Departamento de Biología Molecular
Facultad de Ciencias
Universidad Autónoma de Madrid

Role of arachidonic acid metabolites in *Trypanosoma cruzi* infection

Tesis doctoral

Néstor Adrián Guerrero Gutiérrez

Madrid, 2013

Tesis doctoral

Role of arachidonic acid metabolites in Trypanosoma cruzi infection

Esta memoria ha sido presentada por el Licenciado en Bioquímica ***Néstor Adrián Guerrero Gutiérrez*** para optar al grado de Doctor en Biología Molecular

Directores de la tesis

Dr. Manuel Fresno Escudero
Catedrático del Dpto. de Biología Molecular de la UAM

Dra. Núria Gironès Pujol
Profesor contratado doctor del Dpto. de Biología Molecular de la UAM

A mis padres, por su apoyo en todo momento de mi carrera

Y al Clan que me enseñó
mi lugar en el mundo

INDEX

SUMMARY

ABSTRACT

In Chagas disease, caused by *Trypanosoma cruzi,* inflammation plays an important role in the pathophysiology. Lipid mediators derived from arachidonic acid (AA), as prostaglandins and leukotrienes, are considered regulators of homeostasis and inflammation. These molecules are produced by a biosynthetic pathway controlled by enzymes as cyclooxygenases and lipoxygenases. The role of cyclooxygenase-2 (COX-2) in immunosuppression during the acute phase of *T. cruzi* infection has been described using non-steroidal anti-inflammatory drugs, which are inhibitors of this enzyme. In this study, we first investigated the expression of enzymes involved in AA metabolism during *T. cruzi* infection. Susceptible and non-susceptible models of infection were used to further analyze the role of lipid mediators in *T. cruzi* infection. Our results confirm the expression of several of these enzymes in *T. cruzi* infected heart, in particular COX-2. $CD68^+$ heart-infiltrating macrophages were the major cell type expressing COX-2. $CD11b^+$ heart-infiltrating myeloid cells were purified and produced prostaglandins PGE_2 and $PGF_{2\alpha}$. In contrast, no AA metabolite was produced by the parasite itself. Studies using gene-deficient animal models indicate that regulation of COX-2 and PGE_2 (through Prostaglandin E receptor 2 signaling) is in part responsible of cardiac inflammation in *T. cruzi* infected mice. We also describe the indirect participation of COX-2 in immunosuppression in the acute phase of infection by increasing inducible nitric oxide synthase expression. The key role of lipid mediators in Chagas disease inflammation and the availability of drugs which inhibit their synthesis and their receptors could be useful for the treatment of this neglected disease.

RESUMEN

En la Enfermedad de Chagas, causada por *Trypanosoma cruzi,* la inflamación juega un papel muy importante en la fisiopatología. Los mediadores lipídicos derivados del ácido araquidónico (AA), como prostaglandinas y leucotrienos, son considerados reguladores de la homeostasis y de la inflamación. Estas moléculas son producidas por una ruta biosintética controlada por las enzimas ciclooxigenasas y las lipoxigenasas. El papel de la ciclooxigenasa-2 (COX-2) en la inmunosupresión que ocurre durante la fase aguda de la infección con *T. cruzi* ha sido descrito usando antinflamatorios no esteroideos, los cuales son inhibidores de la enzima. En este trabajo hemos investigado la expresión de enzimas relacionadas con el metabolismo del AA en la infección por *T. cruzi*. Modelos susceptibles y no susceptibles fueron utilizados para profundizar el análisis del papel de los mediadores lipídicos en la infección por *T. cruzi*. Nuestros resultados confirman la expresión de algunas de estas enzimas en el corazón infectado por *T. cruzi*, siendo COX-2 una de ellas. Los macrófagos $CD68^+$ son el principal tipo celular de los que infiltra el corazón que expresa COX-2. Células mieloides $CD11b^+$del corazón infectado fueron purificadas y produjeron prostaglandinas PGE_2 y $PGF_{2\alpha}$. Por el contrario, el parásito no produjo mediadores lipídicos por sí solo. El uso de modelos animales genéticamente deficientes nos lleva a concluir que la regulación por COX-2 y PGE_2 (a través del receptor 2 de prostaglandina E) son en parte responsables de la inflamación cardiaca en ratones infectados por *T. cruzi*. También describimos la participación indirecta de COX-2 en la inmunosupresión que ocurre durante la fase aguda incrementando la expresión de la enzima óxido nítrico sintasa inducible. El papel clave de estos mediadores lipídicos en la inflamación de la Enfermedad de Chagas, junto con la disponibilidad de drogas que inhiben las enzimas productoras y los receptores, podrían ser de utilidad en tratamientos futuros para esta enfermedad olvidada.

ABBREVIATION LIST

AA	Arachidonic Acid
APC	Antigen presenting cell
bp	Base pair
BSA	Bovine serum albumin
cAMP	Cyclic Adenosine Monophosphate
CD	Cluster of Differentiation
CTL	Cytotoxic T lymphocyte
DNA	Deoxyrribonucleic acid
d.p.i	Days post infection
ELISA	Enzyme Linked Immunosorbent Assay
ET-1	Endothelin-1
EP-2	Prostaglandin E receptor 2
FC	Flow citometry
FCS	Fetal calf serum
HETE	Hydroxyeicosatetraenoic
HBSS	Hank´s Balanced Salt Solution
HPLC	High-Performance Liquid Chromatography
IHF	Immunohistofluorescence
IFN	Interferon
Ig	Immunoglobulin
IL	Interleukin
LPS	Lipopolysaccharide
LT	Leukotriene
LX	Lipoxin
M1	Classically activated macrophage
M2	Alternatively activated macrophage
MHC	Major Histocompatibility Complex
M.O.I.	Multiplicity of Infection
MyD88	Myeloid differentiation primary response gene 88
NFAT	Nuclear Factor of Activated T-cells
NF-κB	Nuclear Factor κB
NI	Not Infected
NK	Natural Killer
NO	Nitric oxide
NSAID	Non-steroidal antinflammatory drug
PAMP	Pathogen Associated Molecular Pattern
PBS	Phosphate Buffer Solution
PECS	Peritoneal exudate cells
PG	Prostaglandin
PLA_2	A2 Phospholipase
PPR	Patter recognition receptor
qPCR	Quantitative Polymerase Chain Reaction
RIPA	Radio-Immunoprecipitation Assay
RNA	Ribonucleic acid
RQ	Relative quantity
TCR	T cell Receptor
Th	T helper lymphocyte
TIRAP	Toll/IL-1R(TIR)-domain-containing adaptor protein
TLR	Toll like receptor
TRIF	TIR-domain-containing adaptor inducing interferon-β
TNF	Tumor Necrosis Factor
WB	Western Blot

Genes and proteins abbreviations are listed in Materials & Methods. Table 2

INTRODUCTION

Chagas disease

Chagas disease is a multisystemic disorder that due to the scarcity of preventive and therapeutic tools and population at risk is considered as a neglected tropical disease (Hotez et al., 2007; Morillo, 2013). Carlos Chagas described for the first time the disease and its causative agent *Trypanosoma cruzi* in 1909 (Chagas, 1909). The burden of Chagas disease in Latin America has decreased over recent years but the number of infected people is still over 8 million. More than 40.000 new infected people and 12.550 deaths per year are estimated. The high rate of migration towards non-endemic countries has spread the boundaries of the infection. Non-vectorial transmission is possible through blood transfusion, organ transplantation and from infected mother to child. The risk is related to the country of origin of the migrants and the rate of prevalence in a given region (Moncayo and Silveira, 2009). Spain is the second non-endemic country with more infected immigrants. In 2009 the estimation was between 47.000 and 67.000 infected people (Gascon et al., 2009).

Trypanosoma cruzi is a kinetoplastid protozoan of the *Tripanosomatidae* family. Its life cycle involves stages in invertebrate and vertebrate hosts including domestic and wild vertebrates (**Fig. 1**). The insect vectors that transmit the parasite are blood sucking bugs of the *Reduviidae* family. Parasites replicate in the insect proximal gut in the form of epimastigote. In the distal part of the intestine it transforms into metacyclic trypomastigote. When the insect feeds on blood, it releases the infective parasite with the faeces. Due to scratching close to the site of the bite, the parasite can enter the bloodstream. Another route of entry is the intact mucosa. The metacyclic trypomastigote scapes from the parasitophorous vacuole and localizes in the cytoplasm of the infected cell, where it converts to the amastigote form. As obligate intracellular parasites, *T. cruzi* amastigotes use the nutrient pool present in the host cell cytoplasm for replication and transform into blood trypomastigotes. Parasites released from the host cell disseminate throughout the body via lymph and blood system and infect other cells. Although any nucleated mammalian cell can be parasitized by these organisms, cells of the reticulo-endothelial, nervous and muscle systems, including the heart, are usually targets of infection. Once the bug feeds on and infected host the cycle is completed. (Teixeira et al., 2012; Tyler and Engman, 2001).

Pathology of Chagas disease

Clinically *T. cruzi* infection progress can be divided in two phases, acute and chronic. In the acute phase, after infection, a local inflammatory lesion can appear at the site of the bite. Then, parasite dissemination through the body occurs, and circulating blood trypomastigotes can be observed. Death occurs occasionally in the acute phase (<5–10% of symptomatic cases) as a result of severe myocarditis or meningoencephalitis, or both. But frequently this phase shows very mild and unspecific symptoms and the infection can pass easily unnoticed. About 60–70% of the infected people will never develop clinically apparent disease. These patients have the indeterminate form of chronic Chagas disease, which is characterized by positivity for antibodies against *T. cruzi* in serum, normal electrocardiogram, and normal radiological examination of the chest, esophagus, and colon. The remaining 30–40% of patients develops the most severe pathology of the disease that appears between one and three decades after infection with *T. cruzi*. During this phase, circulating parasites cannot be detected in blood, but progressive damage

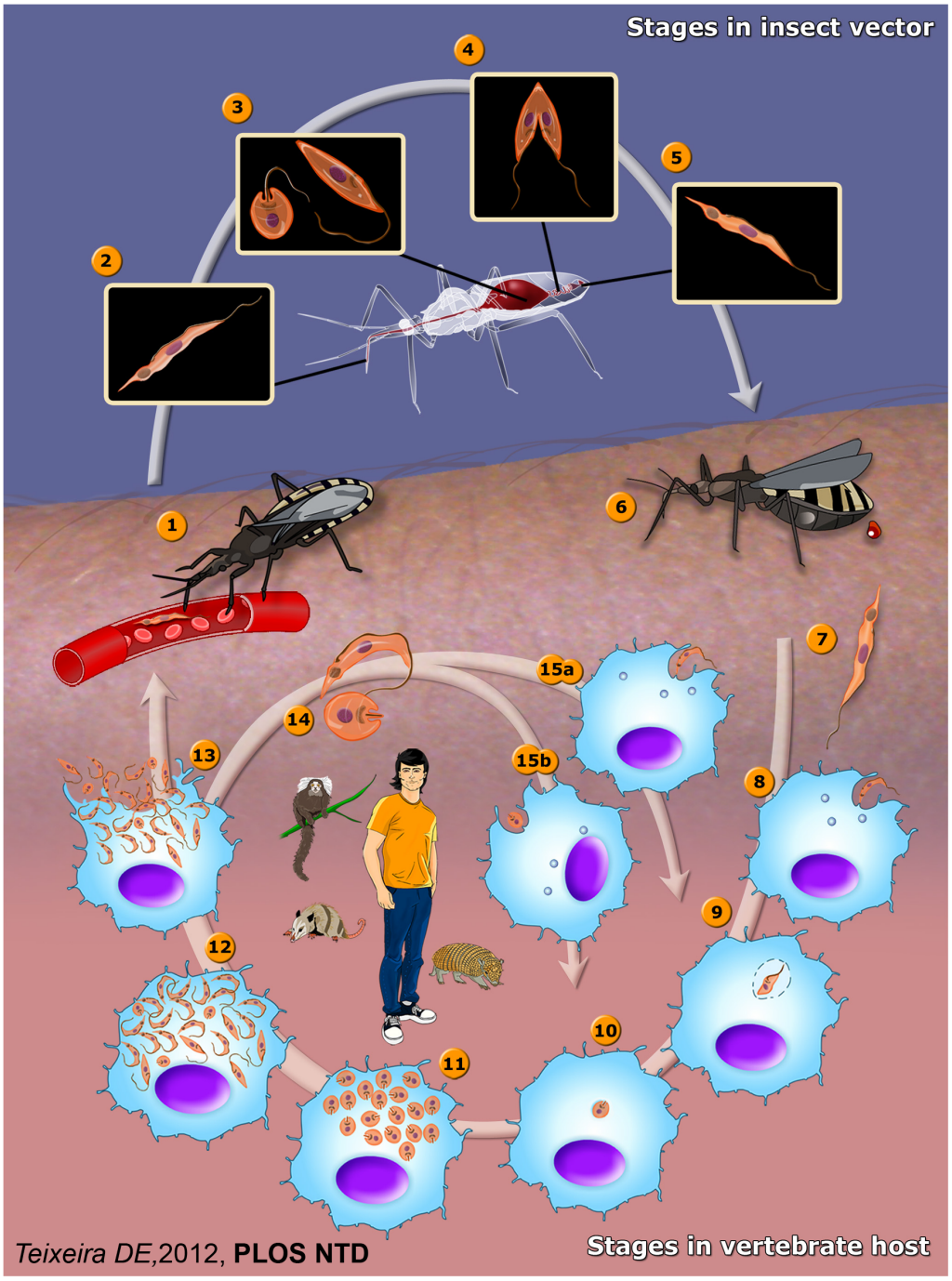

Figure I1 | Schematic representation of the life cycle of *Trypanosoma cruzi*. When hemiptera (*Fam. Reduviidae*) bites an infected vertebrate (1), trypomastigotes in the blood are taken by the bug (2) and turn into epimastigotes (3) in the gut where they reproduce (4). In the distal intestine epimastigotes differentiate back to metacyclic trypomastigotes (5). *T. cruzi* infected hemiptera during blood sucking (6) releases metacyclic trypomastigotes with the faeces that penetrate the host (7), infect cells (8), multiply as amastigotes (11) and break out the cell to the bloodstream in the form of trypomastigotes (13). These parasites can infect new host cells (15) or can be taken up by invertebrate vectors to complete the cycle (1). Adapted from Teixeira *et al. PLOS NtD* (2012)

occurs in tissues. Disease can evolve into different pathologies: cardiac (cardiomegaly), digestive (megaoesophagus and megacolon), or cardiodigestive affections have been described. In the chronic phase, the heart is the most commonly affected organ; cardiomyopathy frequently develops in congestive heart failure, the most common cause of death in these patients (Machado et al., 2012; Rassi et al., 2012; Rassi et al., 2010) (**Fig. 2**).

Two main mechanisms have been proposed for the origin of chronic pathology. The first one states that the pathology is directly linked to parasite persistence and destruction of the infected tissues, resulting in chronic inflammation (Kierszenbaum, 2005; Tarleton, 2001; Viotti et al., 1994). The second one postulates an autoimmune etiology, and it is based in the scarcity of parasites in affected organs during the chronic phase. It claims that *T. cruzi* infection induces an immune response against self-tissues (Cunha-Neto et al., 2011). Indeed, some groups consider the inflammatory cardiomyopathy of Chagas disease a genetically driven autoimmune disease (Teixeira et al., 2011). But both events, autoimmunity and persistence, might not be mutually exclusive (Girones et al., 2005; Girones and Fresno, 2003; Levin, 1996; Soares et al., 2001).

Besides, it has been proposed that the diversity in the clinical manifestations of Chagas disease depends on host genetic background (Andrade et al., 2002; del Puerto et al., 2012). Different studies have demonstrated that *T. cruzi* is genetically heterogeneous with a typical clonal population structure (Zingales

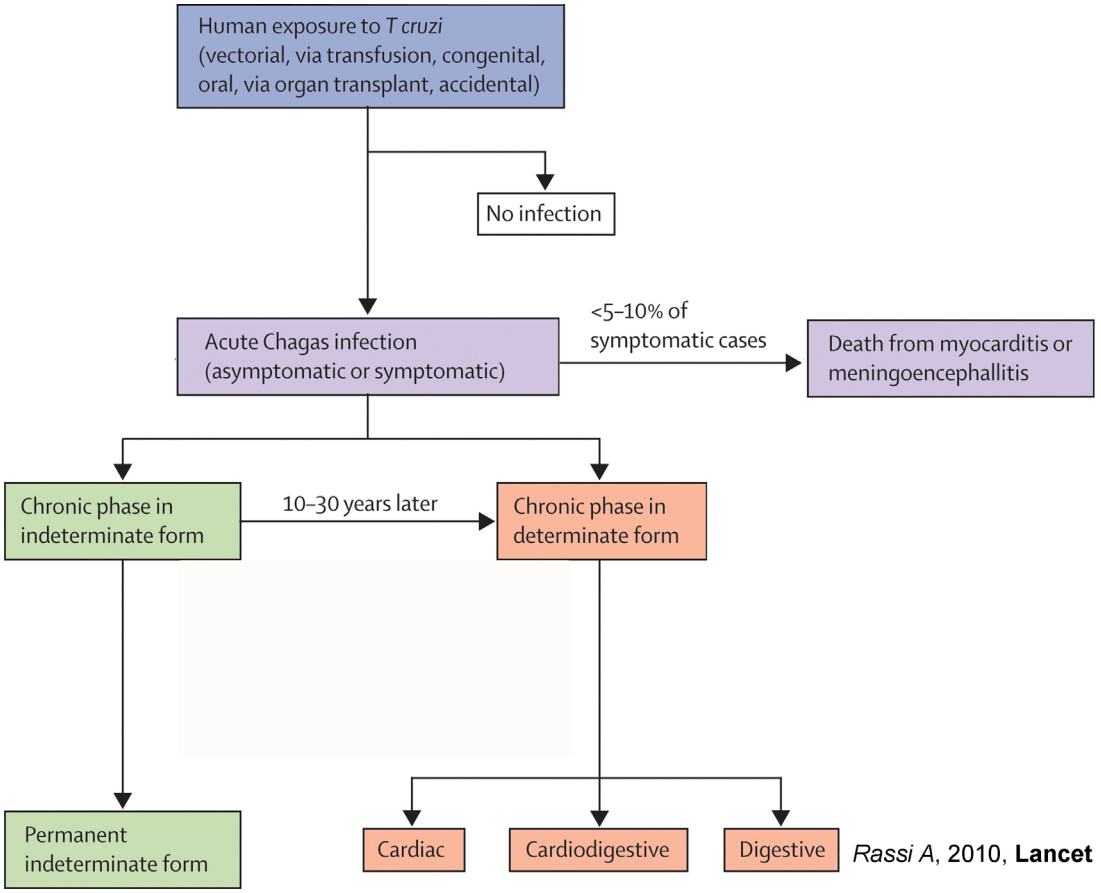

Figure I2 | Chagas disease phases in humans. *Trypanosoma cruzi* infection generates different pathologies in humans. Adapted from Rassi *et al. Lancet* (2010)

et al., 2012). In spite of seldom recombination events (Sturm and Campbell, 2010) DNA markers as ribosomal DNA and miniexon have generated a consensus about the existence of six main phylogenetic lineages (Lewis et al., 2009), with different geographical distribution. There is indirect evidence that genetic variability could generate the different clinical forms of the disease associated with different geographic areas (Zingales et al., 2012). However, a well characterized direct correlation between parasite genetic diversity and clinical outcome of the disease has not yet been established.

Innate response to *Trypanosoma cruzi* infection

T. cruzi infection elicits a complex immune response. Different cell types can recognize *T. cruzi* and react on different ways for controlling infection. Detection and direct destruction of parasites by phagocytes, like macrophages and dendritic cells, which are activated to become APCs and initiate the adaptive immune response is fundamental. Also non-hematopoietic cells, as primary targets of invasion, can sense infection and can contribute to control the infection. (Truyens and Carlier, 2010)

Parasite entry through the skin and mucosa barriers triggers the host immune response. The first cells of the immune system which interacts with the parasite are the phagocytes. These cells detect and respond to pathogen associated molecular patterns (PAMPs) through pathogen pattern recognition receptors (PRRs). PAMPs are repetitive molecular structures of proteic, lipidic, glycolipidic and nucleotidic nature not found in the host. The better characterized PRRs are the Toll-like receptors (TLRs). TLRs activate nuclear factor κB (NF-κB) and interferon regulatory factor (IRF)–dependent pathways via their interaction with adaptor molecules like MyD88, TRIF and TIRAP, leading to IL-1, IL-6, IL-10, IL-12, TNF-α, IFN-γ and COX-2 production (Trinchieri and Sher, 2007).

TLR-2, TLR-4 and TLR-9 can recognize *T. cruzi* molecules. The use of TLR deletion murine models of infection as well as the adaptor molecules MyD88 and TRIF revealed the important role of this pathway in *T. cruzi* immune response (Kayama and Takeda, 2010; Oliveira et al., 2010; Tarleton, 2007). Other PRRs, such as cell surface mannose receptor and cytosolic receptors of the nucleotide-binding oligomerization domain (NOD)-like also activate immune cells after interaction with PAMPs. Nod1-dependent responses have been related to host resistance against *T. cruzi* infection (Silva et al., 2011).

Upon *T. cruzi* infection macrophages secrete IL-12, which activates natural killer (NK) cells to produce IFN-γ (Aliberti et al., 1996; Antunez and Cardoni, 2000). IFN-γ plays a crucial role in activation of macrophages acting synergistically with TNF-α to express inducible nitric oxide synthase (iNOS) (Derouich-Guergour et al., 2001; Munoz-Fernandez et al., 1992) and Cyclooxygenase-2 (COX-2) (**Fig. 3**). In macrophages, nitric oxide (NO) is synthesized by iNOS from L-arginine (L-Arg) and oxygen. iNOS can generate both NO and Superoxide (O^{-2}) that interact to form the potent oxidant peroxynitrite ($ONOO^-$) involved in killing intracellular parasites (Xia and Zweier, 1997). Susceptibility to *T. cruzi* infection has been demonstrated in mice defective in IFN-γ and IL-12 (Graefe et al., 2003; Torrico et al., 1991). IL-6 is produced during *T. cruzi* infection (Truyens et al., 1994) and is related to protective responses against the parasite (Gao and Pereira, 2002).

NO production of IFN-γ activated macrophages is reduced by IL-10 impairing its ability to kill intracellular *Trypanosoma cruzi* (Gazzinelli et al., 1992). But it has been found that

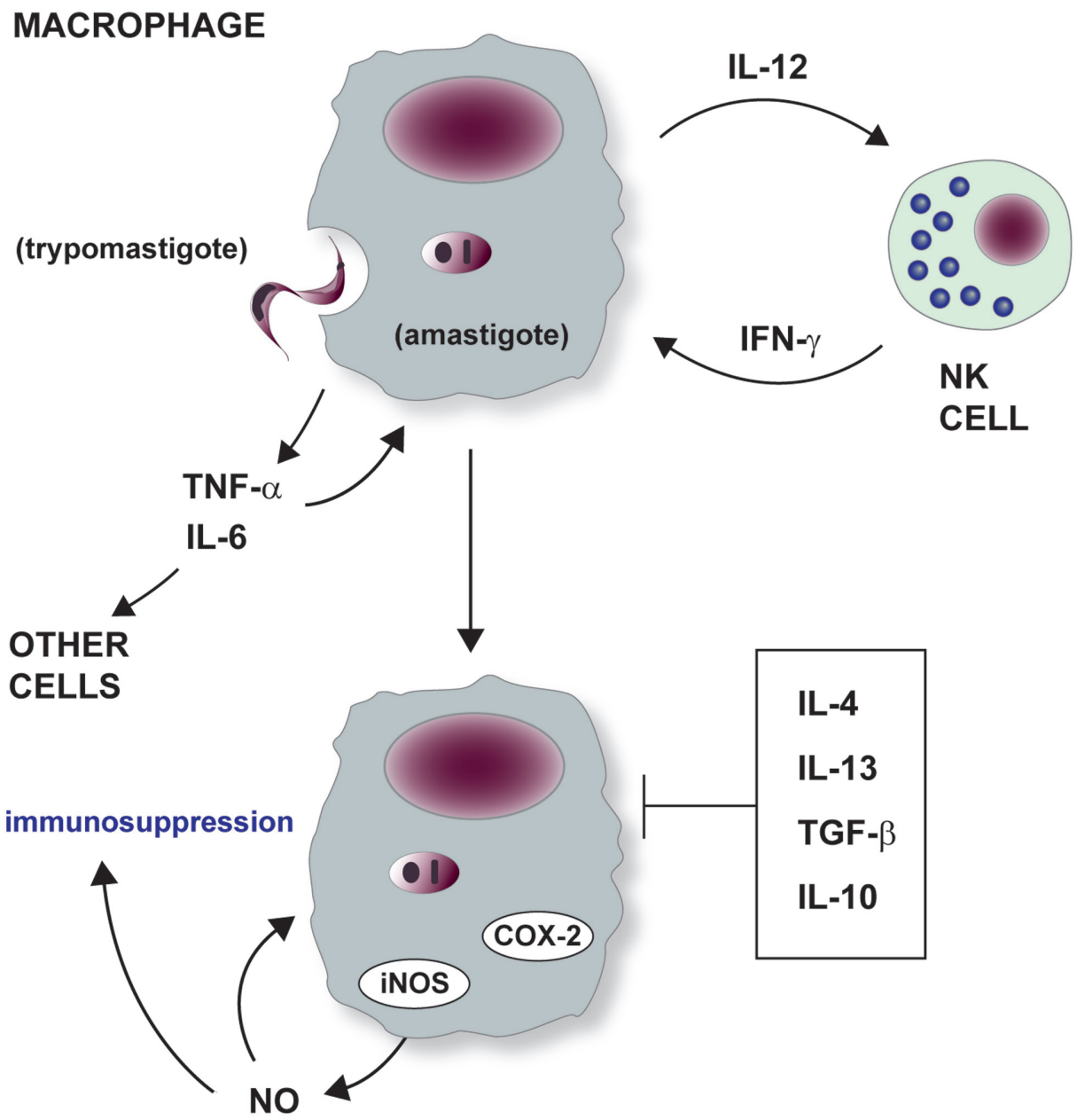

Figure I3 | Macrophage activation in *Trypanosoma cruzi* infection. Upon *T. cruzi* infection macrophages secrete IL-12, which activates natural killer (NK) cells to produce IFN-γ. IFN-γ activates macrophages triggering, with TNF-α, the expression of inducible nitric oxide synthase (iNOS) and Cyclooxygenase-2 (COX-2). TNF-α and IL-6 are produced by activated macrophages and cooperate in the initiation of inflammation acting in other immune and non-immune cells. It has been described that IL-4, IL-13, IL-10 and TGF-β inactive inflammatory macrophages to prevent an excessive and damaging response. In macrophages, nitric oxide (NO) synthesized by iNOS is involved in killing intracellular parasites but also generates immunosuppression inhibiting T cell proliferation.

IL-10 is required to prevent an excessive pro-inflammatory response during *T. cruzi* infection (Hunter et al., 1997) and something similar occurs with tumor growth factor beta (TGF-β) (Silva et al., 1991). It has been proposed that IL-4 down-regulates IFN-γ and inflammation acting cooperatively with IL-10 (Abrahamsohn et al., 2000). IL-13 might also be involved in the down-regulation of IFN-γ release (Antunez and Cardoni, 2001)(**Fig. 3**).

However, NO produced by macrophages also mediates the immunosuppression in the acute phase of *T. cruzi* infection and can also cause oxidative stress, which is especially harmful for the host causing tissue damage (Abrahamsohn and Coffman, 1995; Gutierrez et al., 2009). There are other mechanisms proposed to participate in the immunosuppression, like IL-2 receptor down-regulation (Majumder and Kierszenbaum, 1996), NO production by $CD11b^{+}Gr\text{-}1^{+}$ myeloid suppressor cells (Goni et al., 2002) and prostaglandin E_2 (PGE_2) production (Michelin et al., 2005).

The enzyme arginase-1 (Arg-1) is involved in the urea cycle and the polyamines synthesis pathway, which are needed for proliferation of all eukaryotic cells including parasites. Arg-1 is mainly induced by Th2 cytokines (IL-4, IL-10) and PGE_2 (Corraliza et al., 1995). Due to substrate sharing with iNOS, both enzymes have been involved in regulation of the Th1/Th2 balance during immune processes, and have been used as markers for M1 and M2 macrophage activation (Mills et al., 2000). In addition, it has been shown that iNOS and Arg-1 expressing $CD11b^{+}Ly6C^{+}Ly6G^{-}$ monocytic myeloid-derived suppressor cells (MDSCs) infiltrate cardiac tissue during *T. cruzi* infection can suppress the effector response (Cuervo et al., 2011; Cuervo et al., 2008).

During the acute phase of infection when parasitism is high, there is a burst of chemokine synthesis in the myocardium (Machado et al., 2008; Teixeira et al., 2002). It appears that chemokine synthesis and myocarditis occur mainly in response to parasite molecules. CCL2 is highly expressed in infected cardiac tissue and plays a key role in leukocyte recruitment and parasite resistance (Paiva et al., 2009) . Also CCL3, CCL5 and CXCL9 have been described to play a protective role in experimental models of infections (Hardison et al., 2006; Roffe et al., 2010).

Endothelial cells also collaborate in defense against *T. cruzi* infection by secreting molecules as Endothelin-1 (ET-1), the most potent endogenous vasoconstrictor (Mukherjee et al., 2004). ET-1 has been implied in the vasculature damage generated during *T. cruzi* infection (Machado and Camargos, 2008; Petkova et al., 2001). ET-1 receptor antagonist has a protective role in heart tissue (Rachid et al., 2006) and central nervous system (Rachid et al., 2010) in the rat model of infection. In contrast, a minor effect was found when infected mice were treated with the endothelin receptor antagonist (Roffe et al., 2010).

Adaptive response to *Trypanosoma cruzi* infection

Parasites that do not escape the parasitophorous vacuole or soluble parasite antigens are presented to helper $CD4^{+}$ T cells by professional APCs through MHC-II, despite the fact that MHC-II expression is down-regulated during *T. cruzi* infection (Alba Soto et al., 2003). T helper cells are very important to orchestrate the immune response and when became activated converts into different Th subsets with distinct cytokine expression profiles and functions. In addition, due to the ability of *T. cruzi* to invade a high variety of mammalian cell types, non-professional APCs are also able

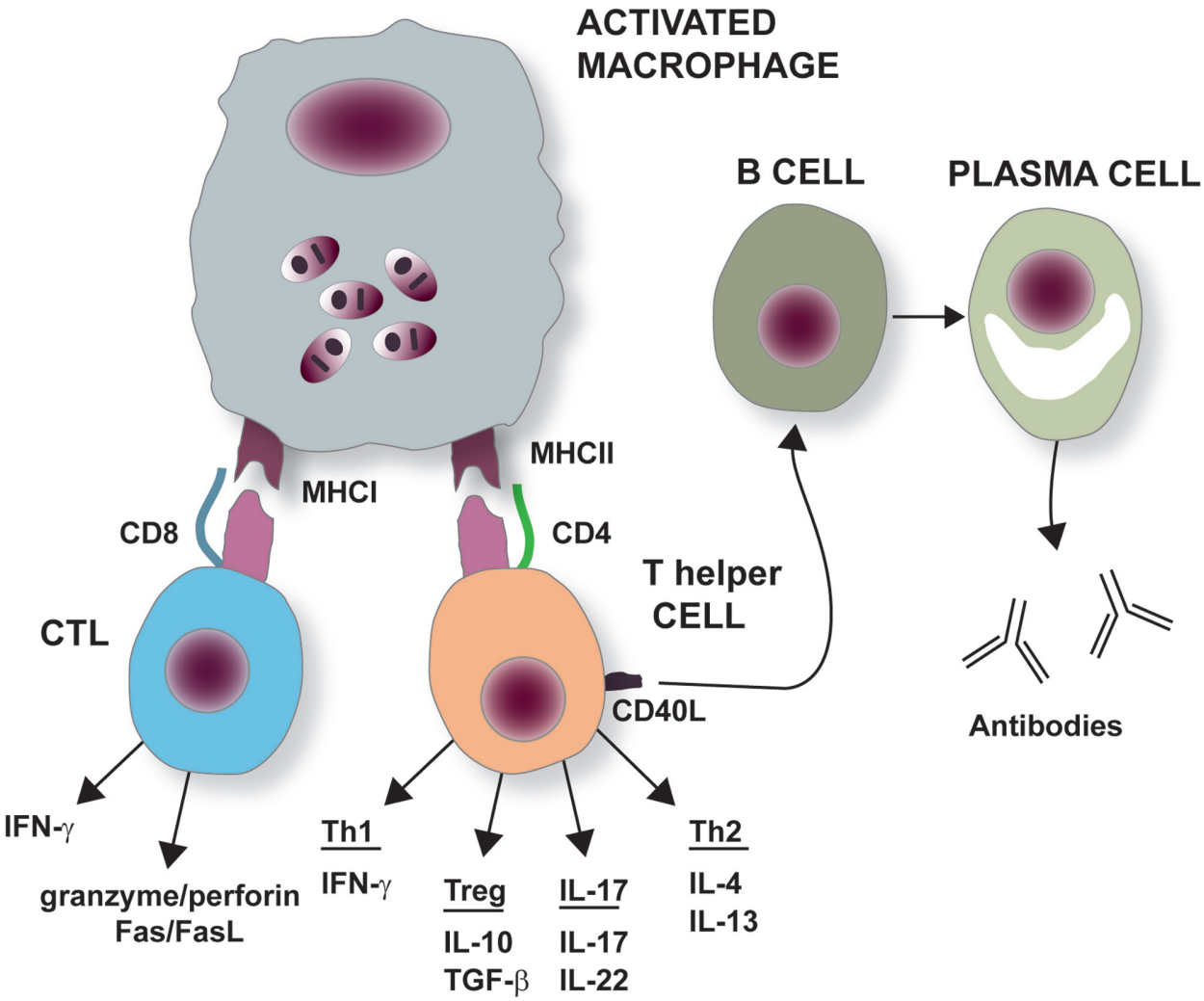

Figure I4 | Adaptative response to *Trypanosoma cruzi* infection. Following an antigenic challenge at a peripheral site, antigen-presenting cells (APCs) migrate to draining lymph nodes in order to present parasite antigens to naïve T cells. This antigen presentation process is mediated by interaction of the TCR (T cell receptor) in $CD8^+$ T cells with major histocompatibility complex class (MHC)-I, or in $CD4^+$ T cells with MHC-II. Antigen presentation leads to T cell activation and proliferation. This is followed by the differentiation of naïve $CD4^+$ T cells to distinct T helper subtypes that secrete different cytokines: T helper (Th)1 cells (IFN-γ), regulatory T (Treg) cells (TGF-β,IL-10), Th17 (IL-217, IL-22) and Th2 (IL-4, IL-13). T helper cells through their TCR and CD40L play a key role in B cell proliferation and differentiation to plasma cell in order to produce antibodies. Naïve $CD8^+$ cells differentiate into CTL (Citotoxic T lymphocytes) that eliminate infected cells through granzyme/perforin and Fas/FasL mechanisms, also secrete IFN-γ to activate macrophages and promote differentiation of Th1 cells.

to present parasite peptides to cytotoxic $CD8^+$ lymphocytes through MHC-I, thus participating in the inflammatory and immune responses (**Fig. 4**). (Garg et al., 1997).

B cell activation is not a generalized response and depends on host susceptibility. (Bryan et al., 2010). Nevertheless, antibody response is necessary because B cell-deficient mice succumb to *T. cruzi* infection (Kumar and Tarleton, 1998). Although it was initially published that perforin/granzyme mediated killing was not necessary for resistance to infection (Kumar and Tarleton, 1998), subsequent studies reported that cytotoxic $CD8^+$ T lymphocytes are important to control intracellular infection through perforin/granzyme mediated killing of infected cells and/or FAS-mediated apoptosis (Martin and Tarleton, 2004; Muller et al., 2003). About the control of the reaction against parasite

infection, cytokines are important regulators in the induction and type of immune response. But no clear Th1 or Th2 polarization was observed when mice susceptible or resistant to *T. cruzi* infection were analyzed (Zhang and Tarleton, 1996).

Nevertheless, we should keep in mind that *T. cruzi* immune evasion mechanisms are important to understand the outcome of the disease. They interfere with innate and adaptive responses at several levels. Evasion of complement, cell surface modification, suppression of T cell proliferation and production of phospholipase A_2 are a few of them (reviewed in (Osorio et al., 2012).

Cyclooxygenases

Derivatives of arachidonic acid (AA) belong to the eicosanoid family, which includes prostanoids (prostaglandins, thromboxanes and prostacyclins), leukotrienes and lipoxins. These mediators act at nanomolar concentration in an autocrine/paracrine manner and have been considered regulators of homeostasis and inflammation. AA is released from the plasma membrane by the action of phospholipase A_2 and is further processed by cyclooxygenase (COX) (Harris et al., 2002; Smith et al., 1996). COX is a bifunctional enzyme that performs a complex reaction by acting successively as a bis-dioxygenase and peroxidase. It begins by catalyzing the oxygenation and cyclation of AA to form the hydroperoxy arachidonate metabolite. Thereupon, the peroxidase activity of the enzyme reduces the carbon 15 position hydroperoxide to its corresponding alcohol to form prostaglandin H_2 (PGH_2) (Nugteren and Hazelhof, 1973). There are two main isoforms involved in the metabolism of AA, COX-1 and COX-2. While COX-1 is constitutively expressed in most cells and tissues COX-2 is usually undetectable, being rapidly induced when cells are activated by inflammatory stimuli (Dubois et al., 1998). Although not exclusive, it is generally accepted that COX-1 is involved in cellular and tissue homeostasis whereas COX-2 is expressed primarily at inflammatory sites. Formation of prostanoids from PGH_2 occurs through the activities of a group of synthases that are expressed in a tissue and cell type-selective manner. These terminal synthases include prostaglandin E synthase (PGES) (Tanaka et al., 1987), prostaglandin D synthase (PGDS) (Shimizu et al., 1982), prostaglandin F synthase (PGFS) (Hayashi et al., 1989), thromboxane A synthase (TXAS) (Ullrich and Haurand, 1983) and prostaglandin I synthase (PGIS) (DeWitt and Smith, 1983), which form PGE_2, PGD_2, $PGF_{2\alpha}$, TXA_2 and PGI_2 respectively. Differential expression of these cyclooxygenases and terminal synthases determines the profile of prostanoid production. Different, but not incompatible mechanisms have been proposed to explain this biosynthetic profile. Firstly, it has been suggested that physical compartmentalization of COX-1 and COX-2 with specific terminal synthases could link the activity of these enzymes with the synthesis of specific prostaglandin (Naraba et al., 1998). One of these compartments are cytoplasmic lipid-rich organelles, named lipid bodies, consisting of a hydrophobic core containing neutral lipids surrounded by a phospholid monolayer, with a particular fatty acid composition and proteins (Bozza et al., 2011). In addition, nuclear distribution of cyclooxygenases has been reported (Parfenova et al., 2001). Secondly, some of the terminal synthases are inducible and their expression may be regulated by external signals (Kudo and Murakami, 2005; Shimura et al., 2010) **(Fig. 5)**. Eventually, it has been proposed that differences in substrate affinity and kinetics of terminal synthases account for different production profiles of resting and

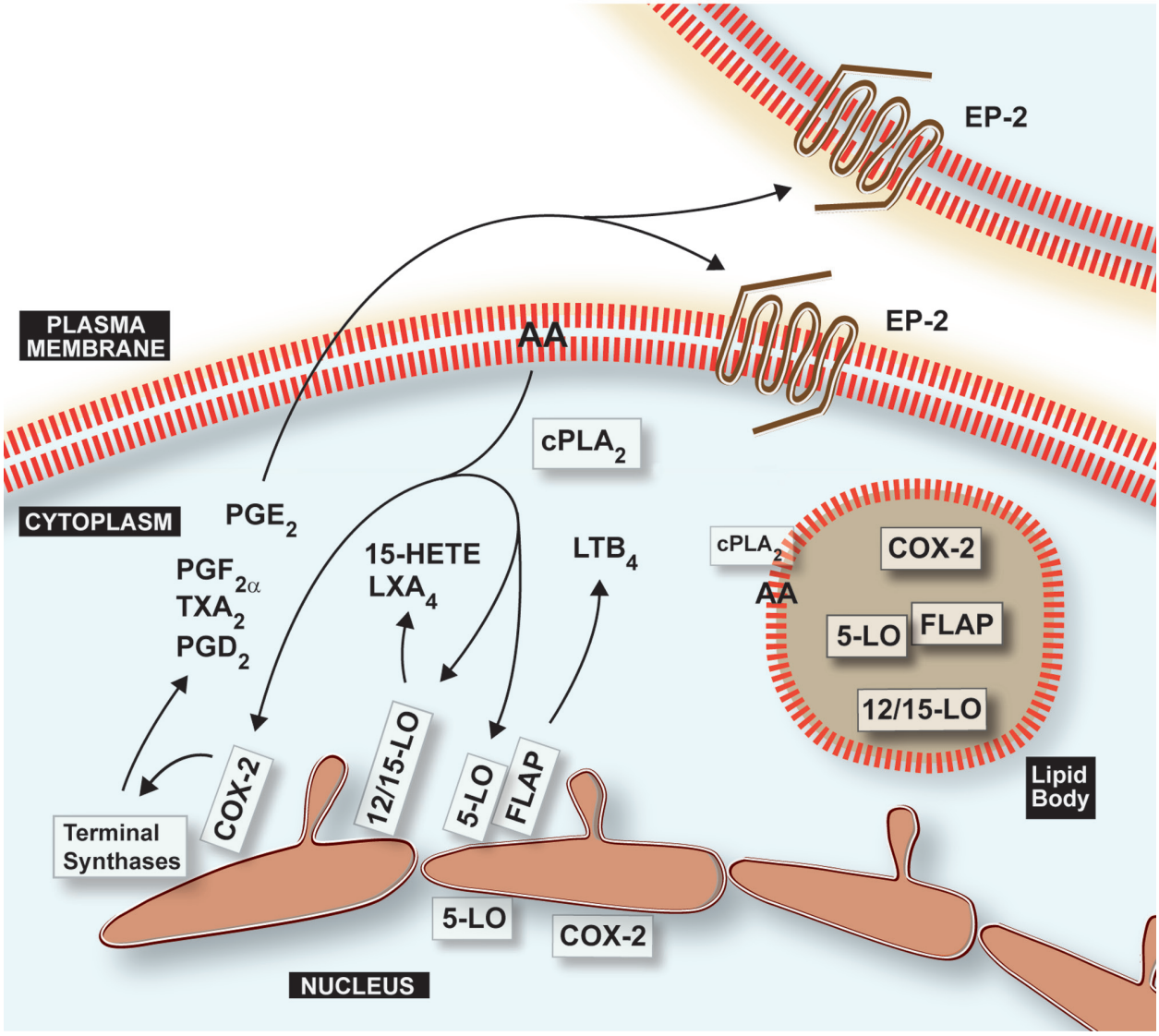

Figure I5 | Arachidonic acid metabolism in inflammation. The precursor arachidonic acid (AA) is derived from membranes phospholipids by the action of the enzyme Phospholipase A2. This free fatty acid is then metabolize by lipoxygenases (12/15 LO, 5-LO with collaboration of FLAP) to produce derivatives as 15-HETE, LXA_4 or LTB_4. Cyclooxygenase enzymes can convert AA into PGH_2 which is further modified by terminal synthase into molecules like $PGF_{2\alpha}$, PGD_2, TXA_2 or PGE_2. These molecules are secreted and act in an autocrine or paracrine manner by binding to G protein coupled receptor like EP-2 for PGE_2. Converting enzymes are mainly distributed in perinuclear area bound to endoplasmic reticulum membrane or nuclear envelop. They have been detected also in lipid bodies, organelle that has a lipid monolayer, neutral lipids and proteins. Presence of COX-2 and 5-LO have been also reported in the nucleus. Eicosanoids synthesis can also occur through transcellular byosinthesis (see text).

activated cells (Penglis et al., 2000; Shimura et al., 2010). There is also evidence that the two COX isoforms may differentially contribute to the synthesis of distinct prostanoids. For instance, in primary peritoneal macrophages COX-1 produces a balance of prostanoids, while COX-2 preferentially generates only PGE_2 and PGI_2 (Brock et al., 1999).

Prostanoids

Prostanoids are generated in most tissues and cells, modulating many biological processes such as smooth muscle tone, vascular permeability, fever and platelet aggregation. Indeed, the clinical importance of prostanoids is emphasized by the fact that their biosynthesis is the target of non-steroidal anti-inflammatory drugs (NSAIDs), one of the most widely group

of drugs used for the treatment of chronic inflammatory diseases (Stables and Gilroy, 2011). Prostanoids have also been implied in cardiovascular diseases (Alfranca et al., 2006; Grosser et al., 2006) and cancer (Greenhough et al., 2009). The maintenance of cardiovascular health is dependent on a balance between vasodilator PGI_2 and pro-thrombotic TXA_2 (Grosser et al., 2006).

PGE_2 and PGI_2 are the predominant pro-inflammatory prostanoids. Both enhance vasodilation and vascular permeability and oedema generation (Funk, 2001; Schror, 1992). PGE_2 exerts pro-inflammatory properties (Krause et al., 2009) but also has immunosuppressive effects through up-regulation of intracellular cAMP (van der Pouw Kraan et al., 1995). PGE_2 binds to four G-protein coupled Prostaglandin E receptors, termed EP-1, EP-2, EP-3 and EP-4, whereas PGI_2 binds to only one receptor (IP) (Cheng et al., 2002). PGE2 receptors, both EP2 and EP4 are coupled to G-proteins, leading to increased production of cAMP and activation of protein kinase A (PKA) (Narumiya et al., 1999). PGE_2 and PGI_2 also reduce the ability of macrophages to phagocytize and kill microorganisms (Aronoff et al., 2004; Weinberg et al., 1985), and inhibit the production of downstream pro-inflammatory mediators (Aronoff et al., 2007; Dorris and Peebles, 2012; Kunkel et al., 1988) yet enhance IL-10 production (Harizi et al., 2002). PGE_2 has a multitude of functions in cell activation and differentiation and these effects vary depending on the micro-environment, maturation and activation state of the cell, type of EP receptor involved and local concentration of prostaglandin. (Chemnitz et al., 2006; Loffler et al., 2008; Napolitani et al., 2009; Yao et al., 2009).

PGD_2 can elicit anti-inflammatory response via ligation to DP1 and PD2 receptors. It can also act through its non-enzymatically dehydrated product 15-deoxy-Δ12,14-PGJ_2 (15d-PGJ_2). This metabolite acts via ligation to the nuclear receptor PPAR-γ, decreasing pro-inflammatory cytokine release and inhibiting the actions of IκB kinase and NF-κB transcription factor (Scher and Pillinger, 2009). However, PGD_2 acts as an important mediator in allergic asthma increasing eosinophilic infiltration, IL-4 secretion with subsequent Th2 activation (Arima and Fukuda, 2011). Dual actions of prostanoids are frequently seen in immune and allergic reactions, where different type of prostanoids and their receptors often exert opposite actions in a single process (Narumiya, 2009).

Both iNOS and COX-2 enzymes are induced upon inflammation stimuli. Crosstalk regulation of the expression and activity between both enzymes through its products PGE_2 and NO has been described. Nitric oxide produced by iNOS increases the enzymatic activity of COX-2 activating the peroxidase activity (Salvemini et al., 2013; Salvemini et al., 1993). The mechanism of COX-2 activation seems to be mediated through peroxynitrite (Landino et al., 1996) (Cuzzocrea and Salvemini, 2007). Regulation of iNOS by COX-2 and its products has been scarcely studied. However, it seems that COX-2 activity is important for iNOS expression in macrophages of rat intestine (Hori et al., 2001) and Küpffer cells (Gaillard et al., 1992), and PGE_2 signaling through EP4 is necessary for iNOS expression in murine breast cancer cell (Timoshenko et al., 2004).

Lipoxygenases

Interestingly, the PGE_2 generated during the onset phase of inflammation collaborates also in its termination by inducing the transcription of enzymes required for the generation of other classes of bioactive lipids that are pro-resolutive mediators, such as lipoxins (LXs). These mediators inhibit granulocyte functional responses, modulate the expression of chemokines and cytokines, stimulate monocyte recruitment and enhance macrophage phagocytosis of apoptotic leukocytes. These events are critical in the control of self-limiting inflammatory responses (Levy et al., 2001). LXs have also been implicated in wound healing (Gronert et al., 2005) and regulation of fibrosis (Kronke et al., 2012).

There are two major routes for LXs production. These routes can be distinguished by the type of lipoxygenase (LO) which begins AA oxygenation, which distribution depends on the cell type. One pathway involves the insertion of molecular oxygen at C-5 by 5-Lipoxygenase (5-LO) with its partner, 5-LO activating protein (FLAP), to produce 5-hydroperoxyeicosatetrenoic acid (5-HpETE). Which is further metabolized by 5-LO to generate leukotriene A_4 (LTA_4). This pathway is conducted only by leukocytes, since the distribution of 5-LO is largely restricted to these cell types. LTA_4 is readily transferred to adjacent platelets, usually leading to its processing to other leukotrienes (Sala et al., 2010). Although, adherent platelets, *via* 12-LO could also convert LTA_4, donated by leukocytes, to LXA_4 and LXB_4 (Folco and Murphy, 2006). The other major route of LX biosynthesis involves the initial conversion of AA to 15(S)-HpETE by 12/15-Lipoxygenase (12/15-LO). This enzyme is abundant in epithelial cells of the respiratory or gastrointestinal tracts, as well as in diverse leukocytes, including macrophages, monocytes and eosinophils. Following secretion, 15(S)-HpETE is taken up by neutrophils or monocytes and converted through a 5-LO/FLAP dependent mechanism to LXA_4 and LXB_4 (Levy et al., 1993). In addition, epimers of LXA_4 and LXB_4 can be produced following aspirin treatment. Aspirin irreversibly acetylates COX-2, inhibiting its ability to produce prostanoids. Nonetheless, acetylated COX-2 can metabolize AA to 15(R)-HETE, which could then be processed into "aspirin-triggered" lypoxin by 5-LO (Chiang et al., 2005; Serhan, 1997).

Eicosanoids in infections

COX-2 expression is up regulated upon bacterial infection and PGE_2 has been shown to play an immunosuppressive role in this process (Goldmann et al., 2010). A COX-2 deficient ($COX\text{-}2^{-/-}$) mouse (Dinchuk et al., 1995) was used in different infection models with apparently contradictorily results. COX-2 deletion seems to be beneficial for the host in the case of bacterial septicemia (Ejima et al., 2003) and viral lung infection (Carey et al., 2005). Supporting this, PGE_2 secretion after infection is associated to viral replication (Janelle et al., 2002). However $COX\text{-}2^{+/-}$ mice presented more inflammatory myocardial damage in viral myocarditis than $COX\text{-}2^{+/+}$ with similar viral burden (Takahashi et al., 2005). In addition, $mPGES\text{-}1^{-/-}$ mice showed higher parasite burden upon *Mycobaterium tuberculosis* infection (Chen et al., 2008).

Pathogen generation of eicosanoids

Analysis of pathogen eicosanoid production is a complex issue. Eicosanoid production has been documented in fungi, helminthes and protozoans that infect humans. The role of these products and its relation with infection is far to be completely understood. Eukaryotic microbes like *Plasmodium falciparum, Toxoplasma gondii,*

Candida albicans, Trypanosoma brucei and Trypanosoma cruzi express a phospholipase-like enzyme. This enzyme releases AA from phospholipid layer allowing its conversion in bioactive lipids. No cyclooxygenase related protein has been described in pathogen microbes and some COX-independent mechanisms of lipid mediators have been proposed (Noverr et al., 2003).

Prostaglandin generation by *T. cruzi* and *T. brucei* has been analyzed. PGF synthase activity has been described and TbPGFS and TcPGFS have been cloned. These enzymes are also related with drug metabolism and activation (Kubata et al., 2007). *Trypanosoma brucei* extracts are able to metabolize AA into $PGE_{2,}$ PGD_2 and $PGF_{2\alpha}$ (Kubata et al., 2000). PGD_2 production by *T. brucei* has been related with the control of parasite density inside the host, probably contributing to disease symptomatology (Figarella et al., 2005).

Trypanosoma cruzi production of prostaglandin and thromboxane has been reported (Kubata et al., 2007; Machado et al., 2011). But only the role of *T. cruzi*- derived TXA_2 has already been studied *in vivo* by Ashton *el al*. These authors proposed that *T. cruzi*- derived TXA_2 is important to control host survival and modulates cell activation and vasoconstriction (Ashton et al., 2007).

Host eicosanoid production after *T. cruzi* infection

Little is known about the role of eicosanoids in human chagasic pathology (de Barros-Mazon et al., 2004; Sousa et al., 2008). In addition, all the research regarding the role of eicosanoids in *Trypanosoma cruzi* infection was performed in the rodent models of acute infection. During the acute phase of infection in the murine model, plasma $PGF_{2\alpha}$, TXB_2, 6-keto-$PGF_{1\alpha}$ (Cardoni and Antunez, 2004) and PGE_2 levels (Celentano et al., 1995) were increased. Macrophages from infected rats show an increased number of lipid bodies, where COX-2 produces PGE_2 (D'Avila et al., 2011). Also $CD8^+$ T lymphocytes from infected mice secrete PGE_2 (Gorelik et al., 1990; Sterin-Borda et al., 1996).

Due to the availability of inhibitors of both enzymes (COX-1 and COX-2) and COX-2-selective inhibitors (NSAIDs), different research groups have used them with experimental model of *T.cruzi* infection. Unfortunately, the use of distinct parasite isolates and mouse strains in those studies have generated a body of controversial data. In some cases pharmacological inhibition of one or both isoforms increases mortality, parasitemia and cardiac parasite nests regardless of mouse or parasite strain used (Celentano et al., 1995; Hideko Tatakihara et al., 2008; Pinge-Filho et al., 1999; Sterin-Borda et al., 1996). But others have found that inhibition of prostaglandin synthesis ablates parasitemia and increases survival in mice (Abdalla et al., 2008; Freire-de-Lima et al., 2000; Michelin et al., 2005). These differences cannot be easy explained, and the effects of NSAIDs on *T. cruzi* infection have been puzzling since the publication on the issue (Celentano et al., 1995). In addition, differences in the ability to produce PGE_2 between mouse strains, as BALB/c and C57BL/6 mice, (Kuroda and Yamashita, 2003), in cytokine serum levels (Roggero et al., 2002) or cardiac cytokine expression profile (Cuervo et al., 2008) after infection could be responsible for the observed discrepancies.

The effects of anti-inflammatory PGD_2 derivative $15dPGJ_2$ have been studied also in *T. cruzi* experimental infection. When added to infected cardiomyocytes *in vitro*, the expression of pro-inflammatory mediators is reduced and parasite burden increases. PPAR-γ and NF-κB

pathways have been implied in this process (Hovsepian et al., 2011). Treatment of infected mice with $15dPGJ_2$ leads to a decrease TNF-α cardiac expression meanwhile IL-10 plasma level increase. No changes were observed in survival of the infected mice compared with the $15dPGJ_2$ treated ones. However, cardiac parasite burden data differed depending on the study (Penas et al., 2013; Rodrigues et al., 2010).

The role of 5-lipoxygenase in and its derivatives *T. cruzi* infection seems to be mouse and parasite strain-dependent (Borges et al., 2009). Again, there is contradictory data in the literature regarding the infection of 5-LO deficient model or the treatment with inhibitors (Pavanelli et al., 2010; Panis et al., 2011). However, despite of divergences due to mouse strain and parasite inoculum, the 5-lipoxygenase and its metabolite LTB_4 is always related to nitric oxide (NO), key mediator in parasite killing (Vespa et al., 1994) and immunosuppression (Abrahamsohn and Coffman, 1995). Thus, previous *in vitro* studies have demonstrated that LTB_4 augment NO level in *T. cruzi* infected macrophages (Talvani et al., 2002).

OBJECTIVES

Lipid mediators produced by cyclooxygenases and lipoxygenases have a wide range of functions in the immune response against infection. One of those functions is the regulation of the initiation and resolution of inflammation. On the other hand, acute phase of *Trypanosoma cruzi* infection is characterized by inflammation with high secretion of cytokines and chemokines. After this phase, usually, parasite burden is dramatically reduced and inflammation resolves. Our hypothesis sustains that lipid mediators produced by cyclooxygenases and lipoxygenases have a role in *T. cruzi* elicited inflammation and resolution.

The main objective of this work was therefore to study the role of these mediators in initiation and resolution of inflammation during the acute phase of *Trypanosoma cruzi* infection. Three specific objectives were proposed:

1. To analyze the expression of cyclooxygenases and lipoxygenases in hearts of mice infected with *Trypanosoma cruzi.*

2. To study the effect of the inhibition and deletion of cyclooxygenase-2 and Prostaglandin E receptor 2 in the outcome of *Trypanosoma cruzi* infection.

3. To determine the role of cyclooxygenases and Prostaglandin E receptor 2 in the immunosuppression observed in the acute phase of *Trypanosoma cruzi* infection.

MATERIALS & METHODS

1. Parasites and mice

Murine models

Young adult (6 to 8-week-old) BALB/c and C57BL/6 mice were purchased from Harlan, Interfauna Iberica or CharlesRiver. IL-4 Receptor deficient BALB/c mice (Mohrs et al., 1999) were a gift from Dr. Beschin (Vrije Universiteit Brussel, Belgium). COX-2 deficient mice: B6;129S7-Ptgs2^{tm1Jed}/J were purchased from Jackson Laboratories (Bar Harbor, ME, USA). Mixed background C57BL/6-129 mice were used as control for the studies with COX-2 deficient model. EP-2 deficient C57BL/6: Ptger2^{tm1Sna} mice were a gift form Dr. Shu Narumiya, (Faculty of Medicine, University of Kyoto, Japan). Genotype of gene deficient mice was determined by PCR protocol. Due to COX-2 $^{-/-}$ and EP-2$^{-/-}$ female inability to reproduce we bred the animals using homozygous males and heterozygous females in both strains. All mice were maintained under pathogen-free conditions in the animal facility at the Centro de Biología Molecular, Universidad Autónoma de Madrid (Spain) in compliance with local and European ethical norms.

Genotyping:

COX-2 deficient genotyping mice primers	
547	caccatagaatccagtccgg
677	gttcacaatgttccagactcc
345	gtgaactatgaagttaggtcctctg
Neoas	cgccttcttgacgagttcttctg
EP-2 deficient genotyping mice primers	
2716	ctggccattatgaccatcaccttcgcca
2701	ctgagcaacacccatgtttctatcctgg
NeoB	tatcaggacatagcgttggct

345+547 primers amplify a 354 bp fragment from the wild type allele
345+677 primers amplify a 580 bp fragment from the wild type allele
Neoas+547 primers amplify a 442 bp fragment from the mutant allele
Neoas+677 primers amplify a 677 bp fragment from the mutant allele
2716+2701 primers amplify a 470 bp fragment from the wild type allele
2716+NeoB primers amplify a 650 bp fragment from the mutant allele

When necessary, drugs were administered as following. Treatment with etoricoxib (COX-2 selective inhibitor) was administered in drinking water with saccharin to improve tolerance. Etoricoxib was renewed every 2 days in colored bottles for light protection to avoid its degradation. The concentration of drug was calculated to obtain a dose of 5mg/kg/day. Bosentan (dual antagonist of ET A/ET B receptors of endothelin-1) treatment was given by gavage (100 mg/ kg/ day) starting the day before infection and until the day of sacrifice.

Infection model

In vivo infections were performed with Y *Trypanosoma cruzi* strain (obtained from Dr. John David, Department of medicine, Harvard Medical School, Boston, Massachusetts, U.S.A.). Blood trypomastigotes were routinely maintained by infecting IFN-γ receptor deficient mice (129 Ifngrt^{tm1Agt}/J) (Huang et al., 1993) purifying parasites from their blood. These mice were a gift from Manfred Kopf (Max-Planck-Intitute for Immunobiology, Freiburg, Germany).

Groups of 3-6 mice were infected with 2.000 typomastigotes per mice (unless stated different) by intraperitoneal injection, keeping a group of non-infected mice. Parasitemia levels were checked every 2 days by directly inspection with a microscope. Parasite counting was performed using 5 µl drop of tail vein blood. At different days post infection mice were euthanized in a CO_2 chamber and blood and various tissues were collected. Samples were processed for RNA, DNA and protein isolation, histology, confocal immunofluorescence analyses, magnetic cell sorting or cell culture.

TABLE 1. ANTIBODIES

ANTIGEN	REFERENCE	PROVIDER	APPLICATION	DILUTION	POSITIVE CONTROL
iNOS	sc-650	Santa Cruz Biotechnology	WB	1:1000	RAW cells + LPS
COX-2	610203	BD Transduction Laboratories	WB	1:500	RAW cells + LPS
COX-2	160126	Cayman Chemical	WB	1:500	RAW cells + LPS
COX-2	160106	Cayman Chemical	IHF	1:200	RAW cells + LPS
Actin	sc-1616	Santa Cruz Biotechnology	WB	1:1000	
Arg-1	sc-18354	Santa Cruz Biotechnology	WB	1:1000	Liver, infected heart
hPGDS	160013	Cayman Chemical	WB	1:200	hPGDS transfected Jurkat cells
COX-1	160109	Cayman Chemical	WB	1:500	Mouse kidney
12/15 LO		Gift from Kühn H.	WB	1:2500	Fresh peritoneal cell
			IHF	1:200	Fresh peritoneal cell
5LO	160402	Cayman Chemical	WB	1:1000	Commercial control (CaymanChem)
FLAP	sc-181187	Cayman Chemical	WB	1:500	cell line SK-N-MC (ATCC.HTB-10)
EP2	101750	Cayman Chemical	WB	1:500	
CD68	MCA1957GA	AbD Serotec	IHF	1:200	Peritoneal cells
CD4	557681	BD Pharmigen	IHF	1:200	Thymus
F4/80	14-4801-81	eBioscience	IHF	1:200	Liver Küpffer cells
Vimentin	9856 S	Cell Signaling	IHF	1:200	Epithelial cells (VERO
CD11b	557686	BD Pharmigen	Flow Cit.	1:100	
GR-1	12-5931.	eBioscience	Flow Cit.	1:100	
MHC-II (I-A/I-E)	12-5321.	BD Bioscience	Flow Cit.	1:100	
CD11b	130-049-601	Miltenyi Biotec	Magn. Sort.		
Ly6G+	130-092-332	Miltenyi Biotec	Magn. Sort.		
Rat IgG	A-21208	Invitrogen	IHF	1:200	
	A-21434	Invitrogen	IHF	1:200	
	A-21247	Invitrogen	IHF	1:200	
Rabbit IgG	A-31572	Invitrogen	IHF	1:200	
	A-31573	Invitrogen	IHF	1:200	
Goat IgG	A-21431	Invitrogen	IHF	1:200	
	A-21447	Invitrogen	IHF	1:200	
Guinea Pig IgG	A-21435	Invitrogen	IHF	1:200	

TABLE 2. QUANTITATIVE PCR PROBES

CODE (A&B)	GENE	PROTEIN
Mm 00477214_m1	*Ptgs1*	Cyclooxygenase 1, COX-1
Mm 00478374_m1	*Ptgs2*	Cyclooxygenase 2, COX-2
Mm 00452105_m1	*Ptges*	Prostaglandin E synthase, mPGES1
Mm01330613_m1	*Ptgds*	Lipocalin type prostaglandin D synthase, LPGDS
Mm 00479846_m1	*Hpgds*	Hematopoietic prostaglandin D synthase, HPGDS
Mm00495553_m1	*Tbxas1*	Thromboxane synthase, TXAS
Mm 00545833_m1	*Alox12*	Arachidonate 12-lipoxygenase, 12-LO
Mm 00507789_m1	*Alox15*	Arachidonate 15-lipoxygenase, 12/15-LO
Mm 01182743_m1	*Alox5*	Arachidonate 5-lipoxygenase, 5-LO
Mm 00802100_m1	*Alox5ap*	Arachidonate 5-lipoxygenase activating protein, FLAP
Mm 99999056_m1	*Ccl2*	Chemokine (C-C motif) ligand 2, MCP-1
Mm 00441259_G1	*Ccl3*	Chemokine (C-C motif) ligand 3, MIP-1-α
Mm 00443111_m1	*Ccl4*	Chemokine (C-C motif) ligand 4, MIP-1-β
Mm 01302427_m1	*Ccl5*	Chemokine (C-C motif) ligand 5, RANTES
Mm 00443113_m1	*Ccl7*	Chemokine (C-C motif) ligand 7, MCP-3
Mm 00434946_m1	*Cxcl9*	Chemokine (C-X-C motif) ligand 9, MIG
Mm 00443258_m1	*Tnf*	Tumor necrosis factor alpha, TNF-α
Mm 00801778_m1	*Ifng*	Gamma interferon , IFN-γ
Mm 00446190_m1	*Il6*	Interleukin 6, IL-6
Mm 00434165_m1	*Il12a*	Interleukin 12a, IL-12
Mm 00439616_m1	*Il10*	Interleukin 10, IL-10
Mm 00434204_m1	*Il13*	Interleukin 13, IL-13
Mm 00445259_m1	*Il4*	Interleukin 4, IL-4
Mm 00442754_m1	*Cd4*	CD4 antigen, CD4
Mm 00839636_g1	*Cd68*	CD68 antigen, CD68
Mm 01182107_g1	*Cd8a*	CD8 antigen, alpha chain, CD8
Mm 00498698_m1	*Itgax*	Integrin alpha X, CD11c
Mm 00802530_m1	*Emr1*	F4/80
Mm00448463_m1	*Ptprc*	CD45
Mm 00475988_m1	*Arg1*	Arginase 1, ARG-1
Mm 00440502_m1	*Nos2*	Nitric oxide synthase 2, iNOS
Mm 00438656_m1	*Edn1*	Endothelin 1, ET-1
Hs99999901_s1	*18S*	Eukaryotic 18S rRNA

TABLE 3. BUFFERS & SOLUTIONS

BUFFER	COMPOSITION	APPLICATION
Protein Lysis Buffer	50 mM Tris-HCl (pH 7.5), 250mM NaCl, 3 mM EDTA and EGTA, 1.5% Triton X-100 10% glycerol, Complete Mini Protease inhibitor Cocktail tablets (Roche) in distilled water	Protein lysis
RIPA Buffer	50 mM Tris-HCl (pH 8), 50 mM NaCl, 1 mM EDTA, Complete Mini Protease inhibitor Cocktail tablets (Roche), 0,1% SDS, 1% Triton-X100, 0,5% sodium deoxycholate in distilled water	Protein lysis
Erythrocyte lysis buffer	123mM Cl NH_4, 10 mM CO_3HK, EDTA 0,1M, (pH 7,4) in distilled water	Leukocyte isolation
AA assay (w hematin)	100 mM sodium phosphate (pH 7.0), 2 μM hematin, and 5 mM tryptophan in distilled water	AA conversion assay
AA assay (w/o hematin)	100 mM sodium phosphate (pH 7.0), and 5 mM tryptophan in distilled water	AA conversion assay
FC staining buffer	2% BSA and 1% FCS in PBS	Flow Citometry
IHF blocking buffer	0,1% Triton X-100, 5 % BSA 2% respective secondary antibody normal serum in PBS	IHF
HBSS (Ca2+ and Mg2+)	1.26 mM $CaCl_2$, 0.49 mM $MgCl_2$, 0.41 mM $MgSO_4$, 5.3 mM KCl, 0,44 mM KH_2PO_4, 4.17 mM $NaHCO_3$, 137.93 mM NaCl, 0,34 mM Na_2HPO_4, 5,55 mM glucose in distilled water	Magnetic sorting
LIT medium	68.4 mM NaCl, 5.36 mM KCl, 44.95 mM $Na_2HPO_4(H_20)_2$, 11.1mM Glucose, 3 g Liver infusion, 5 g Tryptose	Parasite culture
RMPI 1640 medium	RPMI complete medium containing 5% FCS, 2mM L-glutamine, 100U/ml penicillin, 100μg/ml streptomycin, 1000u/ml and 0,1 mM non-essential amino acids	Cell culture

2. *In vitro* generation of parasites and infection

Vero (ATCC number CCl-81) epithelial cells were grown in RPMI complete medium containing 5% FCS, 2mM L-glutamine, 100U/ml penicillin, 100µg/ml streptomycin, 1000U/ml and 0,1 mM non-essential amino acids. (Gibco, Grand Island, NY) at 37°C in an atmosphere containing 5% CO_2. Axenic culture of Y strain trypomastigotes were collected from extracellular medium of Vero cells 5 to 6 days after infection. Only plates without visible extracellular amastigotes or dead cells in the medium were selected for the experiments. Media were shortly centrifuged 2 minutes at 150 x g to remove dead cells and aggregates and always counted and purity checked using a Neubauer hemocytometer. These purified parasites were used to infect adherent cells during 16 hours in the incubator at 37 Celsius degrees with a M.O.I. (multiplicity of infection) 5 parasites per cell in 2% FCS RPMI. After the incubation, culture plates were directly processed for protein extraction or other assays. Warm PBS to wash the cell was used if were necessary.

Three different strains were maintained in epimastigote vital form: Y which belongs to *T. cruzi* II type, CL-Brener (*T. cruzi* VI type) and Dm28 (*T. cruzi* I type), according to their genetic variability (Zingales et al., 2009). Epimastigotes forms of *T. cruzi* were grown in LIT (Liver Infuse Tryptose) medium (Castellani et al., 1967). The macrophage cell line RAW 264.7 (ATTC Code: TIB-71) purchased from ATTC were used in some *in vitro* experiments.

3. Real time PCR for parasite detection

Hearts were perfused with PBS and 0,1% heparin (1.000 U/ml) and were minced into small pieces with an sterile scalpel blade. DNA was isolated with High PurePCR Template preparation Kit (Roche). In order to quantify *T. cruzi* DNA, we followed the qPCR assay described by (Piron et al., 2007). 100, 10, 1, 0.1 and 0.01 pg of DNA purified from Y strain epimastigotes were used to generate the standard curve. Experimental heart tissue qPCR reactions contained 100 ng of total DNA and *Tnf* murine gene was used as a loading control.

4. mRNA analysis by quantitative RT-PCR

Total RNA was extracted from heart tissue perfused with PBS and heparin, cut in small pieces using a sterile scalpel blade, followed by mechanical disruption using a PT 1300 D homogenizer (Kinematica Polytron, Fisher Scientific) in TRIzol reagent (Invitrogen) as indicated by the manufacturer. For quantitative real time polymerase chain reaction (qPCR) analysis, reverse transcription of total RNA was performed using the components of the High Capacity cDNA Archive Kit (Applied Biosystems. Life Sciences) or the SuperScript Enzyme (Invitrogen, Life Sciences). Amplification of different genes using TaqMan MGB probes and the TaqMan Universal PCR Master Mix (Applied Biosystems) on an ABI PRISM 7900 HT instrument (Applied Biosystems. Life Sciences). For cell-cultured cells, samples were treated as mentioned above except for the mechanical disruption. All samples were assayed in triplicate. Quantification of gene expression by real-time PCR was calculated by the comparative threshold cycle (CT) method as described in (Schmittgen and Livak, 2008). RQ= 2-ΔΔCT. All quantifications were normalized to the ribosomal 18S to control variability in the initial concentration of RNA and conversion efficiency of the reverse transcription reaction.

5. Protein expression analyses

Protein extracts were prepared from heart tissue perfused with PBS and heparin, cut

in small pieces using a sterile scalpel blade followed by mechanical disruption using a PT 1300 D homogenizer (Kinematica Polytron, Fisher Scientific) in Triton X-100 based protein lysis or RIPA buffer. Protein concentration was determined by the bicinchonic acid method (BCA, Pierce) using Bovine Serum Albumin for the standard curve. Cultured cells were treated as mentioned above except for the mechanical disruption. Western blot analyses were performed as follows: 15 or 50 µg of cell or tissue extract were fractionated on SDS polyacrylamide gel and transferred to a Nitrocellulose membrane Hybond-ECL (Amersham Biosciences) and blocked in 5% dry fat free milk or 5% bovine serum albumin in 0.1% Tween-20 Tris Buffered Saline. Primary antibodies were diluted in blocking buffer and membranes were incubated overnight at 4-8 Celsius degrees. Then membranes were incubated with horseradish peroxidase conjugated secondary antibody after washing the primary antibody. Detection was carried out with Supersignal detection reagent (Pierce) and photographic film exposure. Fiji package software was used to quantify band intensity normalizing band areas of the sample to their respective loading control.

6. Histological studies

Cardiac tissues from mice were placed, after been cut in two, in 10% neutral buffered formalin for at least 4 hours at room temperature followed by incubation in 70% ethanol overnight. Samples were then embedded in paraffin (Tissue Embedding Station Leica EG1160), and 5µm tissue sections were prepared (motorized Microtome Leica RM2155) over slides. Samples were deparaffinized and rehydrated using a Tissue Processing Station Leica TP1020. Slides were stained using the Masson´s Trichrome staining and mounted permanently in Eukkitt´s quick-hardening mounting medium (Biochemika, Fluka analytical). The sections were microscopically analyzed in a Leica microscope (DMD 108, Leica microsystems Wetzlar GmbH, Germany) using the 20x magnification objective lens. Lamp intensity 10 and f/Stop 12. Ventricular myocardium micrographs were taken avoiding pericardium, endocardium, auricles and big vessels in order to make the process reproducible. Nine different pictures of different sections, separated by at least 50 microns, per heart were taken. The degree of inflammatory-cell infiltration were quantified using the Fiji package (Schindelin et al.) and the plugin Advance Weka Segmentation developed by Ignacio Arganda Carreras (MIT, USA). The macro used is detailed in Appendix2. Classifier used is available in the attached CD.

7. Confocal immunofluorescence

Organs were removed from mice at different times post infection, cut and fixed in a 4% paraformaldehyde PBS buffered solution. After at least 2 hours incubated at room temperature were transferred to a 30% sucrose PBS solution incubate overnight at 4-8 Celsius degrees, until the tissue sections reach the bottom of the tube in order to cryoprotect the sample. Tissues were then embedded in Tissue-Tek OCT in Cryomolds (Sakura, Japan) to allow cryostat sectioning and frozen using dry ice. 10 µm sections were cut using a cryostat Leica CM1900. Slides were fixed in acetone for 10 min at room temperature, washed and incubated 10 min with NH_4Cl to avoid autofluorescence; then were washed with PBS, permeabilized with PBS 0.1% Triton X-100, blocked and incubated overnight at 4˚C with primary antibodies in the blocking buffer. The samples were washed in PBS and secondary antibodies were added at the dilutions shown in Materials table in the blocking buffer and incubated overnight at 4°C

again. After washing with PBS, samples were washed with water. Hydrophobic ink Dako Pen was used when different sections were located in the same slide and different antibodies were used. Nuclei were stained using 1 microgram/ml of DAPI (268298, Merck). Prolong Gold Antifade Reagent (Invitrogen) was used to mount the slides that were kept at 4°C until observation. Transparent nail polish was used to seal the samples. Stained slides were observed with a confocal laser scanning microscope, LSM710 coupled to an Axioimager.M2 microscope (Zeiss). The micrographs were processed using the software ZEN (Zeiss) or Fiji Package. Antibodies controls are shown in Appendix 1.

8. Lipid Droplets staining

Confocal immunofluorescence was used to detect lipid droplets with Oil Red O (ORO) in propylene Glycol 26079-15 purchased from Electron Microscopy Sciences. To set up the staining and detection of lipid droplets, peritoneal cavity macrophages were used. Cells were incubated with deferoxamine 375 µM overnight at 37°C and the following day stained to detect lipid bodies (Hu et al., 2003). These macrophage lipid droplets were used to obtain the absorption/emission spectrum of ORO thanks to the confocal laser scanning microscope, LSM710 coupled to an Axioimager. M2 microscope (Zeiss). Modified protocol of the already described above for confocal immunofluorescence was used to stain lipid droplets in frozen tissues. With the addition of 1 hour of incubation with 0.5 % ORO in Propylene Glycol (PEG) and the following differentiate step with 85% PEG 1min at room temperature. These steps were carried out after the antibody staining and before mounting.

9. PBMCs, spleen cell suspension

Spleens were aseptically removed from mice kept in medium at 4°C until disaggregation in 40µm nylon cell strainers (Falcon). Blood was obtained by cardiac punction and treated with heparin. Single suspension cells were depleted of erythrocytes by hypotonic lysis, washed with cold PBS and processed for RNA isolation or protein extraction. For some experiments cells were cultured in RPMI. (Gibco, Grand Island, NY) 5% FCS at 37°C in an atmosphere containing 5% CO_2.

10. Peritoneal cells isolation

Peritoneal cavity from euthanized mice was washed with 5 ml of sucrose (116g/l) in PBS. Cells were plated in complete RPMI. (Gibco, Grand Island, NY) at 37°C in an atmosphere containing 5% CO_2. After 4h, non-adherent cells were removed by washing three times with warm PBS, and fresh complete RPMI was restored. In several experiments 1 ml of 10% (w/v) thyoglicollate (Gibco, Grand Island, NY) was injected to elicit an aseptic inflammation to recruit macrophage after 4 days. These cells were harvested as described above. In some experiments LPS (L-8273 Sigma-Aldrich) 1 microgram/ml was used in order to obtain a positive control for Western Blot and Confocal Imnunofluorescence. In other cases coverslips were coated with Poly-L-Lisine (Sigma-Aldrich) to allow the binding of not adherent cells.

11. Isolation of LY6G+ and CD11b+ cells by magnetic sorting

15 BALB/c or C57BL/6 mice were infected i.p. with 2.000 Y strain trypomastigotes. At 21 d.p.i. for BALB/c and 14 d.p.i. for C57BL/6 , mice were euthanized in a CO_2 chamber and hearts were aseptically removed, perfused with 10 ml PBS-heparin solution, and kept in cold HBSS. Then, hearts were pooled in a cell culture dish, washed thoroughly with HBSS and minced into small pieces with a sterile surgery blade. Mouse

hearts (maximum 4 per tube) were transferred into the gentleMACS C tube containing 4.7 ml of HBSS. 300µL of Collagenase II solution (600 U/ml) and 10 µl DNase I solution (60U/ml) were added. Then, were disrupted with gentleMACS Dissociator, incubated 30 min at 37ºC and disrupted one more time using the appropriate protocol of disaggregation. After centrifugation homogenized tissue was suspended in HBSS. To obtain a single cell suspension a cell strainer (70µm mesh size) was utilized. After red blood cells lysis cell suspension were washed and processed following Milteny Biotec instructions for magnetic sorting. Same magnetic sorter protocol was used when spleen, peritoneal cavity cells or blood single cell suspension were used.

For $Ly6G^+$ cell sorting, anti Ly-6G MicroBead kit (Milteny Biotec GMbH) was used with MACS LS columns and MACS Separators Magnet (Miltenyi Biotec GmbH) following manufacturer instructions. $Ly6G^-$ fraction of the cell suspension was afterwards processed for $CD11b^+$ cell sorting using CD11b Microbeads (Milteny Biotec GMbH). These purified cells were cultured to perform an AA conversion assay or process to isolate RNA or obtain protein extracts.

12. Proliferative assays

Spleen cells were obtained as mentioned above, counted, suspended in complete RPMI, 5% FCS and 200.000 cells per well were plated in flat 96 well plates. Cells were stimulated with 5µg/ml purified anti-CD3 (clone 145-2C11, BD Pharmingen) and 1 µg/ml purified anti-CD28 (clone 37.51, BD Pharmingen) or with 1µg/ml concanavalin A (Type IV-S γ-irradiated. C0412, Sigma-Aldrich) and, when indicated, cyclooxygenase inhibitors (10 µM Indomethacin, 0.1 µM NS398, 0.1 µM Celecoxib) were added. At these concentrations the inhibitors could efficiently avoid PGE_2 production in LPS activated macrophages. After incubation at 37°C and 5% CO_2 for 48h, 1µCi [^{3}H] thymidine (Amersham, Little Chalfont, UK or PerkinElmer, Massachusetts, USA) was added to each well. The cultures were collected 18 h later and then processed for measurement of incorporated radioactivity. Cultures were transferred to a glass fiber filter using a 96 well plate harvester. After drying, a paraffin film containing the scintillator was melted on the filter and let it solidify (Wallac, Turku, Finland). MicroBeta scintillation counter (Wallac, Turku, Finland) was used to measure [^{3}H] thymidine incorporated into the DNA of the cells.

13. PGE_2, cytokines and anti-*T. cruzi* antibodies by ELISA.

Supernatant of cultured cells or plasma/serum obtained from blood of infected mice were frozen at -70ºC until were assayed. PGE_2 level were measured with PGE_2 EIA KIT from Cayman Chemical (Michigan, USA), TNFα with ELISA kit from R&D systems (Minneapolis, USA). In order to titer anti-*T. cruzi* antibodies 0.1 microgram of *T.cruzi* epimastigote extract were added to each well of MAXISORP plate (NUNC) and incubated overnight. Plasma diluted 1:100 from infected and not infected animal were added after washing and incubated 2.5 hours. Anti-mouse total IgG, IgG2a or IgG1 HRP-conjugated secondary antibodies were used to detect plasma antibodies. O-Phenylenediamine dihydrochloride was (Sigma-Aldrich) was use to reveal the peroxidase activity reading the optic density at 450 nanometers with a Microplate Reader.

14. Migration assay

200.000 mouse thyoglicollate elicited peritoneal cells were cultured in the upper compartment of permeable 8 µm pore TransWell® plates (Corning, Amsterdam, The

Netherlands) during at least 3 hours in 2% FCS RPMI medium. Cells were left to migrate during 24 hours in response to 5% FCS or 5% FCS plus 10 ng/ml of the chemokine CCL5, (478-MR from R&D Systems) located in the lower compartment. To eliminate non-migrating cells of the upper compartment 2 gently washes with PBS were done. . Cells were fixed with 5% Glutaraldehyde (type II, G-6257 Sigma-Aldrich) in PBS during 20 minutes. After washing, the TransWell membrane was stained with 0.5 % Crystal Violet (C-6158, Sigma.-Aldrich) in water/ methanol during 20 minutes. Two washes with PBS and one with water followed the staining. Cells attached to the upper compartment of the membrane were carefully removed using a cotton bud. 8 different micrographs were taken per well to cover almost all its surface. Leica DFC420 C camera coupled to a Leica DM IL microscope at 200x magnification was used. The experiments were performed in duplicate and data is represented as relative migration (number migrated cells to 5% FCS+ RANTES)/ (number migrated cells to 5% FCS).

15. Arachidonic Acid incorporation assay

Y and Dm28 T. *cruzi* strains epimastigotes were cultured as described above. 25, 100 and 250 million parasites were incubated in 0.5 ml LIT medium with 50µM [^{14}C] Arachidonic Acid (PerkinElmer, Massachusetts, USA) for 30 minutes. Cells were centrifuged 5 min at 3.000 x g, supernatants were transferred to a new tube and cell pellets were washed and hypotonic lysed. 2.5ml of scintillation liquid Optiphase Hisafe 2 (Perkin Elmer, Massachusetts, USA) was added , well mixed and after 24 hours of stabilization were measured with the scintillation counter Rack Beta (Wallac, Turku, Finland).

16. Arachidonic Acid conversion assay

250 million Y, Dm28 , Cl-Brener *T.cruzi* strain epimastigotes or 25 millions of trypomastigotes were centrifuged, washed with 0%FCS Medium and suspended in 0.5 ml of medium (0% FCS LIT or RPMI for epimastigotes or trypomastigotes respectively) with or without 2 µM Hematin (Sigma-Aldrich) . Some parasites tubes were sonicated in order to get total parasite extracts before the addition of arachidonic acid (AA).1 million macrophages or other cell type were cultured in 6 well plate and left 1 hour at 37°C before conversion assay was performed. To obtain a positive control macrophages were incubated 6 hours with LPS (Sigma-Aldrich) 1 microgram/ ml and 2,5 ng/ml of gamma-Interferon (Sigma-Aldrich).

25µM [^{14}C] Arachidonic Acid purchased from PerkinElmer (Massachusetts, USA) was added to each sample described above and incubated 30 minutes at 37ºC. 2% acetic acid in cold methanol was added to extract and preserve AA derivatives. Samples were mixed by vortex and the air inside the tube was substituted by inert nitrogen gas. Samples were kept frozen at -70ºC until HPLC was performed.

HPLC device composed by a Beckman Solvent Module 126 with the column Ultraphere ODS (C-18, Beckman-Coulter) 5 µm diameter sphere particle, 4,5 mm and 25 cm column diameter and length respectively and a Beckman 171 Radioisotope Detector. Scintillation liquid Ecoscint H purchased from National Diagnostics.

Prostaglandins were resolved with the isocratic flow (1ml/min) of the mobile phase: Acetonitrile/water/acetic acid 33:67:0.1 v/v/v.

Radioactive standard were kindly donated by Mercedes Camacho (Hospital de la Santa Crey I Sant Pau, Barcelona). These standard

were produced using ^{14}[C] Arachidonic Acid and different cell types expressing the respective enzymes. ^{14}[C] Arachidonic Acid incubated in medium was used like input control.

17. Flow citometry

Surface cell staining was performed in 96 well plates. Fc receptors on cells were blocked by incubating with purified anti-CD16/ CD32 (Mouse BD Fc Block) (clone 2.4G2, BD Pharmingen) for 5 min at 4°C. Cells were then stained with respective directly conjugated antibodies 20 min at 4°C. Cells were washed with cold PBS 1%BSA and single cell suspensions were fixated with paraformaldehyde 1% in PBS for 10 min at 4ºC. Data were analysed with the FlowJo software (TriStar, Ashland, OR, USA).

18. Statistical analysis

For *in vivo* experiments, data are shown as means and SD (Standard deviation) otherwise is mentioned. "n" indicates number of mice or biological replicates of shown data. All *in vitro* experiments were performed at least three times. Significance was evaluated by Student's t-test when two groups were compared. ANOVA one way followed by Tukey post-test was applied when groups of samples from an experiment had different time points. And ANOVA two way followed by Bonferroni post-test when the experiment had time and mice strain as variables. For survival analysis we choose Gehan-Breslow-Wilcoxon method, which gives more weight to deaths at early time points but is more restrictive than regular log-rank test. GraphPad Prism 5.00 software (La Jolla, CA, USA) was used for statistical analysis.

RESULTS

Expression of cyclooxygenases and lipoxygenases during *Trypanosoma cruzi* infection

Trypanosoma cruzi infection modifies the expression of enzymes responsible for production of lipid mediators in the heart

We used the murine model of *Trypanosoma cruzi* infection because mice are easy to handle, can be modified genetically and develop a well described acute phase in the first month after *T. cruzi* infection. Although we already know that human and mouse immune system differ in some important aspects (Mestas and Hughes, 2004), experimental infections of murine models have provided a big amount of important data regarding Chagas disease. It is becoming accepted that host and parasite genetic differences can influence the outcome of the disease. Thus, different strains of mice present distinct susceptibility to parasite infection depending on their genetic background. In our model, BALB/c mice are susceptible to infection, meanwhile C57BL/6 mice are resistant to *T. cruzi* infection with the Y parasite strain. In the C57BL/6 model of infection, cardiac inflammation (analyzed through mRNA expression of cytokines such as IFN-γ, TNF-α, IL-4, and IL-10) ends faster than in the BALB/c model, probably due to a very efficient immune response. No Th1 or Th2 profile is clearly linked to strain susceptibility, although Th1/Th2 balance was higher for C57BL/6 than for BALB/c (Cuervo et al., 2008).

In order to study the main enzymes involved in the arachidonic acid metabolism, we infected BALB/c and C57BL/6 mice intraperitoneally with 2.000 blood trypomastigotes of the Y strain of *T. cruzi*. **Figure 1A** shows that BALB/c infected mice died during the acute phase of infection and C57BL/6 did not. On average, 2 peaks of parasitemia were detected in BALB/c mice at 9 d.p.i. and 21 d.p.i., because in some mice parasitemia increased dramatically before their death. C57BL/6 parasitemia peak was at 9 d.p.i. and was undetectable by 21 d.p.i. (**Fig. 1A**). Histological analysis of the hearts of infected mice shown in **Fig. 1B** revealed high level of cardiac inflammation in BALB/c infected mice (21 d.p.i.). These mice showed more tissue disturbances and parasitism than the C57BL/6 mice as was previously described in our lab. (Cuervo et al., 2008)

Next, we addressed the level of the cyclooxygenases and terminal synthases of prostaglandins and thromboxane, as well aslipoxygenases in the infected cardiac tissue of both murine models over the time of the infection (**Fig. 2**). Cyclooxygenase-2 gene expression (*Ptgs2*), but not Cyclooxygenase-1 (*Ptgs1*), was increased in heart tissue during the acute phase of *T. cruzi* infection in the same magnitude in both mouse strains. Lipocalin-type PGD synthase (*Ptgds*) mRNA was already present in cardiac tissue and did not increase its expression upon *T. cruzi* infection. However, leucocyte type PGD synthase (*Hpgds*) gene expression was increased. PGD_2 can form 15-deoxi-Δ12,14-PGJ_2 and binds to PPARγ which has an anti-inflammatory effect (Liu et al.; Scher and Pillinger, 2009). Thromboxane synthase (*Tbxas1*) gene expression was increased in both strains. It has been described that TXA_2 induce TNF-α production in monocytes (Caughey et al., 1997) and could be in part responsible for the inflammation

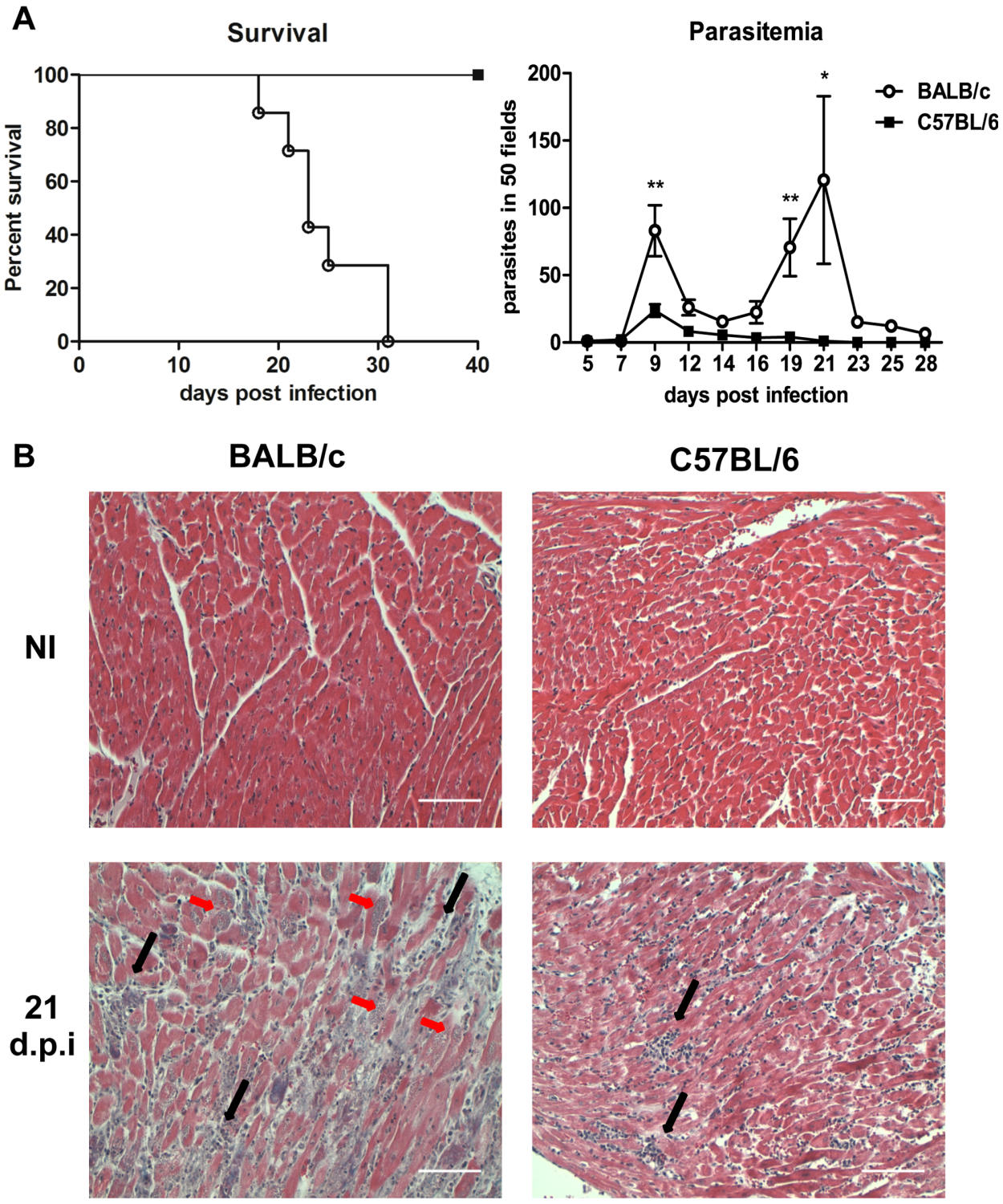

Figure 1 | Survival, parasite burden and inflammation of BALB/c and C57BL/6 mice infected with *Trypanosoma cruzi*. A | Mice survival was monitored daily after infection and parasitemia was quantified every 2 or 3 days. Representative means ± SEM are shown (n=5). ANOVA two way followed by a Bonferroni Post test was performed. Differences between mouse strain are indicated: * p< 0,05 ** p< 0,01. **B |** Cardiac tissue sections from non-infected (NI) and *Trypanosoma cruzi* infected BALB/c and C57BL/6 mice at 21 d.p.i. stained with Masson`s Trichromic. Micrographs were taken as described in Materials and Methods. Representative pictures of each group are shown. Black arrows show infiltrating leukocytes and red arrows indicate parasite nests. Scale bar is 100 microns length.

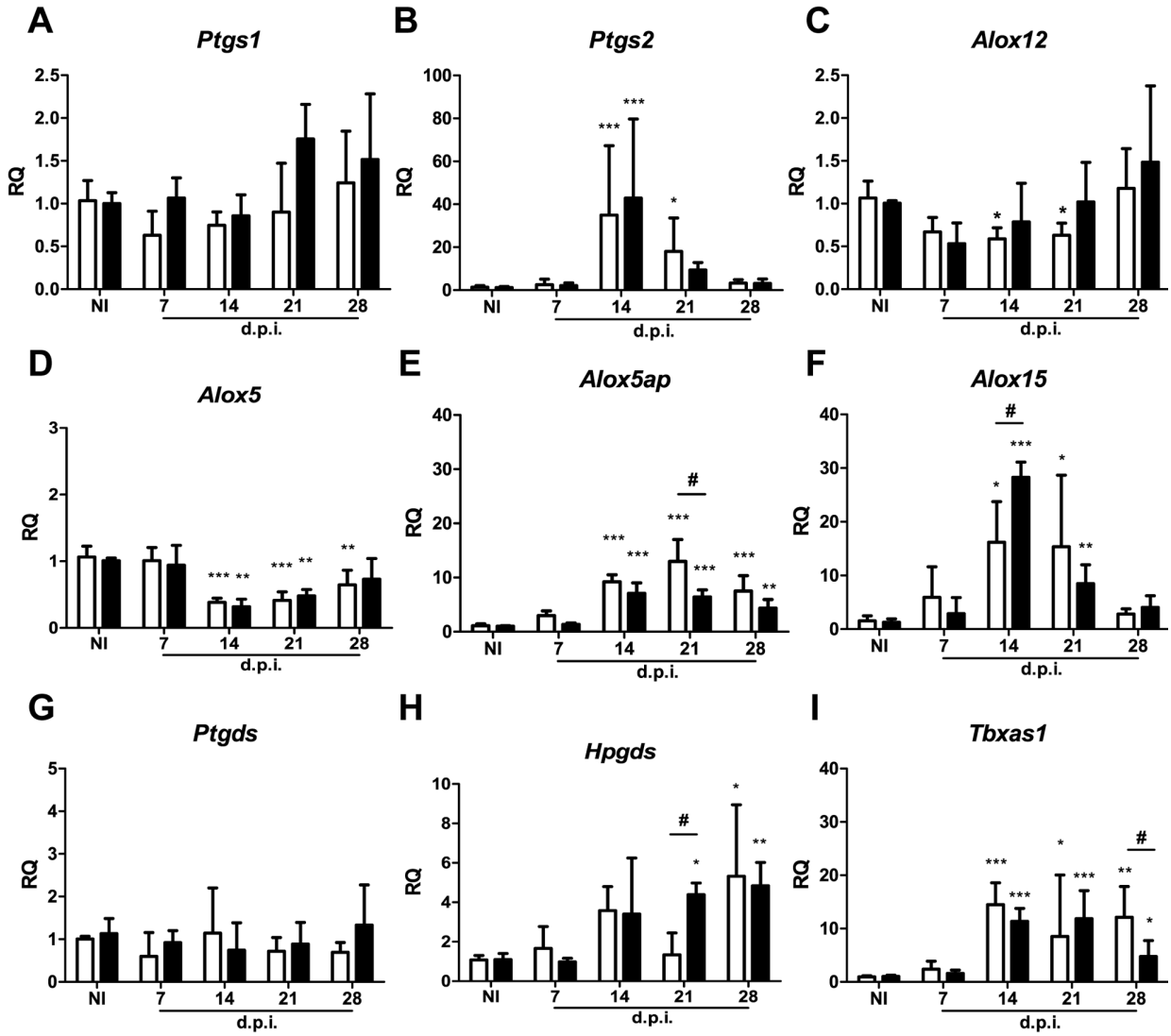

Figure 2 | Arachidonic acid metabolism related enzymes mRNA expression in the heart during *Trypanosoma cruzi* infection. RNA from heart tissue was isolated from mice at different d.p.i. and from non-infected (NI) mice. qPCR was performed as described in Materials and Methods. Results are expressed as RQ calculated from CT values as described in Materials and Methods. Open bars indicate the values of BALB/c mice and filled bars of C57BL/6 mice. Means ± SD from three independent experiments are shown (n=9). Comparison between infected mice respect to non-infected mice for each strain is indicated: * p<0.05 **p<0.01 ***p<0,001. Differences between infected strains is indicated by # p<0.01

generated by *T. cruzi* infection (Ashton et al., 2007).

Expression of the gene encoding 5-lipoxygenase (5-LO, *Alox5),* key enzyme of leukotriene production, decreased in heart tissue of infected mice. In contrast, 5-LO activating protein, FLAP (*Alox5ap)* expression was increased in infected mice (10 fold respect to non-infected mice). Changes in FLAP expression have been involved in post-transcriptional regulation of 5-LO functions (Byrum et al., 1997; Evans et al., 2008). Interestingly, *Alox15,* that codifies 12/15 Lipoxygenase (12/15-LO), involved in resolution of inflammation, showed increased expression in both murine models. The higher level of *Alox15* and *Hpgds* in C57BL/6 mice respect to BALB/c mice at 14 d.p.i. suggests a role of these enzymes in resolution of the infection. In agreement, cardiac inflammation ends earlier in C57BL/6 than in BALB/c mice.

Myeloid cells in inflamed cardiac tissue express COX-2

COX-2 induction in macrophages after infection has been described in different models (Lee et al., 1992). Therefore, we next analysed its expression in magnetic sorted myeloid cells isolated from hearts of *T. cruzi* infected BALB/c and C57BL/6 mice when inflammation was maximal. Using an antibody against Ly6G we obtained the granulocyte population. From Ly6G$^-$ population, CD11b$^+$ cells (monocyte/macrophage) were selected (**Fig. 3**).

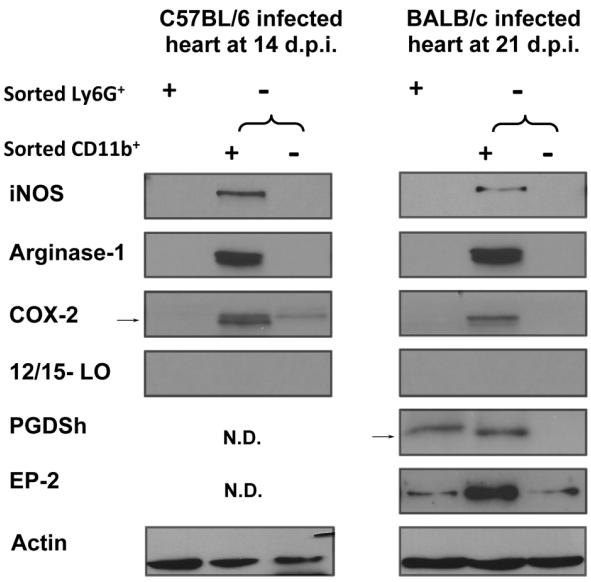

Figure 3 | Protein expression of heart infiltrating myeloid cells during *Trypanosoma cruzi* infection. Ly6G$^+$ and CD11b$^+$ cells were obtained from pooled infected mouse hearts at the peak of inflammation using magnetic separation. Total protein extracts were resolved by SDS-PAGE and transferred to a nitrocellulose membrane. Proteins were detected using specific antibodies. One experiment out of two independent experiments is shown. N.D. stands for non-determined. Arrows indicate the position of loaded positive control bands for COX-2 and PGDSh. Anti-actin antibody was used as a loading control.

As previously described, Arg-1 and iNOS were expressed by Ly6G$^-$ CD11b$^+$ cells (Cuervo et al., 2011). These Ly6G$^-$ CD11b+ cells also expressed COX-2 protein, but 12/15 LO expression could not be detected by immunoblotting, in spite of its mRNA induction in whole cardiac extracts. This suggests that 12/15 LO is not expressed by Ly6G$^+$ or Ly6G$^-$ CD11b$^+$ cells. On the other hand, Ly6G$^-$ CD11b$^+$ cells from BALB/c infected mice expressed hPGDS, which is responsible for production of the pro-resolution prostaglandin PGD_2 (Urade et al., 1989). These cells expressed more EP-2, receptor of PGE_2, than Ly6G$^+$ cells. Interestingly, COX-2 gene expression was much higher in myeloid cells obtained from infected cardiac tissue than in blood, indicating that COX-2 is induced in inflamed tissue (**Fig. 4**).

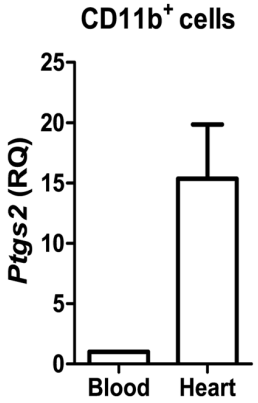

Figure 4 | *Ptgs2* expression in CD11b$^+$ cells isolated from *Trypanosoma cruzi* infected blood and heart tissue. CD11b$^+$ cells were obtained from pooled infected BALB/c mouse hearts or blood at 21 d.p.i. using magnetic beads as described in Materials and Methods RNA was isolated and qPCR was performed. Results are expressed as RQ calculated from CT values as described in Materials and Methods using the infected CD11b$^+$ blood cells for normalization. Means ± SD of two independent experiments is shown.

Hearts from C57BL/6 mice were processed and analysed by confocal microscopy at 14 d.p.i in order to study the pattern of cellular expression of COX-2. CD68 was used as a marker to detected macrophages within the tissue. CD68$^+$cells were clearly present in the infected hearts where they showed a strong and spread intracellular staining due aggrupation of infiltrating cells. We also found that COX-2 was expressed in the perinuclear region of CD68 positive and negative infiltrating cells (**Fig. 5C** and **5D**). No specific staining was

observed in not infected tissues (**Fig. 5A**) or sections incubated with secondary antibodies alone (**Fig. 5B**). COX-2 expression by activated lymphocytes has been previously described (Iniguez et al., 1999), but we could not detect the presence of the enzyme in infiltrating $CD4^+$ cells (**Fig. 6A** to **6C**). Similar results were obtained when BALB/c mice at 21 d.p.i. were analysed with CD68 and CD4 markers (**Not shown**).

$CD68^+$ $Arginase\text{-}1^+$ $iNOS^+$ cells are present in *T. cruzi* infected cardiac tissue and have been characterized as MDSCs (myeloid derived suppressor cells) by their gene signature and suppressor function (Cuervo et al., 2011).

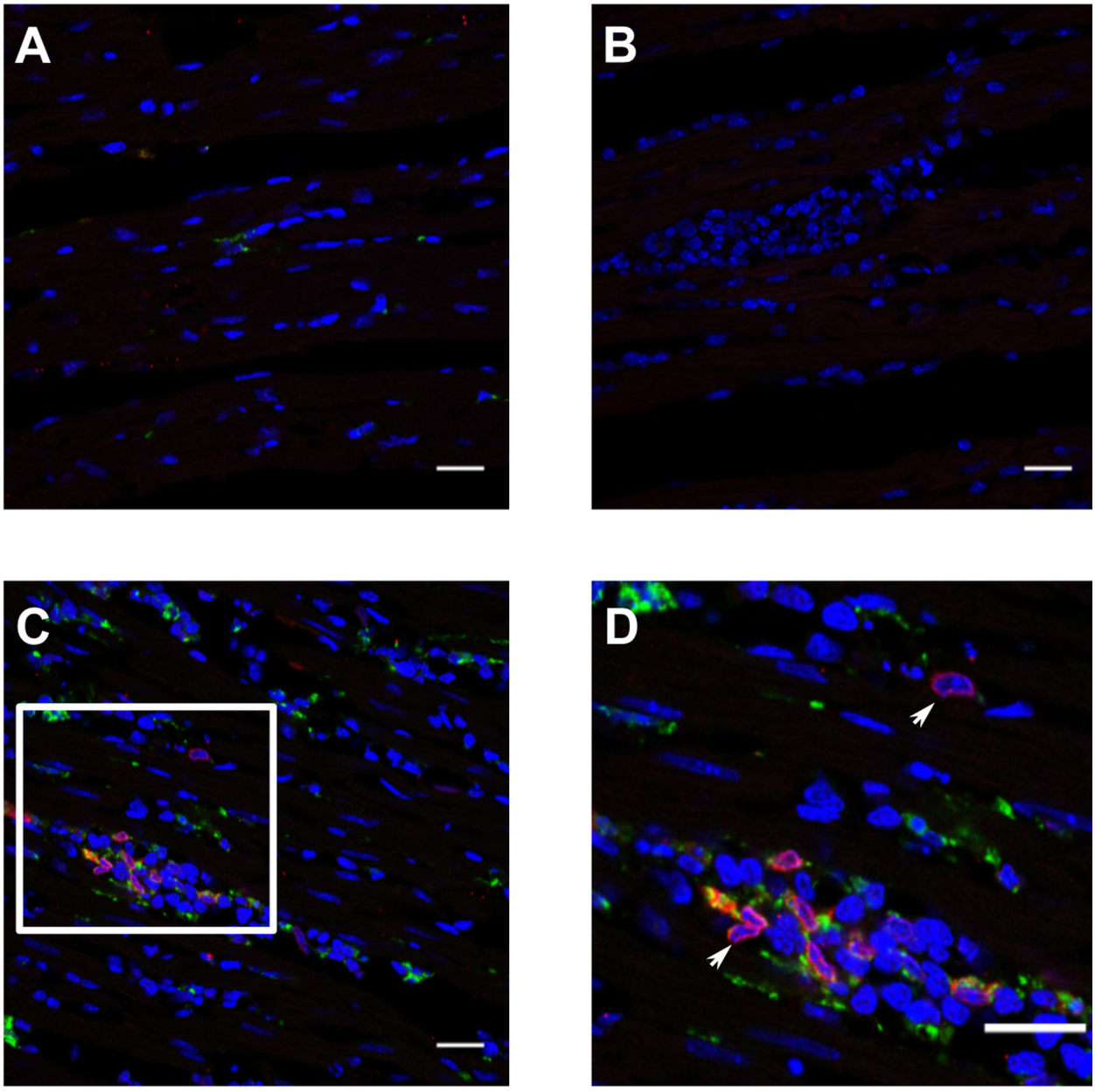

Figure 5 | COX-2 and CD68 expression in *Trypanosoma cruzi* infected cardiac tissue. Heart tissue was isolated at 14 d.p.i. from infected or non-infected C57BL/6 mice and frozen in OCT. Section of the organs were stained with DAPI for **nuclei (blue)** and antibodies against the macrophage marker **CD68 (green)** and the enzyme **COX-2 (red)**. Pictures are representative of more than 3 sections analyzed in at least 3 different mice from three independent experiments. **A** | Non-infected cardiac tissue. **B** | Secondary antibody staining control using infected tissue. **C** | Cardiac tissue from infected mice at 14 d.p.i. **D** | Detail of the infiltrating cells shown in **B**. Magnification of the framed area in **C**. White arrowheads indicate two different $COX\text{-}2^+$ $CD68^-$ cells. Scale bar is 20 microns length.

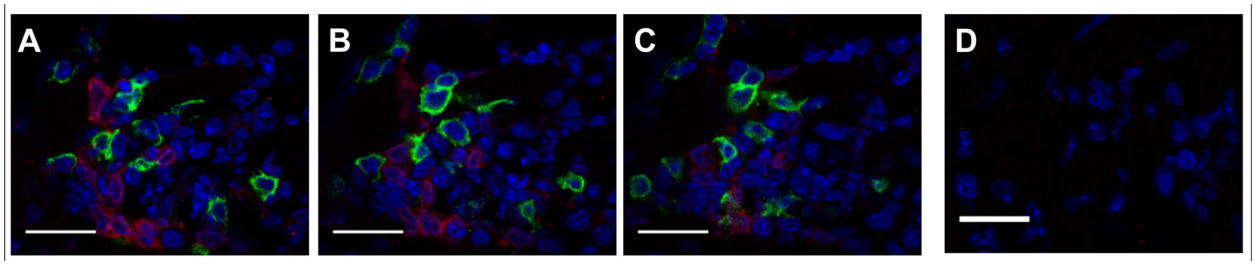

Figure 6 | COX-2 and CD4 expression in *Trypanosoma cruzi* infected cardiac tissue. Heart tissue was isolated at 14 d.p.i. from infected or non-infected C57BL/6 mice and frozen in OCT. Section of organs were stained with DAPI for **nuclei (Blue)** and antibodies against the lymphocyte marker **CD4 (green)** or the enzyme **COX-2 (red)**. Pictures are representative of more than 3 sections analyzed in at least 3 different mice from at least two independent infections. **A - C |** Detail of the infiltrating cells in *T. cruzi* infected heart. 3 confocal sections are shown. **D |** Secondary antibody staining in infected tissue. Scale bar is 20 microns length.

As it was found that Ly6G$^-$ CD11b$^+$ sorted cells expressed the COX-2 enzyme, confocal analysis were performed in heart sections to elucidate if COX-2 co-localized with Arg-1 in MDSCs. Preliminary data showed no cells co-expressing COX-2 and Arg-1 (**Fig. 7**).

Inflammatory cells from infected cardiac tissue but not *T. cruzi* produce PGE_2 and $PGF_{2\alpha}$

In order to identify the arachidonic acid (AA) derivatives produced by the infiltrating myeloid cells of the infected hearts, a

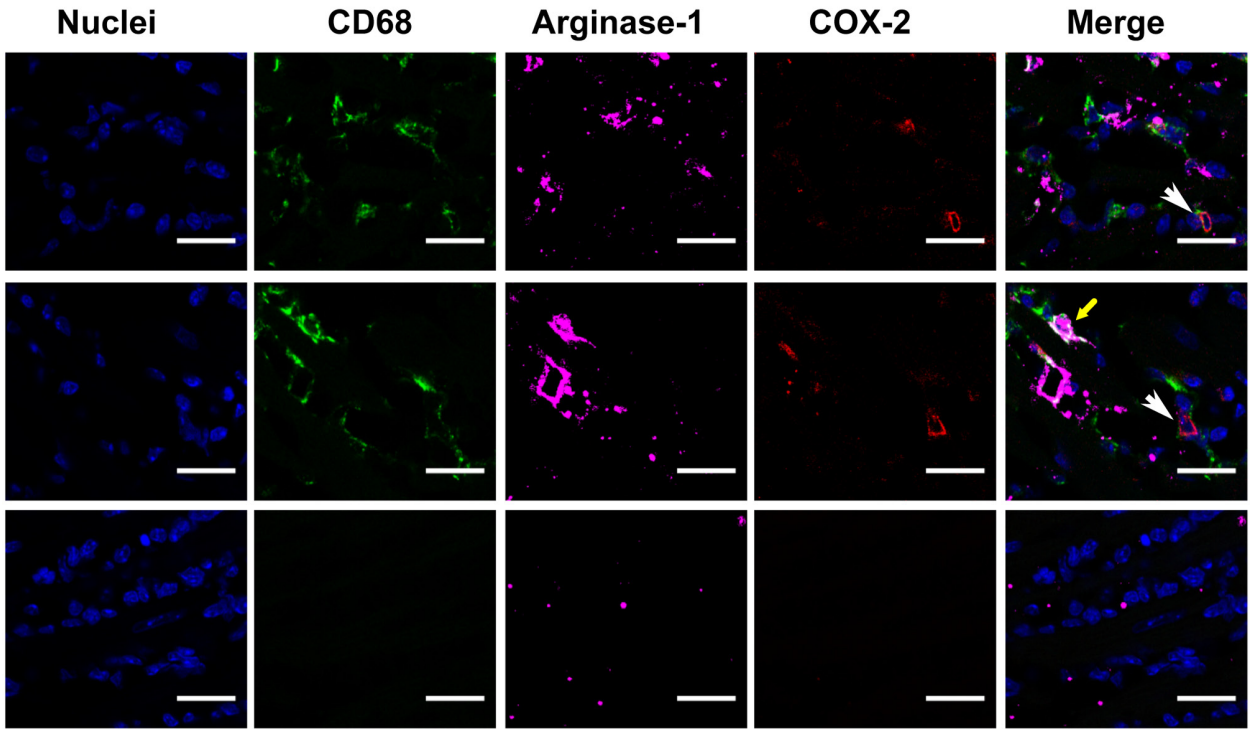

Figure 7 | COX-2 is not expressed by CD68$^+$Arg-1$^+$ cells in *T. cruzi* infected cardiac tissue. Heart tissue was isolated at 21 d.p.i. from infected or non-infected BALB/c mice and frozen in OCT. Section of organs were stained with DAPI for **nuclei (blue)** and antibodies against the macrophage marker **CD68 (green)** and the enzymes **Arg-1 (magenta)** and **COX-2 (red)**. Colocalization of CD68 and Arg-1 results in white color (combination of green and magenta). Upper and middle rows of panels show different pictures of infected cardiac tissue. The yellow arrow indicates an Arg-1 expressing CD68$^+$ cell. White arrows indicate COX-2 expressing cells. Lower row of panel shows the secondary antibody control using infected tissue. Scale bar is 20 microns length. Pictures are representative of several sections analyzed in one experiment.

metabolic assay was performed. LY6G$^+$ and Ly6G$^-$ CD11b$^+$ magnetically purified cells were cultured in the presence of radiolabeled AA. Radioactive PGE_2 and $PGF_{2\alpha}$, but not thromboxane or PGD_2, were present in the supernatants of Ly6G$^-$ CD11b$^+$ cells, but not in Ly6G$^+$ cells (**Fig. 8**). This experiment indicates that the Ly6G$^-$ CD11b$^+$ population is able to synthesize these two prostaglandins from AA without the collaboration of other cell type. Next, we analyzed the production of AA derivative in cells from peritoneal lavages of infected animals. It is known that different stimuli induce macrophage infiltration in the peritoneum (Ghosn et al., 2010). We expected to find macrophages in the peritoneal cavity of *T. cruzi* infected animals because is the route chosen for parasite injection. We found that peritoneal adherent cells from *T. cruzi* infected BALB/c mice are able to convert exogenous AA into PGE_2 (**Fig. 9A**). To further study this, we sorted the peritoneal cells with an antibody against CD11b antigen coupled to magnetic beads. Peritoneal CD11b$^+$ cells from

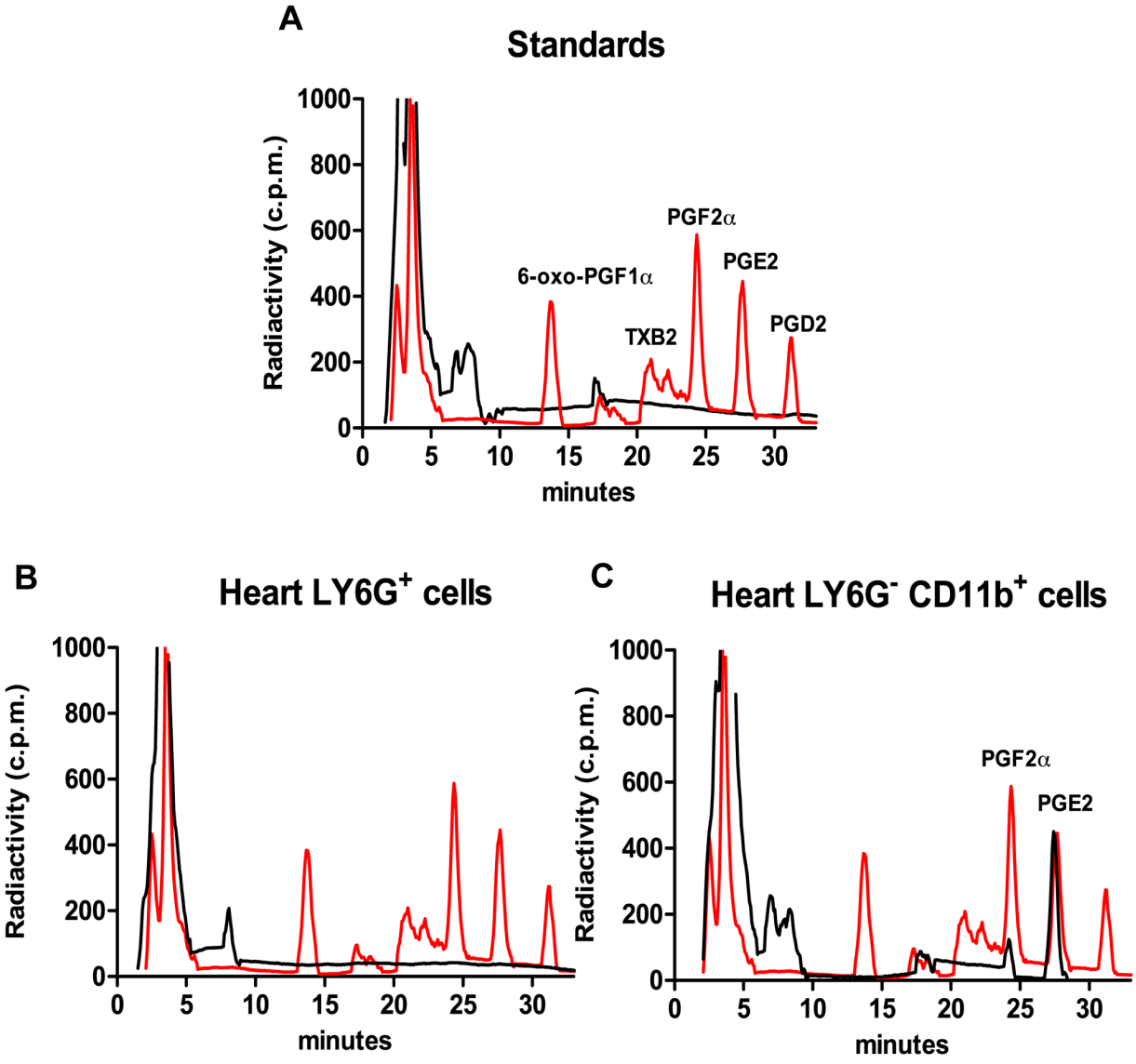

Figure 8 | Cardiac infiltrating myeloid cells metabolyze arachidonic acid into PGE2 and PGF2α. Leukocytes were purified from cardiac tissue of BALB/c mice at 21 d.p.i., Ly6G$^+$ and Ly6G$^-$Cd11b$^+$ cells were sorted magnetically and incubated with 25μM radioactive arachidonic acid. Samples were resolved using HPLC as described in Materials and Methods. Black solid lines represent samples in hematin-containing buffer and red solid line represents the overlaid standards. **A** | Input without cells. **B** | Ly6G$^+$ cells. **C** | Ly6G$^-$CD11b$^+$ cells. Data from one experiment out of two performed is shown.

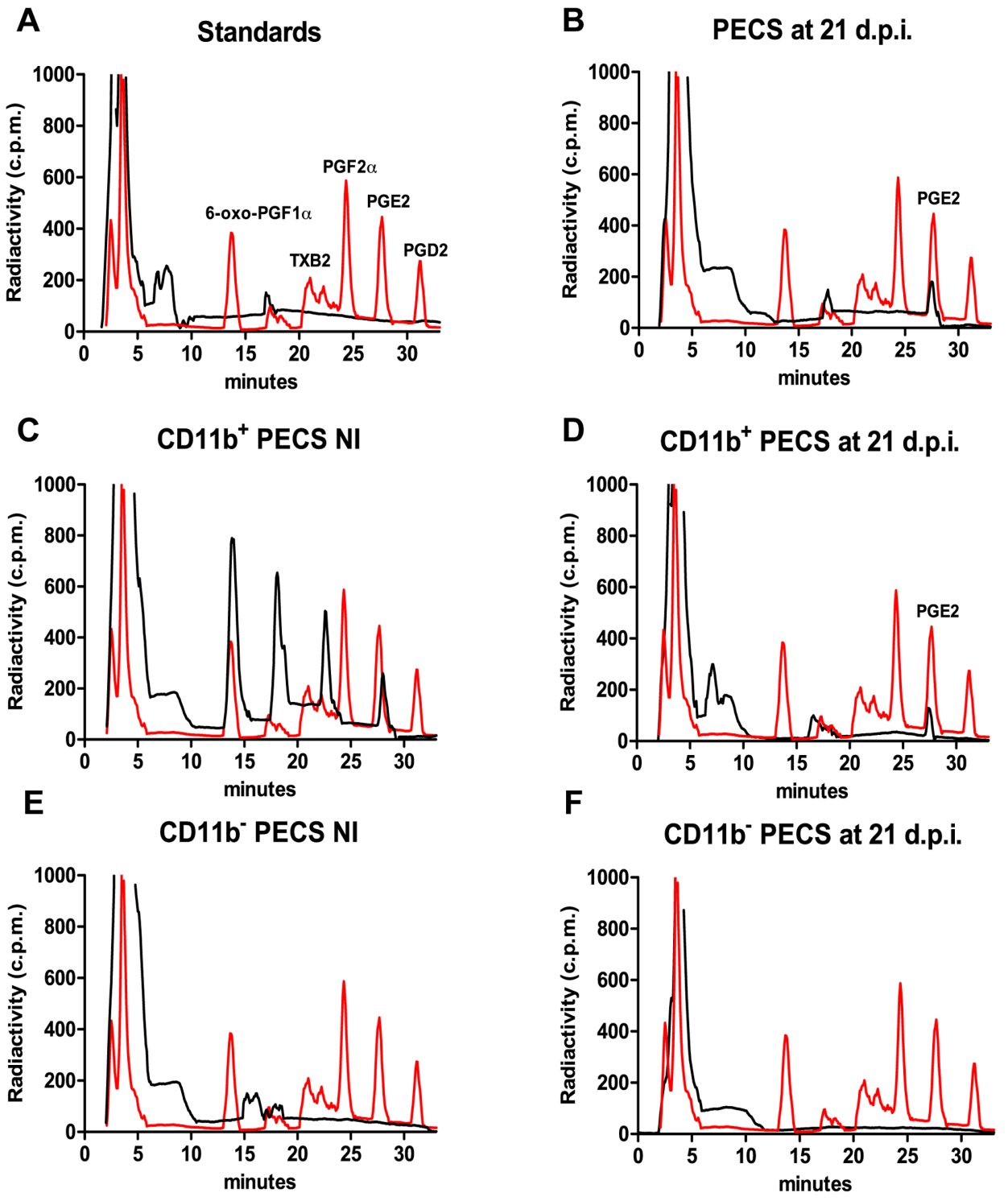

Figure 9 | AA metabolism of peritoneal CD11b⁺ cells from mice infected with *Trypanosoma cruzi*. Leukocytes were obtained from the peritoneal cavity (PECS) of non-infected and infected BALB/c mice at 21 d.p.i by peritoneal lavage. CD11b⁺ cells were magnetically sorted using a specific antibody against CD11b and incubated with radioactive AA. The samples were resolved using HPLC. Black solid line represents samples injected in hematin-containing buffer. Red solid line represents the overlaid standards. **A** | Input without cells. **B** | Total PECS. **C** | CD11b⁺ cells from non-infected mice. **D** | CD11b⁺ cells from infected mice. **E** | CD11b⁻ cells from non-infected mice. **F** | CD11b⁻ cells from infected mice. A representative experiment out of two performed is shown.

not infected animals were able to convert AA in different metabolites (**Fig. 9C**) but interestingly peritoneal CD11b$^+$ from infected animals only produced PGE_2 (**Fig. 9D**). Neither infected nor control CD11b$^-$ cells (**Fig. 9E and 9F**) were able to produce PGE_2. This result suggests that macrophages are a primary source of PGE_2 in different tissues during the acute phase of *T. cruzi* infection.

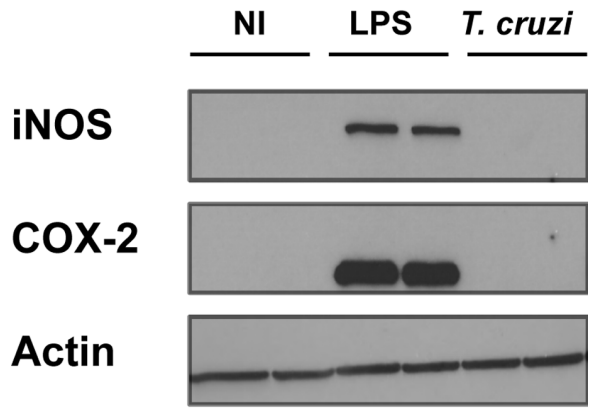

Figure 10 | iNOS and COX-2 protein expression of an *in vitro T. cruzi infected* macrophage cell line. RAW cells were incubated overnight or not with LPS (1 µg/ml) or parasites. Total protein extracts were resolved in duplicate by SDS-PAGE and transferred to a nitrocellulose membrane. The presence of the proteins was detected using specific antibodies. Anti-actin antibody was used as a loading control. A representative experiment out of three is shown.

To clarify whether the production of prostaglandins is due only to the monocyte/macrophage CD11b$^+$ cells, we performed an *in vitro* infection of macrophages. RAW 264.7 cells (a murine macrophage cell line) were infected with purified *T. cruzi* cultured trypomastigotes. **Figure 10** shows that no COX-2 neither iNOS protein expression was detected in infected cells. However, LPS stimulated the expression of both enzymes in RAW 264.7 cells. RAW 264.7 cells produced PGD_2 without stimulation other than culture in the cell plate (**Fig. 11B**). This macrophage cell line metabolized AA into $PGF_{2\alpha}$, PGE_2 and PGD_2 upon stimulation with LPS and IFN-γ (**Fig. 11C**). In fact, preferential PGD_2 over PGE_2 secretion by stimulated RAW 264.7 cell has been described (Cao et al., 2008). However, *T. cruzi* infection did not change the pattern of exogenous AA derivative production by RAW 264.7 cells. (**Fig. 11D**). These data suggest that *T.cruzi* alone is unable to induce COX-2 induction in macrophage cell type.

In vitro production of AA derivatives by *Trypanosoma cruzi* has been previously reported (Kubata et al., 2002)(Ashton et al., 2007). To determine the role of the parasite on AA conversion, we performed similar experiments as described by Ashton et al (Ashton et al., 2007). We used different vital forms of the parasite: axenic epimastigotes, tripomastigotes alone or mixed with amastigotes from *in vitro* infection of fibroblasts. In order to reproduce the protocols used before by others we added hematin. Besides, similar reactions were performed simultaneously in iron-free buffer. No eicosanoids were detected when AA was incubated alone in the iron containing buffer (**Fig. 12A**). Living or homogenized parasites of three different parasite strains were used in these experiments. None of them produced any known prostaglandin or thromboxane when AA was added exogenously without iron in the culture medium (**Fig. 12B-C**). Interestingly, two radioactive peaks appeared at minutes 12 and 32 of the HPLC run. The first AA derivative eluted had approximately the same elution time as 6-oxo-$PGF1_\alpha$, the main metabolite of prostacyclin. The second one did not elute at the time of any of the standards used. However, since production of AA derivatives was iron-dependent, we can conclude that *T. cruzi* parasites alone cannot generate derivatives

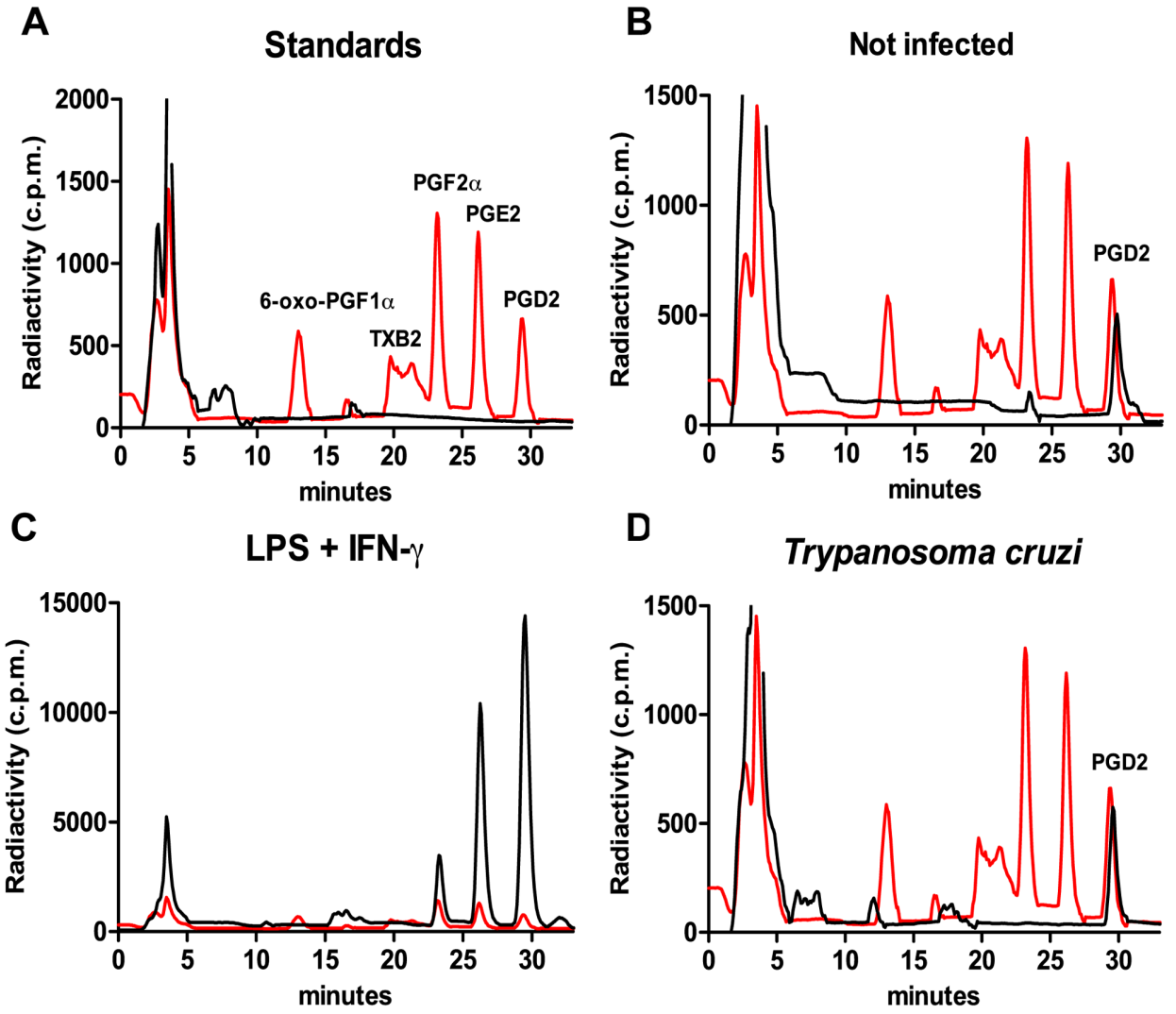

Figure 11 | Arachidonic acid metabolism of *in vitro* infected macrophages. RAW cells were incubated or not with LPS + IFN-γ or infected or non-infected with parasites 5:1 M.O.I. (multiplicity of infection) and 25μM radioactive AA was added. Samples were resolved using HPLC. Solid line represents the injected mock-incubated AA. Red line represents superimposed standards **A** | AA input. **B** | Non-infected cells. **C** | LPS and IFN-γ stimulated cells. **D** | *T. cruzi* infected cells. A representative experiment out of three performed is shown.

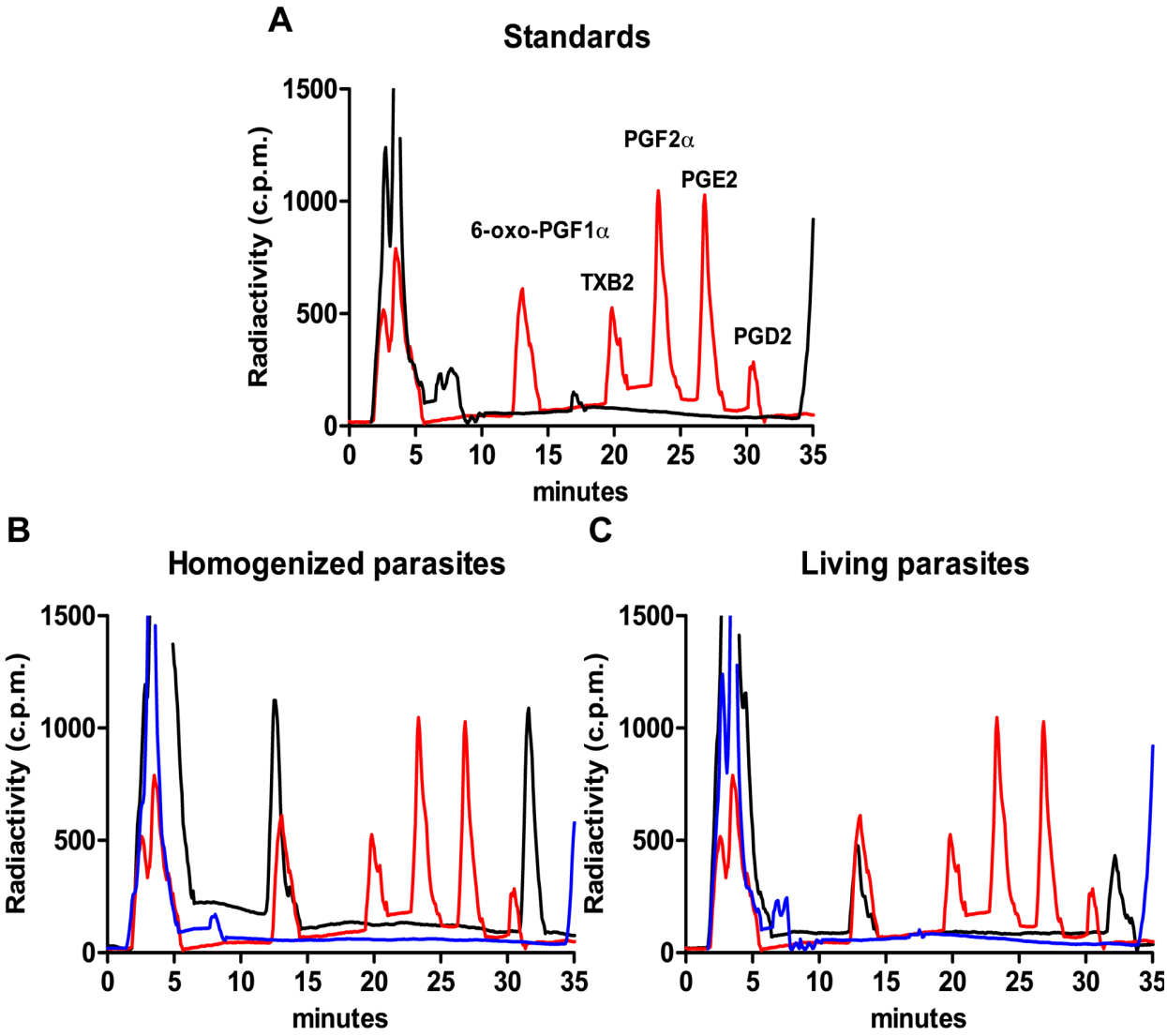

Figure 12 | Arachidonic acid metabolism of *Trypanosoma cruzi* culture parasites. $10x10^8$ living or $15x10^8$ homogenized parasites were incubated with 75μM radioactive AA. The samples were resolved using HPLC as described in Materials and Methods. Black solid lines represent the injected samples in hematin containing buffer. Red solid line represents the superimposed standards. Blue lines represent the injected sample in hematin-free buffer. **A** | AA Input. **B** | Homogenized parasites. **C** | Living parasites. Similar results were obtained when trypomastigotes or trypomastigotes mixed with amastigotes were used. This experiment was performed with three different *T. cruzi* strains (Y, Dm28 and CL-Brener) three times. A representative experiment performed with Y strain is shown.

from AA. To elucidate if parasites efficiently incorporated AA we added radioactive material to the culture and separated the cells from the supernatant by centrifugation. As expected, parasites incorporated radioactive AA into the cells (**Fig. 13**).

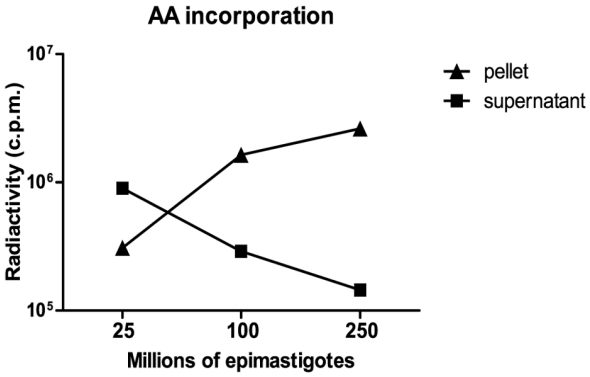

Figure 13 | *Trypanosoma cruzi* incorporation of exogenous arachidonic assay. 25μM radioactive AA was added to different numbers of parasite, incubated, centrifuged and then radioactivity in the pellet and the supernatant was measured in a scintillation counter. The experiment was performed in Y and Dm28 *T. cruzi* strains with similar results. Results for the Dm28 strain experiment are shown.

12/15-Lipoxygenase expression is augmented during *T. cruzi* infection in cardiac tissue

We found that *Alox15* gene was up-regulated during *T. cruzi* infection in the heart, as described before (**Fig. 2F**). We confirmed that the expression of this enzyme was IL-4 dependent as shown by strong reduction when IL-4 receptor deficient mouse were infected (**Fig. 14**). In accordance with a study using a different experimental model (Brinckmann and Kuhn, 1997), the presence of 12/15-Lipoxygenase (12/15-LO) was confirmed by confocal microscopy using the antibody provided by H. Kühn (Dioszeghy et al., 2008). Kayama and collaborators have described a role of cardiomyocyte-expressing 12/15 LO in cardiac failure (Kayama et al., 2009). However, 12/15-LO expression in cardiomyocytes was not observed in *T. cruzi* infected hearts. Rather it seemed to be expressed by inflammatory cells (**Fig. 15**). Next, we tried to characterize the cellular source of 12/15-LO using antibodies to recognize macrophages and fibroblasts. These cells are implied in tissue repair (Lambert et al., 2008; Souders et al., 2009; van den Borne et al.). On the other hand, 12/15-LO expression by these cells is related to wound healing (Gronert et al., 2005). Hence, we used macrophage (CD68) and fibroblast (Vimentin) markers trying to identify 12/15-LO expressing cells. However, 12/15-LO protein was neither found in CD68 nor in vimentin positive cells (**Fig. 16B-C**). Surprisingly, we also detected vimentin staining the parasites indicating a possible surface deposition (**Fig. 16C**). Thus, no cellular 12/15-LO source could be clearly identified in the infected hearts.

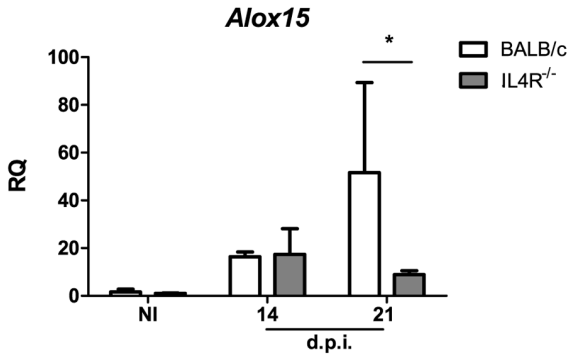

Figure 14 | Expression of 12/15 LO mRNA in cardiac tissue of wild-type and IL-4 receptor deficient mice infected with *Trypanosoma cruzi*. Heart tissue RNA was isolated at different days post infection (d.p.i.) and qPCR was performed.Results are expressed as RQ calculated from CT values as described in Materials and Methods. Open bars indicate the values of BALB/c mice and grey filled bars of IL4-receptor deficient mice. Means ± SD from a representative experiment out of two are shown (n=3). Differences between wild-type and IL-4R$^{-/-}$ mice are indicated with * $p<0.05$.

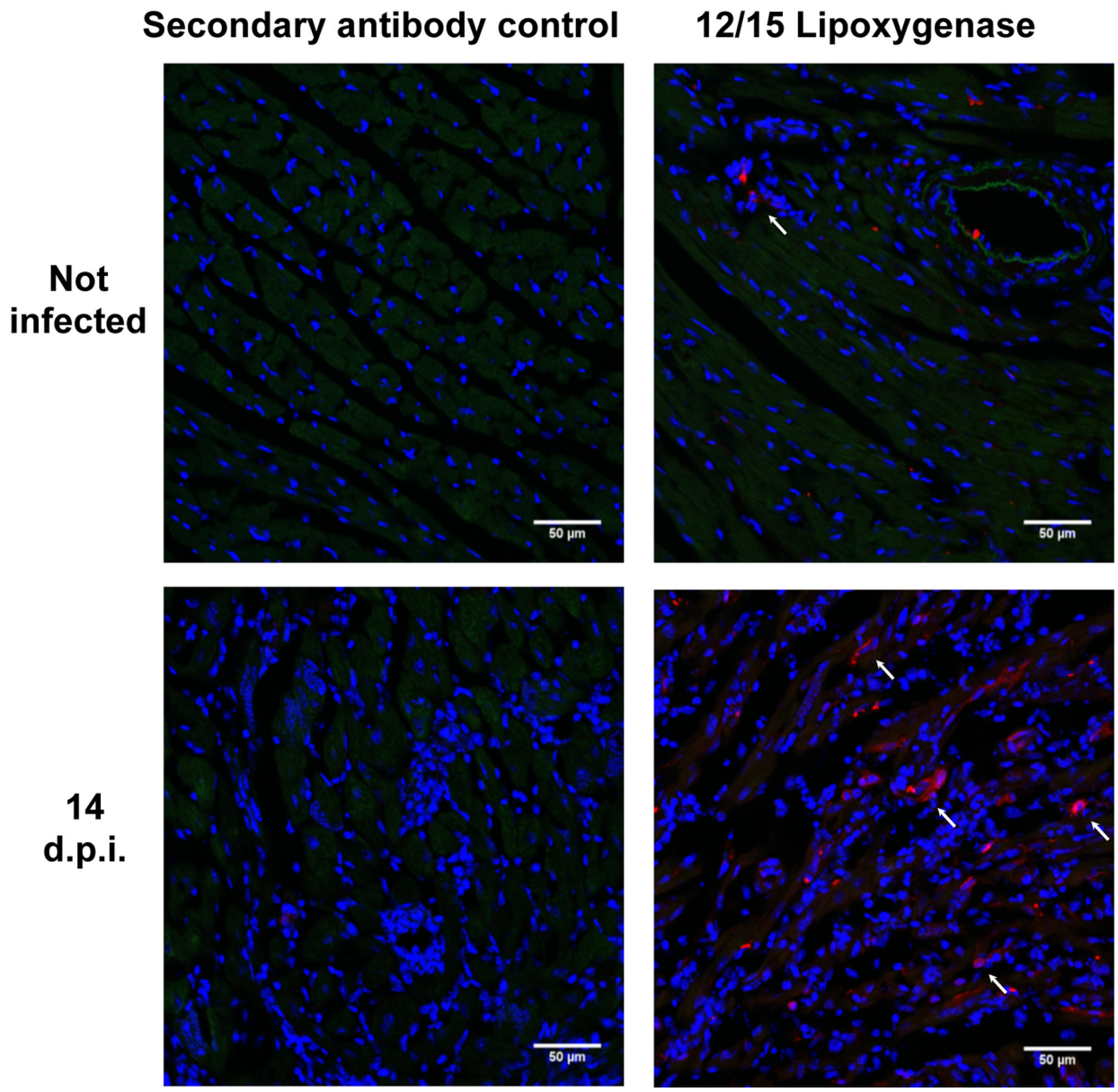

Figure 15 | 12/15-LO expression is augmented during *T. cruzi* infection in cardiac tissue. Hearts were isolated at 21 d.p.i. from infected or non-infected BALB/c mice and frozen in OCT. Sections of organs were stained with DAPI for **nuclei (blue)** and antibodies against **12/15-LO (red)**. The green background signal is due to autofluorescence. Scale bar is 50 microns length. Pictures are representative of several sections analyzed in at least 3 different mice from three different infections. Arrows indicate 12/15-LO positive cells. Similar results were obtained using the C57BL/6 mouse strain.

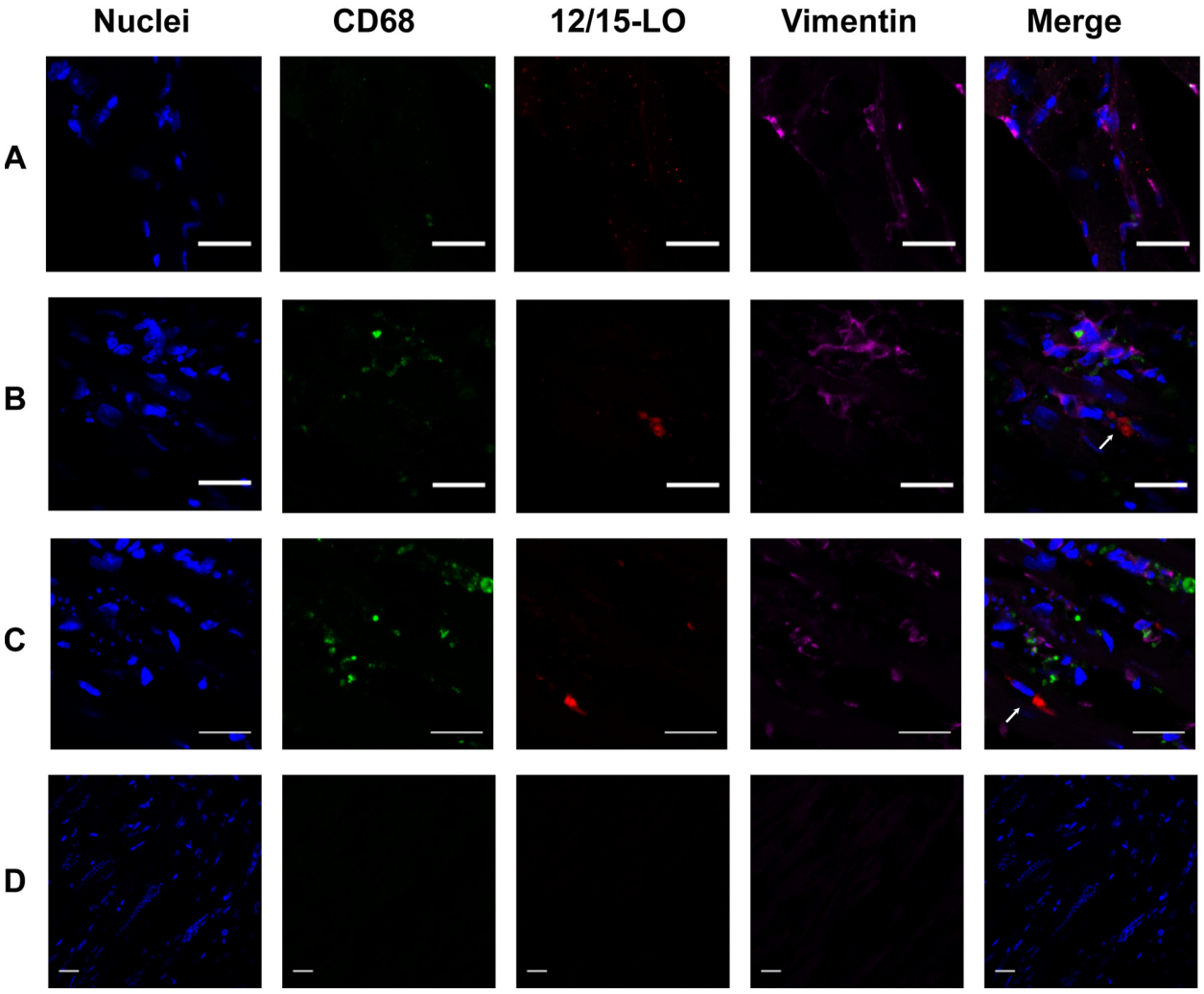

Figure 16 | 12/15-LO is not expressed by infiltrating macrophages nor fibroblasts in *Trypanosoma cruzi* infected cardiac tissue. Hearts were isolated at 14 d.p.i. from infected or non-infected BALB/c mice and frozen in OCT. Section of organs were stained with DAPI for **nuclei (blue)** and antibodies for the macrophage marker **CD68 (green)**, the enzyme **12/15-LO (red)** or the intermediate filament cytoskeleton protein present in fibroblast, **vimentin (magenta)**. Different channels and merge of the same sections are shown. **A** | Upper row represent non-infected stained tissue. **B-C** | Two different micrograph from inflammatory loci of *T. cruzi* infected mice **D** | Secondary antibody control using tissue from non-infected mice Scale bar is 20 microns length. Arrows indicate 12/15-LO positive cells. Pictures are representative of several sections analyzed in at least 3 different mice from at least two different infections.

Role of Cyclooxygenase-2 and PGE_2 in *Trypanosoma cruzi* infected heart

The increase in COX-2 protein expression in infiltrating macrophages and the production of prostaglandins by these cells *ex vivo* suggested that cyclooxygenase may play a pivotal role in initiation, maintenance and resolution of the immune response upon infection. To confirm this, we have used pharmacological inhibition as well as genetically deficient mice for cyclooxygenase-2 and for Prostaglandin E receptor-2. Deficient and treated animals were infected in a similar manner that wild-type mice. Then, immunological and parasitological parameters were measured over infection.

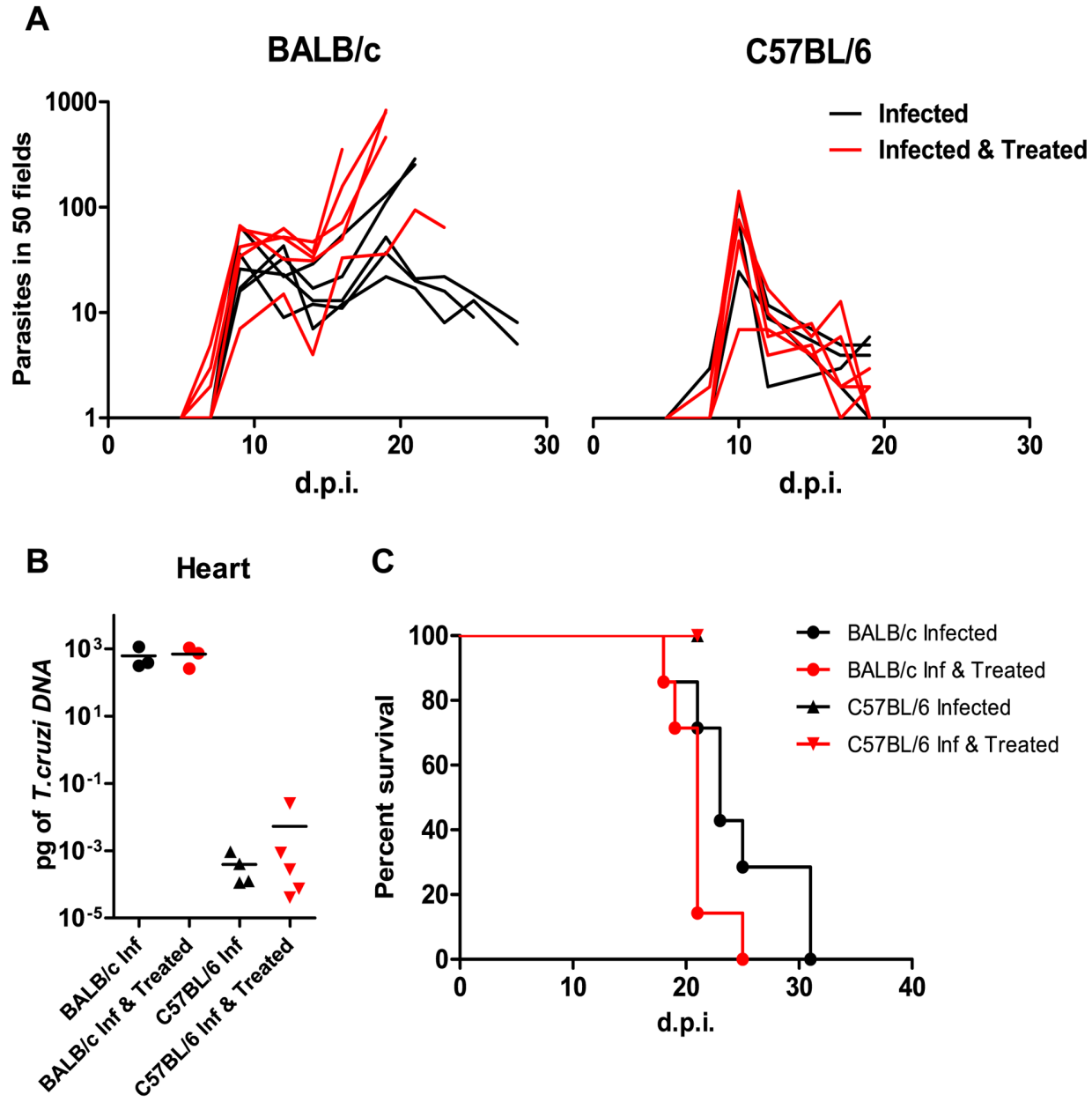

Figure 17 | Effect of inhibition of COX-2 by etoricoxib treatment in *T. cruzi* infected mice. Groups of *T. cruzi* infected mice were treated or not with etoricoxib. Mice survival was monitored daily after infection and parasitemia was checked every 2 or 3 days. Black lines and solid symbols represent data from infected individual mice and red lines and solid symbols represent data from infected and etoricoxib treated mice (n=5). **A |** Parasitemia of BALB/c (left graph) and C57BL/6 (right graph) mice. **B |** DNA from heart tissue was isolated at 21 d.p.i. and qPCR using *T. cruzi* DNA standard was performed (n=3 non-treated mice and n=5 treated mice). **C |** Percent of survival. Gehan-Breslow-Wilcoxon test between BALB/c infected and BALB/c Infected & Treated groups give a p value of 0,0981 (n= 7). Data from a representative experiment are shown.

Pharmacological inhibition of COX-2

COX-2 inhibition slightly decreased survival in the susceptible model of infection.

Both BALB/c and C57BL/6 mice were infected intraperitoneally with 2.000 blood trypomastigotes of *T. cruzi*. Parasitemia and survival was measured over time. COX-2 specific inhibitor Etoricoxib was administered in drinking water as explained in Material and Methods. Mice were sacrificed at maximum of

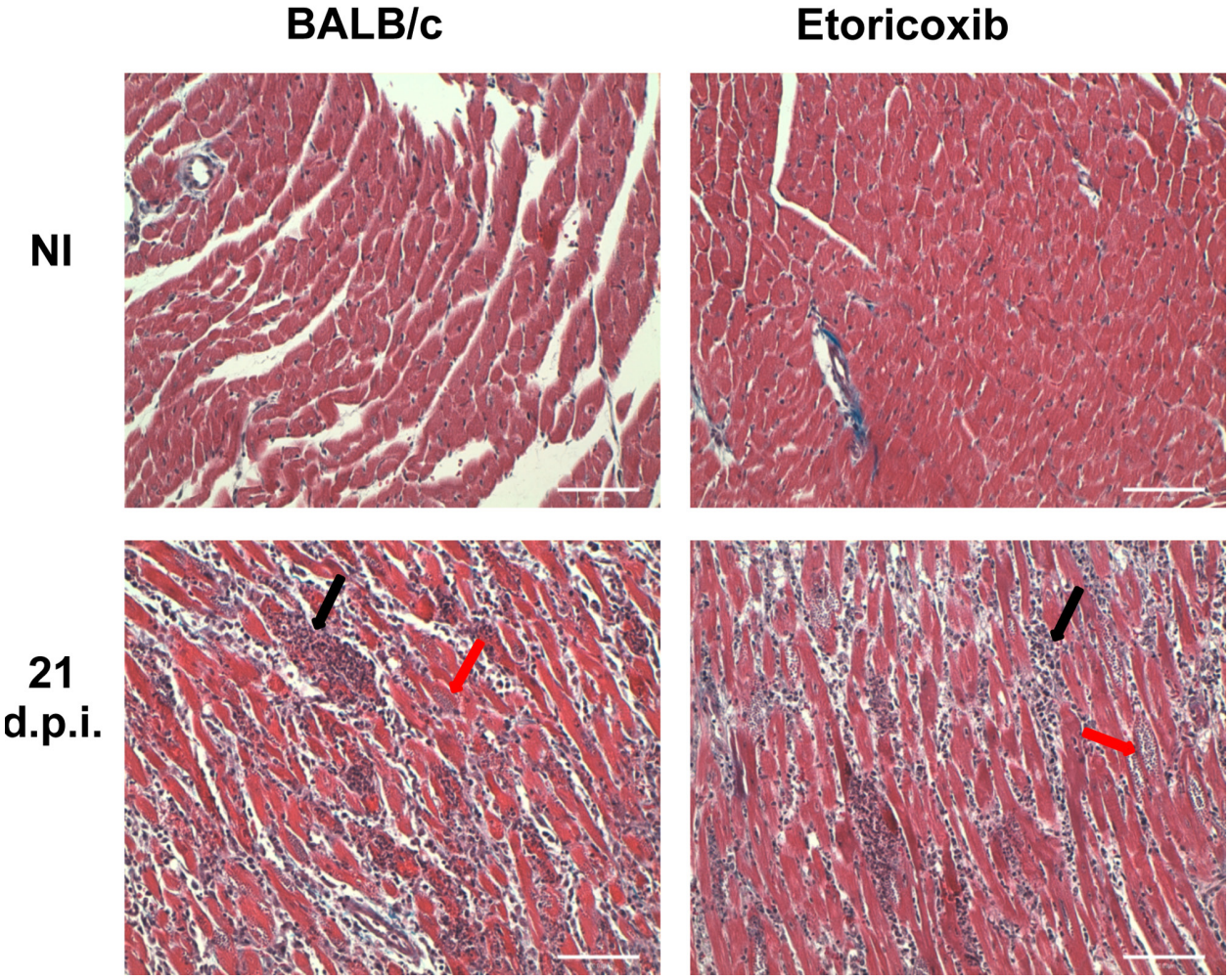

Figure 18 | Histologic analysis of cardiac tissue of BALB/c mice during *Trypanosoma cruzi* infection treated with the COX-2 specific inhibitor etoricoxib. At 21 d.p.i. heart tissue was processed for Masson`s Trichromic staining and micrograph were taken as described in Materials and Methods. Representative pictures of each group were selected. Black arrow shows the infiltrating leukocytes and red arrow indicates parasite nests. Scale bar is 100 microns length.

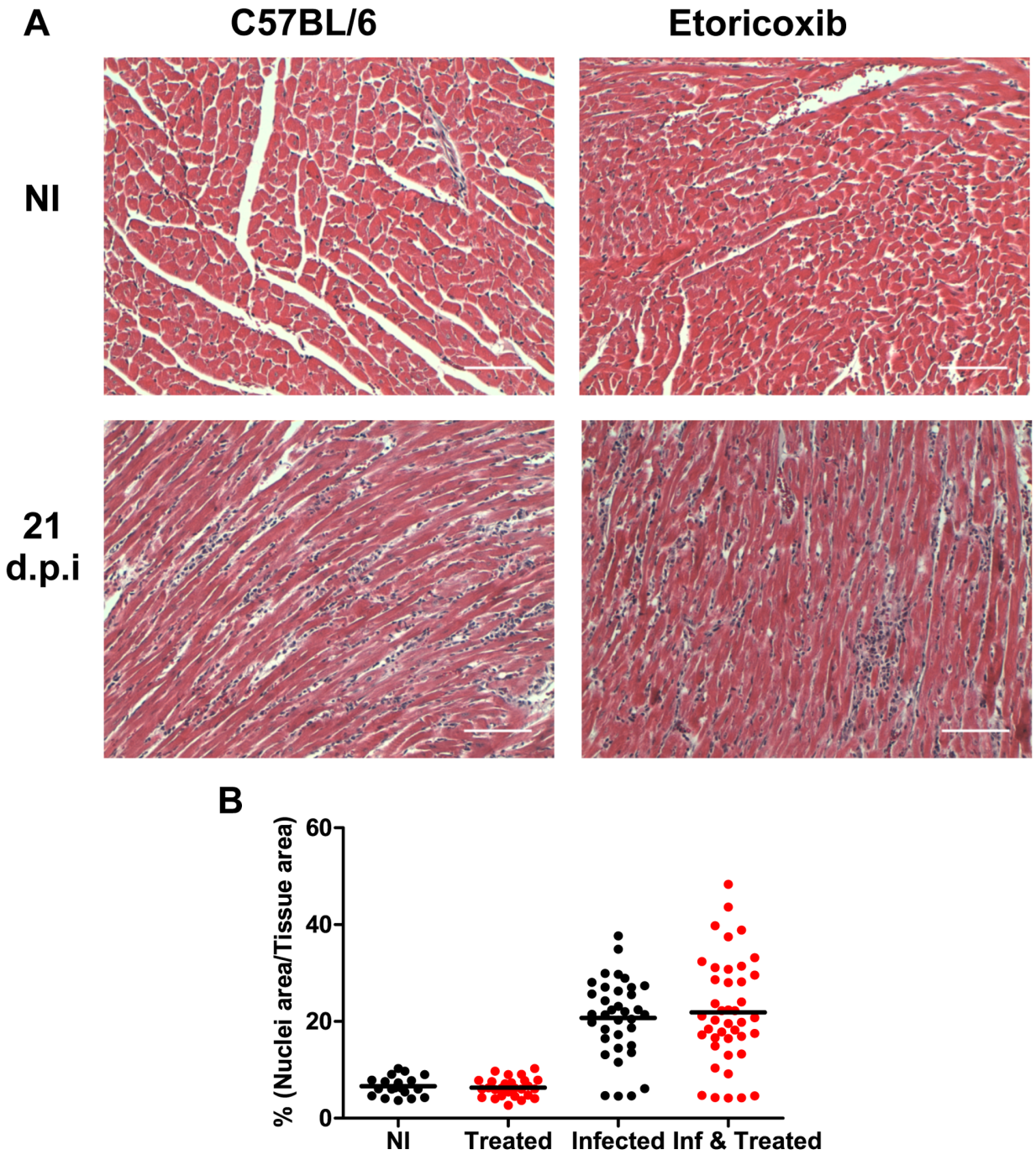

Figure 19 | Histologic analysis of cardiac tissue of C57BL/6 mice treated with the COX-2 specific inhibitor etoricoxib during *Trypanosoma cruzi* infection. At 21 d.p.i. heart tissue was processed for Masson`s Trichromic staining and micrograph were taken as described in Materials and Methods. **A |** Representative pictures of each group were selected. Black arrow shows the infiltrating leukocytes and red arrow indicates a parasite nest. Scale bar is 100 microns length. **B |** Graph showing the quantification of cell infiltration using FIJI software. Not significant changes were observed. Dot plot and means from one experiment are shown (n=4).

cardiac inflammation, 14 d.p.i for C57BL/6 and 21 d.p.i. for BALBc and heart tissue was collected. Etoricoxib treatment exacerbated parasitemia and reduced survival of BALB/c mice but did not change parasitemia or survival of C57BL/6 mice during the acute phase of *T. cruzi* infection. However, heart parasite burden was unaltered (**Fig. 17**). These results indicate that COX-2 inhibition in the BALB/c model increases mice susceptibility in spite of no changes in parasite load in cardiac tissue.

Cardiac inflammation is not altered in treated animals

We next analysed by histology cardiac inflammation in the infected hearts. High leukocyte infiltration and parasite nests were found in BALB/c mice treated or not with the COX-2 inhibitor. Due to the high degree of inflammation, we were not able to quantify cardiac infiltration. However, microscopic examination showed no differences between groups (**Fig. 18**). C57BL/6 model at 14 d.p.i.

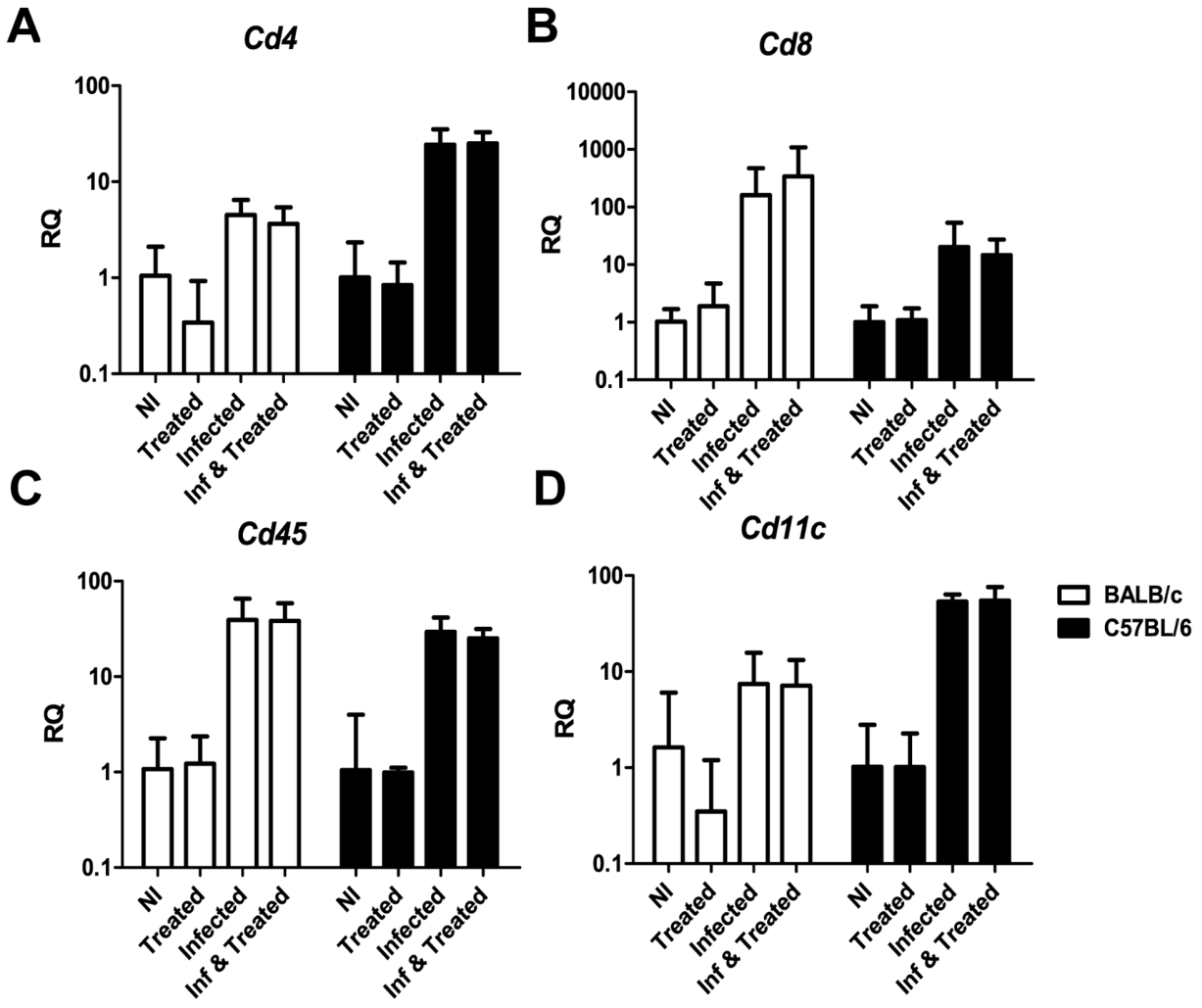

Figure 21 | Expression of cytokines, chemokines and enzymes of L-arginine metabolism related enzymes in the heart of *Trypanosoma cruzi* infected mice treated with the COX-2 specific inhibitor etoricoxib. Heart tissue RNA was isolated at 21 d.p.i. from infected, infected and treated or non-infected BALB/c (open bars) and C57BL/6 (filled bars) mice. Citokine, chemokine and enzyme gene expression was analysed by quantitative PCR with different probes: **A** | *Ifng*, **B** | *Il10*, **C** | *Il6*, **D** | *Ccl2*, **E** | *Ccl5*, **F** | *Cxcl9*, **G** | *Arg1* and **H** | *Nos2*. Not significant changes with the inhibitor treatment were observed. But the differences between infected and non-infected groups were significant. Means ± SD from a representative experiment is shown (n=3 for BALB/c and n=5 for C57BL/6 mice).

showed less inflammation than BALB/c at 21 d.p.i. (**Fig. 19A**) and inflammation was quantified using the FIJI software. No changes between treated and not treated groups were observed (**Fig. 19B**). Thus, treatment with a COX-2 specific inhibitor does not prevent cardiac cell infiltration during the acute phase of *T. cruzi* infection.

Next, we studied the expression of several genes involved in the immune response against *T. cruzi* infection. Infected animals at 14 or 21 d.p.i were compared to their non-infected controls. In agreement with our previous results no changes in immune cell surface receptor expression was observed upon COX-2 inhibitor treatment (**Fig. 20**). In addition, we studied the expression of several genes that

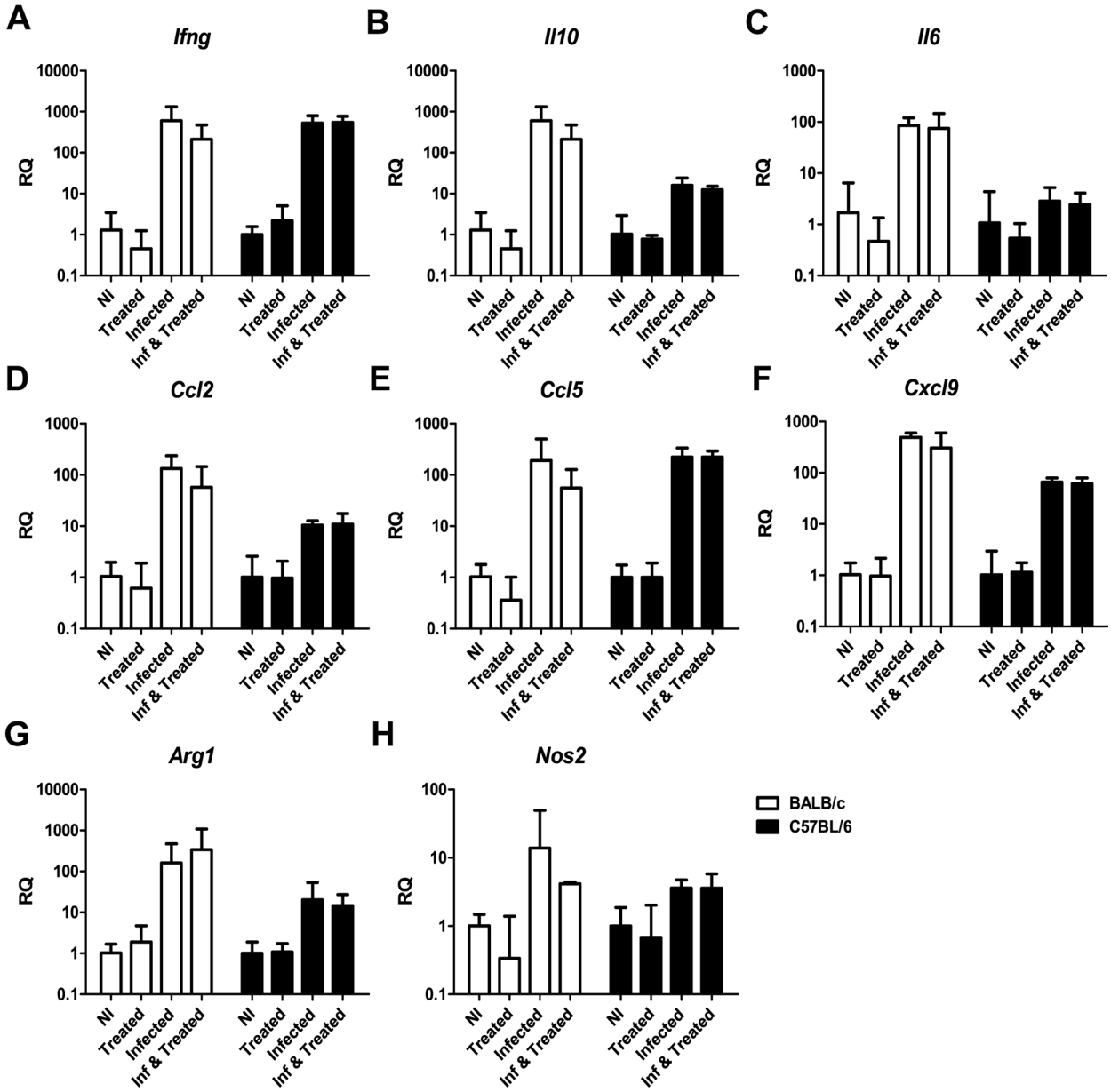

Figure 22 | Parasite burden in *Trypanosoma cruzi* infected wild-type and COX-2$^{-/-}$ mice. Wild-type (open circles and bars) and COX-2$^{-/-}$ (filled circles and bars) mice were infected with *T. cruzi* intraperitoneally. **A |** Parasitemia checked every 2 days. Means ± SD are shown. **B |** DNA from heart tissue was isolated at 7, 14 and 21 d.p.i. and *T. cruzi* specific qPCR with was performed. Representative means ± SD from at least three experiments are shown (n=4, for wild-type and COX-2$^{-/-}$mice). Difference at the peak of parasitemia is significant * p< 0,05.

have previously been related to *T. cruzi*-induced immune response. The expression of cytokines (*Ifng, Il10, Il6*), chemokines (*Ccl2, Ccl3* and *Cxcl9*) and the enzymes *Arg1* and *Nos2* were increased during *T. cruzi* infection but no changes were observed with Etoricoxib treatment. These results indicate the lack of effect in cardiac immune response due to COX-2 inhibition (**Fig. 21**).

Genetic deletion of Cycloxygenase-2

COX-2 deficient mice show less parasitemia but no changes in heart parasite burden

Both wild-type and COX-2 deficient mice were infected intraperitoneally with 2000 blood trypomastigotes of *T. cruzi*. Parasitemia and survival was measured over time. COX-2 deficient mice showed three times less parasitemia than wild-type infected controls at the peak of parasitemia (**Fig. 22A**). However, COX-2 deficiency did not affect cardiac parasite burden in infected mice, indicating that changes in parasitemia were not relevant for the outcome of the disease (**Fig. 22B**). Previous studies in the laboratory with different mouse models of infection, lead us to think that only big changes (at least more than 5 times) in parasitemia may influence the outcome of the disease. No wild-type nor COX-2$^{-/-}$ infected mice died during the experiments that last until 8 weeks in some cases, even when 20.000 trypomastigotes were injected (**Not shown**). These parasitological data indicates that COX-2$^{-/-}$ and wild type (C57BL/6-129Sv) mice are resistant models of infection.

Anti *T. cruzi*-specific antibody production is not altered in COX-2$^{-/-}$ infected mice

IL-4 enhances the production of IgG1. But IFN-γ was shown to stimulate the secretion of IgG2a in concentrations at which it inhibits IL-4 induced production of IgG1 (Coffman et al., 1989). Since serum IgG1/IgG2a balance is related to the Th2/Th1cytokine balance, we determined anti-*T.cruzi* IgG1, IgG2a and total IgG levels throughout acute infection by ELISA. As shown in **Fig. 23**, the antibody level was similar in the two strains of mice over time, independently of COX-2 expression. These

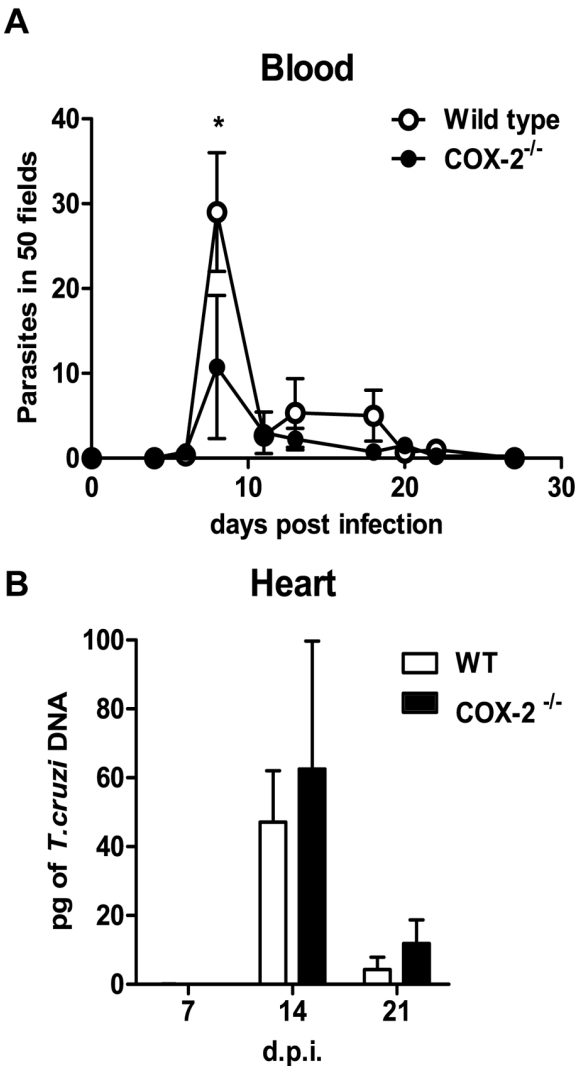

Figure 22 | Parasite burden in *Trypanosoma cruzi* infected wild-type and COX-2$^{-/-}$ mice. Wild-type (open circles and bars) and COX-2$^{-/-}$ (filled circles and bars) mice were infected with *T. cruzi* intraperitoneally. **A** | Parasitemia checked every 2 days. Means ± SD are shown. **B** | DNA from heart tissue was isolated at 7, 14 and 21 d.p.i. and *T. cruzi* specific qPCR with was performed. Representative means ± SD from at least three experiments are shown (n=4, for wild-type and COX-2$^{-/-}$mice). Difference at the peak of parasitemia is significant * p< 0,05.

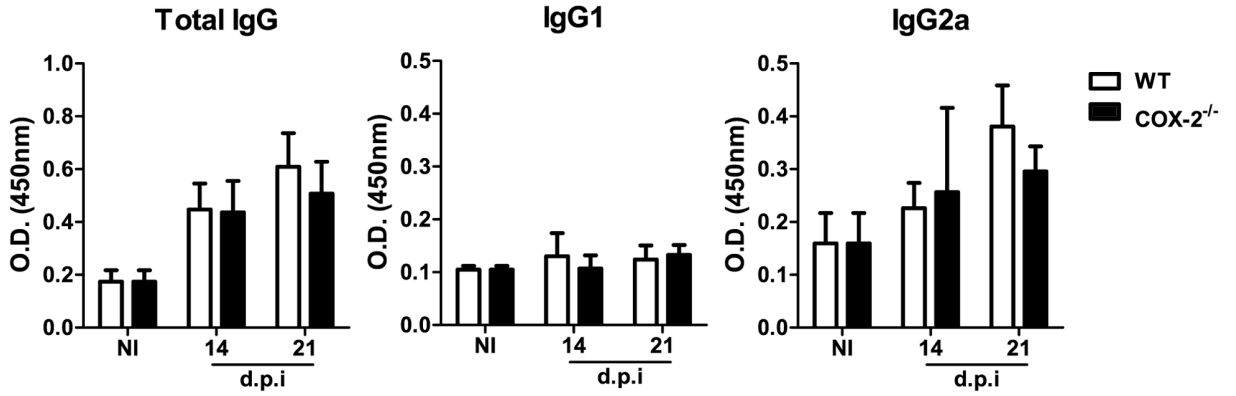

Figure 23 | Plasma antibodies against *Trypanosoma cruzi* during acute phase in COX-2 deficient mice. Blood was obtained by cardiac puncture from infected or non-infected mice and plasma was isolated. The ELISA was performed coating the plate with *T. cruzi* extracts from culture as described in Materials and methods. Means ± SD from two experiments of are shown (n=6, for wild-type and COX-2$^{-/-}$ mice).

results indirectly indicated that deletion of COX-2 gene expression did not alter the Th1/Th2 systemic balance during infection.

Macrophages of COX-2 deficient mice present less lipid bodies than wild-type upon *T. cruzi* infection

It has been previously described that during *T. cruzi* infection macrophages increase the production of lipid bodies. These cellular organelles are one of the prostaglandin production sites identified (D'Avila et al., 2011). We have analyzed the presence of lipid bodies using Oil Red-O staining in infected heart sections and visualized the results by confocal microscopy. We observed that lipid bodies were less in number and smaller in size in cardiac infiltrating macrophages of COX-2 deficient mice than in wild-type mice (**Fig. 24**). Unfortunately, we were not able to quantify the signal due the background of the dye.

Cardiac inflammation is reduced in COX-2$^{-/-}$ mice

Staining of *T. cruzi* infected heart sections from COX-2$^{-/-}$ mice showed less inflammatory infiltrates at 14 and 21 d.p.i. than in wild-type mice (**Fig. 25A**). Infiltration was quantified from images using the FIJI software and the differences of cell infiltration between COX-2$^{-/-}$ and wild-type mice were confirmed (**Fig. 25B**).

In order to analyse the characteristics of the infiltrating cells, gene expression was quantified by RT-PCR and infected animals were compared to their non-infected controls. This would provide information about the nature of COX-2$^{-/-}$ cardiac inflammation and immune

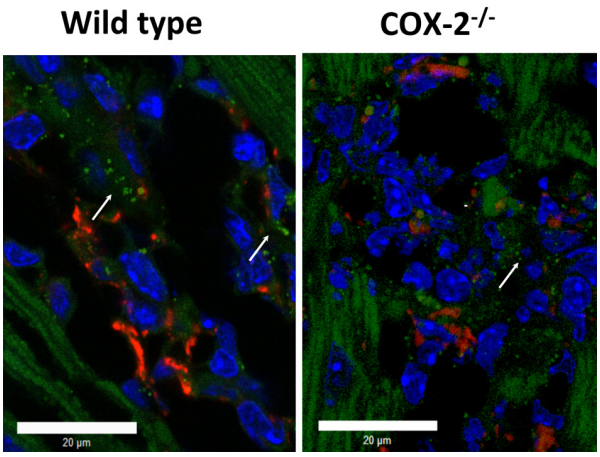

Figure 24 | Lipid bodies formation within inflammatory cells in hearts of wild-type and COX-2 deficient mice Heart tissue was isolated at 14 d.p.i. from infected wild-type or COX-2 deficient mice and frozen in OCT. Sections of organs were stained with DAPI for **nuclei (blue)** and antibodies for the macrophage marker **CD68 (red)** and Oil Red O (ORO) for **lipid bodies (green)**. ORO also slightly stains muscle fibres. White arrows indicate the presence of lipid bodies. Representative images from 3 animals per group are shown. Scale bar is 20 microns length.

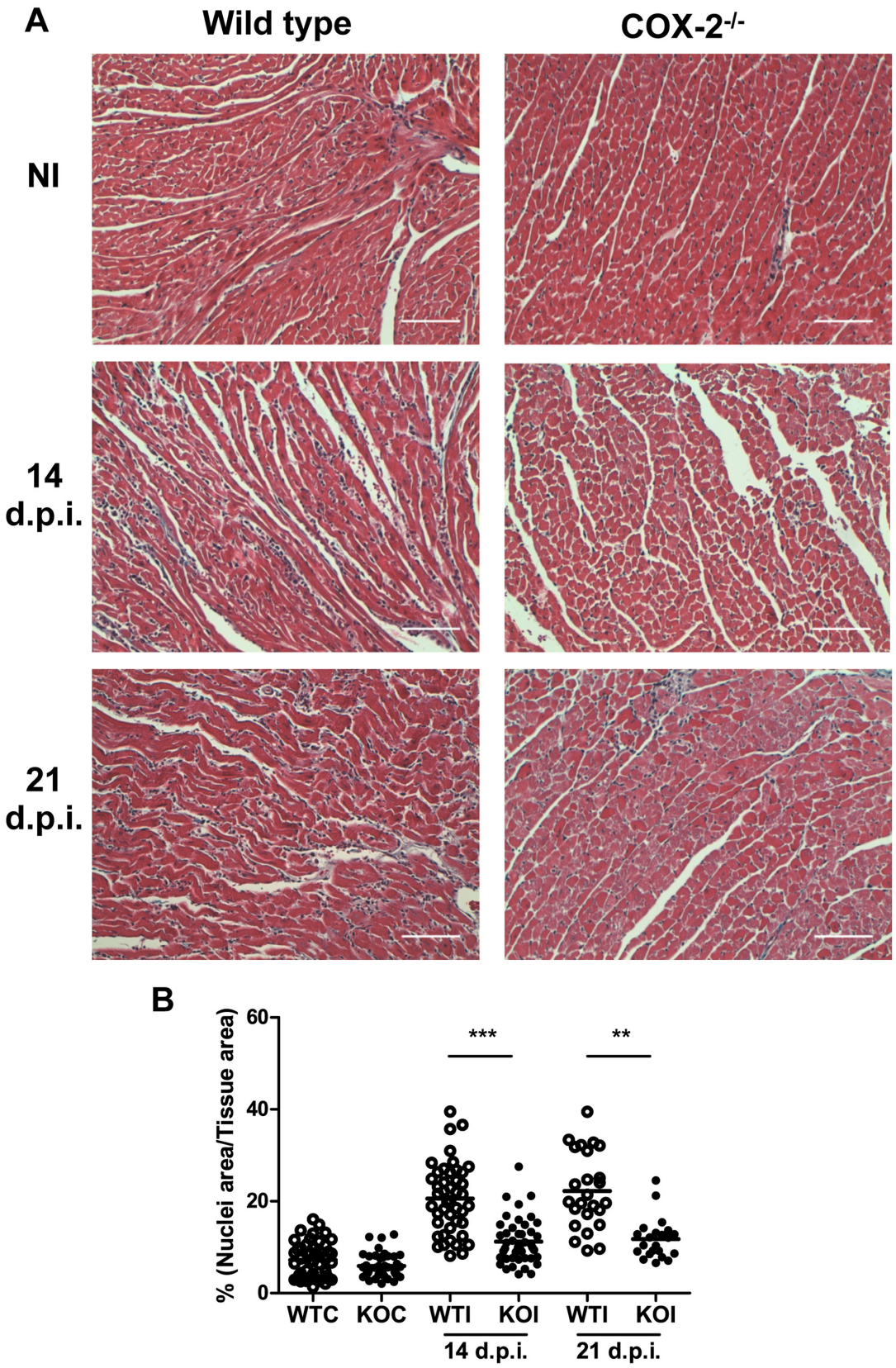

Figure 25 | Histologic analysis of cardiac tissue of *Trypanosoma cruzi* infected wild-type and COX-2$^{-/-}$ mice. Heart tissue was processed for Masson`s Trichromic histology staining at 14 and 21 d.p.i. Micrographs were taken as described in Materials and Methods. **A |** Representative pictures of each group of mice. **B |** Graph showing the quantification of cell infiltration using the FIJI software. Dot plot and means from one representative experiment of two are shown (n=5, for wild type and COX-2$^{-/-}$mice). Differences between mouse strains are indicated *** p<0,001, ** p<0,01. Scale bar is 100 microns length.

response. Samples were collected from the first three weeks of *T. cruzi* infection. Inflammation of cardiac tissue appeared at 14 d.p.i. in both wild-type and COX-2$^{-/-}$ mice. In agreement with histological findings, COX-2$^{-/-}$ mice showed less expression of the common leukocyte marker *Cd45* at 14 d.p.i. than wild-type mice, but no changes were observed at 21 d.p.i. (**Fig, 26A**). Expression of the cellular markers *Cd4, Cd68*, and *Cd11c* gene, related with Th lymphocytes, macrophages and dendritic cells, respectively, was reduced at 14 and 21 d.p.i in COX-2$^{-/-}$ respect to wild-type mice (**Fig, 26B,D,E**). Expression of the CTL marker *Cd8* was reduced in COX-2$^{-/-}$ at 14 d.p.i. and could be related with *Cd45* expression at this moment (**Fig, 26C**). These results confirm the histological findings, revealing that lymphocytes and probably monocytes have a reduced participation in COX-2$^{-/-}$ infected mice cardiac inflammation. In contrast, *Cd8* mRNA was strongly increased at 21 d.p.i. in wild-type and COX-2$^{-/-}$ mice, indicating that CTL activity

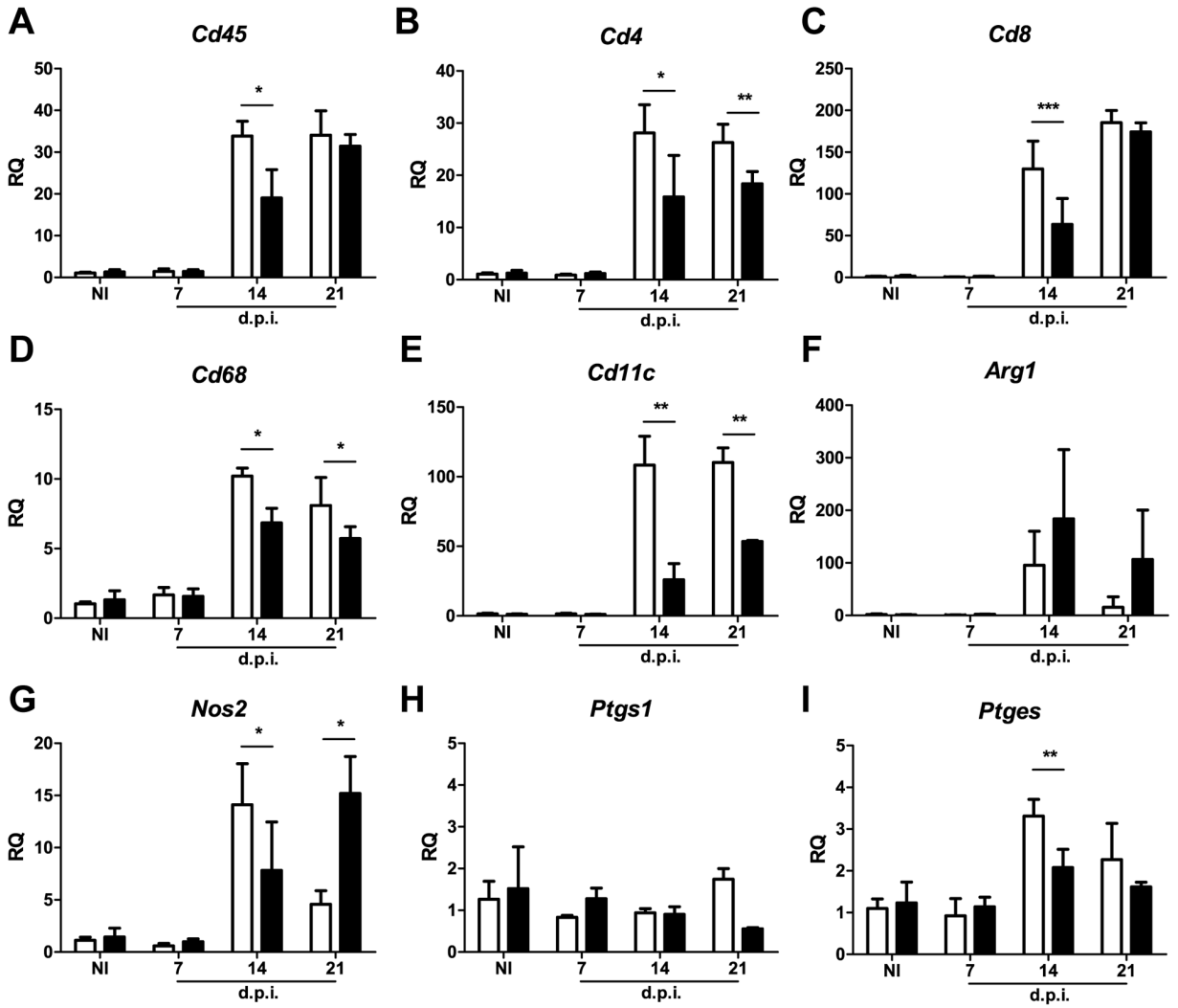

Figure 26 | Cell infiltration, L-arginine and AA metabolizing enzymes expression during *Trypanosoma cruzi* infection in the heart of wild-type and COX-2 deficient mice. Expression was analysed by quantitative PCR. Heart tissue RNA was isolated at 7, 14 and 21 d.p.i. from infected, non-infected wild-type (open bars) or COX-2$^{-/-}$ mice (filled bars). Data were expressed as RQ calculated from CT values . Specific probes were utilized to analyze gene expression corresponding to: **A** | *Cd45*, **B** | *Cd4*, **C** | *Cd8*, **D** | *Cd68*, **E** | *Cd11c* , **F** | *Arg1*, **G** | *Nos2*, **H** | *Ptgs1* and **J** | *Ptges*. Means ± SD from a representative experiment out of four is shown (n=5, for wild-type and COX-2$^{-/-}$ mice). Differences between mouse strains are indicated * p<0.05 **p<0.01 ***p<0,001.

could compensate the decrease in other types of cells infiltrating the heart to fight against infection. There were not differences between mouse strains in *Arg1* expression and data deviation was high within experimental groups (**Fig. 26F**). *Nos2* mRNA decreased in COX-2$^{-/-}$ at 14 d.p.i., but surprisingly, it was higher than in wild-type at 21 d.p.i. (**Fig. 26G**). However, protein analysis by western blot showed less expression of both enzymes related with L-arginine metabolism at 14 d.p.i. in COX-2$^{-/-}$ mice respect to wild-type mice (**Fig. 27**). There was no induction of *Ptgs1* (COX-1) expression to compensate the COX-2$^{-/-}$ deficiency. *Ptges* expression was increased upon infection but was less expressed in heart tissue from COX-2$^{-/-}$ mice (**Fig. 26H,I**). *Ptges* decreased expression seems to be associated with the reduced inflammation found in COX-2$^{-/-}$ *T. cruzi* infected mice. These results suggest that infiltrating leukocytes could be responsible for *Ptges* mRNA levels.

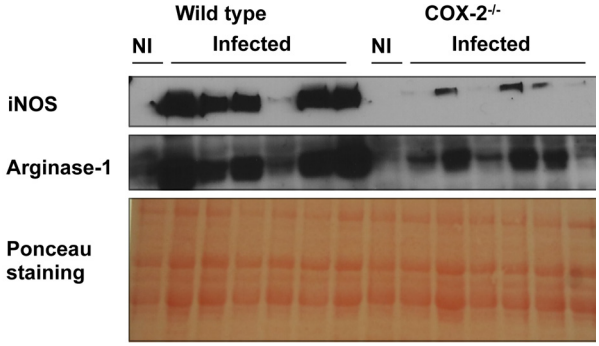

Figure 27 | iNOS and Arginase-1 protein expression in *Trypanosoma cruzi* infected cardiac tissue of wild-type and COX-2 deficient mice. At 14 d.p.i. hearts were collected and total protein extracts were resolved by SDS-PAGE and transferred to a nitrocellulose membrane. Presence of iNOS and Arg-1 in infected and non-infected tissue was detected using specific antibodies. Ponceau staining is presented as a loading control. The extracts from 6 different infected mice were loaded. One representative experiment out of three is shown.

To characterise the immune response in COX-2$^{-/-}$ infected mice, gene expression of cytokines and chemokines were analysed. The expression of chemokines (*Ccl2, Ccl3, Ccl4, Ccl5, Ccl7* and *Cxcl9*) and cytokines (*Ifng, Tnf, Il6, Il4, Il13* and *Il10)* were significantly increased during *T. cruzi* infection of wild-type and COX-2$^{-/-}$ mice (**Fig. 28**). However, chemokine expression presented different patterns in wild-type and COX-2$^{-/-}$ mice. *Ccl3, Ccl5* and *Ccl7* expression was significantly higher in wild-type mice than in COX-2$^{-/-}$ mice at 14 d.p.i., but no significant changes were found between them at 21 d.p.i. (**Fig. 28A,D,E**). In contrast *Ccl3* and *Cxcl9* expression was similar at 14 d.p.i., but higher in COX-2$^{-/-}$ mice than in wild-type mice at 21 d.p.i. (**Fig. 28B,F**). Finally, *Ccl4* expression was significantly reduced at 14 d.p.i. but increased at 21 d.p.i. in COX-2$^{-/-}$ mice respect to wild-type mice (**Fig. 28C**). The decrease in the expression of four out of six chemokines studied could explain the decrease in inflammation observed by histologic analysis at 14 d.p.i. In addition, higher expression of *Cxcl9* could explain how the COX-2$^{-/-}$ model maintains the same level of *Cd8* expression (Kastenmuller et al., 2013). Expression of pro-inflammatory cytokines *Ifng, Tnf* and *Il6* was lower in COX-2$^{-/-}$ at 14 d.p.i respect to wild-type mice (**Fig. 28G,H,I**). Expression of *Il6* was drastically reduced at 21 d.p.i. in both mouse strains (**Fig. 28I**). *Ifng* and *Tnf* expression did not decrease at 21 d.p.i. in COX-2$^{-/-}$ when compared to the group sacrificed at 14 d.p.i. (**Fig. 28G,H**). *Il4* and *Il13* did not decrease in COX-2 deficient mice (**Fig. 28J,K**). *Ifng* was low and *Il4* expression was high at 14 d.p.i. in COX-2$^{-/-}$ mice (**Fig. 28K**), indicating a possible imbalance of the Th1/Th2 profile. The anti-inflammatory cytokine *Il10* showed less expression at both 14 and 21 d.p.i. in the COX-2$^{-/-}$ mouse model. Taken together these data suggest that inflammation is reduced in COX-2$^{-/-}$ but is maintained for longer time.

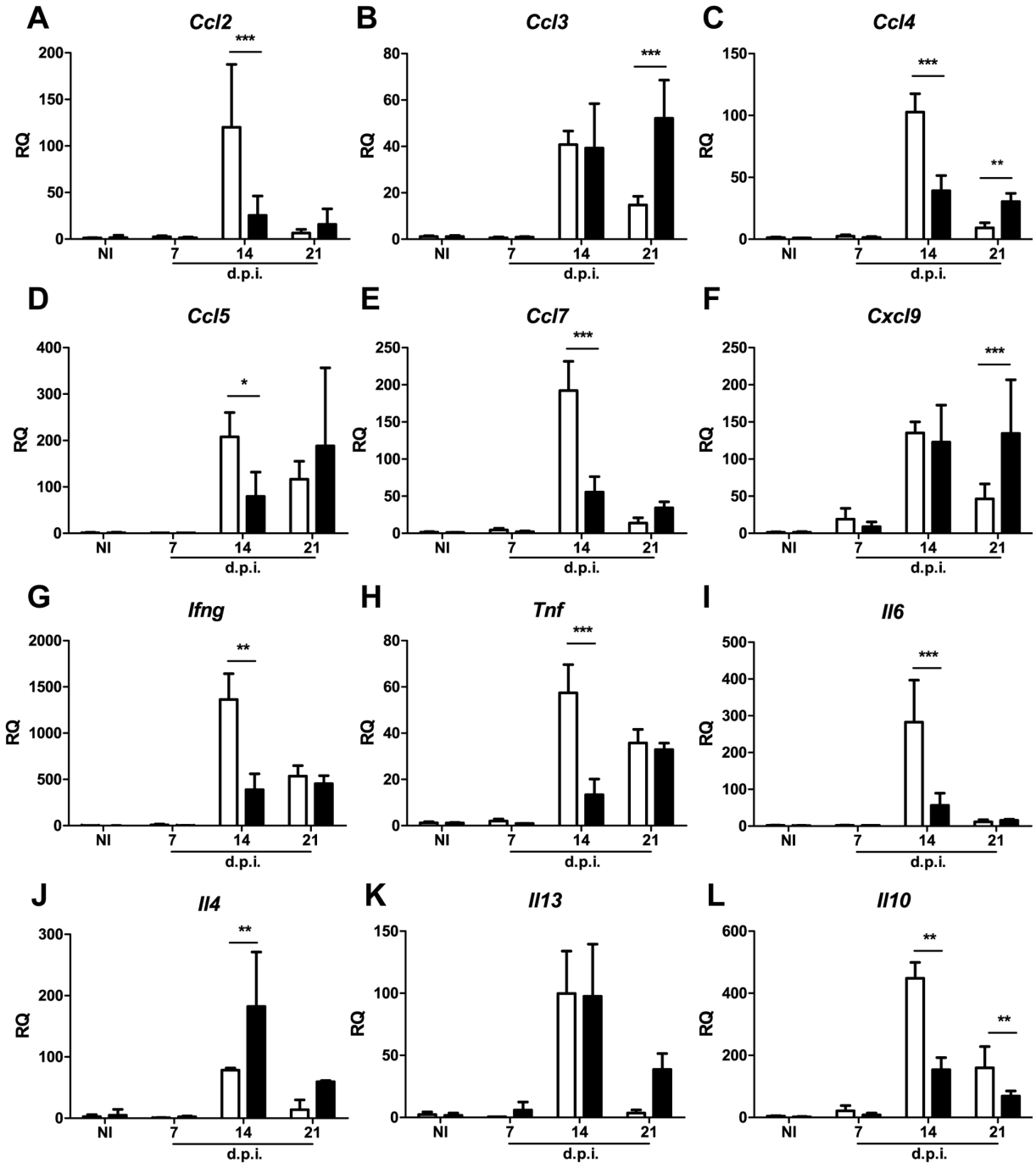

Figure 28| Chemokine and cytokine expression in the heart of wild-type and COX-2 deficient mice during *Trypanosoma cruzi* infection. Expression was analysed by quantitative PCR of the corresponding mRNAs. Heart tissue RNA was isolated at 7, 14 and 21 d.p.i. from infected, non-infected wild-type (open bars) or COX-2$^{-/-}$ mice (filled bars). qPCR was performed and data were expressed as RQ calculated from CT values . Specific probes were utilized to analyze gene expression corresponding to: **A**| *CCl2* **B**| *Ccl3*, **C**| *Ccl4*, **D**|*Ccl5*, **E**|*Ccl7*, **F**| *Cxcl9*, **G**| *Ifng*, **H**| *Tnf*, **I**| *Il6*, **J**| *Il4*, **K**| *Il13*, and **L**|*Il10*. Means ± SD from two representative experiment out of four is shown (n=5, for wild-type and COX-2$^{-/-}$mice). Differences between mouse strains are indicated * p<0.05 **p<0.01 ***p<0,001.

To check whether this process had a systemic incidence, we next analyzed TNF-α plasma level. At 14 d.p.i. TNF-α plasma level was increased in both wild-type and COX-2$^{-/-}$models. But meanwhile wild-type mice showed a decrease in TNF-α plasma level at 21 d.p.i., in COX-2$^{-/-}$ mice was still high. (**Fig. 29**).

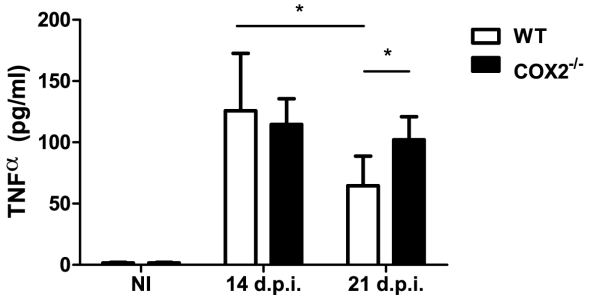

Figure 29 | TNF-α concentration in serum of wild-type and COX-2 deficient mice during *Trypanosoma cruzi* infection. Serum from non-infected and infected wild-type and COX-2$^{-/-}$ mice were collected at 14 and 21 d.p.i. Cytokine quantification by ELISA was performed following manufacturer instructions. Open bars represent the values of wild-type mice and filled bars COX-2$^{-/-}$ mice. Means ± SD from two experiments are shown (n=6, for wild-type and COX-2$^{-/-}$ mice). Differences between mouse strains are indicated * p<0.05.

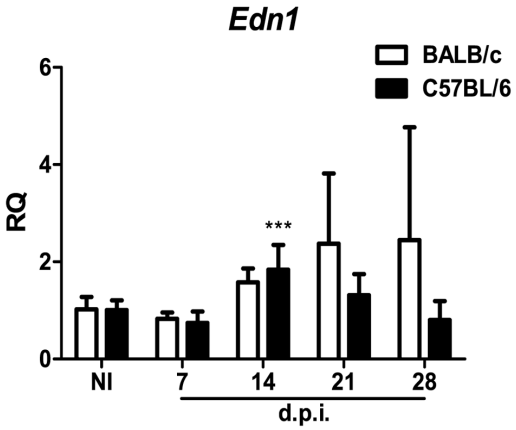

Figure 30 | *Edn1* expression during the acute phase of *Trypanosoma cruzi* infection in cardiac tissue. RNA from heart tissue was isolated at 7, 14, 21 and 28 d.p.i. and qPCR was performed. Results are expressed by RQ calculated from CT values as described in Materials and Methods. Open bars indicate the values for BALB/c mice and filled bars for C57BL/6 mice. Means ± SD from three independent experiments are shown (n=9, for wild-type and COX-2$^{-/-}$ mice). Differences between infected and non-infected mice is indicated ***p<0,001.

Endothelin-1 receptors are not involved in cardiac COX-2 expression

Endothelin-1 (ET-1) is the most potent vasoconstrictor peptide and has been related with *T. cruzi* infection physiopathology (Machado and Camargos, 2008) (Petkova et al., 2001). ET-1 has been found in different experimental models up regulating COX-2 expression, like endothelial (Lin et al., 2013), epithelial (Peng et al., 2008) and smooth muscle cells (Deacon and Knox, 2010). As was previously described, (Petkova et al., 2001) *Edn1* mRNA is induced in *T. cruzi* infected heart in the mouse model (**Fig. 30**). We investigated the effects of treatment with Bosentan, a dual antagonist of ET A/ET B (receptors of ET-1), on the course of *T. cruzi* infection in C57BL/6 mice. Bosentan significantly increased parasitemia

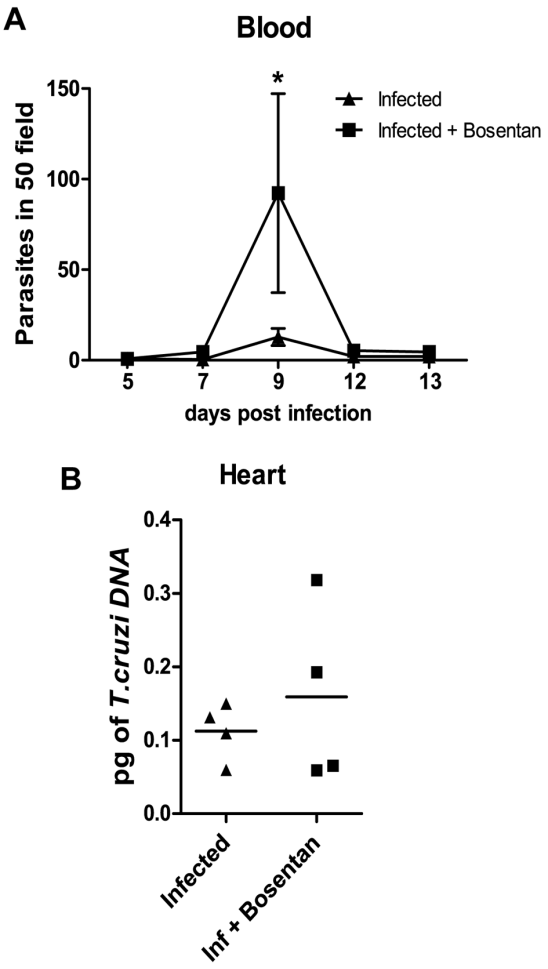

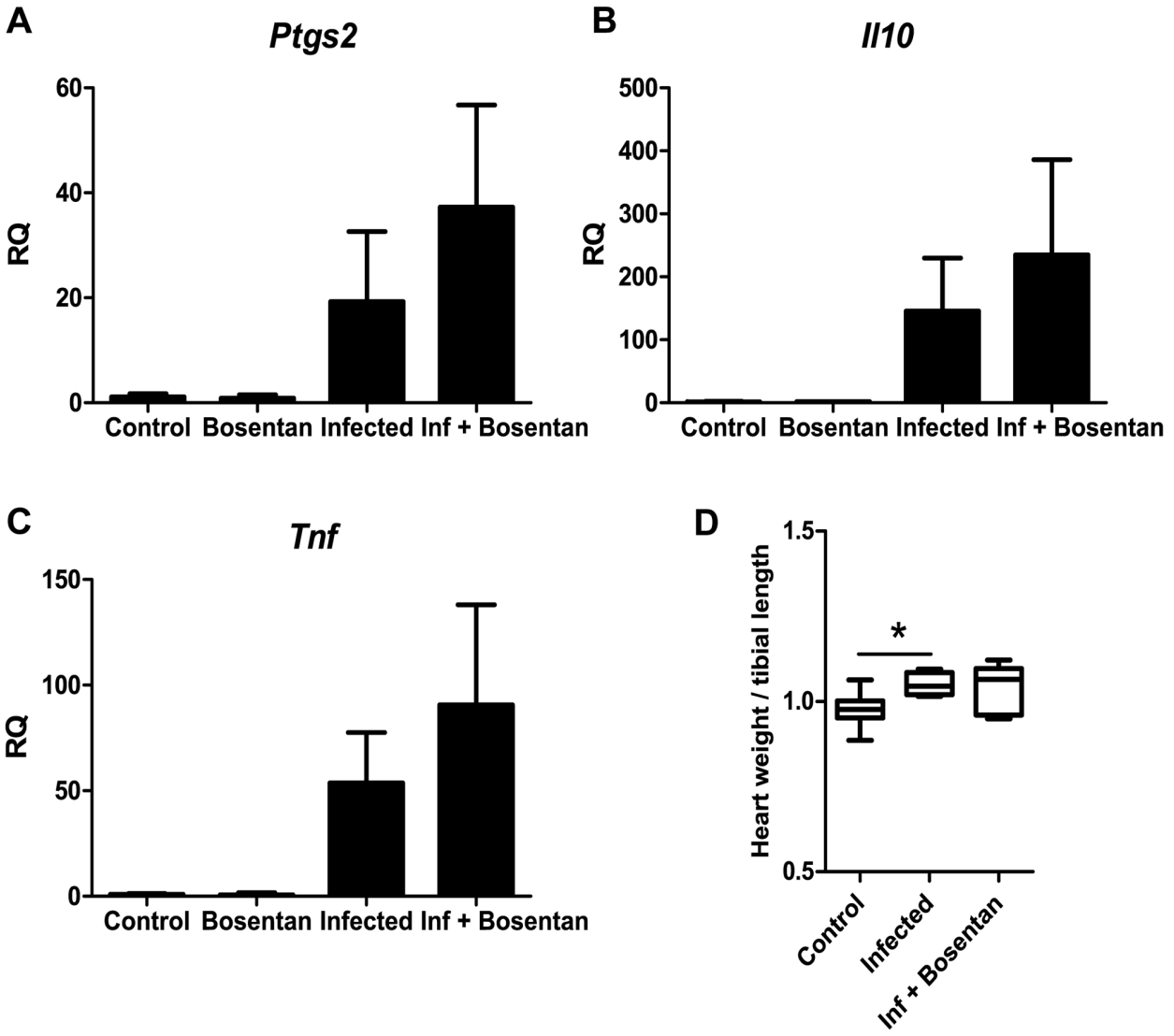

Figure 31 | Parasite burden of *Trypanosoma cruzi* infected mice treated with an inhibitor of endothelin receptors. C57BL/6 mice were infected with *T. cruzi* and one group was treated with the endothelin receptors inhibitor Bosentan by gavage. **A |** Parasitemia was monitored every 2 or 3 days. **B |** DNA from heart tissue was isolated at 14 d.p.i. and qPCR using *T. cruzi* DNA standard was performed. Means ± SD from one experiment are shown (n=4). Differences between treated and non-treated infected mice is indicated * p< 0,05.

Figure 30 | *Edn1* expression during the acute phase of *Trypanosoma cruzi* infection in cardiac tissue. RNA from heart tissue was isolated at 7, 14, 21 and 28 d.p.i. and qPCR was performed. Results are expressed by RQ calculated from CT values as described in Materials and Methods. Open bars indicate the values for BALB/c mice and filled bars for C57BL/6 mice. Means ± SD from three independent experiments are shown (n=9, for wild-type and COX-2$^{-/-}$ mice). Differences between infected and non-infected mice is indicated ***p<0,001.

with no increment of cardiac burden (**Fig. 31**). Bosentan did not affect the infection-associated increase in the cardiac levels of the cytokines *Il10* or *Tnf* (**Fig. 32B,C**). Bosentan treatment of infected animals did not reduce the levels of COX-2 mRNA in the cardiac tissue (**Fig. 32A**). No change in cardiac hypertrophy was observed in Bosentan treated animals (**Fig. 32D**).

Genetic deletion of Prostaglandin E receptor 2 (EP-2)

The COX-2 deficient mouse is an interesting model of infection which has helped us to study the role of this enzyme in inflammation onset of *T. cruzi* infection. This enzyme enhances the production of PGH_2 and with collaboration of the terminal synthases elaborates PGs, prostacyclins and thromboxanes (Stables and Gilroy, 2011). We cannot conclude which mediator is responsible for the effects because the use a COX-$2^{-/-}$ model impairs the production of all metabolites. These mediators act through different G protein coupled receptors and EP-2 is one of the four PGE_2 receptors (Narumiya et al., 1999). PGE_2 is the main COX-2 metabolite found in inflammation and is produced by infiltrating myeloid cells in *T. cruzi* infected cardiac tissue as we shown in Chapter 1. Hence, Dr. Shu Narumiya kindly provided us with the EP-$2^{-/-}$ in C57BL/6 mouse background and the same infection protocol was used to determine the role of this receptor in *T. cruzi* elicited inflammation.

EP-2 deficiency did not modify parasite burden in *Trypanosoma cruzi* infected mice

As in previous experiments, both wild-type and EP-2 deficient mice were infected intraperitoneally with 2000 blood trypomastigotes of *T. cruzi*. Parasitemia and survival was measured every other day. No differences in parasitemia or heart parasite burden were observed between wild-type and EP-2 deficient mice (**Fig. 33**). No EP-$2^{-/-}$ mice died during the *T. cruzi* infection experiments. These results could indicate that the routes of parasite elimination are not directly affected by EP-2 signaling.

Anti-*T. cruzi* specific antibody production is not modified in EP-$2^{-/-}$ infected mice

Since serum IgG1/IgG2a balance is related to the Th2/Th1 balance, we determined anti-*T.cruzi* IgG1, IgG2a and total IgG levels throughout acute infection by ELISA. As shown in **Fig. 34**, the antibody level was similar in the two strains of mice over time, independently of the EP-2 expression.

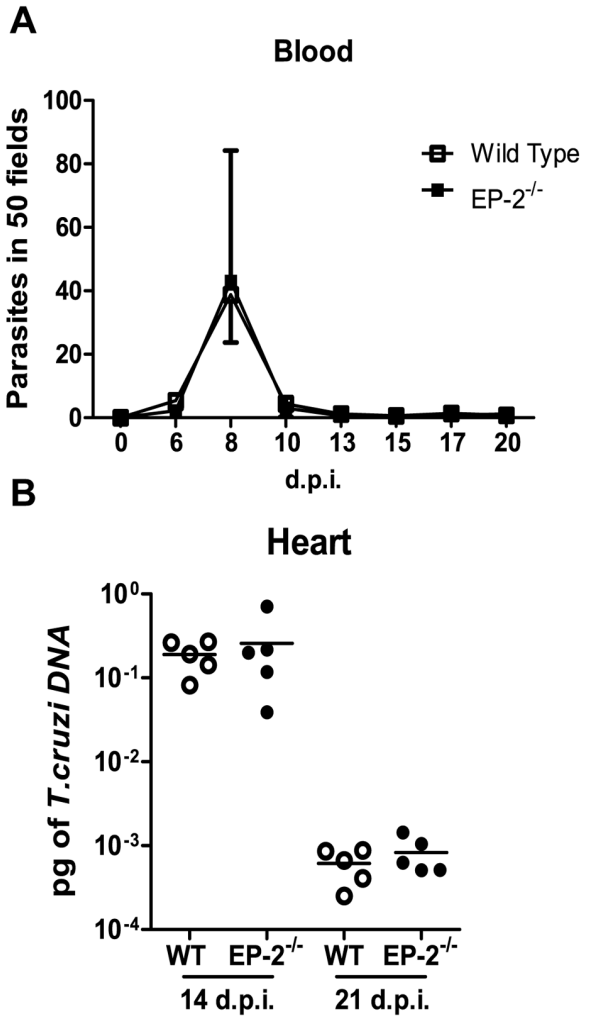

Figure 33| Parasite burden in *Trypanosoma cruzi* infected wild-type and EP-2 $^{-/-}$ mice. Wild-type (open squares) and EP-$2^{-/-}$ (filled squares) mice were infected. **A|** Parasitemia was monitored every 2 or 3 days (means ± SD are shown). **B|** DNA from heart tissue was isolated at 14 and 21 d.p.i. and qPCR using *T. cruzi* DNA standard was performed. (n=5, for wild-type and EP-$2^{-/-}$ mice) and shown as dot plot and mean. Data from a representative experiment out of two performed are shown.

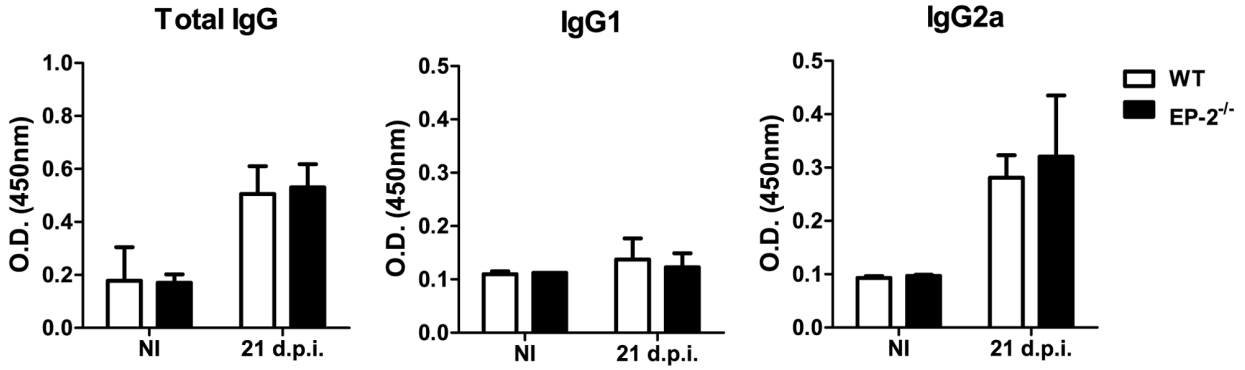

Figure 34 | Plasma antibodies against *Trypanosoma cruzi* during acute phase in EP-2 deficient mice. Blood was obtained by cardiac puncture from infected or non-infected mice at 21 d.p.i and plasma was isolated from wild-type (open bars) and EP-2$^{-/-}$ (filled bars) mice. The ELISA was performed coating the plate with *T. cruzi* extracts from culture. Means ± SD from two representative experiments of are shown (n=9).

PGE_2 signaling through EP-2 inhibition reduces cardiac inflammation

Histologic analysis of cardiac inflammation in *T. cruzi* infected hearts from EP-2$^{-/-}$ showed less inflammatory infiltrates at 14 and 21 d.p.i. (**Fig. 35A**). Images were quantified using the FIJI software and the differences in cell infiltration between EP-2$^{-/-}$ and wild-type mice were confirmed (**Fig. 35B**).

In order to analyse the characteristics of the infiltrating cells, gene expression was quantified by RT-PCR and infected animals were compared to their non-infected controls. Plasma and heart samples were collected at 14 and 21 d.p.i. in both wild-type and EP-2$^{-/-}$ mice. Expression of the common leukocyte marker *Cd45* was decreased in EP-2$^{-/-}$ at 14 d.p.i but not at 21 d.p.i. (**Fig, 36A**). This decrease in *Cd45* could explain the histological findings at 14 d.p.i. Cell surface markers *Cd4, Cd8, F4/80* and *Cd11c* gene expression, related with Th lymphocytes, CTL, macrophages and dendritic cells, respectively, was not reduced at 14 d.p.i. (**Fig, 36B-E**). However, *Cd8, F4/80* and *Cd11c* gene expression was increased at 21 d.p.i. in EP-2$^{-/-}$ respect to wild-type mice (**Fig, 36C-E**). *Ptgs2* (COX-2) gene expression was reduced in EP-2$^{-/-}$ at 14 d.p.i. (**Fig. 36F**), this result is also in agreement with the histologic analysis showing that EP-2$^{-/-}$ mice presented less cardiac inflammation than wild-type mice. No changes were observed in *Alox15* gene expression (**Fig. 36G**). There were no differences between mouse strains in *Nos2* expression (**Fig. 36H**), but *Arg1* mRNA expression was higher in EP-2$^{-/-}$ mice at 14 and 21 d.p.i. (**Fig. 36I**). Increment of several of these genes at 21 d.p.i. may be caused by a failure in the resolution of inflammation due to the EP-2 signalling deficiency.

To characterise the immune response of infected EP-2$^{-/-}$ mice, gene expression of cytokines and chemokines were analysed. The expression of chemokines (*Ccl2, Ccl5* and *Cxcl9*) and cytokines (*Ifng, Tnf, Il6, Il4, Il10* and *Il12)* were significant increased during *T. cruzi* infection of both EP-2$^{-/-}$ and wild-type (**Fig. 37**). When EP-2$^{-/-}$ mice chemokine expression was compared to wild type expression we observed different patterns but quite similar to COX-2$^{-/-}$ infected mice. *Ccl2* expression was reduced at 14 d.p.i. in the EP-2$^{-/-}$ but no significant changes were found at 21 d.p.i. (**Fig. 37A**). In contrast *Cxcl9* expression remained the same at 14 d.p.i. and increased at 21 d.p.i. in EP-2$^{-/-}$ mice (**Fig. 37C**). However, no statistical differences were found in *Ccl5* expression (**Fig. 37B**). Expression of pro-inflammatory cytokines *Ifng, Il12* and *Il6*, the Th2 cytokine *Il4* and the anti-inflammatory cytokine *Il10* was reduced in EP-2$^{-/-}$ at 14 d.p.i.

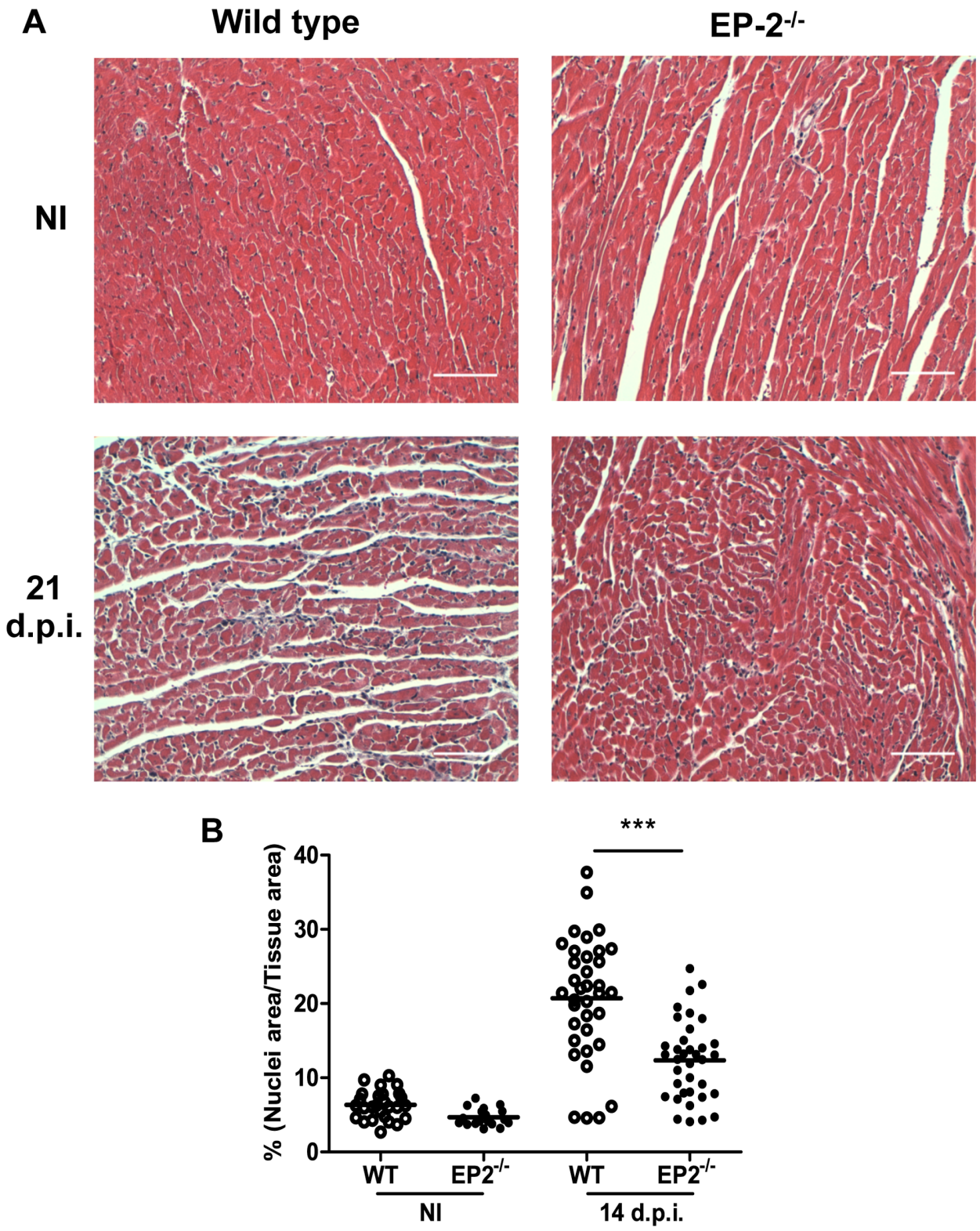

Figure 35 | Histologic analysis of cardiac tissue of *Trypanosoma cruzi* infected wild-type and EP-2$^{-/-}$ mice. Masson`s Trichromic staining was performed in hearts from mice at 21 d.p.i. Micrographs were taken as described in Materials and Methods. Representative pictures of each group were selected. **A** | Representative pictures of infected (21 d.p.i.) and non-infected (NI) wild-type and EP-2$^{-/-}$ mice. **B** | Graph showing the quantification of cell infiltration using the FIJI software. Dot plot and means for wild-type (open circles) and EP-2-/- (filled circles) mice from one experiment are shown (n=4, for each group of mice). Differences between mouse strains are indicated *** p<0,001. Scale bar is 100 microns length.

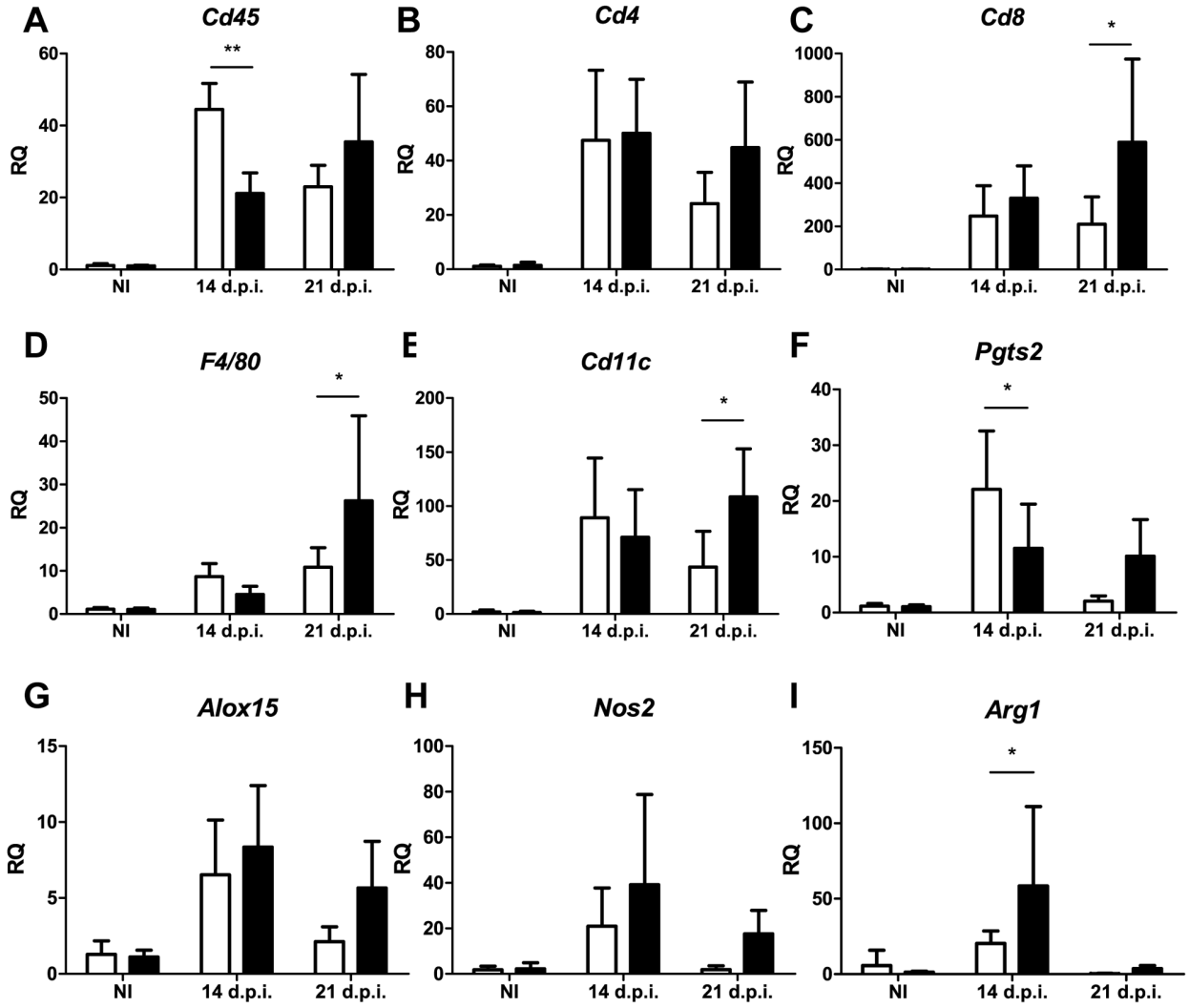

Figure 36 | Cell infiltration and expression of L-arginine and AA metabolizing enzymes during *Trypanosoma cruzi* infection in the heart of wild-type and EP-2 deficient mice. Expression was analysed by quantitative PCR. Heart tissue RNA was isolated at 14 and 21 d.p.i. from infected, non-infected wild-type (open bars) or EP-$2^{-/-}$ mice (filled bars). qPCR was performed and data were expressed as RQ calculated from CT values. Specific probes were utilized to analyze gene expression corresponding to: **A** | *Cd45*, **B** | *Cd4*, **C** | *Cd8*, **D** | *F4/80 (Emr1)* , **E** | *Cd11c* , **F** | *Ptgs2*, **G** | *Alox15*, **H** | *Nos2* and **J** | *Arg1*. Means ± SD from one representative experiment out of two is shown (n=4, for wild-type and EP-$2^{-/-}$ mice). Differences between mouse strains are indicated * $p<0.05$ ** $p<0.01$.

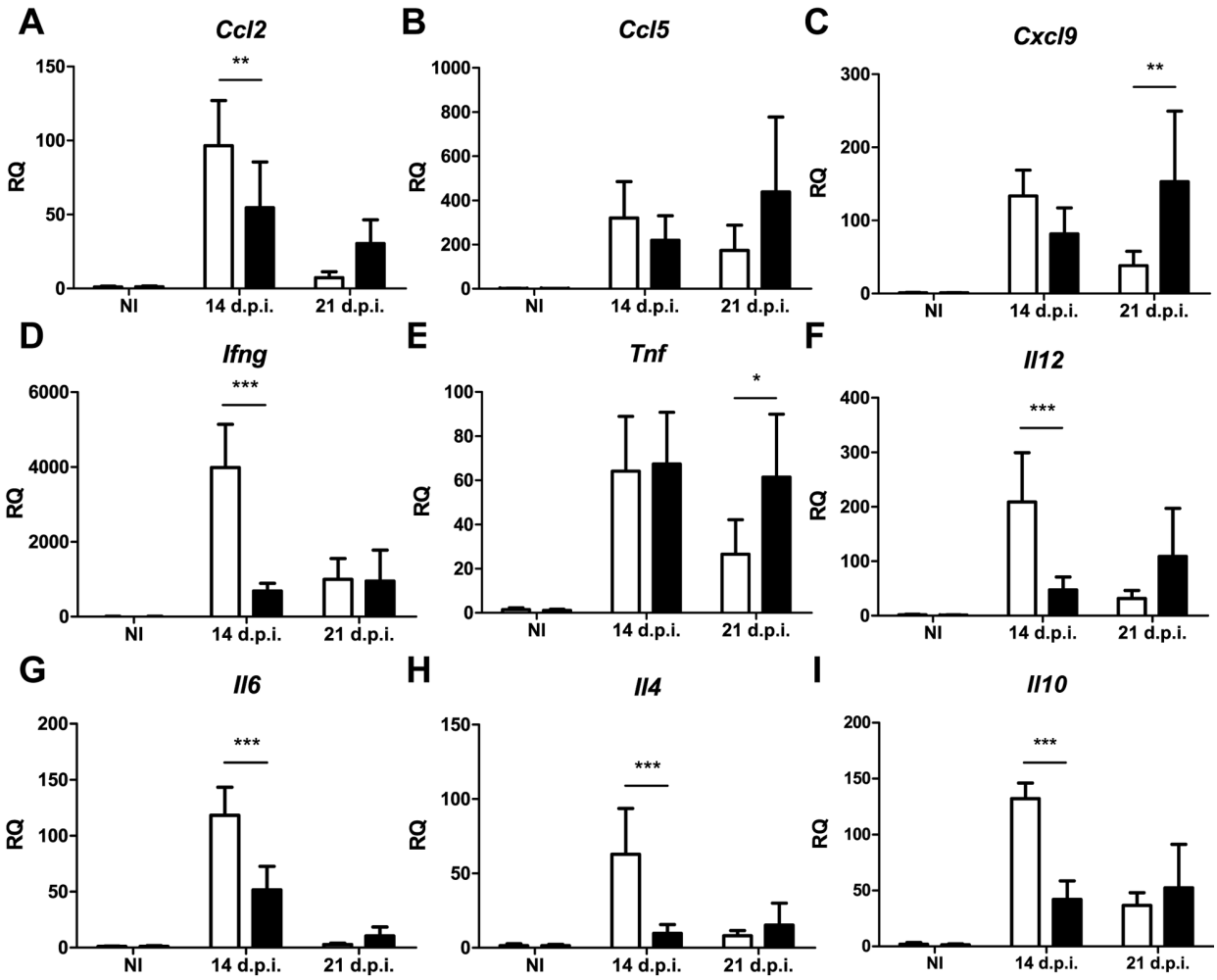

Figure 37| Chemokine and cytokine expression in heart tissue of wild type and EP-2 deficient mice during *Trypanosoma cruzi* infection. Expression was analysed by quantitative PCR of the corresponding mRNAs. Heart tissue RNA was isolated at 14 and 21 d.p.i. from infected and non-infected wild-type (open bars) or EP-$2^{-/-}$ mice (filled bars). qPCR was performed and data were expressed as RQ calculated from CT values. Specific probes were utilized to analyze gene expression corresponding to: **A**| *CCl2* **B**| *Ccl5*, **C**| *Cxcl9*, **D**| *Ifng*, **E**| *Tnf*, **F**| *Il12*, **G**| *Il6*, **H**| *Il4 and* **I**| *Il10*. Means ± SD from a representative experiment out of two is shown (n=4, for wild-type and COX-$2^{-/-}$mice). Differences between mouse strains are indicated * $p<0.05$ ** $p<0.01$ *** $p<0,001$.

compared to wild-type (**Fig. 37D,F,G,H,I**). However, *Tnf* expression did not change at 14 d.p.i. and increased its level at 21 d.p.i. (**Fig. 37E**). No changes were observed in TNF-α plasma levels between the mouse models (**Fig. 38**). Taken together these data suggest that EP-2 signaling has an inflammatory role in *T. cruzi* infected heart. Surprisingly this process seems to be TNF-α-independent.

Macrophage activation and not migration could responsible for the decrease of inflammation of EP-$2^{-/-}$ mice

In order to find an explanation for the reduced inflammation in EP-$2^{-/-}$ infected mice and due to the central role of macrophages in *T. cruzi* infection, we decided to analyze the effects of EP-2 deficiency in migration and activation. Previous works have described a role for PGE_2

in leukocyte migration (Panzer and Uguccioni, 2004). Thus, peritoneal macrophages were used in our migration experiments. We first studied the migration in the aseptic peritonitis model in response to thyoglicollate. No differences were found between EP-2$^{-/-}$ and wild type in total number of cells at 4 days post infection, time at which most of the peritoneal cells were macrophages (**Fig. 39A**). We performed an *in vitro* migration assay using these macrophages placed in a two chamber system separated by permeable membrane with 8 µm pores. CCL5 in RPMI 5% FCS was used as stimulus for cell migration, but neither we found any difference between EP-2$^{-/-}$ and wild type (**Fig. 39B**). As no differences were found in migration, we next focus in activation of macrophages, as they play a key role in the initiation of inflammation. When macrophages become activated they express high levels of MHC-II in order to present antigen to lymphocytes. Spleens from wild-type and EP-2$^{-/-}$mice were collected and cells were analyzed by flow citometry. Myeloid cells were selected using the CD11b marker antibody and MHC-II expression was analyzed

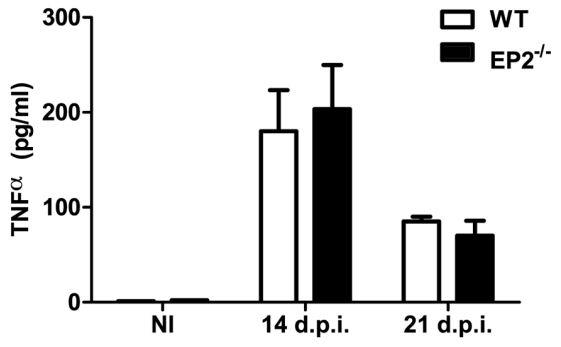

Figure 38 | TNF-α concentration in serum of wild-type and EP-2 deficient mice in *Trypanosoma cruzi* infection. Serum from non-infected and infected wild-type and EP-2$^{-/-}$ mice were collected. Cytokine quantification by ELISA was performed following manufacturer instructions. Open bars represent the values of wild-type mice and filled bars EP2$^{-/-}$ mice. Means ± SD from one experiment are shown (n=5, for each group of mice).

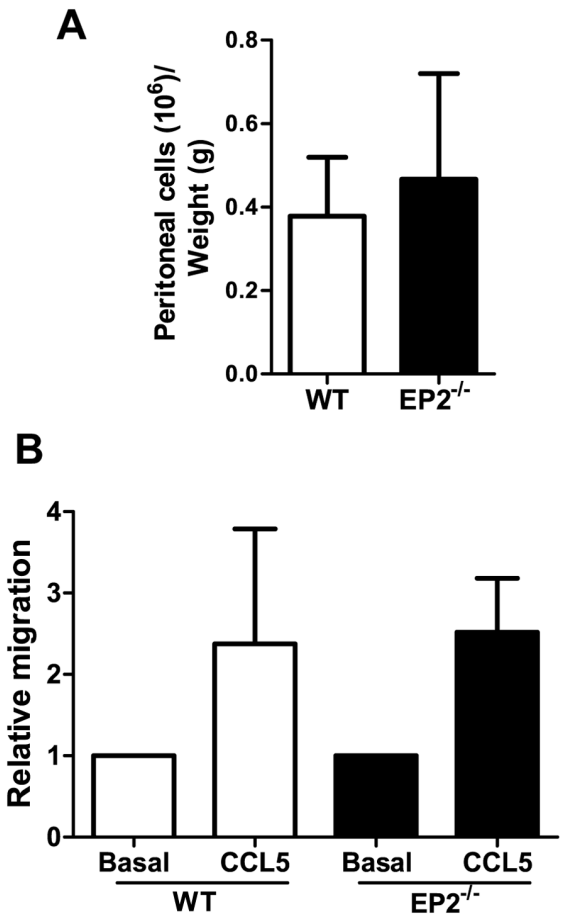

Figure 39 | Cell migration of peritoneal cells in wild type and EP-2 deficient mice. A | Groups of wild-type (open bars) and EP-2$^{-/-}$ (filled bars) mice were injected with thyoglicollate solution and peritoneal exudate cells were collected and counted after 4 days. **B |** Thyoglicollate elicited cells were cultured in Transwell plates as described in Materials and Methods to perform a macrophage migration assay to RANTES. This migration was normalized to migration from 2% FBS to 5% FBS. Means with SD from 5 mice per group are shown.

(**Fig. 40A**). The results show that the percentage of CD11b^{+} cells from EP-2$^{-/-}$ that express MHC-II was lower than wild type. Mean fluorescence intensity (which is related with the level of expression per cell) was also decreased in EP-2$^{-/-}$ and is indicative of activation impairment. Despite we have not analyzed lymphocyte and other cell type activation, we can concluded that EP-2 signaling is important for macrophage MHC-II surface expression and could be related with the reduced cardiac inflammation.

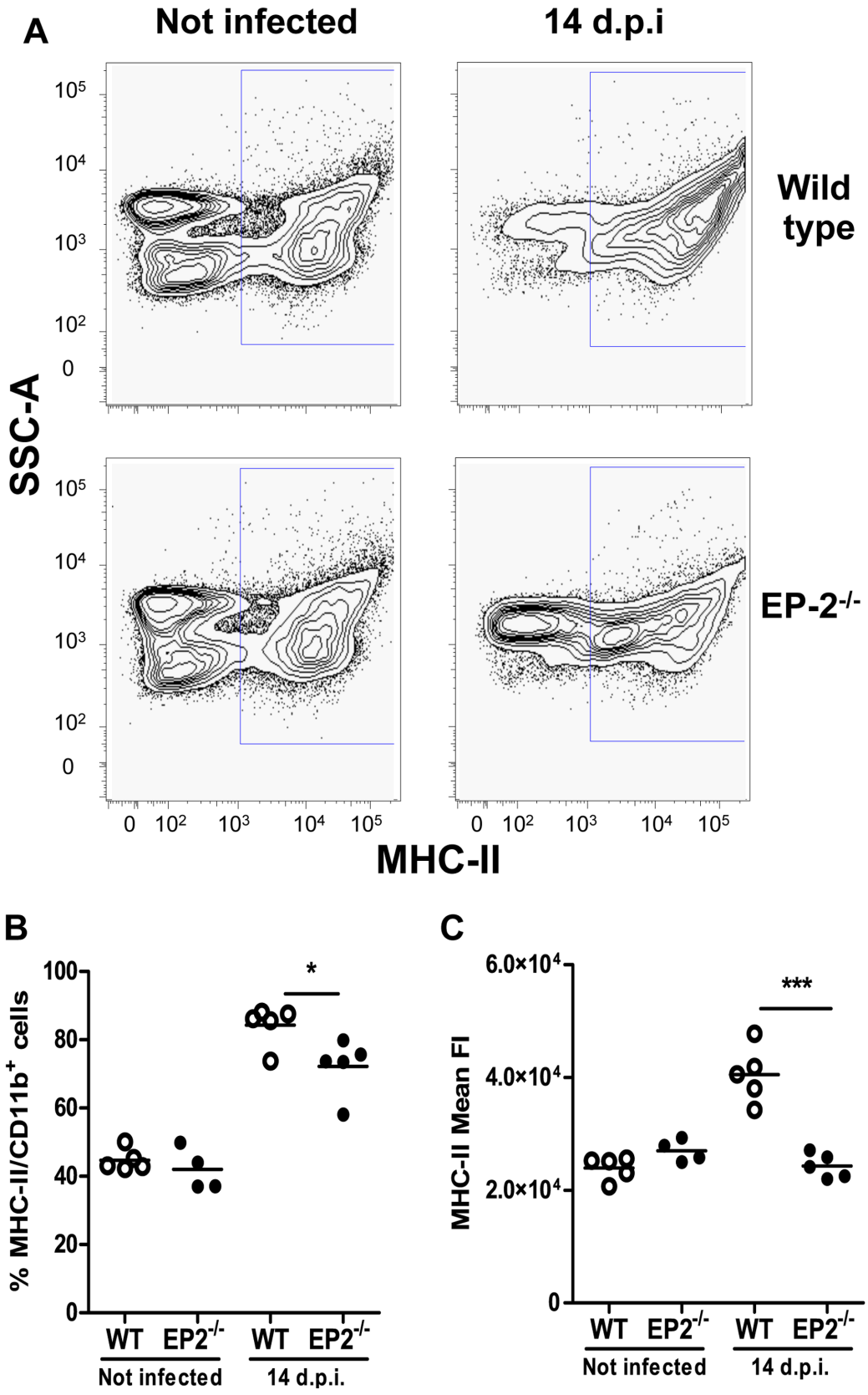

Figure 40 | MHC-II surface expression of EP-2 deficient macrophages. Spleens from infected and non-infected mice, wild-type and EP2$^{-/-}$ mice were collected at 14 d.p.i. mechanically disrupted and analyzed by flow citometry. **A |** Representative quantile countour plots (10% probability) are shown. MHC-II positive cells are gated with a blue square. CD11b^{+} were previously gated according to isotypic controls. **B |** Dot plot representing the percentage of MHC-II expressing cells within CD11b^{+} gated cells. **C |** Dot plot showing mean fluorescence intensity of the same populations. Data from a representative experiment of two are shown (n=5). Differences between mouse strains are indicated *p<0.05, ***p<0.001.

Role of cyclooxygenases in the immunosuppression observed in the acute phase of *Trypanosoma cruzi* infection

A generalized immunosuppression has been described in *T. cruzi* experimental infected animals (Abrahamsohn and Coffman, 1995). Several mechanisms have been proposed to explain this phenomenon being the action of PGE_2 one of them (Michelin et al., 2005).

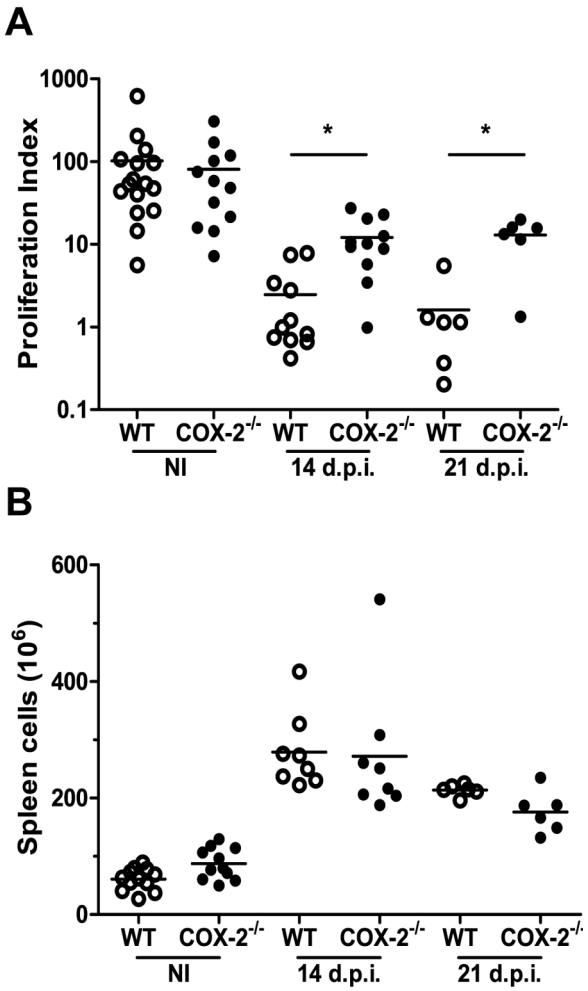

Figure 41 | Splenomegaly and spleen cell proliferation in the acute phase of *Trypanosoma cruzi* infection of wild-type and COX-2 deficient mice. Spleens from infected and non-infected wild type (open circles) and COX-$2^{-/-}$ (filled bars) were collected at 14 and 21 d.p.i. Spleen cells were mechanically obtained counted and cultured in presence of stimulus. **A** | Proliferation of cells stimulated with ConA 1µg/ml. **B** | Splenocytes were counted with a hemocytometer. All differences respect to the non-infected groups were statistically significant (ANOVA two-way). Differences between mouse strain in cell proliferation are indicated *p<0,05 (n=6-12, per each group). Dot plot and means from three independent experiments are shown.

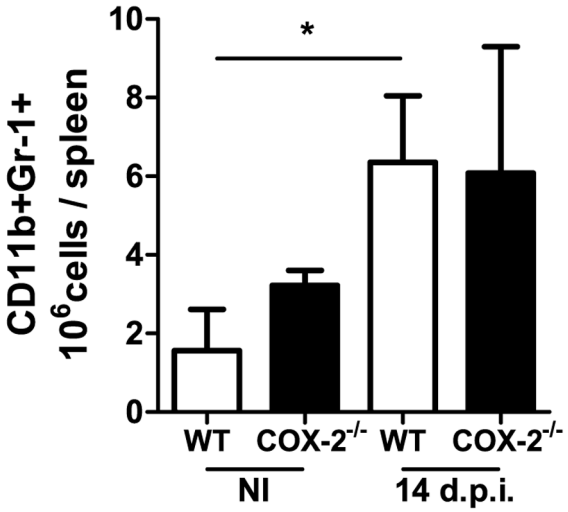

Figure 42 | Analysis of Gr-1^+ cells in spleen of infected COX-2 deficient mice. Spleens from wild-type and COX-$2^{-/-}$ infected and non-infected mice were collected at 14 d.p.i. Organs were disrupted and analyzed by flow citometry. Numbers of CD11b $^+$/ Gr-1^+ of infected wild-type and COX-$2^{-/-}$ mice are shown. Open bars represent wild-type mice and filled bars represent COX-$2^{-/-}$ mice. Data from a representative experiment of two are shown (n=4). Differences between infected and non-infected group are indicated * p<0,05.

All the previous work was performed using COX-2 selective and non-selective inhibitors administered *in vivo* to the infected animals or added *ex vivo* to the cultured cells, reviewed in (Machado et al., 2011). However, the role of PGE_2 in immunosuppression has not been completely elucidated. To further address this we performed *in vitro* stimulation of spleen cells from infected COX-2 deficient mice. As previously described (Goni et al., 2002) spleen cells from *T. cruzi* infected wild type animals showed a NO-dependent suppression of proliferation upon concanavalin A stimulation. Remarkably, a reduced immunosuppression was found at 14 d.p.i and 21 d.p.i. in spleen cells from COX-$2^{-/-}$ infected mice (**Fig. 41A**). However, no changes were observed in the spleen

cell number at any d.p.i. studied (**Fig. 41B**). Production of NO by CD11b^{+} GR-1^{+} spleen infiltrating cells has been previously described to play a role in the immunosuppression in the acute phase of infection (Goni et al., 2002). We performed flow citometry analysis of this cell population in the COX-2 deficient model, finding no changes in cell number respect to wild-type mice (**Fig. 42**). These results lead us to think that the reduced immunosuppression could be due to a functional recovery of T cells more than a change in CD11b^{+} GR-1^{+} infiltration.

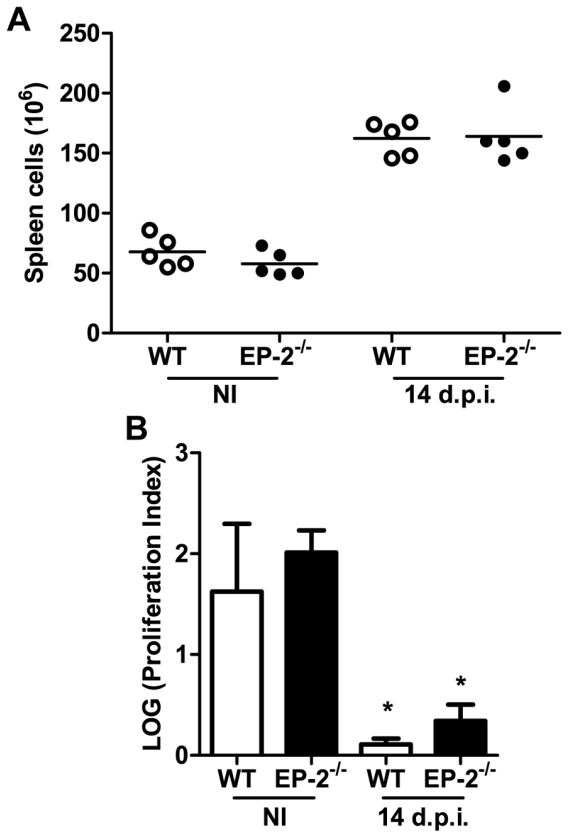

Figure 43 | Splenomegaly and spleen cell proliferation during acute phase of *Trypanosoma cruzi* infection of wild-type and EP-2 receptor deficient mice. Spleens from infected and non-infected wild-type (open circles) and EP-2$^{-/-}$ (filled circles) mice were collected at 14 d.p.i. **A** | Number of spleen cells was counted with a hemocytometer and **B** | cells were cultured in presence of ConA 1μg/ml. Dot plot and means ± SD from a representative experiment of two are shown (n=5, per each group of mice).

Next, we performed the same experiment using the PGE_2 receptor deficient mice (EP-2$^{-/-}$), but no differences with the wild type were found in proliferation or in total cell number (**Fig. 43**). It suggests that EP-2 signalling was not essential for the immunosuppression. In order to analyze whether PGE_2 generation in vitro was necessary for the immunosuppression we added different cyclooxygenase inhibitors to the culture medium of the spleen cells. No recovery from immunosuppression was observed when 10 μM indomethacin, 0,1 μM NS398 or 0,1 μM celecoxib was added to spleen cell cultures (**Fig. 44**). Neither was observed when drugs were used 2 times more concentrated in the case of indomethacin and 10 times more concentrated in the case of NS398 and celecoib (**Not shown**).

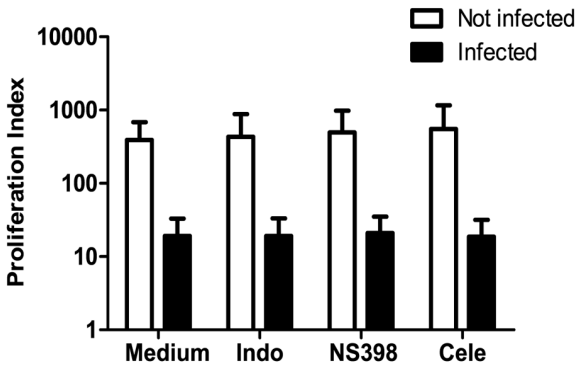

Figure 44 | Effects of cyclooxygenase inhibitors added *ex vivo* in the proliferation of spleen cells proliferation from *Trypanosoma cruzi* infected mice. Spleens from infected and non-infected BALB/c were collected at 21 d.p.i. Spleen cells were cultured in the presence of anti-CD3/CD28 antibodies; 5μg/ml, 1μg/ml . Open and filled bars represent cells from non-infected and infected animals, respectively. Not significant changes were observed when cyclooxygenase inhibitors were added (10 μM Indomethacin, 0,1 μM NS398 or 0,1 μM Celecoxib). Means ± SD from two independent experiments are shown (n=9).

We conclude that COX-2 activity is in part responsible for developing the immunosuppression *in vivo* but COX-2 pharmacological inhibition did not reduce immunosuppression *in vitro*. Consequently, we analyzed PGE_2 secretion of spleen cells from infected COX-$2^{-/-}$ and wild-type mice. Splenocytes from infected wild-type mice at 14 d.p.i. and 21 d.p.i. produced PGE_2 in culture (**Fig. 45A**). When cells from infected COX-2 deficient mice were cultured they surprisingly secreted some PGE_2 to the supernatant (**Fig. 45B**). Nonetheless, we confirmed that expression of COX-2 mRNA was absent in COX-2 deficient mice (**Fig. 46A**).Then, one possibility to explain PGE_2 secretion in COX-2 deficient mice could be by up-regulation of COX-1 expression. Indeed, we found an increase of the expression of COX-1 protein obtained by western blot that could explain PGE_2 secretion by infected COX-2 deficient mice (**Fig. 46C**). In addition, studying the mRNA expression of PGE_2 synthase (*Ptges*) in the infected spleen we found an increment of its expression in COX-2 deficient and wild-type mice (**Fig. 46B).** As nitric oxide produced by iNOS was involved in immunosuppression (Goni et al., 2002)(Gutierrez et al., 2009) we studied the expression of this enzyme in protein extracts from COX-2 deficient spleen cells. We found that COX-2 deficient mice expressed less iNOS protein in spleen after infection (**Fig. 47**). Therefore, a decrease in iNOS expression could explain the partial recovery of proliferation observed in infected COX-2 deficient mice respect to wild-type ones.

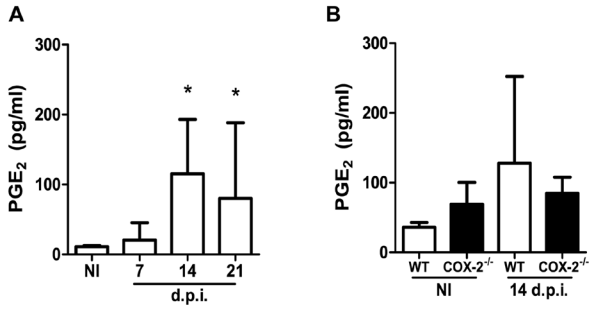

Figure 45| **PGE_2 production by spleen cells from *Trypanosoma cruzi* infected mice during acute phase of infection.** Spleen cells were cultured 48 hours. Supernatants were collected to measure PGE_2 using an EIA kit following manufacturer instructions. **B**| PGE_2 secretion of non-infected and infected C57BL/6 mice at 7, 14 and 21 d.p.i. Differences between infected and non-infected mice are represented *p<0.05. **B**| PGE_2 secretion of non-infected and infected wild type (open bars) and COX-$2^{-/-}$ (filled bars) at 14 d.p.i. Means ± SD from a representative experiment out of two are shown. (n=3, per each group of mice).

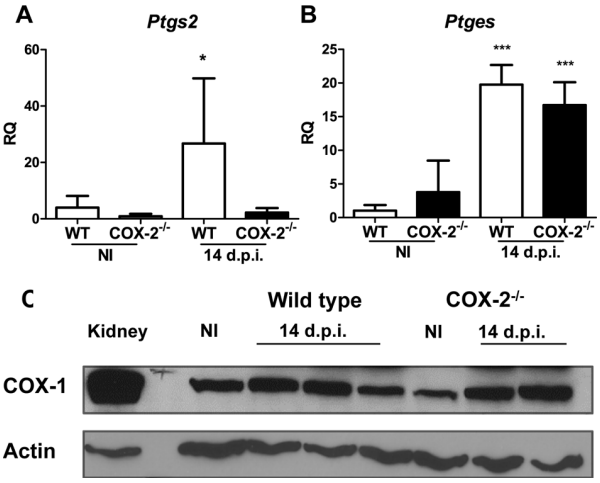

Figure 46| **Expression of cyclooxygenases and prostaglandin E terminal synthase in the spleen during the acute phase of *Trypanosoma cruzi* infection in wild-type and COX-$2^{-/-}$ mice.** Spleens from infected and non-infected wild type (open bars) and COX-$2^{-/-}$ (filled bars) were collected at 14 d.p.i. Spleen cells were mechanically obtained. The RNA was isolated and protein extract were obtained. **A**| Graphs showing mRNA quantification of *Ptgs2* and *Ptges* by qPCR expressed as RQ calculated from CT values as described in Materials and Methods. Means ± SD from a representative experiment of two are shown (n=5, per each group of mice). Enzyme expression of infected mice were compared to their respective non-infected controls ***p<0.001 *p<0.05. **B**|15 micrograms of total protein extracts were resolved by SDS-PAGE and transferred to a nitrocellulose membrane. Presence of COX-1 and actin were detected using specific polyclonal antibodies. Anti-actin antibody was used as a loading control. The extract from 2 or 3 different mice were loaded. A representative experiment out of two is shown.

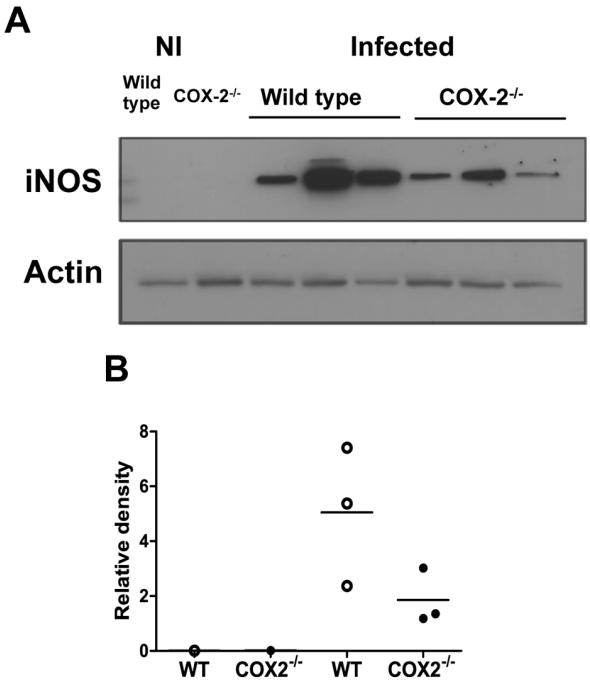

Figure 47 | Expression of iNOS in spleen of *T. cruzi* infected wild-type and COX-2$^{-/-}$mice. Spleens from infected and non-infected WT and COX-2$^{-/-}$ were collected at 14 d.p.i. Spleen cells were mechanically processed and protein extract were obtained. 15 micrograms of total protein extracts were resolved by SDS-PAGE and transferred to a nitrocellulose membrane. The presence of iNOS and actin were detected using specific polyclonal antibodies. Anti-actin antibody was used as a loading control. **A |** The extract from 3 infected mice and non-infected controls were loaded. **B |** Relative density of iNOS specific bands normalized respect to actin bands of one experiment. Data from a representative experiment out of four performed is shown.

CONCLUSIONS

Cycloxygenase-2 (COX-2) is expressed by heart infiltrating macrophages of *Trypanosoma cruzi* infected mice. Purified infiltrating $CD11b^{+}$ myeloid cells are able to produce PGE_2 and $PGF_{2\alpha}$, involved in immune regulation.

12/15 Lipoxygenase gene expression is increased in cardiac tissue during the acute phase of *Trypanosoma cruzi* infection. Enzyme expression is IL-4 receptor dependent.

***Trypanosoma cruzi* alone does not produce prostaglandins nor thromboxans**. *Trypanosoma cruzi* does not have the metabolic routes to elaborate prostaglandins or thromboxans from arachidonic acid.

COX-2 deficiency produces no changes in parasite burden but reduces cardiac inflammation induced by *Trypanosoma cruzi* infection and this acute inflammation seems to be longer. Thus, COX-2 may play a role in the initiation as well as resolution of inflammation.

Defective Prostaglandin E receptor-2 signalling reduces immune cell infiltration and inflammation in the cardiac tissue during the acute phase of *Trypanosoma cruzi* infection. This effect can be related with macrophage inability for full activation as evidenced by the decreased ability of $EP2^{-/-}$ macrophages to express MHC-II in the cell surface.

COX-2 deficiency reduces T cell immunosuppression observed during the acute phase of *Trypanosoma cruzi* infection. Defective iNOS induction in the absence of COX-2 could explain the reduced immunosuppression in spleen cells from $COX\text{-}2^{-/-}$ mice infected by *Trypanosoma cruzi*.

Los macrófagos que infiltran el corazón de ratones infectados con *Trypanosoma cruzi* expresan COX-2. Las células mieloides $CD11b^+$ purificadas del infiltrado son capaces de producir PGE_2 y $PFG_{2\alpha}$.

La expresión de la 12/15-Lipoxigenasa aumenta en el tejido cardiaco durante la fase aguda de la infección por *Trypanosoma cruzi*. La expresión de la enzima es dependiente del receptor de IL-4.

***Trypanosoma cruzi* no es capaz de producir por sí mismo ni prostaglandinas ni tromboxanos.** *Trypanosoma cruzi* no posee las rutas metabólicas para producir prostaglandinas y tromboxanos a partir del ácido araquidónico.

La deficiencia de COX-2 no produce cambios en la carga parasitaria pero reduce la inflamación inducida por la infección con *Trypanosoma cruzi*, aunque prolonga esta inflamación durante la fase aguda. COX-2 podría tener un papel tanto en la iniciación como en la resolución de la inflamación.

La ausencia de la señalización de PGE2 a través del receptor EP-2 reduce la infiltración celular y la inflamación en el tejido cardiaco durante la fase aguda de la infección por *Trypanosoma cruzi*. Este proceso puede estar relacionado con la incapacidad del macrófago de activarse completamente al observarse que los macrófagos deficientes para EP-2 expresan menos MHC-II en la superficie.

La deficiencia de COX-2 reduce la inmunosupresión de las células T que sucede en la fase aguda de la infección por *Trypanosoma cruzi*. La reducción de la inducción de la iNOS en ausencia de COX-2 podría explicar la reducción de la inmunosupresión del bazo en los ratones $COX\text{-}2^{-/-}$ infectados con *Trypanosoma cruzi*.

DISCUSSION

Leukocyte infiltration in *Trypanosoma cruzi* infected heart is a key event in parasite elimination and eventually in pathology generation. During the acute phase of infection a severe myocarditis has been described in humans and experimental models of infection. Many immune cell types have been shown to have a direct or indirect role in parasite elicited immune response (Truyens and Carlier, 2010). The role of cytokines in *T. cruzi* infection has been widely studied (Abrahamsohn and Coffman, 1996; Graefe et al., 2003; Silva et al., 1995). However, non-protein mediators have also an important role in immune response. For instance, nitric oxide is a gas with many biological actions as vasodilation, intracellular-pathogen killing or regulation of protein function by nitrosylation and is related with the damaging oxidative stress and immunosuppression. Besides, derivatives of fatty acids also have a wide range of actions in the organism. Metabolism of the arachidonic acid leads to generation of eicosanoids which includes compounds as prostaglandins, thromboxanes, leukotrienes and lipoxins (Stables and Gilroy, 2011). All these molecules have important roles in homeostasis and immune response regulation (Harris et al., 2002). The enzymes implied in their production, (cyclooxygenases, lipoxygenases, p450 cytochrome) have been investigated for many years (Dubois et al., 1998; Levy et al., 1993). In fact, NSAIDs, the most widely used anti-inflammatory agents, are inhibitors of cyclooxygenases. Despite this, scarce data about the cell source of the key enzymes of eicosanoids production in experimental *Trypanosoma cruzi* infection exists and the few published using pharmacological inhibition of cyclooxygenases are contradictory (Machado et al., 2011). Thus, we addressed the role of these mediators in the acute phase of *T. cruzi* infection using a murine model. The analysis of cardiac tissue revealed an increase of COX-2 and 12/15-LO expression (12/15-LO) upon infection and two cellular sources of COX-2 were characterized: cardiomyocytes and macrophages. Besides, macrophages isolated from infected heart produces PGE_2 from arachidonic acid. We next assessed whether COX-2 and PGE_2 would be important in cardiac inflammation. For this, we used mice deficient in COX-2 and PGE_2 receptor (EP-2) and pharmacological inhibition of COX-2. Our results showed that the extent of myocarditis was reduced in the deficient models, suggesting a pro-inflammatory role of COX-2 and PGE_2 in the onset of cardiac inflammation.

Cyclooxygenases and terminal synthases expression in heart of *Trypanosoma cruzi* infected mice

Increased levels of prostaglandins in serum were observed when mice were infected with *T. cruzi* (Cardoni and Antunez, 2004). Since this and other lipid mediators were suggested as important in *T. cruzi* immune response (Machado et al., 2011), expression of the producing enzymes was analyzed in the infected heart of resistant and susceptible murine models. As expected, COX-2 gene expression was increased in the heart tissue due the inflammation. Our laboratory has also recently published that cardiomyocytes express COX-2 upon *T. cruzi* infection (Corral et al., 2013). Nevertheless, in this work we have focused in the macrophage contribution. A previous study has described an increase in COX-1 and COX-2 protein expression in infected cardiac tissue by immunohistochemistry (Abdalla et al., 2008); however, we consider that appropriate controls were not presented in that study, In contrast, in the present study, COX-2 protein expression was clearly demonstrated in a $CD11b^+$ $CD68^+$ macrophage population in the infected heart. We found a perinuclear

pattern of COX-2 expression in macrophage, as described (Bozza et al., 2011; Morita et al., 1995). Some of the pictures revealed a possible COX-2 expression in the nuclear envelope similar to what has been described in endothelial cells (Parfenova et al., 2001). We corroborated this data by adding radiolabelled arachidonic acid to macrophages isolated from the infected heart, which produced PGE_2 and $PGF_{2\alpha}$. This result is in agreement to published data regarding prostaglandins produced during infection (Cardoni and Antunez, 2004; Oliveira et al., 2010). In order to check if macrophages from other origin produce these prostaglandins during infection we purified $CD11b^+$ cells from the peritoneum of infected mice and PGE_2 production was also evidenced. But these cells were unable to produce all the prostaglandins that the cells from the peritoneum of non-infected animals can produce. Infiltration of $CD11b^+$ COX-2 expressing cells and exit of the resident peritoneal macrophages could explain the different generation of prostaglandins. In this regard, Cassado Ados *et al.* have described how the peritoneal cell populations change during *T. cruzi* infection, from resident to an inflammatory phenotype (Cassado Ados et al.). Moreover, we cannot exclude the presence of B-1 cells in our experiment because is already described that these cells can express CD11b in its surface (Hastings et al., 2006) adhere to the culture plate, transform to phagocytes (Almeida et al., 2001; Parra et al., 2012) and express COX-2 (Graf et al., 1999). In addition, B-1 cell maturation in *T. cruzi* infected mice has been described (Merino et al., 2012). Thus, some of this peritoneal cell PGE_2 generation could come from B-1 cells. Moreover, induction of COX-2 expression by macrophages seems to need a stronger stimuli than infection alone, probably TNF-α and IFN-γ (Munoz-Fernandez et al., 1992) because infection alone could pass mostly unnoticed by the macrophage regarding its activation status (Thi et al., 2012).

We have also found that $CD68^-$ cells express COX-2 in infected cardiac tissue. Since lymphocytes are important regulators in *T. cruzi* elicited immune response (Tarleton et al., 1996; Tarleton et al., 1992), infiltrate the infected heart tissue; (Tarleton et al., 1994) and COX-2 expression has been shown in T cells upon activation (Iniguez et al., 1999), we checked whether infiltrating $CD4^+$ expressed COX-2 cells in our samples. However, no COX-2 expression was detected in $CD4^+$ lymphocytes. Nevertheless, COX-2 expressing $CD8^+$ T cells cannot be ruled out since PGE_2 production by $CD8^+$ T lymphocytes has been described in the context of *T. cruzi* infection (Celentano et al., 1995; Sterin-Borda et al., 1996). Further study is necessary to accurately determine the non-macrophage COX-2 sources in the infected heart. Multicolor flow cytometry analysis could be the best suited technique to clarify this issue.

Increase of *Txas* and *Hpgds* gene expression suggests the production of TXA_2 and PGD_2 and its metabolites respectively in infected cardiac tissue. TXA_2 could have a pro-inflammatory role in monocytes (Caughey et al., 1997) besides its vascular functions (Cheng et al., 2002). In contrast, PGD_2 has anti-inflammatory actions (Bellows et al., 2006; Kanaoka and Urade, 2003). Resistant mice (C57BL/6) showed higher expression of *Hpgds* and lower expression of *Txas* than the susceptible model (BALB/c). This could be related with the fact that inflammation in resistant mice ends earlier than in susceptible mice (Cuervo et al., 2008). The expression of the terminal synthase of prostacyclin, PGI_2 (*Pgis*) (Dorris and Peebles, 2012) was not studied. Nonetheless, it could be of interest to analyze its expression, since PGI_2 metabolite has been detected in infected

animals (Cardoni and Antunez, 2004). Also, PGI_2 could be secreted to counteract the deleterious effect of inflammation (Camacho et al., 2011) and ischemic processes that occurs during infection (Marin-Neto et al., 2007). Accurate quantification of endogenous eicosanoids in the infected cardiac tissue must be performed in order to have a global perspective to integrate the different mediators in their physiological context (Blaho et al., 2009).

On the other hand, COX-2 expressing macrophages seem to be different from the $CD11b^+$ myeloid expressing Arginase 1 (Arg-1) that also infiltrate the infected heart (Cuervo et al., 2008). This remarkable finding suggests a difference in the function of these two macrophage populations. Resident macrophages of C57BL/6 mice heart have a gene expression signature close to M2 (Pinto et al., 2012) and could be implied in tissue repair and fibrosis (Wynn and Barron, 2010). Furthermore, *in situ* proliferation of resident macrophages has been described in a helminth infection model where the Th2 response is important (Jenkins et al., 2011). In our model, monocyte cardiac infiltration could be very important to fight the parasite and also to repair the damaged muscular tissue (Arnold et al., 2007). Arg-1^+ macrophages could be related with repair meanwhile COX-2 expressing macrophages could be linked to inflammation. But this explanation is probably simplistic and far from a more complex reality because macrophages are highly heterogeneous cells that can rapidly change their function in response to local microenviromental signals, playing key roles in the initiation and resolution of inflammation and tissue homeostasis (Murray and Wynn, 2011), therefore this may constitute an amenable hypothesis to test.

Regarding cardiomyocyte contribution to prostaglandin secretion, we recently described that *T. cruzi* infection and Endothelin-1 cooperatively activated the Ca^{2+}/calcineurin/Nuclear Factor of Activated T-cells (NFAT) signaling pathway in atrial myocytes, leading to COX-2 protein expression and increased PGE_2, TXA_2 and $PGF_{2\alpha}$ secretion (Corral et al., 2013). $PGF_{2\alpha}$ and ET-1 (Bouallegue et al., 2007) may contribute in a cooperative way to induce chagasic cardiac hypertrophy (Rossi, 1995; Rossi, 2001) since $PGF_{2\alpha}$ can also activate the NFAT pathway to induce cardiomyocyte enlargement (Lai et al., 1996; Hernandez-Subira E, unpublished results).

Lipoxygenase expression in cardiac tissue during the acute phase of *Trypanosoma cruzi* infection

Lipoxygenases (LO) enzymes generate lipid mediators that are involved in a number of significant physiological and pathological states (Dobrian et al., 2011). In the present work we have analyzed the expression of 5-LO, 5-LO activating protein (FLAP), 12-LO and 12/15-LO. 5-LO and FLAP are responsible for leukotrienes (LTs) synthesis, which have an important active role in inflammation. These enzymes have been studied in different models of cardiovascular disease (Poeckel and Funk, 2010) In addition, LO are considered good targets for anti-inflammatory therapies (Rubin and Mollison, 2007; Sampson, 2009). Previous works with 5-LO deficient mice and enzyme inhibitors were used to define the role of endogenous LTs in inflammatory responses elicited by infection with *T. cruzi.* One group described how the infected 5-$LO^{-/-}$ mice died meanwhile wild type did not (Borges et al., 2009; Panis et al., 2011). However, another group described how 5-LO deficiency improved survival and reduced cardiac inflammation (Pavanelli et al., 2010). Despite the fact that both groups used the

same mouse and parasite strain combination, Pavanelli *et al.* used 50 times less parasite than the others to infect mice and this may be determinant in the final outcome of *T. cruzi* infection. On the other hand, when 5-LO was pharmacologically inhibited during *T. cruzi* infection no changes were found in survival, although LTB_4 induced parasite killing by iNOS *in vitro* (Talvani et al., 2002). In our studies we could not detect any increase of *Alox5* (5-LO) mRNA, in fact we found a reduction of the mRNA expression in the infected hearts. Nevertheless, *Alox5ap* (FLAP) gene expression was increased in both BALB/c and C57BL/6 models of infection. *Alox5ap* induction in the inflamed infected heart could be important, even in absence of changes in *Alox5* levels, because changes in FLAP expression have been shown to modify the profile of LTs produced by 5-LO (Peters-Golden and Brock, 2003). Unfortunately, we could not detect the protein by western blotting in whole cardiac extracts or purified macrophages (**not shown**) and thus, the cell source for FLAP was not identified.

12/15-Lipoxigenase(12/15-LO)is preferentially expressed in mammals by monocyte and macrophages following the action of T helper type 2 cytokines IL-4 and IL-13 (Heydeck et al., 1998). This enzyme is responsible for production of different lipid mediators that have an important role inflammatory diseases (Dobrian et al., 2011). Hydroxyeicosatetraenoic acids (HETEs)metabolites are produced by 12/15-LO that can bind PPAR-γ exerting anti-inflammatory properties (Limor et al., 2008; Subbarayan et al., 2006). Lipoxins (LXs) are other 12/15-LO derivatives with an important role in the resolution of inflammation (Parkinson, 2006). In the present work mRNA analysis in infected cardiac tissue revealed an *Alox15* (12/15-LO gene) expression during the acute phase of *T. cruzi* infection in both BALB/c and C57BL/6 mouse strain. The expression was higher in C57BL/6 than BALB/c, which may be related with a better response against the parasite and faster resolution of inflammation. IL-4 deficient infected mice showed a reduced *Alox15* expression in heart tissue compared to wild-type mice, indicating its dependency on IL-4. When histological sections were analyzed we could not find the cell type that produces the protein. However, we could discard $CD68^{+}$ macrophages and fibroblasts as responsible for the enzyme expression. These results did not fit with the accepted the idea that macrophages are the main cells that express the enzyme (Kuhn and O'Donnell, 2006). However, $CD68^{low}$ macrophages have been described to express 12/15-LO (Rabinowitz and Gordon, 1991). The use of an anti-CD11b and anti-12/15-LO antibodies to stain heart tissue sections could provide an answer to this question.

In order to detect fibroblasts we used an antibody against the intermediate cytoskeleton filament vimentin (Lian et al., 2012). Surprisingly, staining of amastigotes was detected (**Fig. 16C**). One of the reasons for detecting the vimentin signal in the parasites could be unrelated to the cytoskeleton, since vimentin has been described as a macrophage secretion product with antimicrobial properties (Mor-Vaknin et al., 2003), which is deposited in cardiac cells (Ise et al., 2010). Despite the absence of definitive characterization of the cell type producing 12/15-LO the fact that is increased in infected hearts suggests a role in the infection. During local contained inflammation, the first line of host defense, namely the neutrophils, die at the site and can undergo cell death by apoptosis as well as necrosis. As part of resolution, LX signal macrophages to enhance the uptake of the remains of these cells (Serhan et al., 2011). It is known that the uptake of apoptotic cells by macrophages

induces LXs secretion (Freire-de-Lima et al., 2006). This process can modify the functions of the macrophage impairing inflammation and allowing *T. cruzi* persistence (Freire-de-Lima et al., 2000). In this regard, similar results were found in *Leishmania major* infection (van Zandbergen et al., 2006; Wenzel and Van Zandbergen, 2009). Moreover, 12/15-LO has been also linked with cardiac infarct (Kayama et al., 2009) and macrophage recruitment (Wen et al., 2008). Therefore, this enzyme may serve in acute *T.cruzi* infection to enhance macrophage recruitment and once those cells reach the infected heart help to facilitate tissue repair. 12/15-LO deficient mice showed an increased mortality when infected by *Toxoplasma gondii* (and intracellular parasite) (Middleton et al., 2009). Hence, the use of 12/15-LO deficient model (Sun and Funk, 1996) could provide an interesting tool to further analyze the role of the enzyme in *T. cruzi* infection.

Trypanosoma cruzi metabolism of arachidonic acid

Production of arachidonic acid (AA) and other fatty acid bioactive metabolites by human pathogens has been described and reviewed (Kubata et al., 2007). Not only protozoan but also helminthes and fungi can produce these mediators. Compared to mammalian lipid mediator production, little is known regarding the biochemistry of their production by eukaryotic microorganisms and no cyclooxygenase–like gene has been described in parasite sequenced genomes (Noverr et al., 2003). Nonetheless, those lipids may regulate some parasite functions (Figarella et al., 2005) as well as to contribute to host-pathogen communication in the context of the immune responses regulation (Kilunga Kubata et al., 1998). Phospholipases (PLs) are the first enzymes implied in AA metabolism because they could release free fatty acid from membrane phospholipids. Phospholipase activities have been described in *T. brucei, Leishmania sp.* and *T. cruzi*. TcPLA$_1$ enzyme has been even cloned from *T. cruzi*, but despite some evidences, no *T. cruzi* PLA$_2$ has been well characterized (Belaunzaran et al., 2011). Remarkably, no cyclooxygenase activity has been cloned from *T. cruzi*. However, two different research groups in Japan and USA have described a parasite PGF$_{2\alpha}$ synthase activity (Kubata et al., 2002) and a TXA$_2$ synthase activity (Ashton et al., 2007), reviewed in (Machado et al., 2011). In these works, both groups described the conversion of radiolabelled AA into prostaglandins using parasite extracts. In order to check if the PGE$_2$ and PGF$_{2\alpha}$ production that we observed in our experiments could be due to traces of parasites in the culture or in myeloid cells from infected animals harboring intracellular amastigote parasites, we tried to reproduce those published results (Ashton et al., 2007; Kubata et al., 2002). We performed the experiments with living or homogenized parasites from three distinct strains and the three life cycle stages of *T. cruzi.* We could not detect a parasite-derived prostaglandin when the experiments were carried out in absence of hematin. We decided to add the hematin in our reaction buffer in order to reproduce the same published conditions. In those cases we obtained two signals in HPLC runs. One of them seems to correspond to 6-oxo-PGF$_{1\alpha}$ (the main prostacyclin metabolite) and the other did not correspond to any of the standards injected. 6-oxo-PGF$_{1\alpha}$ production has not been described in the previous mentioned reports (Ashton et al., 2007; Kubata et al., 2002). Nevertheless, we think that this could be an experimental artifact. There is no logical reason, in my opinion, to add hematin into the reaction buffer in this kind of experiment. Addition of heme groups is necessary and justified when

a cyclooxygenase activity assay is performed. Hydroperoxides generates the ferryl-oxo complex with the iron of the heme group. This porphyrin-derived complex is a cyclooxygenase prosthetic group key in the catalytic activity (Marnett et al., 1999). Another key aspect leads us to think in a poorly controlled experimental design in Asthon´s report (Ashton et al., 2007). They added stannous chloride to "quench" the reaction. But it has been demonstrated that the addition of stannous chloride converts PGH_2 into $PGF_{2\alpha}$ avoiding spontaneous non-enzymatic PGE_2 and PGD_2 generation (Camacho et al., 1998). This stannous chloride uncontrolled addition is not justified if the aim of the experiment is to characterize the whole prostaglandin profile produced by a cell homogenate. The scarcity of cyclooxygenase activity that we observed in parasites and data regarding AA metabolism in *T. cruzi* makes less plausible even more this justification. However, the parasite could be metabolizing extracellular PGH_2 by a transcellular mechanism. Despite the characterization of terminal synthases in *T. cruzi*, no clear results of prostaglandin generation from AA by *T. cruzi* have been provided in my opinion by those authors. Therefore, their data must been taken carefully. Nonetheless, as previously mentioned, the *T. cruzi* scientific community has accepted that *T. cruzi* produces PGs, further complicating the interpretation of the potential therapeutic role of NSAIDs on Chagas' disease.

COX-2 deficient reduces cardiac inflammation induced by *Trypanosoma cruzi* infection in mice

Since we found that the expression of COX-2 in the *T. cruzi* infected cardiac tissue was increased during infection, we further analyzed its role in the pathophysiology of the disease. For this, we first used a pharmacological approach to inhibit COX-2 using BALB/c (susceptible) and C57BL/6 (resistant) mice. We observed that mortality tended to increase in the susceptible model, but not in the resistant model. However, no changes in inflammation or parasite load were observed after COX-2 inhibition in any of the infected mouse models. We only tried one route of treatment, and it is possible that other routes may deliver the drug more efficiently, and thus our results cannot be considered conclusive. Nevertheless, there are contradictory reports published with COX-2 inhibitors with contradictory data (Machado et al., 2011). In addition, COX-2 inhibitors may interfere with the immune response (Iniguez et al., 1999), but more importantly many COX-2 inhibitors have effects independent of their ability to inhibit cyclooxygenase activity (Iniguez et al., 2010; Schror, 2011; Xu et al., 2001). Altogether, these precedents discouraged us from pursuing this part of the study.

Interestingly, different results were obtained with the COX-2 deficient mice. First, we found a slight reduction (three times less) in parasitemia in COX-$2^{-/-}$ respect to the wild type mice. However, no changes were observed in cardiac parasite burden, in spite that COX-$2^{-/-}$ mice express less iNOS gene, considered to be key for resistance to infection. In a viral model of infection with *influenza*, COX-2 deficient mice presented a decreased pathogen load respect to wild type mice (Carey et al., 2005). We did not observe any significant differences in the levels of *T. cruzi* specific antibodies despite reports showing that immunization of COX-2 deficient animals with a viral vaccine resulted in a decrease in the levels of antibodies (Ryan et al., 2006).

Other laboratories have studied the response to *T. cruzi* infection in mice deficient in other enzymes of the arachidonic acid pathway

(Mukherjee et al., 2011; Sharma et al., 2013). The main drawback to compare our results with those already published is the distinct model of infection used. Sharma *et al*. used a susceptible model and described that deficiency of iPLA$_2$γ (Ca^{++} independent PLA$_2$ isoform-γ), which is implied in arachidonic acid membrane release, aggravated infection and survival. Others described that COX-1$^{-/-}$ mice showed higher parasitemia than wild-type mice, but did not shown changes in survival (Mukherjee et al., 2011). Using COX-1 and COX-2 deficient mice in non-infectious inflammatory models, the importance of COX-1 in the initiation of inflammation and of COX-2 in cell recruitment has been suggested (Langenbach et al., 1999). COX-2 deficient mice showed a reduced cardiac inflammation induced by *Trypanosoma cruzi* infection. Our results are in agreement with a sepsis model using COX-2$^{-/-}$ mice (Ejima et al., 2003), where they described a less inflammatory response than the wild-type controls. Importantly, we found that COX-2 deficiency reduces infiltration of different cell types as lymphocytes and myeloid cells (including MDSCs) in infected heart tissue that could explain the lower inflammation. An important role of COX-2 derived PGs in migration of immune cells to infected tissues or lymphoid organs is becoming evident from recent results of our laboratory (Diaz_Muñoz et al., J Immunol. submitted; Sreeramkumar, et al submitted). The decrease in cardiac inflammation and the expression of L-arginine metabolizing enzymes (iNOS and Arg-1), cytokines and chemokines observed at 14 d.p.i. together with higher cardiac IL-4 expression in COX$^{-/-}$ infected mice seem to be related with the pro-inflammatory role of PGE$_2$ rather than its immunosuppressive function (Nagamachi et al., 2007; Yao et al., 2009). However, at 21 d.p.i. the levels of expression of *Ccl3, Ccl4* and *Cxcl9* chemokines were higher in COX-2$^{-/-}$ in comparison with wild-type controls. At this time point, the levels of TNF-α and IFN-γ were not reduced compared to 14 d.p.i. In addition, plasma TNF-α levels were higher at 21 d.p.i. This apparently contradictory data can be explained if we take into account the complexity of eicosanoid generation (Stables and Gilroy, 2011). Thus, in general, a first wave of pro-inflammatory mediators (PGE$_2$, PGI$_2$, LTB$_4$) is followed by pro-resolving ones (15d-PGJ$_2$ and lipoxins), process known as lipid mediator class switching. The temporal relationship between separate classes of eicosanoids that represent COX and individual LO pathways remains to be established. These temporal relationships are central to the understanding of the role of lipid mediators in inflammation in general and during *T. cruzi* infection in particular. It has been reported that, during the course of a self-resolving acute inflammatory response that was spatially contained, a clear temporal staging of structurally and functionally distinct classes of eicosanoids occurred . Thus, we believe that a similar effect is taking place in T. *cruzi*-infected COX-2$^{-/-}$ mice.

On the other hand, a Th17 response was found to be protective during the acute phase of *T. cruzi* infection with a low parasite inoculum (da Matta Guedes et al., 2010; Miyazaki et al., 2010), being induced by IL-12 (Cobb and Smeltz, 2012) and osteopontin (Boniface et al., 2009; Santamaria and Corral, 2013). Our laboratory has found that susceptible mice develop a Th17 response that is protective at low parasite inoculum, but pathogenic at high parasite inoculum (Sanoja *et al.* PLoS one submitted). However, when resistant mice (129Sv-C57BL/6 mixed background) were infected with high parasite inoculum, we detected that the expression of genes implied in Th17 development as *Stat-3* and *Irf4* were reduced in COX-2 deficient mice respect to resistant wild-type mice, although

another one as *Rorc* was not and neither *Il17* was detected (**supplementary figure S7**). Considering that PGE_2 can promote Th17 development (Boniface et al., 2009), the reduced inflammation that we found in COX-$2^{-/-}$ mice and the decrease in *Stat3* and *Irf4* expression could be explained by reduced levels of PGE_2 in COX-$2^{-/-}$ mice. However, complete understanding on the role of PGE_2/Th17 in *T. cruzi* infection is difficult. Thus, PGE_2 also affect Th1 cells (Sreeramkumar et al., 2012) and Th1/Th17 have complex interactions in the immune regulation (Damsker et al., 2010; Tournadre and Miossec, 2012). Studying the effect of COX-2 deficiency in a susceptible genetic background mice (i.e. BALB/c), where the role of Th17 is more evident (Sanoja et al PLoS one submitted) may provide a clear answer to this question. Thus, the role of PGE_2 in the Th17 response during *T. cruzi* infection remains an open issue.

ET-1 aggravates the cardiac damage generated during *T. cruzi* infection (Andrade et al., 2012). Moreover, ET-1 receptor antagonist has a protective role in heart tissue (Rachid et al., 2006) and central nervous system (Rachid et al., 2010) in a rat model of *T. cruzi* infection. In contrast, it has been described in mice that the same ET-1 receptor antagonist produces only a minor effect in infected mice (Roffe et al., 2010). We did not detect changes in COX-2 expression upon ET-1 receptor antagonist treatment, in agreement with the previous work performed with mice. However, the effect of ET-1 in COX-2 expression in the *T. cruzi* infected heart is probably being masked by other more powerful ET-1-independent COX-2-inducing mechanisms.

Defective PGE_2 receptor EP-2 signalling reduces immune cell infiltration and inflammation in the cardiac tissue during the acute phase of *Trypanosoma cruzi* infection

COX enzymes are responsible for production of many different prostaglandins with sometimes, opposite actions. This complexity makes hard to obtain clear results from COX deletion models and specific PG-receptor deficient mice should be more suitable for that task (Sugimoto and Narumiya, 2007; Yuhki et al., 2011). Thus, we infected PGE_2,-receptor-2 (EP-2) deficient mice with *T. cruzi*. EP-2-/- mice, generated in the C57BL/6 genetic background did not show any changes in survival, parasite burden or plasma levels of *T. cruzi* specific antibodies. Cell infiltration was also decreased in EP-$2^{-/-}$ mice as COX-$2^{-/-}$ mice did. They showed decreased gene expression of *Ptgs2, Ccl2, Ifng, Il12, Il10, Il6* and *Il4* revealing the important role of PGE_2 in the inflammation onset. However, *Tnf* gene expression and plasma level remains unchanged, in agreement with the *in vivo* results after bacterial infection (Aronoff et al., 2012). Nevertheless, in human macrophages there was a reduction in TNF-α secretion in response to EP-2 signaling (Ratcliffe et al., 2007). It has been described that MHC-II surface expression is decreased by the use of EP-2 agonists (Harizi et al., 2003). In contrast, we found that EP-$2^{-/-}$ spleen macrophages from infected mice express low MHC-II in the cell surface. This apparent discrepancy could be attributed to the difference between cell types and *in vivo* approaches. Nonetheless, the fact that EP-2 is required for $CD4^+$T lymphocyte activation and T cell-dendritic cell interaction (Sreeramkumar , *et al.* submitted) together with the results presented here, further support a more thoroughly analysis of macrophage and lymphocyte function in *T. cruzi* infected EP-$2^{-/-}$ mice.

COX-2 deficiency reduces T cell immunosuppression during the acute phase of *Trypanosoma cruzi* infection

A severe suppression of splenic T cell proliferation to mitogens and antigens is a characteristic of the acute phase of *T. cruzi* infection in mice. The impairment of proliferation is associated with high levels of IFN-γ and NO and with decreased production of IL-2 in the supernatants of spleen cells cultures from infected mice. Adherent cells, mainly macrophages, are key in this process (Abrahamsohn and Coffman, 1995). Besides the well documented participation of NO as suppressive factor (Goni et al., 2002; Gutierrez et al., 2009), studies with pharmacological inhibitors of COX-2 suggested a role of its metabolites in immunosuppression (Abdalla et al., 2008; Michelin et al., 2005; Pinge-Filho et al., 1999). To further clarify this issue we infected COX-2 deficient mice and analyzed *ex vivo* spleen cell proliferation. A reduced immunosuppression was found in the spleens from infected COX-2 deficient mice, compared to control wild-type mice, during the acute phase of *T.cruzi* infection. We observed that reduced immunosuppression in COX-$2^{-/-}$ mice was independent of total and $CD11b^{+}Gr\text{-}1^{+}$ spleen cell number and also from EP-2 signaling. Rather, we found that the effect of COX-2-derided PGs in this phenomenon was related to its ability to modulate iNOS expression, which was decreased in the spleen of COX-$2^{-/-}$ respect to wild-type infected mice. This is in agreement with induction of iNOS expression by COX-2-derived PGs in macrophages in other systems (Gaillard et al., 1992; Hori et al., 2001). Cyclooxygenase inhibition in the spleen cells seems to be irrelevant in our *in vitro* cultures, probably because the immunosuppression at 21 d.p.i. of the BALB/c model was already too severe to be restored pharmacologically, as was published before (Pinge-Filho et al., 1999).

Surprisingly, PGE_2 levels in the supernatant of cells coming from infected COX-$2^{-/-}$ mice were not ablated. COX-1 in cooperation with mPGES-1 can secrete PGE_2. In agreement with this result,, COX-1 and not COX-2 produced PGE_2 in the bronco-alveolar lavage of *influenza* infected mice (Carey et al., 2005). During *T. cruzi* infection COX-1 protein expression was induced in the spleen and could be responsible for some of the published actions of COX inhibitors used in the experiments with splenocytes from infected mice. This enzyme usually is constitutively expressed and is usually assumed that its expression does not change (Smith et al., 1996). However, COX-1 induction in immune cells has been described in other models (Samet et al., 1995), in agreement with our results.

BIBLIOGRAPHY

Abdalla, G.K., G.E. Faria, K.T. Silva, E.C. Castro, M.A. Reis, and M.A. Michelin. 2008. Trypanosoma cruzi: the role of PGE2 in immune response during the acute phase of experimental infection. *Experimental parasitology* 118:514-521.

Abrahamsohn, I.A., and R.L. Coffman. 1995. Cytokine and nitric oxide regulation of the immunosuppression in Trypanosoma cruzi infection. *J Immunol* 155:3955-3963.

Abrahamsohn, I.A., and R.L. Coffman. 1996. Trypanosoma cruzi: IL-10, TNF, IFN-gamma, and IL-12 regulate innate and acquired immunity to infection. *Experimental parasitology* 84:231-244.

Abrahamsohn, I.A., A.P. da Silva, and R.L. Coffman. 2000. Effects of interleukin-4 deprivation and treatment on resistance to Trypanosoma cruzi. *Infection and immunity* 68:1975-1979.

Alba Soto, C.D., G.A. Mirkin, M.E. Solana, and S.M. Gonzalez Cappa. 2003. Trypanosoma cruzi infection modulates in vivo expression of major histocompatibility complex class II molecules on antigen-presenting cells and T-cell stimulatory activity of dendritic cells in a strain-dependent manner. *Infection and immunity* 71:1194-1199.

Alfranca, A., M.A. Iniguez, M. Fresno, and J.M. Redondo. 2006. Prostanoid signal transduction and gene expression in the endothelium: role in cardiovascular diseases. *Cardiovascular research* 70:446-456.

Aliberti, J.C., M.A. Cardoso, G.A. Martins, R.T. Gazzinelli, L.Q. Vieira, and J.S. Silva. 1996. Interleukin-12 mediates resistance to Trypanosoma cruzi in mice and is produced by murine macrophages in response to live trypomastigotes. *Infection and immunity* 64:1961-1967.

Almeida, S.R., L.S. Aroeira, E. Frymuller, M.A. Dias, C.S. Bogsan, J.D. Lopes, and M. Mariano. 2001. Mouse B-1 cell-derived mononuclear phagocyte, a novel cellular component of acute non-specific inflammatory exudate. *International immunology* 13:1193-1201.

Andrade, D., R. Serra, E. Svensjo, A.P. Lima, E.S. Ramos, Jr., F.S. Fortes, A.C. Morandini, V. Morandi, N. Soeiro Mde, H.B. Tanowitz, and J. Scharfstein. 2012. Trypanosoma cruzi invades host cells through the activation of endothelin and bradykinin receptors: a converging pathway leading to chagasic vasculopathy. *British journal of pharmacology* 165:1333-1347.

Andrade, L.O., C.R. Machado, E. Chiari, S.D. Pena, and A.M. Macedo. 2002. Trypanosoma cruzi: role of host genetic background in the differential tissue distribution of parasite clonal populations. *Experimental parasitology* 100:269-275.

Antunez, M.I., and R.L. Cardoni. 2000. IL-12 and IFN-gamma production, and NK cell activity, in acute and chronic experimental Trypanosoma cruzi infections. *Immunology letters* 71:103-109.

Antunez, M.I., and R.L. Cardoni. 2001. Early IFN-gamma production is related to the presence of interleukin (IL)-18 and the absence of IL-13 in experimental Trypanosoma cruzi infections. *Immunology letters* 79:189-196.

Arima, M., and T. Fukuda. 2011. Prostaglandin D(2) and T(H)2 inflammation in the pathogenesis of bronchial asthma. *The Korean journal of internal medicine* 26:8-18.

Arnold, L., A. Henry, F. Poron, Y. Baba-Amer, N. van Rooijen, A. Plonquet, R.K. Gherardi, and B. Chazaud. 2007. Inflammatory monocytes recruited after skeletal muscle injury switch into antiinflammatory macrophages to support myogenesis. *The Journal of experimental medicine* 204:1057-1069.

Aronoff, D.M., I.L. Bergin, C. Lewis, D. Goel, E. O'Brien, M. Peters-Golden, and P. Mancuso. 2012. E-prostanoid 2 receptor signaling suppresses lung innate immunity against Streptococcus pneumoniae. *Prostaglandins & other lipid mediators* 98:23-30.

Aronoff, D.M., C. Canetti, and M. Peters-Golden. 2004. Prostaglandin E2 inhibits alveolar

macrophage phagocytosis through an E-prostanoid 2 receptor-mediated increase in intracellular cyclic AMP. *J Immunol* 173:559-565.

Aronoff, D.M., C.M. Peres, C.H. Serezani, M.N. Ballinger, J.K. Carstens, N. Coleman, B.B. Moore, R.S. Peebles, L.H. Faccioli, and M. Peters-Golden. 2007. Synthetic prostacyclin analogs differentially regulate macrophage function via distinct analog-receptor binding specificities. *J Immunol* 178:1628-1634.

Ashton, A.W., S. Mukherjee, F.N. Nagajyothi, H. Huang, V.L. Braunstein, M.S. Desruisseaux, S.M. Factor, L. Lopez, J.W. Berman, M. Wittner, P.E. Scherer, V. Capra, T.M. Coffman, C.N. Serhan, K. Gotlinger, K.K. Wu, L.M. Weiss, and H.B. Tanowitz. 2007. Thromboxane A2 is a key regulator of pathogenesis during Trypanosoma cruzi infection. *The Journal of experimental medicine* 204:929-940.

Belaunzaran, M.L., E.M. Lammel, and E.L. de Isola. 2011. Phospholipases a in trypanosomatids. *Enzyme research* 2011:392082.

Bellows, C.F., A. Alder, P. Wludyka, and B.M. Jaffe. 2006. Modulation of macrophage nitric oxide production by prostaglandin D2. *The Journal of surgical research* 132:92-97.

Blaho, V.A., M.W. Buczynski, C.R. Brown, and E.A. Dennis. 2009. Lipidomic analysis of dynamic eicosanoid responses during the induction and resolution of Lyme arthritis. *The Journal of biological chemistry* 284:21599-21612.

Boniface, K., K.S. Bak-Jensen, Y. Li, W.M. Blumenschein, M.J. McGeachy, T.K. McClanahan, B.S. McKenzie, R.A. Kastelein, D.J. Cua, and R. de Waal Malefyt. 2009. Prostaglandin E2 regulates Th17 cell differentiation and function through cyclic AMP and EP2/EP4 receptor signaling. *The Journal of experimental medicine* 206:535-548.

Borges, C.L., R. Cecchini, V.L. Tatakihara, A.D. Malvezi, S.F. Yamada-Ogatta, L.V. Rizzo, and P. Pinge-Filho. 2009. 5-Lipoxygenase plays a role in the control of parasite burden and contributes to oxidative damage of erythrocytes in murine Chagas' disease. *Immunology letters* 123:38-45.

Bouallegue, A., G.B. Daou, and A.K. Srivastava. 2007. Endothelin-1-induced signaling pathways in vascular smooth muscle cells. *Current vascular pharmacology* 5:45-52.

Bozza, P.T., I. Bakker-Abreu, R.A. Navarro-Xavier, and C. Bandeira-Melo. 2011. Lipid body function in eicosanoid synthesis: an update. *Prostaglandins, leukotrienes, and essential fatty acids* 85:205-213.

Brinckmann, R., and H. Kuhn. 1997. Regulation of 15-lipoxygenase expression by cytokines. *Advances in experimental medicine and biology* 400B:599-604.

Brock, T.G., R.W. McNish, and M. Peters-Golden. 1999. Arachidonic acid is preferentially metabolized by cyclooxygenase-2 to prostacyclin and prostaglandin E2. *The Journal of biological chemistry* 274:11660-11666.

Bryan, M.A., S.E. Guyach, and K.A. Norris. 2010. Specific humoral immunity versus polyclonal B cell activation in Trypanosoma cruzi infection of susceptible and resistant mice. *PLoS neglected tropical diseases* 4:e733.

Byrum, R.S., J.L. Goulet, R.J. Griffiths, and B.H. Koller. 1997. Role of the 5-lipoxygenase-activating protein (FLAP) in murine acute inflammatory responses. *The Journal of experimental medicine* 185:1065-1075.

Camacho, M., J. Lopez-Belmonte, and L. Vila. 1998. Rate of vasoconstrictor prostanoids released by endothelial cells depends on cyclooxygenase-2 expression and prostaglandin I synthase activity. *Circulation research* 83:353-365.

Camacho, M., C. Rodriguez, A. Guadall, S. Alcolea, M. Orriols, J.R. Escudero, J. Martinez-Gonzalez, and L. Vila. 2011. Hypoxia upregulates PGI-synthase and increases PGI(2) release in human vascular cells exposed to inflammatory stimuli. *Journal of lipid research* 52:720-731.

Cao, H., L. Xiao, G. Park, X. Wang, A.C. Azim, J.W. Christman, and R.B. van Breemen. 2008. An improved LC-MS/MS method for the quantification of prostaglandins E(2) and D(2) production in biological fluids. *Analytical biochemistry* 372:41-51.

Cardoni, R.L., and M.I. Antunez. 2004. Circulating levels of cyclooxygenase metabolites in experimental Trypanosoma cruzi infections. *Mediators of inflammation* 13:235-240.

Carey, M.A., J.A. Bradbury, J.M. Seubert, R. Langenbach, D.C. Zeldin, and D.R. Germolec. 2005. Contrasting effects of cyclooxygenase-1 (COX-1) and COX-2 deficiency on the host response to influenza A viral infection. *J Immunol* 175:6878-6884.

Cassado Ados, A., J.A. de Albuquerque, L.R. Sardinha, L. Buzzo Cde, L. Faustino, R. Nascimento, E.E. Ghosn, M.R. Lima, J.M. Alvarez, and K.R. Bortoluci. 2011. Cellular renewal and improvement of local cell effector activity in peritoneal cavity in response to infectious stimuli. *PloS one* 6:e22141.

Castellani, O., L.V. Ribeiro, and J.F. Fernandes. 1967. Differentiation of Trypanosoma cruzi in culture. *J Protozool* 14:447-451.

Caughey, G.E., M. Pouliot, L.G. Cleland, and M.J. James. 1997. Regulation of tumor necrosis factor-alpha and IL-1 beta synthesis by thromboxane A2 in nonadherent human monocytes. *J Immunol* 158:351-358.

Celentano, A.M., G. Gorelik, M.E. Solana, L. Sterin-Borda, E. Borda, and S.M. Gonzalez Cappa. 1995. PGE2 involvement in experimental infection with Trypanosoma cruzi subpopulations. *Prostaglandins* 49:141-153.

Cobb, D., and R.B. Smeltz. 2012. Regulation of proinflammatory Th17 responses during Trypanosoma cruzi infection by IL-12 family cytokines. *J Immunol* 188:3766-3773.

Coffman, R.L., H.F. Savelkoul, and D.A. Lebman. 1989. Cytokine regulation of immunoglobulin isotype switching and expression. *Seminars in immunology* 1:55-63.

Composto, G., D. Gonzalez, A. Bucknum, D. Silberman, J. Taylor, M. Kozlowski, T. Bloomfield, T. Bartlett, and J. Riggs. 2011. Peritoneal T lymphocyte regulation by macrophages. *Immunobiology* 216:256-264.

Corral, R.S., N.A. Guerrero, H. Cuervo, N. Girones, and M. Fresno. 2013. Trypanosoma cruzi Infection and Endothelin-1 Cooperatively Activate Pathogenic Inflammatory Pathways in Cardiomyocytes. *PLoS neglected tropical diseases* 7:e2034.

Corraliza, I.M., G. Soler, K. Eichmann, and M. Modolell. 1995. Arginase induction by suppressors of nitric oxide synthesis (IL-4, IL-10 and PGE2) in murine bone-marrow-derived macrophages. *Biochemical and biophysical research communications* 206:667-673.

Cuervo, H., N.A. Guerrero, S. Carbajosa, A. Beschin, P. De Baetselier, N. Girones, and M. Fresno. 2011. Myeloid-derived suppressor cells infiltrate the heart in acute Trypanosoma cruzi infection. *J Immunol* 187:2656-2665.

Cuervo, H., M.A. Pineda, M.P. Aoki, S. Gea, M. Fresno, and N. Girones. 2008. Inducible nitric oxide synthase and arginase expression in heart tissue during acute Trypanosoma cruzi infection in mice: arginase I is expressed in infiltrating CD68+ macrophages. *The Journal of infectious diseases* 197:1772-1782.

Cunha-Neto, E., P.C. Teixeira, L.G. Nogueira, and J. Kalil. 2011. Autoimmunity. *Advances in parasitology* 76:129-152.

Cuzzocrea, S., and D. Salvemini. 2007. Molecular mechanisms involved in the reciprocal regulation of cyclooxygenase and nitric oxide synthase enzymes. *Kidney international* 71:290-297.

Chagas, C. 1909. Neue Trypanosomen. *Archiv für schiffs- und tropen-hygiene* 13:120-122.

Chemnitz, J.M., J. Driesen, S. Classen, J.L. Riley, S. Debey, M. Beyer, A. Popov, T. Zander, and J.L. Schultze. 2006. Prostaglandin E2 impairs CD4+ T cell activation by inhibition of lck: implications in Hodgkin's lymphoma. *Cancer research* 66:1114-1122.

Chen, M., M. Divangahi, H. Gan, D.S. Shin, S. Hong, D.M. Lee, C.N. Serhan, S.M. Behar, and H.G. Remold. 2008. Lipid mediators in innate immunity against tuberculosis: opposing roles of PGE2 and LXA4 in the induction of macrophage death. *The Journal of experimental medicine* 205:2791-2801.

Cheng, Y., S.C. Austin, B. Rocca, B.H. Koller, T.M. Coffman, T. Grosser, J.A. Lawson, and G.A. FitzGerald. 2002. Role of prostacyclin in the cardiovascular response to thromboxane A2. *Science (New York, N.Y* 296:539-541.

Chiang, N., M. Arita, and C.N. Serhan. 2005. Anti-inflammatory circuitry: lipoxin, aspirin-triggered lipoxins and their receptor ALX. *Prostaglandins, leukotrienes, and essential fatty acids* 73:163-177.

D'Avila, H., C.G. Freire-de-Lima, N.R. Roque, L. Teixeira, C. Barja-Fidalgo, A.R. Silva, R.C. Melo, G.A. Dosreis, H.C. Castro-Faria-Neto, and P.T. Bozza. 2011. Host cell lipid bodies triggered by Trypanosoma cruzi infection and enhanced by the uptake of apoptotic cells are associated with prostaglandin E(2) generation and increased parasite growth. *The Journal of infectious diseases* 204:951-961.

da Matta Guedes, P.M., F.R. Gutierrez, F.L. Maia, C.M. Milanezi, G.K. Silva, W.R. Pavanelli, and J.S. Silva. 2010. IL-17 produced during Trypanosoma cruzi infection plays a central role in regulating parasite-induced myocarditis. *PLoS neglected tropical diseases* 4:e604.

Damsker, J.M., A.M. Hansen, and R.R. Caspi. 2010. Th1 and Th17 cells: adversaries and collaborators. *Annals of the New York Academy of Sciences* 1183:211-221.

de Barros-Mazon, S., M.E. Guariento, C.A. da Silva, R.L. Coffman, and I.A. Abrahamsohn. 2004. Differential regulation of lymphoproliferative responses to Trypanosoma cruzi antigen in patients with the cardiac or indeterminate form of Chagas disease. *Clinical immunology (Orlando, Fla* 111:137-145.

Deacon, K., and A.J. Knox. 2010. Endothelin-1 (ET-1) increases the expression of remodeling genes in vascular smooth muscle through linked calcium and cAMP pathways: role of a phospholipase A(2)(cPLA(2))/ cyclooxygenase-2 (COX-2)/prostacyclin receptor-dependent autocrine loop. *The Journal of biological chemistry* 285:25913-25927.

del Puerto, F., J.E. Nishizawa, M. Kikuchi, Y. Roca, C. Avilas, A. Gianella, J. Lora, F.U. Velarde, S. Miura, N. Komiya, K. Maemura, and K. Hirayama. 2012. Protective human leucocyte antigen haplotype, HLA-DRB1*01-B*14, against chronic Chagas disease in Bolivia. *PLoS neglected tropical diseases* 6:e1587.

Derouich-Guergour, D., M.P. Brenier-Pinchart, P. Ambroise-Thomas, and H. Pelloux. 2001. Tumour necrosis factor alpha receptors: role in the physiopathology of protozoan parasite infections. *International journal for parasitology* 31:763-769.

DeWitt, D.L., and W.L. Smith. 1983. Purification of prostacyclin synthase from bovine aorta by immunoaffinity chromatography. Evidence that the enzyme is a hemoprotein. *The Journal of biological chemistry* 258:3285-3293.

Dinchuk, J.E., B.D. Car, R.J. Focht, J.J. Johnston, B.D. Jaffee, M.B. Covington, N.R. Contel, V.M. Eng, R.J. Collins, P.M. Czerniak, and et al. 1995. Renal abnormalities and an altered inflammatory response in mice lacking cyclooxygenase II. *Nature* 378:406-409.

Dioszeghy, V., M. Rosas, B.H. Maskrey, C. Colmont, N. Topley, P. Chaitidis, H. Kuhn, S.A. Jones, P.R. Taylor, and V.B. O'Donnell. 2008. 12/15-Lipoxygenase regulates the inflammatory response to bacterial products in vivo. *J Immunol* 181:6514-6524.

Dobrian, A.D., D.C. Lieb, B.K. Cole, D.A. Taylor-Fishwick, S.K. Chakrabarti, and J.L. Nadler. 2011. Functional and pathological roles of the 12- and 15-lipoxygenases. *Progress in lipid research* 50:115-131.

Dorris, S.L., and R.S. Peebles, Jr. 2012. PGI2 as a regulator of inflammatory diseases. *Mediators of inflammation* 2012:926968.

Dubois, R.N., S.B. Abramson, L. Crofford, R.A. Gupta, L.S. Simon, L.B. Van De Putte, and P.E. Lipsky. 1998. Cyclooxygenase in biology and disease. *Faseb J* 12:1063-1073.

Ejima, K., M.D. Layne, I.M. Carvajal, P.A. Kritek, R.M. Baron, Y.H. Chen, J. Vom Saal, B.D. Levy, S.F. Yet, and M.A. Perrella. 2003. Cyclooxygenase-2-deficient mice are resistant to endotoxin-induced inflammation and death. *Faseb J* 17:1325-1327.

Evans, J.F., A.D. Ferguson, R.T. Mosley, and J.H. Hutchinson. 2008. What's all the FLAP about?: 5-lipoxygenase-activating protein inhibitors for inflammatory diseases. *Trends in pharmacological sciences* 29:72-78.

Figarella, K., M. Rawer, N.L. Uzcategui, B.K. Kubata, K. Lauber, F. Madeo, S. Wesselborg, and M. Duszenko. 2005. Prostaglandin D2 induces programmed cell death in Trypanosoma brucei bloodstream form. *Cell death and differentiation* 12:335-346.

Folco, G., and R.C. Murphy. 2006. Eicosanoid transcellular biosynthesis: from cell-cell interactions to in vivo tissue responses. *Pharmacological reviews* 58:375-388.

Freire-de-Lima, C.G., D.O. Nascimento, M.B. Soares, P.T. Bozza, H.C. Castro-Faria-Neto, F.G. de Mello, G.A. DosReis, and M.F. Lopes. 2000. Uptake of apoptotic cells drives the growth of a pathogenic trypanosome in macrophages. *Nature* 403:199-203.

Freire-de-Lima, C.G., Y.Q. Xiao, S.J. Gardai, D.L. Bratton, W.P. Schiemann, and P.M. Henson. 2006. Apoptotic cells, through transforming growth factor-beta, coordinately induce anti-inflammatory and suppress pro-inflammatory eicosanoid and NO synthesis in murine macrophages. *The Journal of biological chemistry* 281:38376-38384.

Funk, C.D. 2001. Prostaglandins and leukotrienes: advances in eicosanoid biology. *Science (New York, N.Y* 294:1871-1875.

Gaillard, T., A. Mulsch, H. Klein, and K. Decker. 1992. Regulation by prostaglandin E2 of cytokine-elicited nitric oxide synthesis in rat liver macrophages. *Biological chemistry Hoppe-Seyler* 373:897-902.

Gao, W., and M.A. Pereira. 2002. Interleukin-6 is required for parasite specific response and host resistance to Trypanosoma cruzi. *International journal for parasitology* 32:167-170.

Garg, N., M.P. Nunes, and R.L. Tarleton. 1997. Delivery by Trypanosoma cruzi of proteins into the MHC class I antigen processing and presentation pathway. *J Immunol* 158:3293-3302.

Gascon, J., C. Bern, and M.J. Pinazo. 2009. Chagas disease in Spain, the United States and other non-endemic countries. *Acta tropica* 115:22-27.

Gazzinelli, R.T., I.P. Oswald, S. Hieny, S.L. James, and A. Sher. 1992. The microbicidal activity of interferon-gamma-treated macrophages against Trypanosoma cruzi involves an L-arginine-dependent, nitrogen oxide-mediated mechanism inhibitable by interleukin-10 and transforming growth factor-beta. *European journal of immunology* 22:2501-2506.

Ghosn, E.E., A.A. Cassado, G.R. Govoni, T. Fukuhara, Y. Yang, D.M. Monack, K.R. Bortoluci, S.R. Almeida, L.A. Herzenberg, and L.A. Herzenberg. 2010. Two physically, functionally, and developmentally distinct peritoneal macrophage subsets. *Proceedings of the National Academy of Sciences of the United States of America* 107:2568-2573.

Girones, N., H. Cuervo, and M. Fresno. 2005. Trypanosoma cruzi-induced molecular mimicry and Chagas' disease. *Current*

topics in microbiology and immunology 296:89-123.

Girones, N., and M. Fresno. 2003. Etiology of Chagas disease myocarditis: autoimmunity, parasite persistence, or both? *Trends in parasitology* 19:19-22.

Goldmann, O., E. Hertzen, A. Hecht, H. Schmidt, S. Lehne, A. Norrby-Teglund, and E. Medina. 2010. Inducible cyclooxygenase released prostaglandin E2 modulates the severity of infection caused by Streptococcus pyogenes. *J Immunol* 185:2372-2381.

Goni, O., P. Alcaide, and M. Fresno. 2002. Immunosuppression during acute Trypanosoma cruzi infection: involvement of Ly6G (Gr1(+))CD11b(+)immature myeloid suppressor cells. *International immunology* 14:1125-1134.

Gorelik, G., A.M. Genaro, L. Sterin-Borda, S. Gonzalez Cappa, and E.S. Borda. 1990. Antibodies bind and activate beta adrenergic and cholinergic lymphocyte receptors in Chagas' disease. *Clinical immunology and immunopathology* 55:221-236.

Graefe, S.E., T. Jacobs, I. Gaworski, U. Klauenberg, C. Steeg, and B. Fleischer. 2003. Interleukin-12 but not interleukin-18 is required for immunity to Trypanosoma cruzi in mice. *Microbes and infection / Institut Pasteur* 5:833-839.

Graf, B.A., D.A. Nazarenko, M.A. Borrello, L.J. Roberts, J.D. Morrow, J. Palis, and R.P. Phipps. 1999. Biphenotypic B/macrophage cells express COX-1 and up-regulate COX-2 expression and prostaglandin E(2) production in response to pro-inflammatory signals. *European journal of immunology* 29:3793-3803.

Greenhough, A., H.J. Smartt, A.E. Moore, H.R. Roberts, A.C. Williams, C. Paraskeva, and A. Kaidi. 2009. The COX-2/PGE2 pathway: key roles in the hallmarks of cancer and adaptation to the tumour microenvironment. *Carcinogenesis* 30:377-386.

Gronert, K., N. Maheshwari, N. Khan, I.R. Hassan, M. Dunn, and M. Laniado Schwartzman. 2005. A role for the mouse 12/15-lipoxygenase pathway in promoting epithelial wound healing and host defense. *The Journal of biological chemistry* 280:15267-15278.

Grosser, T., S. Fries, and G.A. FitzGerald. 2006. Biological basis for the cardiovascular consequences of COX-2 inhibition: therapeutic challenges and opportunities. *The Journal of clinical investigation* 116:4-15.

Gutierrez, F.R., T.W. Mineo, W.R. Pavanelli, P.M. Guedes, and J.S. Silva. 2009. The effects of nitric oxide on the immune system during Trypanosoma cruzi infection. *Mem Inst Oswaldo Cruz* 104 Suppl 1:236-245.

Hardison, J.L., R.A. Wrightsman, P.M. Carpenter, T.E. Lane, and J.E. Manning. 2006. The chemokines CXCL9 and CXCL10 promote a protective immune response but do not contribute to cardiac inflammation following infection with Trypanosoma cruzi. *Infection and immunity* 74:125-134.

Harizi, H., C. Grosset, and N. Gualde. 2003. Prostaglandin E2 modulates dendritic cell function via EP2 and EP4 receptor subtypes. *Journal of leukocyte biology* 73:756-763.

Harizi, H., M. Juzan, V. Pitard, J.F. Moreau, and N. Gualde. 2002. Cyclooxygenase-2-issued prostaglandin e(2) enhances the production of endogenous IL-10, which down-regulates dendritic cell functions. *J Immunol* 168:2255-2263.

Harris, S.G., J. Padilla, L. Koumas, D. Ray, and R.P. Phipps. 2002. Prostaglandins as modulators of immunity. *Trends in immunology* 23:144-150.

Hastings, W.D., S.M. Gurdak, J.R. Tumang, and T.L. Rothstein. 2006. CD5+/Mac-1- peritoneal B cells: a novel B cell subset that exhibits characteristics of B-1 cells. *Immunology letters* 105:90-96.

Hayashi, H., Y. Fujii, K. Watanabe, Y. Urade, and O. Hayaishi. 1989. Enzymatic conversion of prostaglandin H2 to prostaglandin F2

alpha by aldehyde reductase from human liver: comparison to the prostaglandin F synthetase from bovine lung. *The Journal of biological chemistry* 264:1036-1040.

Heydeck, D., L. Thomas, K. Schnurr, F. Trebus, W.E. Thierfelder, J.N. Ihle, and H. Kuhn. 1998. Interleukin-4 and -13 induce upregulation of the murine macrophage 12/15-lipoxygenase activity: evidence for the involvement of transcription factor STAT6. *Blood* 92:2503-2510.

Hideko Tatakihara, V.L., R. Cecchini, C.L. Borges, A.D. Malvezi, V.K. Graca-de Souza, S.F. Yamada-Ogatta, L.V. Rizzo, and P. Pinge-Filho. 2008. Effects of cyclooxygenase inhibitors on parasite burden, anemia and oxidative stress in murine Trypanosoma cruzi infection. *FEMS immunology and medical microbiology* 52:47-58.

Hori, M., M. Kita, S. Torihashi, S. Miyamoto, K.J. Won, K. Sato, H. Ozaki, and H. Karaki. 2001. Upregulation of iNOS by COX-2 in muscularis resident macrophage of rat intestine stimulated with LPS. *Am J Physiol Gastrointest Liver Physiol* 280:G930-938.

Hotez, P.J., D.H. Molyneux, A. Fenwick, J. Kumaresan, S.E. Sachs, J.D. Sachs, and L. Savioli. 2007. Control of neglected tropical diseases. *The New England journal of medicine* 357:1018-1027.

Hovsepian, E., G.A. Mirkin, F. Penas, A. Manzano, R. Bartrons, and N.B. Goren. 2011. Modulation of inflammatory response and parasitism by 15-Deoxy-Delta(12,14) prostaglandin J(2) in Trypanosoma cruzi-infected cardiomyocytes. *International journal for parasitology* 41:553-562.

Hu, C.J., L.Y. Wang, L.A. Chodosh, B. Keith, and M.C. Simon. 2003. Differential roles of hypoxia-inducible factor 1alpha (HIF-1alpha) and HIF-2alpha in hypoxic gene regulation. *Molecular and cellular biology* 23:9361-9374.

Huang, S., W. Hendriks, A. Althage, S. Hemmi, H. Bluethmann, R. Kamijo, J. Vilcek, R.M. Zinkernagel, and M. Aguet. 1993. Immune response in mice that lack the interferon-gamma receptor. *Science (New York, N.Y* 259:1742-1745.

Hunter, C.A., L.A. Ellis-Neyes, T. Slifer, S. Kanaly, G. Grunig, M. Fort, D. Rennick, and F.G. Araujo. 1997. IL-10 is required to prevent immune hyperactivity during infection with Trypanosoma cruzi. *J Immunol* 158:3311-3316.

Iniguez, M.A., C. Punzon, C. Cacheiro-Llaguno, M.D. Diaz-Munoz, J. Duque, R. Cuberes, I. Alvarez, E.M. Andres, J. Buxens, H. Buschmann, J.M. Vela, and M. Fresno. 2010. Cyclooxygenase-independent inhibitory effects on T cell activation of novel 4,5-dihydro-3 trifluoromethyl pyrazole cyclooxygenase-2 inhibitors. *International immunopharmacology* 10:1295-1304.

Iniguez, M.A., C. Punzon, and M. Fresno. 1999. Induction of cyclooxygenase-2 on activated T lymphocytes: regulation of T cell activation by cyclooxygenase-2 inhibitors. *J Immunol* 163:111-119.

Ise, H., S. Kobayashi, M. Goto, T. Sato, M. Kawakubo, M. Takahashi, U. Ikeda, and T. Akaike. 2010. Vimentin and desmin possess GlcNAc-binding lectin-like properties on cell surfaces. *Glycobiology* 20:843-864.

Janelle, M.E., A. Gravel, J. Gosselin, M.J. Tremblay, and L. Flamand. 2002. Activation of monocyte cyclooxygenase-2 gene expression by human herpesvirus 6. Role for cyclic AMP-responsive element-binding protein and activator protein-1. *The Journal of biological chemistry* 277:30665-30674.

Jenkins, S.J., D. Ruckerl, P.C. Cook, L.H. Jones, F.D. Finkelman, N. van Rooijen, A.S. MacDonald, and J.E. Allen. 2011. Local macrophage proliferation, rather than recruitment from the blood, is a signature of TH2 inflammation. *Science (New York, N.Y* 332:1284-1288.

Kanaoka, Y., and Y. Urade. 2003. Hematopoietic prostaglandin D synthase. *Prostaglandins, leukotrienes, and essential fatty acids* 69:163-167.

Kastenmuller, W., M. Brandes, Z. Wang, J. Herz, J.G. Egen, and R.N. Germain. 2013. Peripheral Prepositioning and Local CXCL9 Chemokine-Mediated Guidance Orchestrate Rapid Memory CD8(+) T Cell Responses in the Lymph Node. *Immunity*

Kayama, H., and K. Takeda. 2010. The innate immune response to Trypanosoma cruzi infection. *Microbes and infection / Institut Pasteur* 12:511-517.

Kayama, Y., T. Minamino, H. Toko, M. Sakamoto, I. Shimizu, H. Takahashi, S. Okada, K. Tateno, J. Moriya, M. Yokoyama, A. Nojima, M. Yoshimura, K. Egashira, H. Aburatani, and I. Komuro. 2009. Cardiac 12/15 lipoxygenase-induced inflammation is involved in heart failure. *The Journal of experimental medicine* 206:1565-1574.

Kierszenbaum, F. 2005. Where do we stand on the autoimmunity hypothesis of Chagas disease? *Trends in parasitology* 21:513-516.

Kilunga Kubata, B., N. Eguchi, Y. Urade, K. Yamashita, T. Mitamura, K. Tai, O. Hayaishi, and T. Horii. 1998. Plasmodium falciparum produces prostaglandins that are pyrogenic, somnogenic, and immunosuppressive substances in humans. *The Journal of experimental medicine* 188:1197-1202.

Kinoshita, M., T. Uchida, A. Sato, M. Nakashima, H. Nakashima, S. Shono, Y. Habu, H. Miyazaki, S. Hiroi, and S. Seki. 2010. Characterization of two F4/80-positive Kupffer cell subsets by their function and phenotype in mice. *Journal of hepatology* 53:903-910.

Krause, P., M. Bruckner, C. Uermosi, E. Singer, M. Groettrup, and D.F. Legler. 2009. Prostaglandin E(2) enhances T-cell proliferation by inducing the costimulatory molecules OX40L, CD70, and 4-1BBL on dendritic cells. *Blood* 113:2451-2460.

Kronke, G., N. Reich, C. Scholtysek, A. Akhmetshina, S. Uderhardt, P. Zerr, K. Palumbo, V. Lang, C. Dees, O. Distler, G. Schett, and J.H. Distler. 2012. The 12/15-lipoxygenase pathway counteracts fibroblast activation and experimental fibrosis. *Annals of the rheumatic diseases* 71:1081-1087.

Kubata, B.K., M. Duszenko, Z. Kabututu, M. Rawer, A. Szallies, K. Fujimori, T. Inui, T. Nozaki, K. Yamashita, T. Horii, Y. Urade, and O. Hayaishi. 2000. Identification of a novel prostaglandin f(2alpha) synthase in Trypanosoma brucei. *The Journal of experimental medicine* 192:1327-1338.

Kubata, B.K., M. Duszenko, K.S. Martin, and Y. Urade. 2007. Molecular basis for prostaglandin production in hosts and parasites. *Trends in parasitology* 23:325-331.

Kubata, B.K., Z. Kabututu, T. Nozaki, C.J. Munday, S. Fukuzumi, K. Ohkubo, M. Lazarus, T. Maruyama, S.K. Martin, M. Duszenko, and Y. Urade. 2002. A key role for old yellow enzyme in the metabolism of drugs by Trypanosoma cruzi. *The Journal of experimental medicine* 196:1241-1251.

Kudo, I., and M. Murakami. 2005. Prostaglandin E synthase, a terminal enzyme for prostaglandin E2 biosynthesis. *Journal of biochemistry and molecular biology* 38:633-638.

Kuhn, H., and V.B. O'Donnell. 2006. Inflammation and immune regulation by 12/15-lipoxygenases. *Progress in lipid research* 45:334-356.

Kumar, S., and R.L. Tarleton. 1998. The relative contribution of antibody production and CD8+ T cell function to immune control of Trypanosoma cruzi. *Parasite immunology* 20:207-216.

Kunkel, S.L., M. Spengler, M.A. May, R. Spengler, J. Larrick, and D. Remick. 1988. Prostaglandin E2 regulates macrophage-derived tumor necrosis factor gene expression. *The Journal of biological chemistry* 263:5380-5384.

Kuroda, E., and U. Yamashita. 2003. Mechanisms of enhanced macrophage-mediated prostaglandin E2 production and its suppressive role in Th1 activation in Th2-dominant BALB/c mice. *J Immunol* 170:757-764.

Lai, J., H. Jin, R. Yang, J. Winer, W. Li, R. Yen, K.L. King, F. Zeigler, A. Ko, J. Cheng, S. Bunting, and N.F. Paoni. 1996. Prostaglandin F2 alpha induces cardiac myocyte hypertrophy in vitro and cardiac growth in vivo. *The American journal of physiology* 271:H2197-2208.

Lambert, J.M., E.F. Lopez, and M.L. Lindsey. 2008. Macrophage roles following myocardial infarction. *International journal of cardiology* 130:147-158.

Landino, L.M., B.C. Crews, M.D. Timmons, J.D. Morrow, and L.J. Marnett. 1996. Peroxynitrite, the coupling product of nitric oxide and superoxide, activates prostaglandin biosynthesis. *Proceedings of the National Academy of Sciences of the United States of America* 93:15069-15074.

Langenbach, R., C. Loftin, C. Lee, and H. Tiano. 1999. Cyclooxygenase knockout mice: models for elucidating isoform-specific functions. *Biochemical pharmacology* 58:1237-1246.

Lee, S.H., E. Soyoola, P. Chanmugam, S. Hart, W. Sun, H. Zhong, S. Liou, D. Simmons, and D. Hwang. 1992. Selective expression of mitogen-inducible cyclooxygenase in macrophages stimulated with lipopolysaccharide. *The Journal of biological chemistry* 267:25934-25938.

Levin, M.J. 1996. In chronic Chagas heart disease, don't forget the parasite. *Parasitology today (Personal ed* 12:415-416.

Levy, B.D., C.B. Clish, B. Schmidt, K. Gronert, and C.N. Serhan. 2001. Lipid mediator class switching during acute inflammation: signals in resolution. *Nature immunology* 2:612-619.

Levy, B.D., M. Romano, H.A. Chapman, J.J. Reilly, J. Drazen, and C.N. Serhan. 1993. Human alveolar macrophages have 15-lipoxygenase and generate 15(S)-hydroxy-5,8,11-cis-13-trans-eicosatetraenoic acid and lipoxins. *The Journal of clinical investigation* 92:1572-1579.

Lewis, M.D., J. Ma, M. Yeo, H.J. Carrasco, M.S. Llewellyn, and M.A. Miles. 2009. Genotyping of Trypanosoma cruzi: systematic selection of assays allowing rapid and accurate discrimination of all known lineages. *The American journal of tropical medicine and hygiene* 81:1041-1049.

Lian, H., Y. Ma, J. Feng, W. Dong, Q. Yang, D. Lu, and L. Zhang. 2012. Heparin-binding EGF-like growth factor induces heart interstitial fibrosis via an Akt/mTor/p70s6k pathway. *PloS one* 7:e44946.

Limor, R., O. Sharon, E. Knoll, A. Many, G. Weisinger, and N. Stern. 2008. Lipoxygenase-derived metabolites are regulators of peroxisome proliferator-activated receptor gamma-2 expression in human vascular smooth muscle cells. *American journal of hypertension* 21:219-223.

Lin, C.C., H.L. Hsieh, R.H. Shih, P.L. Chi, S.E. Cheng, and C.M. Yang. 2013. Up-regulation of COX-2/PGE2 by endothelin-1 via MAPK-dependent NF-kappaB pathway in mouse brain microvascular endothelial cells. *Cell Commun Signal* 11:8.

Liu, X., H. Yu, L. Yang, C. Li, and L. Li. 2012. 15-Deoxy-Delta(12,14)-prostaglandin J(2) attenuates the biological activities of monocyte/macrophage cell lines. *European journal of cell biology* 91:654-661.

Loffler, I., M. Grun, F.D. Bohmer, and I. Rubio. 2008. Role of cAMP in the promotion of colorectal cancer cell growth by prostaglandin E2. *BMC cancer* 8:380.

Machado, C.R., and E.R. Camargos. 2008. Endothelins role in the control of the acute phase of Trypanosoma cruzi infection. *Mini reviews in medicinal chemistry* 8:820-827.

Machado, F.S., W.O. Dutra, L. Esper, K.J. Gollob, M.M. Teixeira, S.M. Factor, L.M. Weiss, F. Nagajyothi, H.B. Tanowitz, and N.J. Garg. 2012. Current understanding of immunity to Trypanosoma cruzi infection and pathogenesis of Chagas disease. *Seminars in immunopathology* 34:753-770.

Machado, F.S., S. Mukherjee, L.M. Weiss, H.B. Tanowitz, and A.W. Ashton. 2011. Bioactive lipids in Trypanosoma cruzi infection. *Advances in parasitology* 76:1-31.

Machado, F.S., J.T. Souto, M.A. Rossi, L. Esper, H.B. Tanowitz, J. Aliberti, and J.S. Silva. 2008. Nitric oxide synthase-2 modulates chemokine production by Trypanosoma cruzi-infected cardiac myocytes. *Microbes and infection / Institut Pasteur* 10:1558-1566.

Majumder, S., and F. Kierszenbaum. 1996. Mechanisms of Trypanosoma cruzi-induced down-regulation of lymphocyte function. Inhibition of transcription and expression of IL-2 receptor gamma (p64IL-2R) and beta (p70IL-2R) chain molecules in activated normal human lymphocytes. *J Immunol* 156:3866-3874.

Marin-Neto, J.A., E. Cunha-Neto, B.C. Maciel, and M.V. Simoes. 2007. Pathogenesis of chronic Chagas heart disease. *Circulation* 115:1109-1123.

Marnett, L.J., S.W. Rowlinson, D.C. Goodwin, A.S. Kalgutkar, and C.A. Lanzo. 1999. Arachidonic acid oxygenation by COX-1 and COX-2. Mechanisms of catalysis and inhibition. *The Journal of biological chemistry* 274:22903-22906.

Martin, D., and R. Tarleton. 2004. Generation, specificity, and function of CD8+ T cells in Trypanosoma cruzi infection. *Immunological reviews* 201:304-317.

Merino, M.C., C.L. Montes, E.V. Acosta-Rodriguez, D.A. Bermejo, M.C. Amezcua-Vesely, and A. Gruppi. 2012. Peritoneum from Trypanosoma cruzi-infected mice is a homing site of Syndecan-1 neg plasma cells which mainly provide non-parasite-specific antibodies. *International immunology* 22:399-410.

Mestas, J., and C.C. Hughes. 2004. Of mice and not men: differences between mouse and human immunology. *J Immunol* 172:2731-2738.

Michelin, M.A., J.S. Silva, and F.Q. Cunha. 2005. Inducible cyclooxygenase released prostaglandin mediates immunosuppression in acute phase of experimental Trypanosoma cruzi infection. *Experimental parasitology* 111:71-79.

Middleton, M.K., A.M. Zukas, T. Rubinstein, M. Kinder, E.H. Wilson, P. Zhu, I.A. Blair, C.A. Hunter, and E. Pure. 2009. 12/15-lipoxygenase-dependent myeloid production of interleukin-12 is essential for resistance to chronic toxoplasmosis. *Infection and immunity* 77:5690-5700.

Mills, C.D., K. Kincaid, J.M. Alt, M.J. Heilman, and A.M. Hill. 2000. M-1/M-2 macrophages and the Th1/Th2 paradigm. *J Immunol* 164:6166-6173.

Miyazaki, Y., S. Hamano, S. Wang, Y. Shimanoe, Y. Iwakura, and H. Yoshida. 2010. IL-17 is necessary for host protection against acute-phase Trypanosoma cruzi infection. *J Immunol* 185:1150-1157.

Mohrs, M., B. Ledermann, G. Kohler, A. Dorfmuller, A. Gessner, and F. Brombacher. 1999. Differences between IL-4- and IL-4 receptor alpha-deficient mice in chronic leishmaniasis reveal a protective role for IL-13 receptor signaling. *J Immunol* 162:7302-7308.

Moncayo, A., and A.C. Silveira. 2009. Current epidemiological trends for Chagas disease in Latin America and future challenges in epidemiology, surveillance and health policy. *Mem Inst Oswaldo Cruz* 104 Suppl 1:17-30.

Mor-Vaknin, N., A. Punturieri, K. Sitwala, and D.M. Markovitz. 2003. Vimentin is secreted by activated macrophages. *Nature cell biology* 5:59-63.

Morillo, C.A. 2013. Infection with T. cruzi and Progression to Cardiomyopathy: What is the Evidence and is the Tide Finally Turning Around? *Circulation*

Morita, I., M. Schindler, M.K. Regier, J.C. Otto, T. Hori, D.L. DeWitt, and W.L. Smith. 1995. Different intracellular locations for prostaglandin endoperoxide H synthase-1 and -2. *The Journal of biological chemistry* 270:10902-10908.

Mukherjee, S., H. Huang, S.B. Petkova, C. Albanese, R.G. Pestell, V.L. Braunstein, G.J. Christ, M. Wittner, M.P. Lisanti, J.W. Berman, L.M. Weiss, and H.B. Tanowitz. 2004. Trypanosoma cruzi infection activates extracellular signal-regulated kinase in cultured endothelial and smooth muscle cells. *Infection and immunity* 72:5274-5282.

Mukherjee, S., F.S. Machado, H. Huang, H.S. Oz, L.A. Jelicks, C.M. Prado, W. Koba, E.J. Fine, D. Zhao, S.M. Factor, J.E. Collado, L.M. Weiss, H.B. Tanowitz, and A.W. Ashton. 2011. Aspirin treatment of mice infected with Trypanosoma cruzi and implications for the pathogenesis of Chagas disease. *PloS one* 6:e16959.

Muller, U., V. Sobek, S. Balkow, C. Holscher, A. Mullbacher, C. Museteanu, H. Mossmann, and M.M. Simon. 2003. Concerted action of perforin and granzymes is critical for the elimination of Trypanosoma cruzi from mouse tissues, but prevention of early host death is in addition dependent on the FasL/Fas pathway. *European journal of immunology* 33:70-78.

Munoz-Fernandez, M.A., M.A. Fernandez, and M. Fresno. 1992. Activation of human macrophages for the killing of intracellular Trypanosoma cruzi by TNF-alpha and IFN-gamma through a nitric oxide-dependent mechanism. *Immunology letters* 33:35-40.

Murray, P.J., and T.A. Wynn. 2011. Protective and pathogenic functions of macrophage subsets. *Nat Rev Immunol* 11:723-737.

Nagamachi, M., D. Sakata, K. Kabashima, T. Furuyashiki, T. Murata, E. Segi-Nishida, K. Soontrapa, T. Matsuoka, Y. Miyachi, and S. Narumiya. 2007. Facilitation of Th1-mediated immune response by prostaglandin E receptor EP1. *The Journal of experimental medicine* 204:2865-2874.

Napolitani, G., E.V. Acosta-Rodriguez, A. Lanzavecchia, and F. Sallusto. 2009. Prostaglandin E2 enhances Th17 responses via modulation of IL-17 and IFN-gamma production by memory CD4+ T cells. *European journal of immunology* 39:1301-1312.

Naraba, H., M. Murakami, H. Matsumoto, S. Shimbara, A. Ueno, I. Kudo, and S. Oh-ishi. 1998. Segregated coupling of phospholipases A2, cyclooxygenases, and terminal prostanoid synthases in different phases of prostanoid biosynthesis in rat peritoneal macrophages. *J Immunol* 160:2974-2982.

Narumiya, S. 2009. Prostanoids and inflammation: a new concept arising from receptor knockout mice. *Journal of molecular medicine (Berlin, Germany)* 87:1015-1022.

Narumiya, S., Y. Sugimoto, and F. Ushikubi. 1999. Prostanoid receptors: structures, properties, and functions. *Physiological reviews* 79:1193-1226.

Noverr, M.C., J.R. Erb-Downward, and G.B. Huffnagle. 2003. Production of eicosanoids and other oxylipins by pathogenic eukaryotic microbes. *Clinical microbiology reviews* 16:517-533.

Nugteren, D.H., and E. Hazelhof. 1973. Isolation and properties of intermediates in prostaglandin biosynthesis. *Biochimica et biophysica acta* 326:448-461.

Oliveira, A.C., B.C. de Alencar, F. Tzelepis, W. Klezewsky, R.N. da Silva, F.S. Neves, G.S. Cavalcanti, S. Boscardin, M.P. Nunes, M.F. Santiago, A. Nobrega, M.M. Rodrigues, and M. Bellio. 2010a. Impaired innate immunity in Tlr4(-/-) mice but preserved CD8+ T cell responses against Trypanosoma cruzi in Tlr4-, Tlr2-, Tlr9- or Myd88-deficient mice. *PLoS pathogens* 6:e1000870.

Oliveira, L.G., C.C. Kuehn, C.D. Santos, M.P. Toldo, and J.C. do Prado, Jr. 2010b. Enhanced protection by melatonin and meloxicam combination in experimental infection by Trypanosoma cruzi. *Parasite immunology* 32:245-251.

Osorio, L., I. Rios, B. Gutierrez, and J. Gonzalez. 2012. Virulence factors of Trypanosoma cruzi: who is who? *Microbes and infection / Institut Pasteur* 14:1390-1402.

Paiva, C.N., R.T. Figueiredo, K. Kroll-Palhares, A.A. Silva, J.C. Silverio, D. Gibaldi, S. Pyrrho Ados, C.F. Benjamim, J. Lannes-Vieira, and M.T. Bozza. 2009. CCL2/MCP-1 controls parasite burden, cell infiltration, and mononuclear activation during acute Trypanosoma cruzi infection. *Journal of leukocyte biology* 86:1239-1246.

Panis, C., T.L. Mazzuco, C.Z. Costa, V.J. Victorino, V.L. Tatakihara, L.M. Yamauchi, S.F. Yamada-Ogatta, R. Cecchini, L.V. Rizzo, and P. Pinge-Filho. 2011. Trypanosoma cruzi: effect of the absence of 5-lipoxygenase (5-LO)-derived leukotrienes on levels of cytokines, nitric oxide and iNOS expression in cardiac tissue in the acute phase of infection in mice. *Experimental parasitology* 127:58-65.

Panzer, U., and M. Uguccioni. 2004. Prostaglandin E2 modulates the functional responsiveness of human monocytes to chemokines. *European journal of immunology* 34:3682-3689.

Parfenova, H., V.N. Parfenov, B.V. Shlopov, V. Levine, S. Falkos, M. Pourcyrous, and C.W. Leffler. 2001. Dynamics of nuclear localization sites for COX-2 in vascular endothelial cells. *American journal of physiology* 281:C166-178.

Parkinson, J.F. 2006. Lipoxin and synthetic lipoxin analogs: an overview of anti-inflammatory functions and new concepts in immunomodulation. *Inflammation & allergy drug targets* 5:91-106.

Parra, D., A.M. Rieger, J. Li, Y.A. Zhang, L.M. Randall, C.A. Hunter, D.R. Barreda, and J.O. Sunyer. 2012. Pivotal advance: peritoneal cavity B-1 B cells have phagocytic and microbicidal capacities and present phagocytosed antigen to CD4+ T cells. *Journal of leukocyte biology* 91:525-536.

Pavanelli, W.R., F.R. Gutierrez, F.S. Mariano, C.M. Prado, B.R. Ferreira, M.M. Teixeira, C. Canetti, M.A. Rossi, F.Q. Cunha, and J.S. Silva. 2010. 5-lipoxygenase is a key determinant of acute myocardial inflammation and mortality during Trypanosoma cruzi infection. *Microbes and infection / Institut Pasteur* 12:587-597.

Penas, F., G.A. Mirkin, E. Hovsepian, A. Cevey, R. Caccuri, M.E. Sales, and N.B. Goren. 2013. PPARgamma ligand treatment inhibits cardiac inflammatory mediators induced by infection with different lethality strains of Trypanosoma cruzi. *Biochimica et biophysica acta* 1832:239-248.

Peng, H., P. Chen, Y. Cai, Y. Chen, Q.H. Wu, Y. Li, R. Zhou, and X. Fang. 2008. Endothelin-1 increases expression of cyclooxygenase-2 and production of interlukin-8 in hunan pulmonary epithelial cells. *Peptides* 29:419-424.

Penglis, P.S., L.G. Cleland, M. Demasi, G.E. Caughey, and M.J. James. 2000. Differential regulation of prostaglandin E2 and thromboxane A2 production in human monocytes: implications for the use of cyclooxygenase inhibitors. *J Immunol* 165:1605-1611.

Peters-Golden, M., and T.G. Brock. 2003. 5-lipoxygenase and FLAP. *Prostaglandins, leukotrienes, and essential fatty acids* 69:99-109.

Petkova, S.B., H. Huang, S.M. Factor, R.G. Pestell, B. Bouzahzah, L.A. Jelicks, L.M. Weiss, S.A. Douglas, M. Wittner, and H.B. Tanowitz. 2001. The role of endothelin in the pathogenesis of Chagas' disease. *International journal for parasitology* 31:499-511.

Pinge-Filho, P., C.E. Tadokoro, and I.A. Abrahamsohn. 1999. Prostaglandins mediate suppression of lymphocyte proliferation and cytokine synthesis in acute Trypanosoma cruzi infection. *Cellular immunology* 193:90-98.

Pinto, A.R., R. Paolicelli, E. Salimova, J. Gospocic, E. Slonimsky, D. Bilbao-Cortes, J.W. Godwin, and N.A. Rosenthal. 2012. An abundant tissue macrophage population in the adult murine heart with a distinct alternatively-activated macrophage profile. *PloS one* 7:e36814.

Piron, M., R. Fisa, N. Casamitjana, P. Lopez-Chejade, L. Puig, M. Verges, J. Gascon, J. Gomez i Prat, M. Portus, and S. Sauleda. 2007. Development of a real-time PCR assay for Trypanosoma cruzi detection in blood samples. *Acta tropica* 103:195-200.

Poeckel, D., and C.D. Funk. 2010. The 5-lipoxygenase/leukotriene pathway in preclinical models of cardiovascular disease. *Cardiovascular research* 86:243-253.

Rabinowitz, S.S., and S. Gordon. 1991. Macrosialin, a macrophage-restricted membrane sialoprotein differentially glycosylated in response to inflammatory stimuli. *The Journal of experimental medicine* 174:827-836.

Rachid, M.A., E.R. Camargos, L. Barcellos, C.A. Marques, E. Chiari, H. Huang, H.B. Tanowitz, M.M. Teixeira, and C.R. Machado. 2006. Blockade of endothelin ET(A)/ET(B) receptors favors a role for endothelin during acute Trypanosoma cruzi infection in rats. *Microbes and infection / Institut Pasteur* 8:2113-2119.

Rachid, M.A., A.L. Teixeira, L.S. Barcelos, C.R. Machado, E. Chiari, H.B. Tanowitz, E.R. Camargos, and M.M. Teixeira. 2010. Role of endothelin receptors in the control of central nervous system parasitism in Trypanosoma cruzi infection in rats. *Journal of neuroimmunology* 220:64-68.

Rassi, A., Jr., A. Rassi, and J. Marcondes de Rezende. 2012. American trypanosomiasis (Chagas disease). *Infectious disease clinics of North America* 26:275-291.

Rassi, A., Jr., A. Rassi, and J.A. Marin-Neto. 2010. Chagas disease. *Lancet* 375:1388-1402.

Ratcliffe, M.J., A. Walding, P.A. Shelton, A. Flaherty, and I.G. Dougall. 2007. Activation of E-prostanoid4 and E-prostanoid2 receptors inhibits TNF-alpha release from human alveolar macrophages. *Eur Respir J* 29:986-994.

Rodrigues, W.F., C.B. Miguel, J.E. Chica, and M.H. Napimoga. 2010. 15d-PGJ(2) modulates acute immune responses to Trypanosoma cruzi infection. *Mem Inst Oswaldo Cruz* 105:137-143.

Roffe, E., F. Oliveira, A.L. Souza, V. Pinho, D.G. Souza, P.R. Souza, R.C. Russo, H.C. Santiago, A.J. Romanha, H.B. Tanowitz, J.G. Valenzuela, and M.M. Teixeira. 2010. Role of CCL3/MIP-1alpha and CCL5/RANTES during acute Trypanosoma cruzi infection in rats. *Microbes and infection / Institut Pasteur* 12:669-676.

Roggero, E., A. Perez, M. Tamae-Kakazu, I. Piazzon, I. Nepomnaschy, J. Wietzerbin, E. Serra, S. Revelli, and O. Bottasso. 2002. Differential susceptibility to acute Trypanosoma cruzi infection in BALB/c and C57BL/6 mice is not associated with a distinct parasite load but cytokine abnormalities. *Clinical and experimental immunology* 128:421-428.

Rossi, M.A. 1995. Pathogenesis of chronic Chagas' myocarditis. *Sao Paulo medical journal = Revista paulista de medicina* 113:750-756.

Rossi, M.A. 2001. Connective tissue skeleton in the normal left ventricle and in hypertensive left ventricular hypertrophy and chronic chagasic myocarditis. *Med Sci Monit* 7:820-832.

Rubin, P., and K.W. Mollison. 2007. Pharmacotherapy of diseases mediated by 5-lipoxygenase pathway eicosanoids. *Prostaglandins & other lipid mediators* 83:188-197.

Ryan, E.P., C.M. Malboeuf, M. Bernard, R.C. Rose, and R.P. Phipps. 2006. Cyclooxygenase-2 inhibition attenuates antibody responses against human papillomavirus-like particles. *J Immunol* 177:7811-7819.

Sala, A., G. Folco, and R.C. Murphy. 2010. Transcellular biosynthesis of eicosanoids. *Pharmacol Rep* 62:503-510.

Salvemini, D., S.F. Kim, and V. Mollace. 2013. Invited Review: Reciprocal regulation of the nitric oxide and cyclooxygenase pathway in pathophysiology; relevance and clinical implications. *Am J Physiol Regul Integr Comp Physiol*

Salvemini, D., T.P. Misko, J.L. Masferrer, K. Seibert, M.G. Currie, and P. Needleman. 1993. Nitric oxide activates cyclooxygenase enzymes. *Proceedings of the National Academy of Sciences of the United States of America* 90:7240-7244.

Samet, J.M., M.B. Fasano, A.N. Fonteh, and F.H. Chilton. 1995. Selective induction of prostaglandin G/H synthase I by stem cell factor and dexamethasone in mast cells. *The Journal of biological chemistry* 270:8044-8049.

Sampson, A.P. 2009. FLAP inhibitors for the treatment of inflammatory diseases. *Curr Opin Investig Drugs* 10:1163-1172.

Santamaria, M.H., and R.S. Corral. 2013. Osteopontin-dependent regulation of Th1 and Th17 cytokine responses in Trypanosoma cruzi-infected C57BL/6 mice. *Cytokine* 61:491-498.

Scher, J.U., and M.H. Pillinger. 2009. The anti-inflammatory effects of prostaglandins. *J Investig Med* 57:703-708.

Schindelin, J., I. Arganda-Carreras, E. Frise, V. Kaynig, M. Longair, T. Pietzsch, S. Preibisch, C. Rueden, S. Saalfeld, B. Schmid, J.Y. Tinevez, D.J. White, V. Hartenstein, K. Eliceiri, P. Tomancak, and A. Cardona. 2012. Fiji: an open-source platform for biological-image analysis. *Nature methods* 9:676-682.

Schmittgen, T.D., and K.J. Livak. 2008. Analyzing real-time PCR data by the comparative C(T) method. *Nat Protoc* 3:1101-1108.

Schror, K. 1992. Role of prostaglandins in the cardiovascular effects of bradykinin and angiotensin-converting enzyme inhibitors. *Journal of cardiovascular pharmacology* 20 Suppl 9:S68-73.

Schror, K. 2011. Pharmacology and cellular/molecular mechanisms of action of aspirin and non-aspirin NSAIDs in colorectal cancer. *Best practice & research* 25:473-484.

Serhan, C.N. 1997. Lipoxins and novel aspirin-triggered 15-epi-lipoxins (ATL): a jungle of cell-cell interactions or a therapeutic opportunity? *Prostaglandins* 53:107-137.

Serhan, C.N., S. Krishnamoorthy, A. Recchiuti, and N. Chiang. 2011. Novel anti-inflammatory--pro-resolving mediators and their receptors. *Current topics in medicinal chemistry* 11:629-647.

Sharma, J., C.S. Eickhoff, D.F. Hoft, D.A. Ford, R.W. Gross, and J. McHowat. 2013. Absence of myocardial calcium-independent phospholipase A2gamma results in impaired PGE2 production and decreased survival in mice with acute Trypanosoma cruzi infection. *Infection and immunity*

Shimizu, T., S. Yamamoto, and O. Hayaishi. 1982. Purification of PGH-PGD isomerase from rat brain. *Methods in enzymology* 86:73-77.

Shimura, C., T. Satoh, K. Igawa, K. Aritake, Y. Urade, M. Nakamura, and H. Yokozeki. 2010. Dendritic cells express hematopoietic prostaglandin D synthase and function as a source of prostaglandin D2 in the skin. *The American journal of pathology* 176:227-237.

Silva, G.K., F.R. Gutierrez, P.M. Guedes, C.V. Horta, L.D. Cunha, T.W. Mineo, J. Santiago-Silva, K.S. Kobayashi, R.A. Flavell, J.S. Silva, and D.S. Zamboni. 2011. Cutting edge: nucleotide-binding oligomerization domain 1-dependent responses account for murine resistance against Trypanosoma cruzi infection. *J Immunol* 184:1148-1152.

Silva, J.S., D.R. Twardzik, and S.G. Reed. 1991. Regulation of Trypanosoma cruzi infections in vitro and in vivo by transforming growth factor beta (TGF-beta). *The Journal of experimental medicine* 174:539-545.

Silva, J.S., G.N. Vespa, M.A. Cardoso, J.C. Aliberti, and F.Q. Cunha. 1995. Tumor necrosis factor alpha mediates resistance to Trypanosoma cruzi infection in mice by inducing nitric oxide production in infected gamma interferon-activated macrophages. *Infection and immunity* 63:4862-4867.

Smith, W.L., R.M. Garavito, and D.L. DeWitt. 1996. Prostaglandin endoperoxide H synthases (cyclooxygenases)-1 and -2. *The Journal of biological chemistry* 271:33157-33160.

Soares, M.B., L. Pontes-De-Carvalho, and R. Ribeiro-Dos-Santos. 2001. The pathogenesis of Chagas' disease: when autoimmune and parasite-specific immune responses meet. *Anais da Academia Brasileira de Ciencias* 73:547-559.

Souders, C.A., S.L. Bowers, and T.A. Baudino. 2009. Cardiac fibroblast: the renaissance cell. *Circulation research* 105:1164-1176.

Sousa, A.S., S.S. Xavier, G.R. Freitas, and A. Hasslocher-Moreno. 2008. Prevention strategies of cardioembolic ischemic stroke in Chagas' disease. *Arquivos brasileiros de cardiologia* 91:306-310.

Sreeramkumar, V., M. Fresno, and N. Cuesta. 2012. Prostaglandin E2 and T cells: friends or foes? *Immunology and cell biology* 90:579-586.

Stables, M.J., and D.W. Gilroy. 2011. Old and new generation lipid mediators in acute inflammation and resolution. *Progress in lipid research* 50:35-51.

Sterin-Borda, L., G. Gorelik, N. Goren, S.G. Cappa, A.M. Celentano, and E. Borda. 1996. Lymphocyte muscarinic cholinergic activity and PGE2 involvement in experimental Trypanosoma cruzi infection. *Clinical immunology and immunopathology* 81:122-128.

Sturm, N.R., and D.A. Campbell. 2010. Alternative lifestyles: the population structure of Trypanosoma cruzi. *Acta tropica* 115:35-43.

Subbarayan, V., P. Krieg, L.C. Hsi, J. Kim, P. Yang, A.L. Sabichi, N. Llansa, G. Mendoza, C.J. Logothetis, R.A. Newman, S.M. Lippman, and D.G. Menter. 2006. 15-Lipoxygenase-2 gene regulation by its product 15-(S)-hydroxyeicosatetraenoic acid through a negative feedback mechanism that involves peroxisome proliferator-activated receptor gamma. *Oncogene* 25:6015-6025.

Sugimoto, Y., and S. Narumiya. 2007. Prostaglandin E receptors. *The Journal of biological chemistry* 282:11613-11617.

Sun, D., and C.D. Funk. 1996. Disruption of 12/15-lipoxygenase expression in peritoneal macrophages. Enhanced utilization of the 5-lipoxygenase pathway and diminished oxidation of low density lipoprotein. *The Journal of biological chemistry* 271:24055-24062.

Takahashi, T., S.J. Zhu, H. Sumino, S. Saegusa, T. Nakahashi, K. Iwai, S. Morimoto, and T. Kanda. 2005. Inhibition of cyclooxygenase-2 enhances myocardial damage in a mouse model of viral myocarditis. *Life sciences* 78:195-204.

Talvani, A., F.S. Machado, G.C. Santana, A. Klein, L. Barcelos, J.S. Silva, and M.M. Teixeira. 2002. Leukotriene B(4) induces nitric oxide synthesis in Trypanosoma cruzi-infected murine macrophages and mediates resistance to infection. *Infection and immunity* 70:4247-4253.

Tanaka, Y., S.L. Ward, and W.L. Smith. 1987. Immunochemical and kinetic evidence for two different prostaglandin H-prostaglandin E isomerases in sheep vesicular gland microsomes. *The Journal of biological chemistry* 262:1374-1381.

Tarleton, R.L. 2001. Parasite persistence in the aetiology of Chagas disease. *International journal for parasitology* 31:550-554.

Tarleton, R.L. 2007. Immune system recognition of Trypanosoma cruzi. *Current opinion in immunology* 19:430-434.

Tarleton, R.L., M.J. Grusby, M. Postan, and L.H. Glimcher. 1996. Trypanosoma cruzi infection in MHC-deficient mice: further evidence for the role of both class I- and class II-restricted T cells in immune resistance and disease. *International immunology* 8:13-22.

Tarleton, R.L., B.H. Koller, A. Latour, and M. Postan. 1992. Susceptibility of beta 2-microglobulin-deficient mice to Trypanosoma cruzi infection. *Nature* 356:338-340.

Tarleton, R.L., J. Sun, L. Zhang, and M. Postan. 1994. Depletion of T-cell subpopulations results in exacerbation of myocarditis and parasitism in experimental Chagas' disease. *Infection and immunity* 62:1820-1829.

Teixeira, A.R., M.M. Hecht, M.C. Guimaro, A.O. Sousa, and N. Nitz. 2011. Pathogenesis of chagas' disease: parasite persistence and autoimmunity. *Clinical microbiology reviews* 24:592-630.

Teixeira, D.E., M. Benchimol, P.H. Crepaldi, and W. de Souza. 2012. Interactive multimedia to teach the life cycle of Trypanosoma cruzi, the causative agent of Chagas disease. *PLoS neglected tropical diseases* 6:e1749.

Teixeira, M.M., R.T. Gazzinelli, and J.S. Silva. 2002. Chemokines, inflammation and Trypanosoma cruzi infection. *Trends in parasitology* 18:262-265.

Thi, E.P., U. Lambertz, and N.E. Reiner. 2012. Sleeping with the enemy: how intracellular pathogens cope with a macrophage lifestyle. *PLoS pathogens* 8:e1002551.

Timoshenko, A.V., P.K. Lala, and C. Chakraborty. 2004. PGE2-mediated upregulation of iNOS in murine breast cancer cells through the activation of EP4 receptors. *International journal of cancer* 108:384-389.

Torrico, F., H. Heremans, M.T. Rivera, E. Van Marck, A. Billiau, and Y. Carlier. 1991. Endogenous IFN-gamma is required for resistance to acute Trypanosoma cruzi infection in mice. *J Immunol* 146:3626-3632.

Tournadre, A., and P. Miossec. 2012. Interleukin-17 in inflammatory myopathies. *Current rheumatology reports* 14:252-256.

Trinchieri, G., and A. Sher. 2007. Cooperation of Toll-like receptor signals in innate immune defence. *Nat Rev Immunol* 7:179-190.

Truyens, C., A. Angelo-Barrios, F. Torrico, J. Van Damme, H. Heremans, and Y. Carlier. 1994. Interleukin-6 (IL-6) production in mice infected with Trypanosoma cruzi: effect of its paradoxical increase by anti-IL-6 monoclonal antibody treatment on infection and acute-phase and humoral immune responses. *Infection and immunity* 62:692-696.

Truyens, C., and Y. Carlier. 2010. Protective Host Response to Parasite and Its Limitations. In American Trypanosomiasis Chagas Disease. One hundred years of research. M.T. Jenny Telleira, editor Elsevier,

Tyler, K.M., and D.M. Engman. 2001. The life cycle of Trypanosoma cruzi revisited. *International journal for parasitology* 31:472-481.

Ullrich, V., and M. Haurand. 1983. Thromboxane synthase as a cytochrome P450 enzyme. *Advances in prostaglandin, thromboxane, and leukotriene research* 11:105-110.

Urade, Y., M. Ujihara, Y. Horiguchi, K. Ikai, and O. Hayaishi. 1989. The major source of endogenous prostaglandin D2 production is likely antigen-presenting cells. Localization of glutathione-requiring prostaglandin D synthetase in histiocytes, dendritic, and Kupffer cells in various rat tissues. *J Immunol* 143:2982-2989.

van den Borne, S.W., J. Diez, W.M. Blankesteijn, J. Verjans, L. Hofstra, and J. Narula. 2010. Myocardial remodeling after infarction: the role of myofibroblasts. *Nature reviews* 7:30-37.

van der Pouw Kraan, T.C., L.C. Boeije, R.J. Smeenk, J. Wijdenes, and L.A. Aarden. 1995. Prostaglandin-E2 is a potent inhibitor of human interleukin 12 production. *The Journal of experimental medicine* 181:775-779.

van Zandbergen, G., A. Bollinger, A. Wenzel, S. Kamhawi, R. Voll, M. Klinger, A. Muller, C. Holscher, M. Herrmann, D. Sacks, W. Solbach, and T. Laskay. 2006. Leishmania disease development depends on the presence of apoptotic promastigotes in the virulent inoculum. *Proceedings of the National Academy of Sciences of the United States of America* 103:13837-13842.

Vespa, G.N., F.Q. Cunha, and J.S. Silva. 1994. Nitric oxide is involved in control of Trypanosoma cruzi-induced parasitemia and directly kills the parasite in vitro. *Infection and immunity* 62:5177-5182.

Viotti, R., C. Vigliano, H. Armenti, and E. Segura. 1994. Treatment of chronic Chagas' disease with benznidazole: clinical and serologic evolution of patients with long-term follow-up. *Am Heart J* 127:151-162.

Weinberg, D.A., L.K. Weston, and J.E. Kaplan. 1985. Influence of prostaglandin I2 on fibronectin-mediated phagocytosis in vivo and in vitro. *Journal of leukocyte biology* 37:151-159.

Wen, Y., J. Gu, G.E. Vandenhoff, X. Liu, and J.L. Nadler. 2008. Role of 12/15-lipoxygenase in the expression of MCP-1 in mouse macrophages. *Am J Physiol Heart Circ Physiol* 294:H1933-1938.

Wenzel, A., and G. Van Zandbergen. 2009. Lipoxin A4 receptor dependent leishmania infection. *Autoimmunity* 42:331-333.

Wynn, T.A., and L. Barron. 2010. Macrophages: master regulators of inflammation and fibrosis. *Seminars in liver disease* 30:245-257.

Xia, Y., and J.L. Zweier. 1997. Superoxide and peroxynitrite generation from inducible nitric oxide synthase in macrophages. *Proceedings of the National Academy of Sciences of the United States of America* 94:6954-6958.

Xu, H., D.J. Izon, C. Loftin, and L.M. Spain. 2001. The COX-2 inhibitor NS-398 causes T-cell developmental disruptions independent of COX-2 enzyme inhibition. *Cellular immunology* 214:184-193.

Yao, C., D. Sakata, Y. Esaki, Y. Li, T. Matsuoka, K. Kuroiwa, Y. Sugimoto, and S. Narumiya. 2009. Prostaglandin E2-EP4 signaling promotes immune inflammation through Th1 cell differentiation and Th17 cell expansion. *Nature medicine* 15:633-640.

Yuhki, K., F. Kojima, H. Kashiwagi, J. Kawabe, T. Fujino, S. Narumiya, and F. Ushikubi. 2011. Roles of prostanoids in the pathogenesis of cardiovascular diseases: Novel insights from knockout mouse studies. *Pharmacology & therapeutics* 129:195-205.

Zhang, L., and R.L. Tarleton. 1996. Characterization of cytokine production in murine Trypanosoma cruzi infection by in situ immunocytochemistry: lack of association between susceptibility and type 2 cytokine production. *European journal of immunology* 26:102-109.

Zingales, B., S.G. Andrade, M.R. Briones, D.A. Campbell, E. Chiari, O. Fernandes, F. Guhl, E. Lages-Silva, A.M. Macedo, C.R. Machado, M.A. Miles, A.J. Romanha, N.R. Sturm, M. Tibayrenc, and A.G. Schijman. 2009. A new consensus for Trypanosoma cruzi intraspecific nomenclature: second revision meeting recommends TcI to TcVI. *Mem Inst Oswaldo Cruz* 104:1051-1054.

Zingales, B., M.A. Miles, D.A. Campbell, M. Tibayrenc, A.M. Macedo, M.M. Teixeira, A.G. Schijman, M.S. Llewellyn, E. Lages-Silva, C.R. Machado, S.G. Andrade, and N.R. Sturm. 2012. The revised Trypanosoma cruzi subspecific nomenclature: rationale, epidemiological relevance and research applications. *Infect Genet Evol* 12:240-253.

APPENDIX 1
Supplementary data

In this appendix we show the experiments we perform to set up the different histological staining of our preparations.

We have used the fluorochrome directly conjugated antibody against CD4 tested to flow citometry (557681 ,BD Pharmigen) to perform confocal immunofluorescence experiments. In **Fig. S1** peritoneal lymphocytes (Composto et al., 2011) and mouse thymus are positively stained.

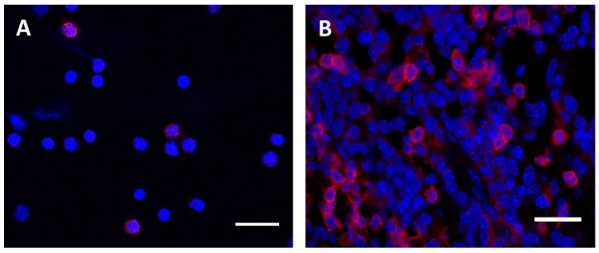

Figure S1 | CD4 is expressed in lymphocytes.

A | Mouse peritoneal cells were bound to Poly-L lysine coverslips and prepared for confocal immunofluorescence. Coverslips were stained with DAPI for **nuclei (blue)** and the directly conjugated antibody specific for lymphocyte marker **CD4 (red)** **B** | Normal thymus were isolated from BALB/c mice, frozen in OCT and prepared for confocal immunofluorescence. Slices were stained with DAPI for **nuclei** and the directly conjugated antibody especific for lymphocyte marker **CD4**. Scale bar is 20 microns length. Pictures are representative of two different coverslips or slices.

To set up the staining of the macrophage marker F4/80 antigen antibody (14-4801-81, eBioscience) mouse liver was used (**Fig. S2**) because it is known that Küpffer cells express the marker (Kinoshita et al., 2010).

In order to set up COX-2 and 12/15- LO enzymes staining peritoneal macrophages were selected. After try with different antibodies against COX-2, reference 106160 from Cayman Chemical was selected due to its well performance. LPS activated peritoneal macrophages (Lee et al., 1992) were used like a positive control in **Fig. S3**. 12/15-LO antiserum raised in guinea pig was a gift from Kühn H (Germany) (Dioszeghy et al., 2008). We have used freshly isolated peritoneal cells like a positive control in **Fig. S4**. These cells have been described like one of the higher 12/15-LO expressing cells in mice (Heydeck et al., 1998). Anti-CD68 (macrophage marker) antibody (MCA1957GA ,AbD Serotec) was tested also in this peritoneal cells.

Anti-Vimentin antibody directly conjugated to Alexa Fluor 647™ (9856 S from Cell Signaling) was used to stain the intermediate filament cytoskeleton in fibroblast and heart tissue, **Fig. S5 A** and **B** respectively.

Confocal immunofluorescence was used to detect lipid droplets with Oil Red O (ORO) in propylene Glycol 26079-15 purchased from Electron Microscopy Sciences. To set up the staining and detection of lipid droplets peritoneal cavity macrophages were used **Fig. S6** (Hu et al., 2003).

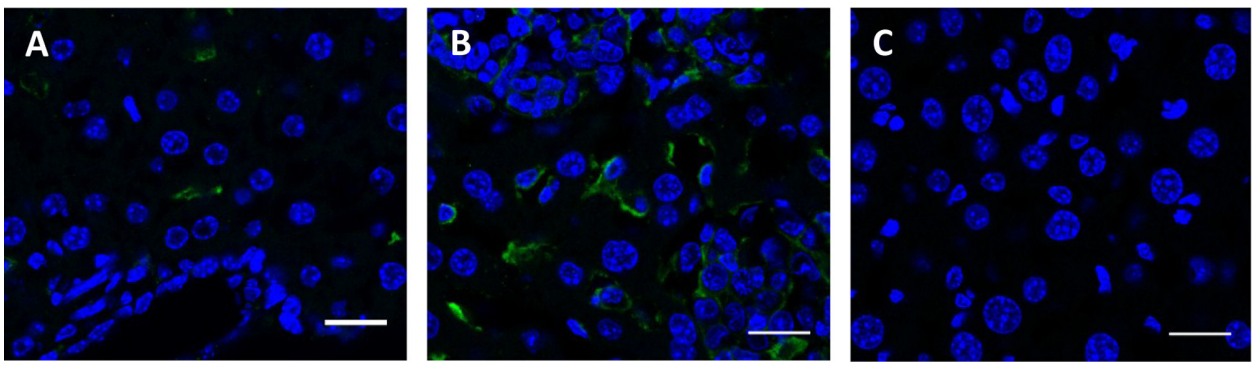

Figure S2 | F4/80 is expressed by liver macrophages. Livers form infected and not infected BALB/c mice were collected, frozen in OCT and prepared for confocal immunofluorescence. DAPI staining was used to visualize **nuclei (blue)** and the antibody raised against **F4/80 (green)** to visualized macrophages. **A** | Not infected liver **B** | Infected liver **C** | Secondary antibody control using infected tissue. Scale bar is 20 microns length. Pictures are representative of three different organs.

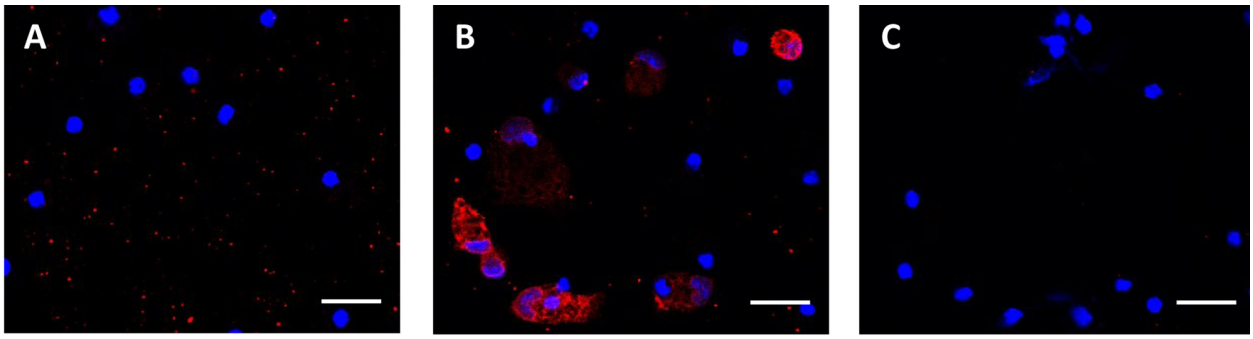

Figure S3 | COX-2 is expressed in LPS-stimulated macrophages. Peritoneal macrophages were cultured in coverslips and treated or not with *E.coli* LPS (1 microgram/ml) and prepared for confocal immunofluorescence. Coverslip stained with DAPI for **nuclei (blue)** and the antibody raised against the enzyme **COX-2 (red)** **A** | Non stimulated macrophages **B** | LPS treated macrophages. **C** | Secondary antibody control using LPS activated macrophages. Scale bar is 20 microns length. Pictures are representative of two different coverslips.

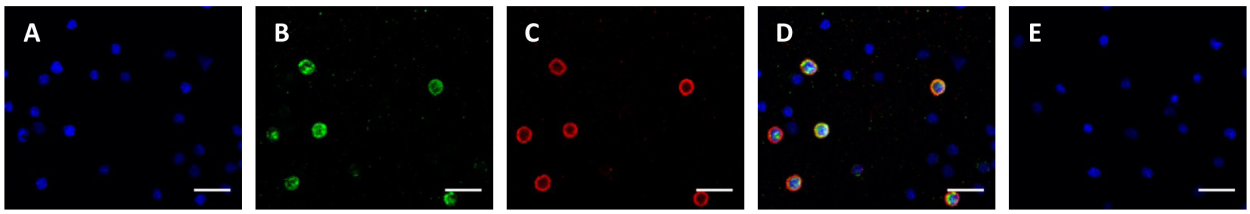

Figure S4 | 12/15 Lipoxygenase (12/15-LO) is highly expressed in freshly purified not activated peritoneal macrophages. Peritoneal cells were bound to Poly-L lysine coverslips and treated and prepared for confocal immunofluorescence. Coverslip were stained with DAPI for **nuclei (blue)** and the antibody raised against the macrophage marker **CD68 (green)** or the enzyme **12/15-LO (red)**. Upper set of panels represent the separated channels of the same confocal adquisition **A** | Nuclei stained with DAPI **B** | CD68 positive macrophages **C** | 12/15 LO expressing cells **D** | Merge **E** | Merge of secondary antibody control. Scale bar is 20 microns length. Pictures are representative of at least two different coverslips.

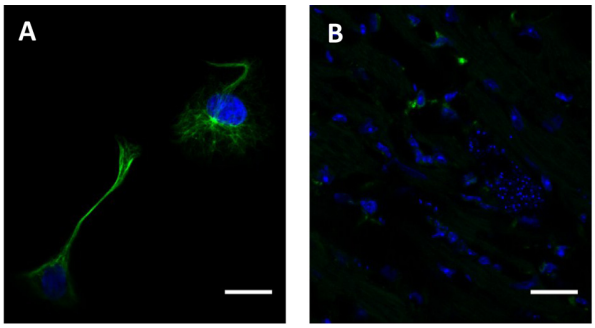

Figure S5 | Vimentin is abundant in intermediate filaments cytoskeleton. A | Vero cells were bound to coverslips and prepared for confocal immunofluorescence. **A** | Coverslips were stained with DAPI for **nuclei (blue)** and the directly conjugated antibody raised against **vimentin (green)** **B** | Infected heart tissue were isolated from BALB/c mice, frozen in OCT and prepared for confocal immunofluorescence, stained with DAPI for **nuclei** and the directly conjugated antibody raised against **vimentin** . Scale bar is 20 microns length. Pictures are representative of two different coverslips or organs.

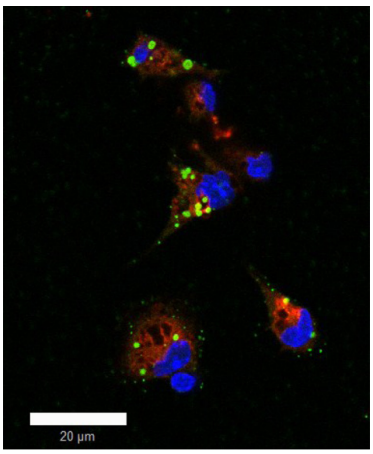

Figure S6 | Lipid bodies are produced in macrophages. Peritoneal macrophages were incubated with deferoxamine 375 µM overnight at 37°C and the following day stained to detect lipid bodies in coverslips. Coverslips were stained with DAPI for **nuclei (blue)**, the antibody raised against the macrophage marker **CD68 (red)** and **Oil Red O (green)** to detect lipid bodies. Scale bar is 20 microns length. Pictures are representative of two different coverslips.

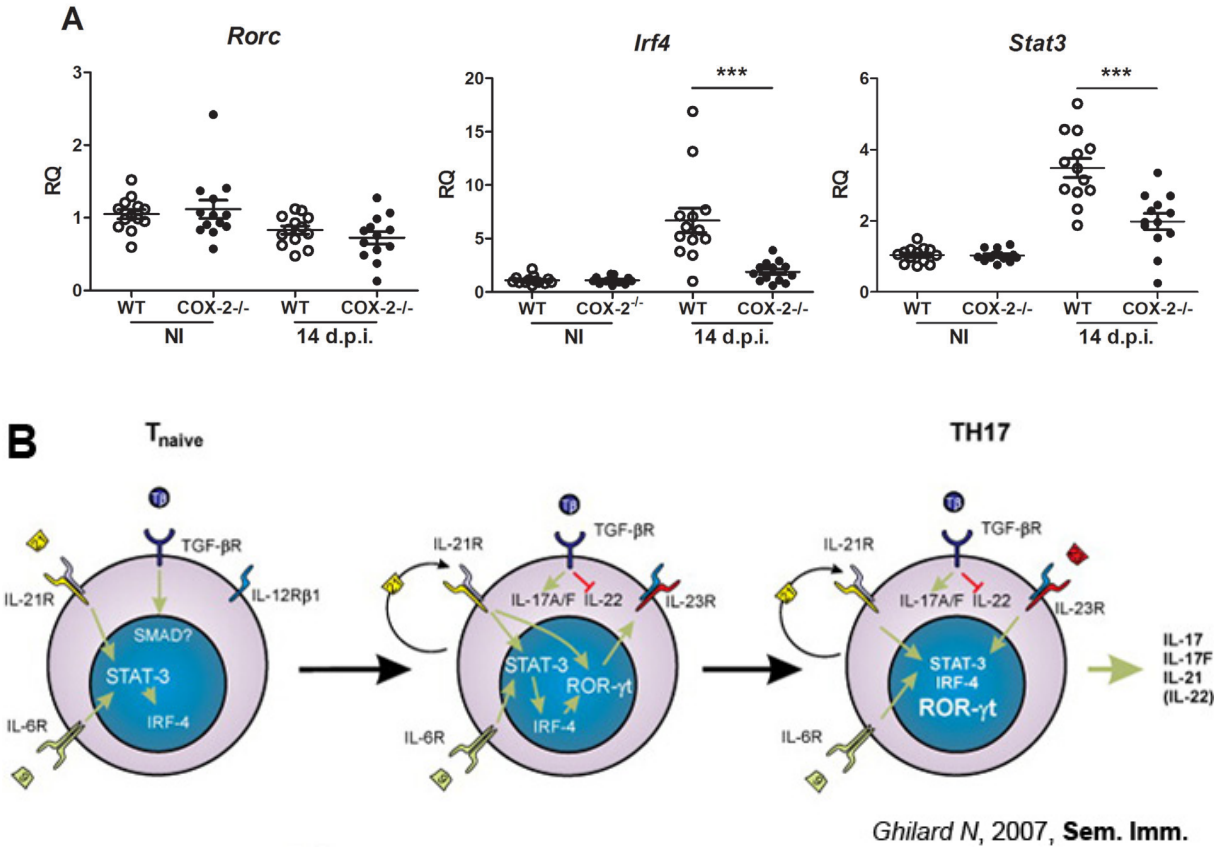

Figure S7 | Expression of gene related with Th17 differentiation in cardiac tissue of wild-type and COX-2 deficient mice infected with *Trypanosoma cruzi*. A | Heart tissue RNA was isolated at 14 d.p.i. and qPCR was performed. Results are expressed as RQ calculated from CT values as described in Materials and Methods. No amplification of IL-17 was detected Open circles indicate the values of wild-type mice closed circles of COX-2 deficient mice. Means ± SD from four experiments are shown (n=13). Differences between wild-type and COX-$2^{-/-}$ mice are indicated with * $p<0.05$. **B |** Scheme of Th17 differentiation. Adapted from *Ghilardi N*, 2007, Seminar in Immunology

IMAGE J MACRO USED TO AUTOMATE IMAGE ANALYSIS

```
origen = getDirectory("Elige la carpeta con las imagenes originales a
procesar");

resultados = getDirectory("Elige la carpeta para guardar los resultados ");

lista = getFileList(origen);

setBatchMode(false);

for (z=0; z<lista.length; z++) {

      showProgress(z+1, lista.length);

      open(origen+lista[z]);

      nombre = lista[z];

      run("Advanced Weka Segmentation", "origen + nombre");

      selectWindow("Advanced Weka Segmentation");

      call("trainableSegmentation.Weka_Segmentation.loadClassifier", "C:\\
Users\\vlabrador\\Desktop\\clasificador.model");

      wait(3000);

      call("trainableSegmentation.Weka_Segmentation.applyClassifier", origen,
nombre, "showResults=true", "storeResults=false", "probabilityMaps=false",
"");

      selectWindow("Advanced Weka Segmentation");

      selectWindow("Classification result");

      saveAs(".tiff", resultados + nombre + "-Binary");

      run("Set Scale...", "distance=313.67 known=100 pixel=1 unit=µm
global");

      run("Set Measurements...", "area area_fraction limit display
redirect=None decimal=3");

      class1 = nombre + "__Fibrosis";

      rename(class1);

      //run("Threshold...");

      setThreshold(175, 255);
```

```
        run("Measure");
        class2 = nombre + "__Fondo";
        rename(class2);
        //run("Threshold...");
        setThreshold(150, 174);
        run("Measure");
        class3 = nombre + "__Nucleos";
        rename(class3);
        //run("Threshold...");
        setThreshold(75, 100);
        run("Measure");
        class4 = nombre + "__Tejido y Eritrocitos";
        rename(class4);
        //run("Threshold...");
        setThreshold(0, 74);
        run("Measure");
        close();
        close();
        close();
        close();
}
selectWindow("Results");
saveAs("Text", resultados + "Resultados.xls");
run("Close");
```

APPENDIX 2
Published articles

OPEN ACCESS Freely available online

PLOS | NEGLECTED TROPICAL DISEASES

Trypanosoma cruzi Infection and Endothelin-1 Cooperatively Activate Pathogenic Inflammatory Pathways in Cardiomyocytes

Ricardo S. Corral[1]*, Néstor A. Guerrero[2,3], Henar Cuervo[2¤], Núria Gironès[2,3], Manuel Fresno[2,3]

1 Servicio de Parasitología-Chagas, Hospital de Niños Ricardo Gutiérrez, Buenos Aires, Argentina, **2** Centro de Biología Molecular Severo Ochoa, Consejo Superior de Investigaciones Científicas, Universidad Autónoma de Madrid, Cantoblanco, Madrid, Spain, **3** Instituto de Investigación Sanitaria Princesa, Hospital Universitario de La Princesa, Madrid, Spain

Abstract

Trypanosoma cruzi, the causative agent of Chagas' disease, induces multiple responses in the heart, a critical organ of infection and pathology in the host. Among diverse factors, eicosanoids and the vasoactive peptide endothelin-1 (ET-1) have been implicated in the pathogenesis of chronic chagasic cardiomyopathy. In the present study, we found that *T. cruzi* infection in mice induces myocardial gene expression of cyclooxygenase-2 (*Cox2*) and thromboxane synthase (*Tbxas1*) as well as endothelin-1 (*Edn1*) and atrial natriuretic peptide (*Nppa*). *T. cruzi* infection and ET-1 cooperatively activated the Ca^{2+}/calcineurin (Cn)/nuclear factor of activated T cells (NFAT) signaling pathway in atrial myocytes, leading to COX-2 protein expression and increased eicosanoid (prostaglandins E_2 and $F_{2\alpha}$, thromboxane A_2) release. Moreover, *T. cruzi* infection of ET-1-stimulated cardiomyocytes resulted in significantly enhanced production of atrial natriuretic peptide (ANP), a prognostic marker for impairment in cardiac function of chagasic patients. Our findings support an important role for the Ca^{2+}/Cn/NFAT cascade in *T. cruzi*-mediated myocardial production of inflammatory mediators and may help define novel therapeutic targets.

Citation: Corral RS, Guerrero NA, Cuervo H, Gironès N, Fresno M (2013) *Trypanosoma cruzi* Infection and Endothelin-1 Cooperatively Activate Pathogenic Inflammatory Pathways in Cardiomyocytes. PLoS Negl Trop Dis 7(2): e2034. doi:10.1371/journal.pntd.0002034

Editor: Helton da Costa Santiago, National Institutes of Health, United States of America

Received August 17, 2012; **Accepted** December 12, 2012; **Published** February 7, 2013

Funding: This work was supported by grants to M.F. from Ministerio de Ciencia y Tecnología, Spain (SAF2007-61716; SAF2005-02220); Red Temática de Investigación en Enfermedades Cardiovasculares (RECAVA RD06/0014/1013); Red de Investigación de Centros de Enfermedades Tropicales (RICET RD06/0021/0016); European Union (HEALTH-FE-2008-22303, ChagasEpiNet); Universidad Autónoma de Madrid and Comunidad de Madrid (CC08-UAM/SAL-4440/08); Fundación Ramón Areces and Agencia Española de Cooperación Internacional para el Desarrollo (AECID, A/9418/07 and A/017500/08 to M.F. and R.S.C.); and Fondo de Investigaciones Sanitarias (PS09/00538 to N.G.). R.S.C. is a Member of Research Career from Consejo Nacional de Investigaciones Científicas y Técnicas (CONICET), Argentina. M.F. and N.G. are professors at the "Biología Molecular" Department, Universidad Autónoma de Madrid. N.G. is a holder of a fellowship from Red de Investigación Cooperativa en Enfermedades Tropicales (RICET). N.A.G. was a recipient of a contract from RICET. The funders had no role in study design, data collection and analysis, decision to publish, or preparation of the manuscript.

Competing Interests: The authors have declared that no competing interests exist.

* E-mail: ricardocorral56@hotmail.com

¤ Current address: Laboratory for Accelerated Vascular Research, Division of Vascular Surgery, Department of Surgery, University of California, San Francisco, San Francisco, California, United States of America

Introduction

Chagas' disease, caused by the infection with the protozoan parasite *Trypanosoma cruzi*, constitutes the major cause of infectious heart disease in Latin America. It is estimated that 10 million people are infected with *T. cruzi* in the Central and South America, 100–120 million are at potential risk of infection and around 50,000 new cases occur each year [1]. In humans, an acute phase displays frequently as a non-apparent form with a few or no symptoms. Thereafter, the patients enter into an asymptomatic, indeterminate stage, which lasts throughout life in the majority of infected subjects. The remaining 20–30% of chronically infected individuals develop cardiac or digestive complications, typically years or decades after infection. Chronic cardiomyopathy is the most common and severe manifestation of human Chagas' disease, causing congestive heart failure, arrhythmias and conduction abnormalities, which often lead to stroke and sudden death. This type of dilated cardiomyopathy is associated with chronic inflammation and fibrosis, cardiac hypertrophy and thrombo-embolic events [2].

Compromised microcirculation, caused by *T. cruzi* infection, involves endothelial alterations, vasospasm, reduced blood flow and focal ischemia [3]. Cardiovascular production of vasoactive mediators has been implicated in the pathogenesis of the vasculopathy seen in chagasic heart disease [4]. Among other vasculitis-promoting factors, *T. cruzi* infection triggers myocardial overexpression and increased plasma levels of endothelin-1 (ET-1) in mice and chronic chagasic patients, which correlate with heart dysfunction [5,6]. A bulk of evidence supports the participation of this vasoactive peptide, produced by myocardial and endothelial cells among others, in Chagas' disease pathogenesis [4,5,7,8–10]. ET-1 activity may result in vascular injury, cardiac remodeling and enhanced liberation of inflammatory agents [11].

Endothelin-1 is involved in different signaling pathways that include increase in intracellular calcium levels ($[Ca^{2+}]_i$) and ERK1/2 activation leading to expression of cyclin D1 and inflammation-linked genes, all of them contributing to *T. cruzi*-mediated cardiac pathology [12,13]. Moreover, ET-1 has been shown to induce cell hypertrophy in primary cultures of rat

Author Summary

Chronic cardiomyopathy is the most common and severe manifestation of human Chagas' disease, caused by the protozoan parasite *Trypanosoma cruzi*. Among diverse inflammation-promoting moieties, eicosanoids and the vasoactive peptide endothelin-1 (ET-1) have been implicated in its pathogenesis. Nevertheless, the link between these two factors has not yet been identified. In the present study, we found that *T. cruzi* infection induces gene expression of ET-1 and eicosanoid-forming enzymes in the heart of infected mice. We also demonstrated that HL-1 atrial myocytes respond to ET-1 stimulus and *T. cruzi* infection by induction of cyclooxygenase-2 through activation of the Ca^{2+}/calcineurin/NFAT intracellular signaling pathway. Moreover, the cooperation between *T. cruzi* and ET-1 leads to overproduction of eicosanoids (prostaglandins E_2 and $F_{2\alpha}$, thromboxane A_2) and the pro-hypertrophic atrial natriuretic peptide. Our results support an important role for NFAT in *T. cruzi* plus ET-1-dependent induction of key agents of pathogenesis in chronic chagasic cardiomyopathy. Identification of the Ca^{2+}/calcineurin/NFAT cascade as mediator of cardiovascular pathology in Chagas' disease advances our understanding of host-parasite interrelationship and may help define novel potential targets for therapeutic interventions to ameliorate or prevent cardiomyopathy during chronic *T. cruzi* infection.

cardiomyocytes through a calcineurin (Cn)/nuclear factor of activated T cells (NFAT)-dependent mechanism [14,15]. The NFAT family includes four 'classical' members displaying a high degree of homology: NFATc1-4, each of which is expressed in heart tissue [16]. NFAT exists in a highly phosphorylated form in the cytoplasm, which translocates into the nucleus upon dephosphorylation by the phosphatase Cn in response to increases in $[Ca^{2+}]_i$, where it binds to enhancer elements of downstream genes leading to transcriptional activation [17].

One of the NFAT target genes associated with inflammation is cyclooxygenase-2 (COX-2), the inducible enzyme that catalyzes the rate-limiting step in prostanoid biosynthesis [18–20]. ET-1 is able to stimulate protein expression of COX-2 and prostacyclin release in cardiomyocytes [21]. In addition, experimental murine infection with *T. cruzi* has been shown to raise the number of cardiac cells positive for COX-1 and COX-2, as well as the circulating levels of cyclooxygenase metabolites [22,23]. Both host- and parasite-derived prostaglandins (PG) and thromboxane A_2 (TXA_2) are key regulators of pathogenesis during *T. cruzi* infection [24]. Remarkably, ET-1 stimulation of cardiac myocytes also results in NFATc4-dependent up-regulation of hypertrophy response genes such as atrial natriuretic peptide (ANP) and B-type natriuretic peptide (BNP) [25,26], potential markers of myocardial compromise in Chagas' disease [27,28].

Although ET-1 and eicosanoids have been proposed to play a role in Chagas' disease pathogenesis, the link between them has not yet been addressed. Thus, we have examined the regulation of *Cox2* expression and activity by the combined effect of ET-1 and *T. cruzi* infection of cardiomyocytes. Our results show that induction of *Cox2* expression by ET-1 plus *T. cruzi* in HL-1 atrial myocytes requires activation of the Ca^{2+}/Cn/NFAT pathway. NFAT is translocated to the nucleus upon stimulation with the peptide and subsequent infection where it binds to NFAT response elements in the promoter region of *Cox2* that are essential for transcriptional induction of the gene. Moreover, trypomastigote infection of ET-1-pre-treated HL-1 cardiomyocytes significantly enhanced production of eicosanoids and ANP by these cells. These findings demonstrate the participation of NFAT in [*T. cruzi*+ET-1]-mediated induction of genes involved in the pathogenesis of chronic Chagas' heart disease.

Materials and Methods

Ethics statement

This study was carried out in strict accordance with the recommendations of Spanish Legislation and the European Council Directive from the Convention for the Protection of Vertebrate Animals Used for Experimental and Other Scientific Purposes. All mice were maintained under pathogen-free conditions in the animal facility at the Centro de Biología Molecular, Universidad Autónoma de Madrid (Madrid, Spain). The animal protocol was approved by the Comité de Ética de la Investigación de la Universidad Autónoma de Madrid. Animals had free access to food and water and were handled in compliance with European codes of practice. Mice were euthanized in a CO_2 chamber, and all efforts were made to minimize suffering.

Cell culture, primary cardiomyocytes and infection

Mouse HL-1 cardiomyocytes were plated onto gelatin/fibronectin pre-coated flasks and cultured in Claycomb medium (Sigma-Aldrich) supplemented with 10% fetal calf serum, 100 U/ml penicillin, 100 µg/ml streptomycin and 2 mM L-glutamine as previously described [29]. Primary cardiomyocytes were isolated from BALB/c mice and cultured according to standard protocols [30]. HL-1 and primary cardiomyocytes were seeded in 6- (5×10^5/well) or 24- (1×10^5/well) well plates and infected with *T. cruzi* trypomastigotes (cell:parasite ratio 1:5), Y strain, routinely propagated in Vero cells. In some experiments, cell cultures were starved for 18 h and then treated with recombinant murine interferon-γ (25 U/ml IFN-γ, R&D Systems), 1 µg/ml lipopolysaccharide (LPS, Sigma-Aldrich) or 0.3 nM ET-1 (Sigma-Aldrich) for 2 h before infection. Endotoxin level in the ET-1 batch was <1 EU/mg, as determined using a *Limulus* amoebocyte lysate analysis kit (Whittaker Bioproducts). Plates were rinsed to remove free parasites and further incubated in complete medium at 37°C, 5% CO_2 for the indicated times.

In vivo infection

Young adult (6- to 8-wk-old) C57BL/6 mice were purchased from Charles River Laboratories. For infection experiments, 2×10^3 blood trypomastigotes (Y strain) per mouse were inoculated by intraperitoneal injection as described [31], keeping a group of non-infected mice. Age-matched BALB/c mice were infected in parallel. Parasitemia levels were checked every 2 days by direct inspection and counting parasites in a 5 µl drop of tail vein blood. Weekly during one month post-infection, groups of 3 mice were euthanized in a CO_2 chamber, and blood and various tissues were collected. Samples were processed for RNA or histological analysis.

RNA isolation, reverse transcription and polymerase chain reaction (PCR)

Total RNA was extracted from HL-1 cells and mouse heart tissue by using Trizol reagent (Invitrogen) according to the manufacturer's instructions. First-strand cDNA was prepared by incubation of 1 µg of total RNA with murine leukemia virus reverse transcriptase and random hexamer oligonucleotides (Bio-Rad Laboratories) at 40°C for 45 min. Then, 5 µl of the reaction products was amplified by PCR with 1.25 U of *Taq* DNA polymerase (Invitrogen). PCR amplification consisted of 94°C for

45 s for denaturation, 60°C for 45 s for annealing, and 72°C for 45 s for extension, performed for 30 cycles. The sense and antisense primers used for murine *Cox2* were: 5′-tcctcctggaacatg-gactc-3′ and 5′-gctcggcttccagtattgag-3′, respectively [32]. Aliquots of 10 µl of the PCR products were electrophoresed in a 1.6% agarose gel containing ethidium bromide.

Real-time PCR of infected heart tissue

Quantitative real-time RT-PCR analysis was performed using the High Capacity cDNA Archive Kit (Applied Biosystems), and amplification of different murine genes (*Cox2*, *Cox1*, *Tbxas1*, *Nppa*, *Edn1* and ribosomal 18S) was performed in triplicate with the use of TaqMan MGB probes and the TaqMan Universal PCR Master Mix (Life Technologies) on an ABI Prism 7900 HT instrument (Applied Biosystems), as reported previously [31]. Quantification of gene expression was calculated using the comparative threshold cycle (C*t*) method, normalized to the ribosomal 18S control and efficiency of the RT reaction (relative quantity, $2^{-\Delta\Delta C}T$).

Histological and immunohistochemical analysis of heart

Cardiac tissues from mice were placed after been cut in two pieces in 10% neutral buffered formalin for at least 4 h at room temperature followed by overnight incubation in 70% ethanol. Samples were them embedded in paraffin (Tissue Embedding Station Leica EG1160), and 5-µm tissue sections were prepared using a motorized Microtome Leica RM2155. Samples were deparaffinized and rehydrated using a Tissue Processing Station Leica TP1020. Slides were stained using the Masson's trichrome staining and mounted permanently in Eukkitt's quick hardening mounting system medium (Biochemika, Fluka Analytical). The sections were analyzed in a Leica DMD 108 microscope (Leica Microsystems, Germany). For immunohistochemical studies, myocardial sections were deparaffinized by routine procedures and analyzed using anti-murine COX-2 rabbit polyclonal antibody (Abcam) and biotinylated swine antiserum to rabbit immunoglobulin (Dako), following a procedure previously described [33].

Immunoblot analysis

Immunoblotting was carried out as described elsewhere [19]. Cardiac cells were disrupted and solubilized extracts (20 µg) were separated in 6% (only for analysis of NFAT translocation to the nucleus) or 10% sodium dodecyl sulfate-polyacrylamide gels, and transferred to nitrocellulose filters. After blocking for 2 h with 5% non-fat dried milk in Tris-buffered saline containing 0.1% Tween-20, the membranes were probed 2 h at 37°C with murine monoclonal antibodies against COX-2 (diluted 1:250 in blocking buffer, BD Biosciences), α-tubulin (1:1000, Sigma-Aldrich), and with rabbit polyclonal antibodies against NFAT (c1 to c4 isoforms, 1:200, Santa Cruz Biotechnology), prostaglandin E synthase-2 (microsomal, 1:500), thromboxane synthase (1:500, Cayman) and prostaglandin F synthase/AK31C3 (1:2,000, ProSci). The filters were washed and incubated with the corresponding secondary antibody linked to horseradish peroxidase at 1:10,000 dilution, and the stained bands were visualized by a chemiluminescent peroxide substrate (Amersham Pharmacia).

Plasmid constructs

Cox2 promoter constructs spanning from −1796 (P2-1900-LUC) and −170 (P2-274-LUC) to +104 bp relative to the transcription start site of the human *Cox2* gene and the P2-274-LUC plasmid with binding sites for NFAT, or AP-1, or both mutated were described [19]. The pSH102CD418 expression vector derives from pBJ5 and encodes an NFATc1 deletion mutant (1–418) that functions as a dominant negative for all NFAT isoforms [34].

Transfection and luciferase assays

HL-1 cells were transfected by Lipofectamine (Invitrogen) as described [19]. Briefly, exponential growing cells (2×10^5/well) cultured in 24-well plates were incubated for 3 h at 37°C with a mixture of 0.5–1 µg of the corresponding reporter plasmid and Lipofectamine-containing Opti-MEM (Invitrogen). The total amount of DNA in each transfection was kept constant by using the empty expression vectors. Complete medium was then added to cells and incubated at 37°C for additional 16 h. Transfected cells were exposed to different stimuli (0.3 nM ET-1, or phorbol 12-myristate 13-acetate -PMA- plus A23187 calcium ionophore -Ion-, Sigma-Aldrich) and/or *T. cruzi*-infected as indicated. In some experiments, FK506 (100 ng/ml, Sandoz Ltd., Tokyo, Japan) was added for 1 h. Then, cells were harvested and lysed. Luciferase activity was determined by using a luciferase assay system (Promega) with a luminometer Monolight 2010 (Analytical Luminescence). Transfection experiments were performed in triplicate. Data of luciferase activity are presented as fold induction (observed experimental relative luciferase units (RLU)/basal RLU in absence of any stimulus). Results were normalized for extract protein concentrations measured with a Bradford assay kit (Pierce, Thermo Fisher Scientific).

Intracellular calcium measurements

Agonist-induced changes in $[Ca^{2+}]_i$ were detected using the Ca^{2+}-sensitive dye Fura-2/AM as described [35]. Briefly, cell monolayers at 80% confluence were trypsinized, washed and then loaded with 1 µM Fura-2/AM under continuous stirring for 30 min at 37°C. The cells (2×10^6/ml) were exposed to 0.3 nM ET-1 and/or infected with *T. cruzi* trypomastigotes (cell:parasite ratio 1:5), and placed in an Aminco Bowman Series 2 spectrofluorometer (Thermo). Uninfected cultures were used as controls. At the indicated times, the fluorescence signal of Fura-2 was recorded, with excitation and emission at 340 and 510 nm, respectively.

Electrophoretic mobility shift assay (EMSA)

Nuclear extracts were prepared from ET-1-treated and/or *T. cruzi*-infected HL-1 cells as described [36] with minor modifications. Purity of fractions was proven by analyzing cytoplasmic and nuclear marker proteins including α-tubulin (cytoplasmic), and topoisomerase IIβ and c-jun (nuclear). In brief, 5 µg of nuclear protein was incubated with 1 µg of poly(dI–dC) DNA carrier in DNA binding buffer (10% (wt/vol) polyvinylethanol, 12.5% (vol/vol) glycerol, 50 mM Tris, pH 8, 2.5 mM dithiothreitol, 2.5 mM ethylenediaminetetraacetic acid) for 30 min at 4°C. Then, 10^5 counts per minute (c.p.m.) (10^8 c.p.m./µg) of the ^{32}P-labeled double-stranded oligonucleotide (2 µg) were added, and the reaction was incubated at room temperature for 30 min. A synthetic oligonucleotide containing the NFAT consensus sequence 5′-gggtggggtggggaaagccgaggcgga-3′ (nucleotides −98 to −73) in the rat Cox-2 promoter was used as probe/competitor in EMSAs. For competition experiments, a 50-fold molar excess of unlabeled oligonucleotide was added before the addition of the probe. Supershift assays were performed by incubating nuclear extracts with either normal rabbit IgG or anti-NFATc4 antibody for 15 min at 4°C before the addition of the probe. DNA-protein complexes were resolved by electrophoresis in 4% non-denaturing polyacrylamide gels and were subjected to autoradiography.

Measurements of metabolites

For eicosanoid measurements, HL-1 cells were maintained for 12 h in culture medium supplemented with 0.5% fetal calf serum, then pre-treated or not with 10 μM indomethacin (Sigma-Aldrich) or 10 μM NS-398 (Alexis) for 1 h, and further stimulated with 0.3 nM ET-1 for 2 h. After treatment, cardiomyocytes were infected with *T. cruzi* trypomastigotes for 24 h. At that time, media supernatants were collected and analysed for PGE_2, $PGF_{2\alpha}$ and TXB_2 by ELISA (Cayman) according to manufacturer's specifications. In addition, eicosanoid levels were determined by ELISA in the sera from both uninfected and *T. cruzi*-infected C57BL/6 mice at 21 days of infection.

For ANP measurements, 24-h supernatants from ET-1-stimulated and/or *T. cruzi*-infected HL-1 cells, as well as serum specimens from both uninfected and *T. cruzi*-infected mice, were analyzed by ELISA (Kamiya Biomedical) following the instructions of the supplier.

For ET-1 measurements, the sera from uninfected and *T. cruzi*-infected mice were analyzed by ELISA (Phoenix Pharmaceuticals), according to the manufacturer's guidelines.

Statistical analysis

Statistical analysis was performed by using GraphPad Prism 5.0 software. Arithmetics means and standard error of the means (s.e.m.) were calculated. Significant differences among groups were made by using the one-way analysis of variance test followed by Tukey's test. A difference between groups of $P<0.05$ was considered significant.

Results

Trypanosoma cruzi infection induces the expression of markers of cardiac damage and eicosanoid enzymes in the heart

As shown in previous works from our group [30,37], C57BL/6 mice proved susceptible to infection with the Y strain of *T. cruzi*, albeit less severely than BALB/c mice, and survived acute infection (Figure 1A,B). Intense myocardial parasitism and inflammatory pathology were observed at 21 days of infection, together with enhanced COX-2 expression revealed by immunohistochemistry in both cardiomyocytes and heart-infiltrating leukocytes (Figure 1C). Accordingly, *T. cruzi*-infected C57BL/6 mice showed an augmented (up to 100 fold) expression of myocardial *Cox2* mRNA (Figure 1D) coincident with the highest parasite burden in the heart and maximum severity of myocarditis [30]. In addition, we detected a parallel increase (up to 15 fold) in the expression of the TXS gene (*Tbxas1*). However, no effect was observed on the expression of *Cox1* mRNA (data not shown). Overall, results similar to those above were found in *T. cruzi*-infected BALB/c mice. Moreover, mRNA levels of ET-1 (*Edn1*) and ANP (*Nppa*), a prognostic marker for impairment in cardiac function of chagasic patients [28], were up-regulated in heart tissue of infected C57BL/6 mice (Figure 1D). Upon infection, ET-1 increased in the two mouse genetic backgrounds. This enhanced mRNA expression in the heart of infected animals was accompanied by elevated serum levels of both peptides and circulating eicosanoids (TXB_2 and $PGF_{2\alpha}$) (Figure 1E). It is important to note that observed values from BALB/c and C57BL/6 animals cannot be directly compared to each other, since data are normalized to non-infected values that can differ between both mouse strains.

Trypanosoma cruzi- and endothelin-1-regulated *Cox2* expression in mouse cardiomyocytes

The observed *Cox2* mRNA expression in infected heart could come from infected cardiomyocytes, endothelial cells, fibroblasts and/or infiltrating leukocytes. Hence, we tested whether cardiomyocytes up-regulate *Cox2* upon *T. cruzi* infection *in vitro*. A strong induction of COX-2 protein expression was observed in neonatal cardiomyocyte primary cultures infected with *T. cruzi*, comparable to that induced by a well-known pro-inflammatory stimulus as LPS plus IFNγ (Figure 2A). To better examine the molecular regulatory mechanism of gene expression of this inducible enzyme by infection, we used the terminally differentiated murine HL-1 cardiomyocyte cell line infected with *T. cruzi*. Although some reports have described an impaired inflammatory ability of HL-1 cells to express NO synthase-2 or to activate NF-κB [38], others find the opposite [39]. Nonetheless, in our hands these cells retain contractile and phenotypic characteristics of the adult cardiomyocytes and they are much better suitable for transfection experiments than immature cardiac myocytes, as it has been described [40]. After 3 h of parasite infection, *Cox2* mRNA could not be detected. Similarly, a very weak *Cox2* induction was also noted in cardiomyocytes cultured in the presence of 0.3 nM ET-1. However, when ET-1-pre-treated HL-1 cells were infected with *T. cruzi* trypomastigotes ([*T. cruzi*+ET-1]), a strong increase in *Cox2* mRNA expression was detected (Figure 2B). These findings were confirmed by analysing COX-2 protein (Figure 2C).

The above results suggested that the combined effect of *T. cruzi* infection and ET-1 treatment on *Cox2* expression was taking place at the transcriptional level. To confirm this, HL-1 cardiac cells were transfected with a *Cox2* promoter/luciferase construct spanning from nucleotide −1796 to +104 bp relative to the human *Cox2* gene transcription start site (P2-1900-Cox-2-LUC). As shown in Figure 2D, *T. cruzi* plus ET-1 (0.3 nM) induced a four-fold increment ($P<0.05$) in luciferase activity in transiently transfected cells compared to untreated controls. In contrast, *T. cruzi*-infected cardiomyocytes and ET-1-stimulated uninfected cells showed very little increase. Interestingly, addition of the Cn inhibitor FK506 (100 ng/ml) significantly attenuated [*T. cruzi*+ET-1]-mediated induction of *Cox2* promoter.

Transcriptional regulation of the *Cox2* promoter by the combined effect of *Trypanosoma cruzi* and endothelin-1

To map the *Cox2* promoter region responsible for [*T. cruzi*+ET-1] inducibility, we used several *Cox2* promoter deletion/mutation constructs. Deletion up to −170 (P2-1900 to P2-274) of the *Cox2* promoter region did not significantly affect [*T. cruzi*+ET-1] inducibility (Figure 2E). Given the relevance of the region spanning from nucleotides −170 to −46 for the recorded induction of the *Cox2* promoter, we next determined the contribution of the known transcription factor sites present in this region [19] to the overall transcriptional regulation of [*T. cruzi*+ET-1]-dependent *Cox2* expression. Transfection experiments showed that mutation of the dNFAT (P2-274 dNFAT mut) or pNFAT (P2-274 pNFAT mut) sites resulted in a 65 and a 60% loss in the [*T. cruzi*+ET-1]-induced *Cox2* promoter activity, respectively, whereas double mutation of both NFAT (P2-274 p- and dNFAT mut) sites drastically reduced this activation. Conversely, mutagenesis of the AP-1-like site (P2-274 AP-1 mut) present in this region did not significantly diminish the inducibility of the *Cox2* promoter by [*T. cruzi*+ET-1]. To further confirm the central role of NFAT activation in the transcriptional regulation mediated by *T. cruzi* in ET-1-stimulated HL-1 cells, we co-transfected a dominant-negative version of NFAT (dnNFAT), previously

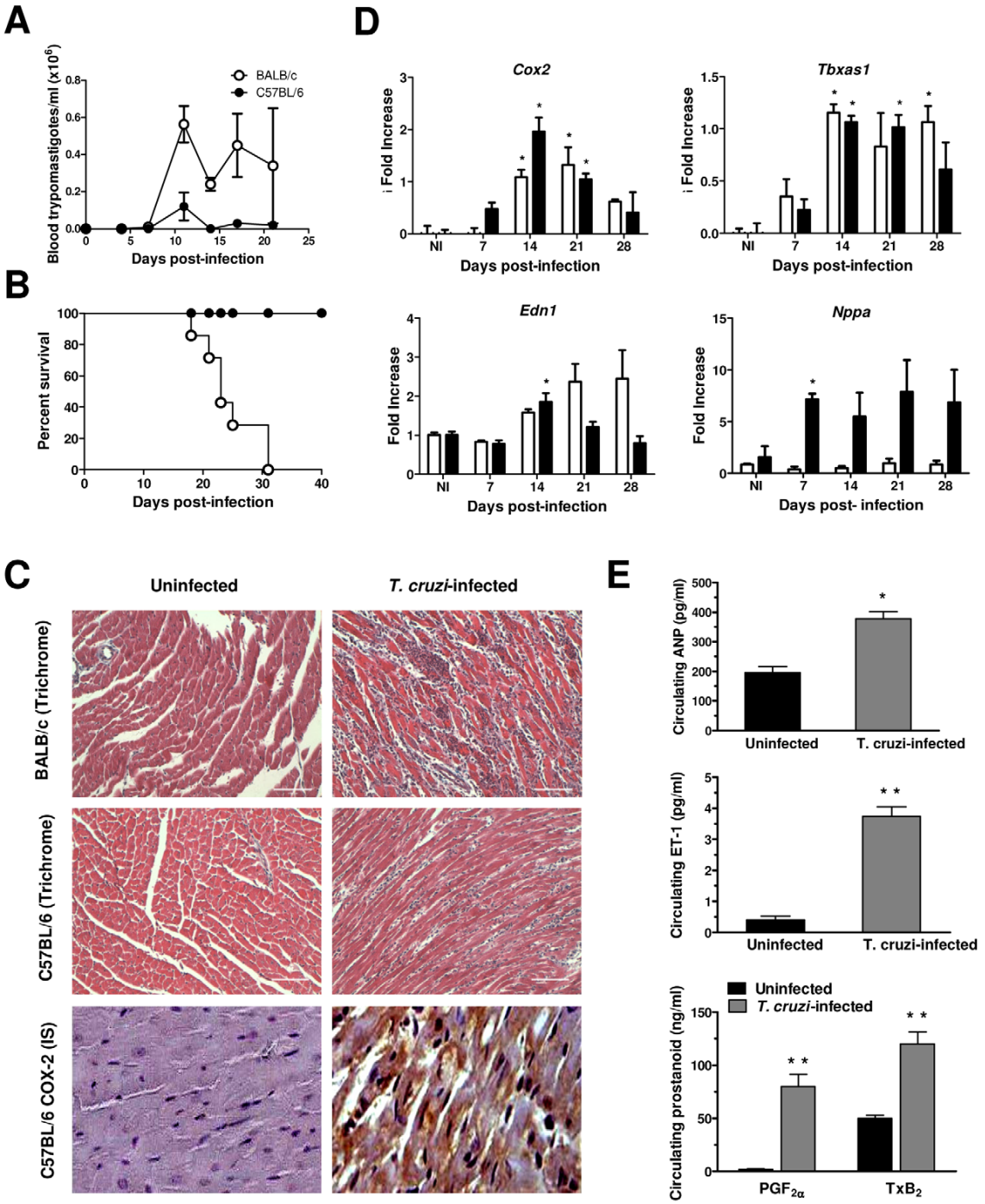

Figure 1. *Trypanosoma cruzi* infection induces *Cox2*, *Tbxas1*, *Edn1* and *Nppa* in infected heart tissue. (A and B) C57BL/6 (*black circles*) and BALB/c (*white circles*) mice were infected with 2×10^3 blood-trypomastigote forms of the Y strain. (A) Parasitemia expressed as the mean ± standard error of the mean (s.e.m.) of the number of parasites per 5 µl of blood. (B) Percent of mice survival. Results are representative of 2 independent experiments, each performed with 6 mice per group. (C) Tissue inflammation, parasitism and COX-2 expression in heart from uninfected (left panels) and *T. cruzi*-infected (21 days post-infection, right panels) mice. Representative results of histological analysis (Mason's trichrome staining) of cardiac tissue specimens from BALB/c and C57BL/6 mice (top and center panels, respectively) are shown. Bars = 100 µm. Bottom panels display representative results of COX-2 immunostaining (IS) in the hearts from C57BL/6 mice. Original magnification for microphotographs ×400. (D) *Cox2* (COX-2), *Tbxas1* (TXS), *Edn1* (ET-1) and *Nppa* (ANP) gene expression in the heart during the acute phase of infection in C57BL/6 and BALB/c mice. RNA from heart tissue at different days post-infection was used to perform RT-PCR with specific probes, and normalized to ribosomal 18S RNA as described in 'Materials and Methods'. Values are expressed as means ± s.e.m. from 3 independent infections, each performed with 3 mice per group.

*$P<0.05$. (E) Levels of circulating peptides (ET-1 and ANP) and eicosanoids ($PGF_{2\alpha}$ and TxB_2) in the sera of uninfected (*black bars*) and *T. cruzi*-infected (*grey bars*) C57BL/6 mice. Mouse sera were collected before and after 21 days of infection, and were assayed in triplicate by capture ELISA for ANP (top panel), ET-1 (central panel), $PGF_{2\alpha}$ and TxB_2 (bottom panel). Each bar represents the mean values for groups of 6 mice ± s.e.m. Similar results were obtained in two additional experiments. *$P<0.05$; **$P<0.01$.
doi:10.1371/journal.pntd.0002034.g001

described to abolish NFAT-dependent promoter activity [19], together with the P2-274-Cox-2-LUC plasmid. Interestingly, expression of dnNFAT abrogated [*T. cruzi*+ET-1]-induced transcription of the reporter (Figure 2E), supporting the hypothesis of the involvement of NFAT signaling in the regulation of *Cox2* gene expression by the cooperation between ET-1 and *T. cruzi* infection in cardiomyocytes.

Trypanosoma cruzi infection leads to activation of the Ca^{2+}/Calcineurin/NFAT intracellular signaling pathway in endothelin-1-treated cardiomyocytes

T. cruzi trypomastigote invasion of cardiac myocytes triggers a transient $[Ca^{2+}]_i$ elevation [41]. Similarly, upon the addition of trypomastigotes to HL-1 cells, we observed a transient $[Ca^{2+}]_i$ response associated to a considerable, sustained increase in $[Ca^{2+}]_i$ during the invasion process (Figure 3A). Comparable outcome, although with higher $[Ca^{2+}]_i$ levels, was obtained in *T. cruzi*-infected HL-1 cells pre-treated with 0.3 nM ET-1.

In HL-1 cells, basal expression of several isoforms of NFAT proteins (c1, c3 and c4) was detected by immunoblot analysis. Interestingly, stimulation with *T. cruzi* plus ET-1 induced a remarkable increase in the expression of NFATc4 and to a lesser extent, NFATc1 and NFATc3 (Figure 3B). Moreover, NFATc4 was present in the cytoplasm of untreated cardiac cells, but upon parasite infection of ET-1-stimulated cardiomyocytes, it was translocated into the nucleus. Pre-treatment with FK506 (100 ng/ml), a Cn inhibitor, prevented this translocation, thereby resulting in an accumulation of cytoplasmic NFATc4 protein (Figure 3C). To a much lesser extent, we also observed NFATc1 and NFATc3 migration to the nucleus (data not shown). Together, the above results indicate the activation of the NFATc4 isoform by [*T. cruzi*+ET-1] through a Ca^{2+}/Cn signaling process.

To analyse NFATc4 binding to the NFAT sequences of the *Cox2* promoter, we performed EMSAs with nuclear extracts of atrial HL-1 myocytes (Figure 3D). PMA (15 ng/ml) supplemented with Ion (1 μM) was used as a control stimulus. The NFAT oligonucleotide probe from *Cox2* promoter specifically bound nuclear proteins from [*T. cruzi*+ET-1]- and [PMA+Ion]-treated HL-1 cells, which was efficiently competed with a 50-fold molar excess of cold oligonucleotide (Cox-2-NFAT). These inducible complexes were severely diminished in nuclear extracts from cells stimulated with *T. cruzi* plus ET-1 in the presence of FK506. No NFAT binding could be demonstrated in response to ET-1 stimulation in the absence of parasites or *T. cruzi* infection alone. To determine unambiguously the presence of the NFATc4 protein in the complexes, we performed super shifting with an NFATc4-specific antibody. This antibody clearly displaced the migration of the bound probe, allowing the formation of more retarded complexes likely constituted by DNA/NFAT/antibody (Figure 3D). As the NFATc4-specific antibody completely supershifted the complex, it is indicative that c4, but no other NFAT isoform, is bound to *Cox2* promoter DNA in detectable amount. As a negative control, normal rabbit IgG was used. Taken together, these data suggest the binding of NFATc4 to the corresponding sites within the *Cox2* promoter in response to *T. cruzi* infection of ET-1-pre-treated HL-1 cells.

Trypanosoma cruzi infection of endothelin-1-treated HL-1 cardiomyocytes enhances the production of eicosanoids and atrial natriuretic peptide

To assess whether [*T. cruzi*+ET-1]-mediated induction of *Cox2* expression was associated with an increase in its enzymatic activity, eicosanoid release by HL-1 cells was measured. Compared to mock-treated cells, stimulation of myocytes with 0.3 nM ET-1, or trypomastigote infection over a 24-h period, or the combination of both, induced a significant production of COX metabolites, mainly TXB_2, the stable metabolite of TXA_2, and prostaglandins E_2 (PGE_2) and $PGF_{2\alpha}$. Particularly, a striking increase of TXB_2 levels, significantly higher than those obtained with *T. cruzi* and ET-1 separately, was detected in response to [*T. cruzi*+ET-1] (Figure 4A). Likewise, induction of the Ca^{2+}/Cn/NFAT/COX-2 pathway and eicosanoid production were also achieved in ET-1-primed HL-1 cells exposed to a parasite lysate preparation, thereby suggesting that cardiac cell invasion by trypomastigotes is not absolutely required to produce the cooperative effect with the peptide (not shown). TXB_2, PGE_2 and $PGF_{2\alpha}$ synthesis was drastically reduced in the cells incubated with indomethacin (10 μM), a non-steroidal anti-inflammatory drug known to inhibit both COX-1 and COX-2 enzymatic activity, or with a COX-2-selective inhibitor (NS398, 10 μM), indicating the important involvement of COX-2 in eicosanoid production upon ET-1 stimulation and *T. cruzi* infection of HL-1 cardiomyocytes. Treatment of HL-1 cells with COX inhibitors or Cn antagonist had no significant effect on cardiomyocyte-*T. cruzi* association and did not affect the capacity of the parasites to transform into amastigotes and multiply intracellularly (not shown). Furthermore, analyses for microsomal prostaglandin E synthase-2 (mPGES-2), prostaglandin F synthase (PGFS) and thromboxane synthase (TXS), enzymes that convert the COX product PGH_2 to PGE_2, $PGF_{2\alpha}$ and TXA_2, respectively, revealed that [*T. cruzi*+ET-1] also induced the expression of TXS and PGFS proteins in atrial HL-1 myocytes (Figure 4B).

In addition, stimulation with ET-1 promoted a three-fold increased ($P<0.05$) release of ANP. Compared to that observed in mock-treated controls, *T. cruzi* also up-regulated ANP levels in the supernatants of 24-h-infected cells, which were significantly augmented by the cooperative action of [*T. cruzi*+ET-1] (Figure 4C).

Discussion

Trypanosoma cruzi induces multiple responses in the heart, a critical organ of infection and pathology in the host. We herein demonstrated that *Cox2* mRNA and protein are induced in mouse heart tissue during *T. cruzi* infection correlating with cardiac parasite load and myocarditis. This up-regulation was also associated to induction of TXS and of two markers of heart dysfunction previously implicated in Chagas' disease pathogenesis, such as ET-1 and ANP [7,10,27]. Up-regulation of *Cox2* mRNA and protein in myocardial tissue of infected C57BL/6 mice is consistent with a previous report [22] that revealed increased COX-2 protein expression in the heart of infected BALB/c mice. Moreover, several evidences have suggested a role of cyclooxygenase-derived eicosanoids in the cardiopathogenesis of Chagas' disease (revised in [42,43]).

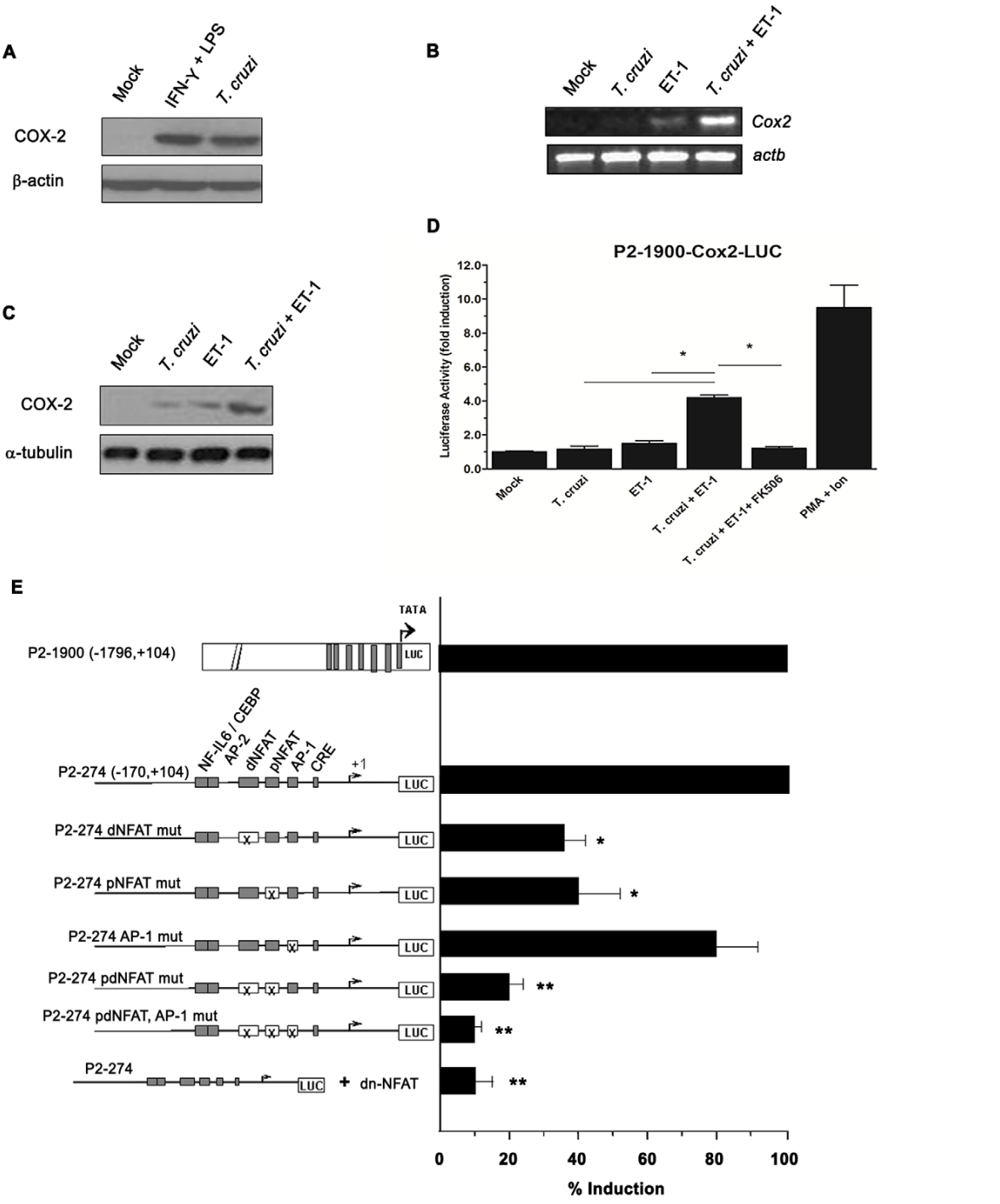

Figure 2. ***Trypanosoma cruzi*** **infection of endothelin-1-pre-treated HL-1 cardiomyocytes induces cyclooxygenase-2 expression.** (A) COX-2 protein expression in primary BALB/c cardiac myocytes infected with *T. cruzi*. Neonatal mouse heart cells were isolated and *ex vivo* infected with Y strain trypomastigotes (cell:parasite ratio 1:5) for 24 h. To obtain a positive control, the cells were incubated with 25 U/ml recombinant IFN-γ plus 1 μg/ml LPS. Uninfected cells (Mock) were used as controls. The levels of COX-2 and β-actin proteins were analysed by immunoblotting as described under 'Materials and methods'. (B) Effects of ET-1 pre-treatment and *T. cruzi* infection of HL-1 cardiomyocytes on *Cox2* mRNA expression. HL-1 atrial muscle cells were stimulated with 0.3 nM ET-1 for 2 h, and/or infected with *T. cruzi* trypomastigotes (cell:parasite ratio 1:5) for 3 h, and the levels of *Cox2* mRNA were assessed by reverse transcription and PCR; *Actb* (β-actin) was used as a loading marker. (C) Effects of ET-1 pre-treatment and *T. cruzi* infection of HL-1 cardiomyocytes on COX-2 protein expression. HL-1 atrial muscle cells were stimulated with 0.3 nM ET-1 for 2 h, and/or infected with *T. cruzi* trypomastigotes for 3 h, and the levels of COX-2 and α-tubulin proteins were analysed by immunoblotting. (D) Effects of ET-1

pre-treatment and *T. cruzi* infection of HL-1 cardiomyocytes on the inducibility of the *Cox2* promoter. Cells were transiently transfected with the P2-1900-Cox-2-LUC reporter construct, and then stimulated with 0.3 nM ET-1 for 2 h, and/or infected with trypomastigotes for 3 h. For some experiments, FK506 (100 ng/ml) was added to [*T. cruzi*+ET-1]-activated cardiomyocytes. PMA+Ion was used as a standard stimulus. Luciferase activity is expressed as fold induction relative to the transfection with empty expression vector. Data are the means ± s.e.m. of three independent experiments, each performed in triplicate. *$P<0.05$. (E) Involvement of NFAT in *Cox2* induction by *T. cruzi* plus ET-1. HL-1 cells were transiently transfected with the P2-1900-Cox-2-LUC reporter construct, with the P2-274-Cox-2 promoter construct, or with the same construct containing distal and/or proximal NFAT sites (dNFAT and pNFAT, respectively), and/or actvated protein-1 (AP-1) site mutated (indicated by X). For some experiments, the cells were transiently co-transfected with the P2-274-Cox-2-LUC reporter plasmid along with a dominant-negative version of NFAT (dn-NFAT). Three hours later, the cells were stimulated with ET-1 (0.3 nM) for 2 h and infected with *T. cruzi* parasites for 3 h. Luciferase activity is expressed as percentage of induction (mean ± s.e.m.) relative to that achieved in P2-1900-Cox-2-LUC transfected cells. One out of three separate experiments performed is shown. *$P<0.05$; ** $P<0.001$ (respect to the P2-274 construct).
doi:10.1371/journal.pntd.0002034.g002

Using adult HL-1 atrial myocytes, we further demonstrated that cooperation between *T. cruzi* and ET-1 stimulated *Cox2* mRNA and protein expression leading to the release of eicosanoids. ET-1 seems to be mainly implicated in the establishment of chagasic cardiomyopathy rather than in the control of infection. Previous studies on *T. cruzi*-infected ET-1 null mice have highlighted the pathogenic role of cardiac myocyte-derived ET-1 in Chagas' heart disease, but these animals did not display higher parasitemia nor lower survival rate than infected wild-type mice [8]. In chagasic heart dysfunction, locally produced ET-1 acts on cardiac myocytes in both an autocrine and/or paracrine manner and chronically induces muscle injury [5,7]. In addition, exposure of neonatal rat ventricular cardiomyocytes to ET-1 has been shown to result in higher COX-2 and prostacyclin formation [21,44]. In our study, ET-1 induced a dose-dependent increase (not shown) in COX-2 activity and eicosanoid biosynthesis in HL-1 cells subsequently infected with *T. cruzi*. To mimic the pathological microenvironment characteristic of *T. cruzi*-mediated cardiomyopathy, a 0.3 nM ET-1 concentration, close to that detected in the circulation of infected mice and patients exhibiting cardiac involvement [5,6], was selected for pre-treatment of cardiomyocytes.

Trypanosoma cruzi invasion of HL-1 cells increased $[Ca^{2+}]_i$, similar to previous report on primary cardiomyocytes [41]. Furthermore, ET-1 induces Ca^{2+} release in cardiac myofibers [45]. Alterations in $[Ca^{2+}]_i$ regulation are frequently recorded in Chagas' disease. In cardiomyocytes from chagasic patients there is a dysregulation of the diastolic $[Ca^{2+}]_i$, while Ca^{2+} channel blockers display therapeutic potential against chronic chagasic cardiomyopathy [46,47]. It has been largely established the requirement for sustained increases, including Ca^{2+} oscillation frequency, in $[Ca^{2+}]_i$ to mediate Cn activation and the nuclear translocation of NFAT [48]. Few studies so far have addressed the impact of *T. cruzi* infection on the Cn/NFAT pathway in host cells. NFAT has been identified as an important element in innate immunity to *T. cruzi* and also involved in parasite immune evasion [49,50]. The Ca^{2+}/Cn/NFAT pathway has proven functional in adult mouse heart muscle cells and ET-1 has been shown to activate this signaling route in HL-1 atrial myocytes [51,52]. Noticeably, NFAT proteins have been described as key molecules for the regulation of *Cox2* gene transcription in many different cell types [19,53–55]. Our present report constitutes the first demonstration that the cooperative effect of ET-1 and *T. cruzi* infection transcriptionally controls *Cox2* expression through activation of the Cn/NFATc4 signaling cascade in cardiomyocytes. Particularly, the two NFAT binding sites in the *Cox2* promoter appear to be critical for the observed induction. Mutation of any of these sites strongly diminished *Cox2* transcription raised by *T. cruzi* infection of ET-1-stimulated cardiomyocytes, and dominant negative NFAT prevented that stimulation.

Interestingly, this Cn/NFAT pathway has a pivotal role in pathological cardiac hypertrophy [26]. In this regard, we found that ET-1 plus *T. cruzi* infection leads to enhanced production of the pro-hypertrophic ANP, a prognostic factor for impairment in cardiac function of chagasic patients [28]. Augmented ANP was previously observed in atrial muscle cells upon ET-1 stimulation [56] and, during *T. cruzi* infection, ET-1 and ANP seem to be important late factors in myocardial remodeling and hypertrophy [10,27]. Increased ANP production is somehow linked to the myocardial regulatory pathway induced by [*T. cruzi*+ET-1]. Thus, PGE_2 and $PGF_{2\alpha}$ are known to promote ANP synthesis and release [57,58], while Ca^{2+} influx is involved in ET-1-triggered ANP expression [59]. More interestingly, NFATc4 was found to regulate several hypertrophy-associated gene transcription in cardiomyocytes, including ANP [26,58]. Taken the data together, it is likely that Ca^{2+} elevation, induced by [*T. cruzi*+ET-1], has led to NFATc4 activation, COX-2 induction and augmented ANP secretion by HL-1 cells.

A dual role of cyclooxygenase-derived eicosanoids in the course of Chagas' disease has been postulated (revised in [42,43]). Morever, the same COX metabolites that mediate host survival during the acute phase may contribute to the progression of cardiac remodeling and heart damage in the chronic phase [60]. The mechanisms involved in the increased prostanoid production in parasite-infected hosts are not yet fully understood. Our findings indicate that the combined effect of ET-1 priming and *T. cruzi* infection mimics what likely takes place in the heart during infection, inducing eicosanoid-forming enzyme activity through the Ca^{2+}/Cn/NFAT signaling pathway, and leading to enhanced release of prostanoids by atrial cardiomyocytes. Acutely infected mice display elevated $PGF_{2\alpha}$ plasma levels, whereas PGE_2 has been found to favor the development of cardiac fibrosis and functional deficits after infection by *T. cruzi* [23,61]. TXA_2, measured as the stable metabolite TXB_2, is the main eicosanoid produced during chronic infection with *T. cruzi* and this pro-inflammatory agent could be responsible of several of the pathophysiological features of chagasic cardiomyopathy [23,24]. TXA_2 may exacerbate cardiomyocyte apoptosis, facilitate cytokine biosynthesis by monocytes, activate endothelial cells, and also promote platelet activation, aggregation and degranulation [62]. It is conceivable that the liberated TXA_2 might play a role in a feedback loop for ET-1 expression/response, as efficient regulation of ET-1 by a TXA_2 mimetic in rat heart smooth muscle cells has been documented [63]. Moreover, the released $PGF_{2\alpha}$ could further induce COX-2 expression and activity, as occurs in carcinoma cells [64]. Enhanced levels of eicosanoids synthesized by [*T. cruzi*+ET-1]-activated HL-1 cells were down-regulated by addition of COX-2 inhibitors, indomethacin or NS398. In this regard, meloxicam or etoricoxib, two specific COX-2 inhibitors, minimized the amount of inflammation and fibrosis in the cardiac tissue of infected mice, whereas delayed treatment with aspirin, which blocks COX-1 and COX-2 indistinctly, improved cardiac dysfunction in a murine model of Chagas' heart disease [22,60]. However, the potential benefits of COX inhibition for chronic

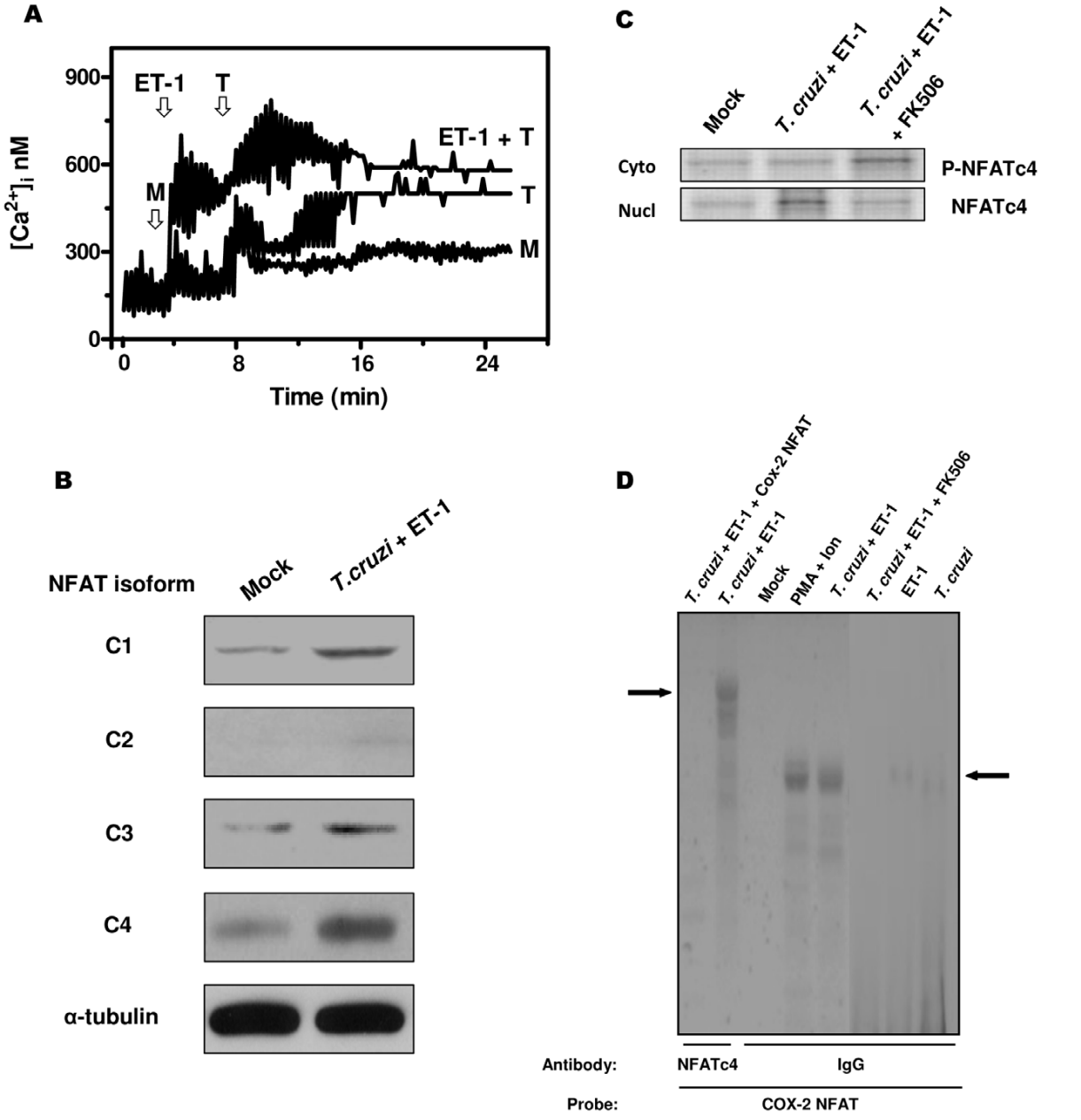

Figure 3. Activation of the Ca^{2+}/Calcineurin/NFAT intracellular signaling pathway in endothelin-1-stimulated and *Trypanosoma cruzi*-infected cardiomyocytes. (A) HL-1 cells, exposed or not to 0.3 nM ET-1, were loaded with the Ca^{2+} indicator Fura-2/M and changes in $[Ca^{2+}]_i$ upon *T. cruzi* infection were recorded. Uninfected cells were used as a control. Arrows indicate the time (min) when either culture medium (M) or *T. cruzi* trypomastigotes (T) was added. The results presented are representative of three independent experiments. (B) ET-1 stimulated and *T. cruzi*-infected HL-1 cardiomyocytes were disrupted and the protein expression of the four NFAT isoforms (c1 to c4) was analysed by immunoblotting. Alpha-tubulin protein levels were determined as a control of loading. (C) HL-1 cells were incubated for 2 h with ET-1 (0.3 nM) and subsequently infected with *T. cruzi* trypomastigotes for 3 h. For some experiments, FK506 (100 ng/ml) was added 1 h before stimulation. Fractionated extracts from both untreated and treated cells were analysed by immunoblotting with an antiserum to NFATc4. The phosphorylated cytosolic (P-NFATc4) or dephosphorylated nuclear (NFATc4) forms of the factor are indicated. Cyto, cytosolic extracts; Nucl, nuclear extracts. (D) Electrophoretic mobility shift assay (EMSA) analysis to determine NFATc4 binding to the NFAT sites of the *Cox2* gene (Cox-2 NFAT). HL-1 myocytes were stimulated with 0.3 nM ET-1 for 2 h and/or infected with *T. cruzi* trypomastigotes for 3 h. For some experiments, FK506 (100 ng/ml) was added 1 h before stimulation. Mock-treated cells were considered as controls. PMA (15 ng/ml) supplemented with 1 μM Ion was used as a standard stimulus. Nuclear extracts were analysed by EMSA using a Cox-2 NFAT radiolabeled probe. A 50-fold molar excess of unlabeled Cox-2 NFAT oligonucleotide (*T. cruzi*+ET-1+Cox-2 NFAT) was added to determine specific binding. NFATc4 antibody or normal rabbit IgG was added to the extracts before incubation with the probe. Arrows indicate specific supershifted complexes. This is representative of at least three independent experiments.
doi:10.1371/journal.pntd.0002034.g003

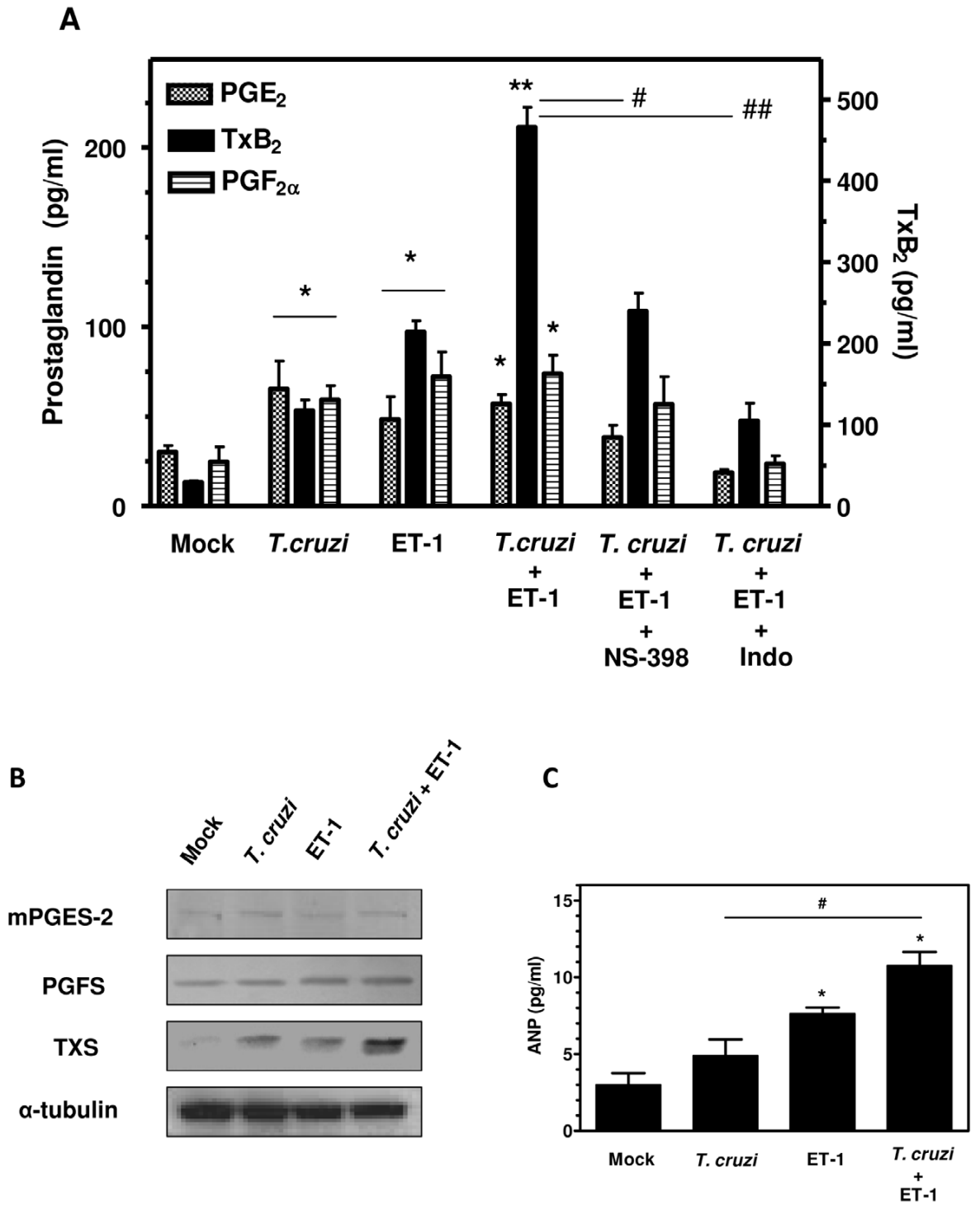

Figure 4. Production of eicosanoids and atrial natriuretic peptide by endothelin-1-stimulated and *Trypanosoma cruzi*-infected HL-1 cardiac cells. (A) Cardiomyocytes were serum-starved for 12 h, then incubated for 1 h in the presence of cyclooxygenase inhibitors (10 μM indomethacin -Indo- or 10 μM NS-398) and further stimulated with 0.3 nM ET-1 for 2 h. After treatment, the cells were infected with *T. cruzi* trypomastigotes for 24 h. HL-1 myocytes infected with the parasite or stimulated with ET-1 alone were included in the assay. Culture supernatants were collected and analysed for PGE_2, $PGF_{2\alpha}$ and TxB_2 (TxA_2 stable metabolite) by ELISA (Cayman). The results represent means ± s.e.m. of three individual experiments assayed in triplicate. $^{*}P<0.05$ and $^{**}P<0.001$ compared with mock-treated cells; $^{\#}P<0.05$ and $^{\#\#}P<0.001$ compared with NS-398- and Indo-treated cells, respectively. (B) Effects of *T. cruzi* infection and ET-1 stimulation on the expression of prostanoid terminal synthases in

HL-1 cardiac cells. Myocytes were incubated with 0.3 nM ET-1 for 2 h and/or infected with *T. cruzi* trypomastigotes for 3 h. Uninfected and mock-treated cells were used as controls. Immunoblot analysis of the protein expression of prostanoid terminal synthases (mPGES-2, PGFS and TXS) after exposure to stimulus and/or parasite is shown. Alpha-tubulin was used as loading control. The results presented are representative of three independent experiments with similar outcome. (C) HL-1 cells were treated with ET-1 (0.3 nM) for 2 h and/or *T. cruzi*-infected for 24 h and supernatants were collected. Uninfected and mock-treated cells were used as controls. ANP release (mean ± s.e.m.) was analyzed using an ELISA kit (Kamiya Biomedical) following the manufacturer's instructions. The results are representative of three independent experiments performed in quadruplicate. Statistically significant differences are indicated (*$P<0.05$, compared with mock; $^{\#}P<0.05$, [*T. cruzi*+ET-1]-activated cells *versus T. cruzi*-infected myocytes).
doi:10.1371/journal.pntd.0002034.g004

chagasic patients are still unknown. Even though *T. cruzi*-derived TXA_2 and $PGF_{2\alpha}$ have been associated with pathogenesis [24,43], no consistent evidence of parasite COX-2 and TXAS expression is available so far. As we detected overexpression of myocardial enzymes by using mouse-specific probes/antibodies and dampened eicosanoid production in cardiomyocytes treated with mammalian enzyme-specific inhibitors, our data mostly reflect the contribution of prostanoids secreted by host cells to Chagas' myocarditis.

In conclusion, we have demonstrated that eicosanoid-converting enzymes are expressed in the infected heart and also that cardiomyocytes respond to ET-1 and *T. cruzi* infection by induction of COX-2 through activation of the Ca^{2+}/Cn/NFAT intracellular signaling pathway. The cooperation between *T. cruzi* and ET-1 also led to overproduction of eicosanoids and the pro-hypertrophic factor ANP. These results support an important role for NFAT in [*T. cruzi*+ET-1]-dependent induction of key agents of pathogenesis in chronic chagasic cardiomyopathy. Identification of the Ca^{2+}/Cn/NFAT cascade as mediator of cardiovascular pathology in Chagas' disease advances our understanding of host-parasite relationship and may help define novel potential targets for therapeutic interventions to ameliorate or prevent cardiomyopathy during chronic *T. cruzi* infection.

Acknowledgments

We are grateful to Dr. W.C. Claycomb, Louisiana State University Health Science Center, New Orleans, LA, for generously providing the HL-1 cell line used in these studies, and to Dr. M.A. Iñiguez, Centro de Biología Molecular Severo Ochoa, Consejo Superior de Investigaciones Científicas, Universidad Autónoma de Madrid, and Dr. G. Crabtree, Stanford University School of Medicine, Stanford, CA, for the plasmid constructs used in transfection experiments.

Author Contributions

Conceived and designed the experiments: RSC MF NG. Performed the experiments: RSC NAG HC. Analyzed the data: RSC MF NG NAG HC. Contributed reagents/materials/analysis tools: RSC MF. Wrote the paper: RSC MF NG.

References

1. PAHO 2007: Pan American Health Organization 2007 (2007) Meeting Conclusions and Recommendations from the Joint IPA-AMCHA Annual Meeting (Quito, Ecuador); Technical Guidelines for Prevention and Control of Chagas Disease; PAHO/MSF Regional Consultation on the Organization and Structure of Health Care (IEC) on Congenital Chagas Disease (CLAP, Montevideo, 17–18 May 2007).
2. Rocha MO, Teixeira MM, Ribeiro AL (2007) An update on the management of Chagas cardiomyopathy. Exper Rev Anti Infect Ther 5: 727–743.
3. Tanowitz HB, Kaul DK, Chen B, Morris SA, Factor SM, et al. (1996) Compromised microcirculation in acute murine *Trypanosoma cruzi* infection. J Parasitol 82: 124–130.
4. Mukherjee S, Huang H, Weiss LM, Costa S, Scharfstein J, et al. (2003) Role of vasoactive mediators in the pathogenesis of Chagas' disease. Front Biosci 8: e410–419.
5. Petkova SB, Tanowitz HB, Magazine HI, Factor SM, Chan J, et al. (2000) Myocardial expression of endothelin-1 in murine *Trypanosoma cruzi* infection. Cardiovasc Pathol 9: 257–265.
6. Salomone OA, Caeiro TF, Madoery RJ, Amuchástegui M, Omelinauk M, et al. (2001) High plasma immunoreactive endothelin levels in patients with Chagas' cardiomyopathy. Am J Cardiol 87: 1217–1220.
7. Petkova SB, Huang H, Factor SM, Bouzahzah B, Pestell RG, et al. (2001) The role of endothelin in the pathogenesis of Chagas' disease. Int J Parasitol 31: 499–511.
8. Huang H, Yanagisawa M, Kisanuki YY, Jelicks LA, Chandra M, et al. (2002) Role of cardiac myocyte-derived endothelin-1 in chagasic cardiomyopathy: molecular genetic evidence. Clin Sci (Lond) 103, Suppl 48: 263S–266S.
9. Tanowitz HB, Wittner M, Morris SA, Zhao W, Weiss LM, et al. (1999) The putative mechanistic basis for the modulatory role of endothelin-1 in the altered vascular tone induced by *Trypanosoma cruzi*. Endothelium 6: 217–230.
10. Tanowitz HB, Huang H, Jelicks LA, Chandra M, Loredo ML, et al. (2005) Role of endothelin 1 in the pathogenesis of chronic chagasic heart disease. Infect Immun 73: 2496–2503.
11. Mulder P, Richard V, Derumeaux G, Hoggie M, Henry JP, et al. (1997) Role of endogenous endothelin in chronic heart failure: effect of long-term treatment with an endothelin antagonist on survival, hemodynamics, and cardiac remodeling. Circulation 96: 1976–1982.
12. Morris SA, Hatcher V, Bilezikian JP, Tanowitz HB, Wittner M (1988) Alterations in intracellular calcium following infection of human endothelial cells with *Trypanosoma cruzi*. Mol Biochem Parasitol 29: 213–221.
13. Hassan GS, Mukherjee S, Nagajyothi F, Weiss LM, Petkova SB, et al. (2006) *Trypanosoma cruzi* induces proliferation of vascular smooth muscle cells. Infect Immun 74: 152–159.
14. Kawamura T, Ono K, Morimoto T, Akao M, Iwai-Kanai E, et al. (2004) Endothelin-1-dependent nuclear factor of activated T lymphocyte signaling associates with transcriptional coactivator p300 in the activation of the B cell leukemia-2 promoter in cardiac myocytes. Circ Res 94: 1492–1499.
15. Zhu W, Zou Y, Shiojima I, Kudoh S, Aikawa R, et al. (2000) Ca^{2+}/calmodulin-dependent kinase II and calcineurin play critical roles in endothelin-1-induced cardiomyocyte hypertrophy. J Biol Chem 275: 15239–15245.
16. Vihma H, Pruunsild P, Timmusk T (2008) Alternative splicing and expression of human and mouse NFAT genes. Genomics 92: 279–291.
17. Hogan PG, Chen L, Nardone J, Rao A (2003) Transcriptional regulation by calcium, calcineurin, and NFAT. Genes Dev 17: 2205–2232.
18. Abdullah HI, Pedraza PL, Hao S, Rodland KD, McGiff JC, et al. (2006) NFAT regulates calcium-sensing receptor-mediated TNF production. Am J Physiol Renal Physiol 290: F1110–F1117.
19. Iñiguez MA, Martínez-Martínez S, Punzón C, Redondo JM, Fresno M (2000) An essential role of the nuclear factor of activated T cells in the regulation of the expression of the cyclooxygenase-2 gene in human T lymphocytes. J Biol Chem 275: 23627–23635.
20. Kataoka A, Tozaki-Saitoh H, Koga Y, Tsuda M, Inoue K (2009) Activation of P2X7 receptors induces CCL3 production in microglial cells through transcription factor NFAT. J Neurochem 108: 115–125.
21. Rebsamen MC, Capoccia R, Vallotton MB, Lang U (2003) Role of cyclooxygenase 2, p38 and p42/44 MAPK in the secretion of prostacyclin induced by epidermal growth factor, endothelin-1 and angiotensin II in rat ventricular cardiomyocytes. J Mol Cell Cardiol 35: 81–89.
22. Abdalla GK, Faria GEL, Silva KT, Castro ECC, Reis MA, et al. (2008) *Trypanosoma cruzi*: The role of PGE2 in immune response during the acute phase of experimental infection. Exp Parasitol 118: 514–521.
23. Cardoni RL, Antúnez MI (2004) Circulating levels of cyclooxygenase metabolites in experimental *Trypanosoma cruzi* infections. Mediators Inflamm 13: 235–240.
24. Ashton AW, Mukherjee S, Nagajyothi FN, Huang H, Braunstein VL, et al. (2007) Thromboxane A2 is a key regulator of pathogenesis during *Trypanosoma cruzi* infection. J Exp Med 204: 929–940.
25. Iwai-Kanai E, Hasegawa K (2004) Intracellular signaling pathways for norepinephrine- and endothelin-1-mediated regulation of myocardial cell apoptosis. Mol Cell Biochem 259: 163–168.
26. Liu CJ, Cheng YC, Lee KW, Hsu HH, Chu CH, et al. (2008) Lipopolysaccharide induces cellular hypertrophy through calcineurin/NFAT-3 signaling pathway in H9c2 myocardiac cells. Mol Cell Biochem 313: 167–178.
27. Benvenuti LA, Aiello VD, Palomino SA, Higuchi M de L (2003) Ventricular expression of atrial natriuretic peptide in chronic chagasic cardiomyopathy is not induced by myocarditis. Int J Cardiol 88: 57–61.

28. Moreira Mda C, Wang Y, Heringer-Walther S, Wessel N, Walther T (2009) Prognostic value of natriuretic peptides in Chagas' disease: a head-to-head comparison of the 3 natriuretic peptides. Congest Heart Fail 15: 75–81.
29. Claycomb WC, Lanson NA Jr, Stallworth BS, Egeland DB, Delcarpio JB, et al. (1998) HL-1 cells: a cardiac muscle cell line that contracts and retains phenotypic characteristics of the adult cardiomyocyte. Proc Natl Acad Sci U S A 95: 2979–2984.
30. Cuervo H, Pineda MA, Aoki MP, Gea S, Fresno M, et al. (2008) Inducible nitric oxide synthase and arginase expression in heart tissue during acute *Trypanosoma cruzi* infection in mice: arginase I is expressed in infiltrating CD68+ macrophages. J Infect Dis 197: 1772–1782.
31. Cuervo H, Guerrero NA, Carbajosa S, Beschin A, De Baetselier P, et al. (2011) Myeloid-derived suppressor cells infiltrate the heart in acute *Trypanosoma cruzi* infection. J Immunol 187: 2656–2665.
32. Zhang D, Li J, Wu K, Ouyang W, Ding J, et al. (2007) JNK1, but not JNK2, is required for COX-2 induction by nickel compounds. Carcinogenesis 28: 883–891.
33. Cutrullis RA, Postan M, Petray PB, Corral RS (2009) Timing of expression of inflammatory mediators in skeletal muscles from mice acutely infected with the RA strain of *Trypanosoma cruzi*. Pathobiology 76: 170–180.
34. Northrop JP, Ho SN, Chen L, Thomas DJ, Timmerman LA, et al. (1994) NF-AT components define a family of transcription factors targeted in T-cell activation. Nature 369: 497–502.
35. Hellmich MR, Ives KL, Udupi V, Soloff MS, Greeley GH Jr, et al. (1999) Multiple protein kinase pathways are involved in gastrin-releasing peptide receptor-regulated secretion. J Biol Chem 274: 23901–23909.
36. Martínez-Martínez S, Gomez del Arco P, Armesilla AL, Aramburu J, Luo C, et al. (1997) Blockade of T-cell activation by dithiocarbamates involves novel mechanisms of inhibition of nuclear factor of activated T cells. Mol Cell Biol 17: 6437–6447.
37. Calderón J, Maganto-Garcia E, Punzón C, Carrión J, Terhorst C, et al. (2012) The receptor Slamf1 on the surface of myeloid lineage cells controls susceptibility to infection by *Trypanosoma cruzi*. PLoS Pathog 8: e1002799.
38. Cuenca J, Goren N, Prieto P, Martín-Sanz P, Boscá L (2007) Selective impairment of nuclear factor-kappaB-dependent gene transcription in adult cardiomyocytes: relevance for the regulation of the inflammatory response in the heart. Am J Pathol 171: 820–828.
39. Boltzen U, Eisenreich A, Antoniak S, Weithaeuser A, Fechner H, et al. (2012) Alternatively spliced tissue factor and full-length tissue factor protect cardiomyocytes against TNF-α-induced apoptosis. J Mol Cell Cardiol 52: 1056–1065.
40. White SM, Constantin PE, Claycomb WC (2004) Cardiac physiology at the cellular level: use of cultured HL-1 cardiomyocytes for studies of cardiac muscle cell structure and function. Am J Physiol Heart Circ Physiol 286: H823–H829.
41. Garzoni LR, Masuda MO, Capella MM, Gil Lopes A, Leal de Meirelles MNS (2003) Characterization of $[Ca^{2+}]_i$ responses in primary cultures of mouse cardiomyocytes induced by *Trypanosoma cruzi* trypomastigotes. Mem Inst Oswaldo Cruz 98: 487–493.
42. Maya JD, Orellana M, Ferreira J, Kemmerling U, López-Muñoz R, et al. (2010) Chagas disease: Present status of pathogenic mechanisms and chemotherapy. Biol Res 43: 323–331.
43. Machado FS, Mukherjee S, Weiss LM, Tanowitz HB, Ashton AW (2011) Bioactive lipids in *Trypanosoma cruzi* infection. Adv Parasitol 76: 1–31.
44. Manque PA, Probst C, Pereira MC, Rampazzo RC, Ozaki LS, et al. (2011) *Trypanosoma cruzi* infection induces a global host cell response in cardiomyocytes. Infect Immun 79: 1855–1862.
45. Higazi DR, Fearnley CJ, Drawnel FM, Talasila A, Corps EM, et al. (2009) Endothelin-1-stimulated InsP3-induced Ca^{2+} release is a nexus for hypertrophic signaling in cardiac myocytes. Mol Cell 33: 472–482.
46. López JR, Espinosa R, Landazuru P, Linares N, Allen P, et al. (2011) Dysfunction of diastolic $[Ca^{2+}]$ in cardiomyocytes isolated from chagasic patients. Rev Esp Cardiol 64: 456–462.
47. De Souza AP, Tanowitz HB, Chandra M, Shtutin V, Weiss LM, et al. (2004) Effects of early and late verapamil administration on the development of cardiomyopathy in experimental chronic *Trypanosoma cruzi* (Brazil strain) infection. Parasitol Res 92: 496–501.
48. Colella M, Grisan F, Robert V, Turner JD, Thomas AP, et al. (2008) Ca^{2+} oscillation frequency decoding in cardiac cell hypertrophy: role of calcineurin/NFAT as Ca^{2+} signal integrators. Proc Natl Acad Sci U S A 105: 2859–2864.
49. Bellio M, Liveira AC, Mermelstein CS, Capella MA, Viola JP, et al. (1999) Costimulatory action of glycoinositolphospholipids from *Trypanosoma cruzi*: increased interleukin 2 secretion and induction of nuclear translocation of the nuclear factor of activated T cells 1. FASEB J 13: 1627–1636.
50. Kayama H, Koga R, Atarashi K, Okoyama M, Kimura T, et al. (2009) NFATc1 mediates Toll-like receptor-independent innate immune responses during *Trypanosoma cruzi* infection. PloS Pathog 5: e1000514.
51. Tang M, Li J, Huang W, Su H, Liang Q, et al. (2010) Proteasome functional insufficiency activates the calcineurin-NFAT pathway in cardiomyocytes and promotes maladaptive remodelling of stressed mouse hearts. Cardiovasc Res 88: 424–433.
52. Poteser M, Schleifer H, Lichtenegger M, Schernthaner M, Stockner T, et al. (2011) PKC-dependent coupling of calcium permeation through transient receptor potential canonical 3 (TRPC3) to calcineurin signaling in HL-1 myocytes. Proc Natl Acad Sci U S A 108: 10556–10561.
53. Sugimoto T, Haneda M, Sawano H, Isshiki K, Maeda S, et al. (2001) Endothelin-1 induces cyclooxygenase-2 expression via nuclear factor of activated T-cell transcription factor in glomerular mesangial cells. J Am Soc Nephrol 12: 1359–1368.
54. Corral RS, Iñiguez MA, Duque J, López-Pérez R, Fresno M (2007) Bombesin induces cyclooxygenase-2 expression through the activation of the nuclear factor of activated T cells and enhances cell migration in Caco-2 colon carcinoma cells. Oncogene 26: 958–969.
55. Yiu GK, Toker A (2006) NFAT induces breast cancer cell invasion by promoting the induction of cyclooxygenase-2. J Biol Chem 281: 12210–12217.
56. Cheng TH, Shih NL, Chen CH, Lin H, Liu JC, et al. (2005) Role of mitogen-activated protein kinase pathway in reactive oxygen species-mediated endothelin-1-induced beta-myosin heavy chain gene expression and cardiomyocyte hypertrophy. J Biomed Sci 12: 123–133.
57. Miyatake S, Manabe-Kawaguchi H, Watanabe K, Hori S, Aikawa N, et al. (2007) Prostaglandin E2 induces hypertrophic changes and suppresses alpha-skeletal actin gene expression in rat cardiomyocytes. J Cardiovasc Pharmacol 50: 548–554.
58. Bai S, Kerppola TK (2011) Opposing roles of FoxP1 and Nfat3 in transcriptional control of cardiomyocyte hypertrophy. Mol Cell Biol 31: 3068–3080.
59. Rebsamen MC, Church DJ, Morabito D, Vallotton MB, Lang U (1997) Role of cAMP and calcium influx in endothelin-1-induced ANP release in rat cardiomyocytes. Am J Physiol 273: E922–E931.
60. Mukherjee S, Machado FS, Huang H, Oz HS, Jelicks LA, et al. (2011) Aspirin treatment of mice infected with *Trypanosoma cruzi* and implications for the pathogenesis of Chagas disease. PLoS One 6: e16959.
61. Freire-de-Lima CG, Nascimento DO, Soares MB, Bozza PT, Castro-Faria-Neto HC, et al. (2000) Uptake of apoptotic cells drives the growth of a pathogenic trypanosome in macrophages. Nature 403: 199–203.
62. Ogletree ML (1987) Overview of physiological and pathophysiological effects of thromboxane A_2. FASEB J 46: 133–138.
63. Chua CC, Hamdy RC, Chua BH (1996) Regulation of endothelin-1 production by a thromboxane A2 mimetic in rat heart smooth muscle cells. Biochim Biophys Acta 1313: 1–5.
64. Jabbour HN, Sales KJ, Boddy SC, Anderson RA, Williams AR (2005) A positive feedback loop that regulates cyclooxygenase-2 expression and prostaglandin F2alpha synthesis via the F-series-prostanoid receptor and extracellular signal-regulated kinase 1/2 signaling pathway. Endocrinology 146:4657–4664.

Myeloid-Derived Suppressor Cells Infiltrate the Heart in Acute *Trypanosoma cruzi* Infection

Henar Cuervo,* Néstor A. Guerrero,*,† Sofía Carbajosa,* Alain Beschin,‡,§ Patrick De Baetselier,‡,§ Núria Gironès,*,†,1 and Manuel Fresno*,†,1

Chagas disease, caused by the protozoan parasite *Trypanosoma cruzi*, affects several million people in Latin America. Myocarditis, observed in the acute and chronic phases of the disease, is characterized by a mononuclear cell inflammatory infiltrate. We previously identified a myeloid cell population in the inflammatory heart infiltrate of infected mice that expressed arginase I. In this study, we purified CD11b$^+$ myeloid cells from the heart and analyzed their phenotype and function. Those CD11b$^+$ cells were ~70% Ly6G$^-$Ly6C$^+$ and 25% Ly6G$^+$Ly6C$^+$. Moreover, purified CD11b$^+$Ly6G$^-$ cells, but not Ly6G$^+$ cells, showed a predominant monocytic phenotype, expressed arginase I and inducible NO synthase, and suppressed anti-CD3/anti-CD28 Ab-induced T cell proliferation in vitro by an NO-dependent mechanism, activity that best defines myeloid-derived suppressor cells (MDSCs). Contrarily, CD11b$^+$Ly6G$^+$ cells, but not CD11b$^+$Ly6G$^-$ cells, expressed S100A8 and S100A9, proteins known to promote recruitment and differentiation of MDSCs. Together, our results suggest that inducible NO synthase/arginase I-expressing CD11b$^+$ Ly6G$^-$ myeloid cells in the hearts of *T. cruzi*-infected mice are MDSCs. Finally, we found plasma L-arginine depletion in the acute phase of infection that was coincident in time with the appearance of MDSCs, suggesting that in vivo arginase I could be contributing to L-arginine depletion and systemic immunosuppression. Notably, L-arginine supplementation decreased heart tissue parasite load, suggesting that sustained arginase expression through the acute infection is detrimental for the host. This is, to our knowledge, the first time that MDSCs have been found in the heart in the context of myocarditis and also in infection by *T. cruzi*. *The Journal of Immunology*, 2011, 187: 2656–2665.

Chagas disease, which is caused by the protozoan parasite *Trypanosoma cruzi*, affects ~18 million people in Latin America, with 120 million at risk, thus remaining a major cause of morbidity and mortality in that region (1). Myocarditis that occurs as a result of infection is the most serious and frequent manifestation of chronic Chagas disease and appears in 30% of infected individuals several years after the infection. The pathogenesis is thought to be dependent on an immune-inflammatory reaction to a low-grade infection (2, 3). *T. cruzi* has a complex life cycle involving several life stages in both vertebrates and insect vectors. It infects and replicates in macrophages and cardiomyocytes and many other cell types. Resistance to the disease is associated with a Th1 response, which efficiently controls infection through IFN-γ production and further increased activity of inducible NO synthase (iNOS; also termed NOS2), which metabolizes L-arginine (a semiessential amino acid) and produces NO (4). In addition, during acute infection, there is suppression of T cell proliferation that is partially caused by NO (5). Moreover, the development of severe cardiomyopathy in Chagas disease is also thought to be due to a Th1-specific immune response (6).

In contrast, L-arginine can also be used by arginase I, which produces ornithine that in turn is metabolized by ornithine decarboxylase to produce polyamines needed for growth of all eukaryotic cells. In this regard, arginase I expression was found to be upregulated in macrophages infected with *T. cruzi* and associated with parasite survival (7, 8).

In mice, arginase I has been described to be expressed by different myeloid cell subsets such as alternatively activated macrophages (also called M2 macrophages) and myeloid-derived suppressor cells (MDSCs), among others. Whereas M2 macrophages are thought to express arginase I but not iNOS (9), MDSCs can express both enzymes (10). M2 macrophages induced by type 2 and regulatory cytokines have been implicated in parasite growth (11) and can be defined by an M2 gene signature (12). In contrast, MDSCs accumulate during acute and chronic immune responses to pathogens, tumor growth, trauma, and other immunological responses (13). These cells are commonly identified in mice by the coexpression of CD11b and Gr-1 (Ly6G/Ly6C) surface markers. However, this population shows important phenotypic differences depending on the anatomical site where they are

*Centro de Biología Molecular Severo Ochoa, Consejo Superior de Investigaciones Científicas, Universidad Autónoma de Madrid, Cantoblanco, 28049 Madrid, Spain; †Instituto de Investigación Sanitaria Princesa, Hospital Universitario de La Princesa, 28006 Madrid, Spain; ‡Department of Molecular and Cellular Interactions, Flemish Institute for Biotechnology, 1050 Brussels, Belgium; and §Laboratory of Cellular and Molecular Immunology, Free University of Brussels, 1050 Brussels, Belgium

[1]N.G. and M.F. contributed equally to the direction of this work.

Received for publication August 31, 2010. Accepted for publication July 1, 2011.

This work was supported by Ministerio de Ciencia y Tecnología (SAF2007-61716 and SAF2005-02220); Fondo de Investigaciones Sanitarias (PS09/00538); Red Tematica de Investigación en Enfermedades Cardiovasculares (RECAVA RD06/0014/1013); Red de Investigación de Centros de Enfermedades Tropicales (RICET RD06/0021/0016); European Union (HEALTH-FE-2008-22303, ChagasEpiNet); Universidad Autónoma de Madrid and Comunidad de Madrid (CC08-UAM/SAL-4440/08); Agencia Española de Cooperación Internacional para el Desarrollo cooperation with Argentina (A/025417/09); and Fundación Ramón Areces. H.C. and N.A.G. were financed by Fondo de Investigaciones Sanitarias, Instituto de salud Carlos III contracts. S.C. was a holder of a Formación de personal investigador fellowship. A.B. was funded by the Interuniversity Attraction Pole Program of the Belgian government.

Address correspondence and reprint requests to Dr. Núria Gironès, Centro de Biología Molecular Severo Ochoa, CSIC-UAM, Departamento de Bioquímica y Biología Molecular, Facultad de Ciencias, Universidad Autónoma de Madrid, Cantoblanco, 28049 Madrid, Spain. E-mail address: ngirones@cbm.uam.es

The online version of this article contains supplemental material.

Abbreviations used in this article: BCA, bicinchoninic acid; BI, PBMCs of infected mice; BNI, PBMCs of noninfected mice; CVB3, Coxsackie virus B3; dpi, days postinfection; HI, hearts of infected mice; iNOS, inducible NO synthase; L-NAME, L-N^G-nitroarginine methyl ester (hydrochloride); L-NMMA, N^G-monomethyl-L-arginine; MDSC, myeloid-derived suppressor cell; NI, noninfected mice; nor-NOHA, N^{ω}-hydroxy-nor-L-arginine; RQ, relative quantity.

www.jimmunol.org/cgi/doi/10.4049/jimmunol.1002928

located or the pathological condition. In addition, in tumor-induced MDSCs, discrete subpopulations with distinct T cell suppressive activity have been identified (14). Therefore, a rigid classification for MDSCs is not actually available, and their definition is still a matter of debate.

Arginase I and iNOS, either separately or in combination, can inhibit T cell responses. L-Arginine is required for T cell proliferation, and the threshold of L-arginine concentration in mammalian plasma that permits fully functional T cell proliferation is 100 μM (15). Moreover, combined activity of arginase I and iNOS enzymes has been shown to be important in the suppressive activity of mouse MDSCs in tumors (16), but there also exists various evidence of the role of MDSCs, iNOS, and L-arginine depletion in infectious diseases such as chronic infections with helminths (17). In addition, in experimental infections with *T. cruzi*, the existence of an IFN-γ–induced, NO-dependent mechanism of T cell suppression has been described (5, 18).

We have previously reported the existence of a population of infiltrating myeloid cells expressing arginase I in the hearts of mice during the acute phase of Chagas disease (19). The aim of this work was to characterize the heart-infiltrating myeloid CD11b$^+$ cells in acute *T. cruzi* infection. We found that the heart-infiltrating myeloid CD11b$^+$ cells included granulocytic Ly6G$^+$ and monocytic Ly6G$^-$ subpopulations; the phenotype and function of the latter cells indicate that they are closely related to the so-called MDSCs. The monocytic myeloid cell subset, but not the granulocytic subset, expressed arginase I and iNOS activity and was able to inhibit T cell proliferation in vitro in an NO-dependent manner. Persistent arginase I expression leads to a decreased plasma L-arginine concentration during acute infection. Notably, supplementation of infected mice with L-arginine diminished parasite load. To our knowledge, this is the first report about MDSCs infiltrating the heart, in the context of myocarditis, and of plasma L-arginine depletion during acute *T. cruzi* infection, which are able to downregulate the immune response. This may have consequences in chronic cardiac Chagas disease.

Materials and Methods

Parasites and mice

Young adult (6- to 8-wk-old) BALB/c and C57BL/6 mice were purchased from Charles River Laboratories. All the infections were performed with the Y strain of *T. cruzi*. Blood trypomastigotes were routinely maintained by infecting mice and purifying them from their blood. For experiments, 2×10^3 trypomastigotes per mouse was inoculated by i.p. injection. Parasitemia was monitored by the Brener method as described (20). When indicated, mice were supplemented with 1 mg/ml L-N^G-nitroarginine methyl ester (hydrochloride) (L-NAME) or 3.75 mg/ml L-arginine in the drinking water, which was replaced every other day.

Ethics statement

This study was carried out in strict accordance with the recommendations of Spanish legislation and the European Council directive from the Convention for the Protection of Vertebrate Animals Used for Experimental and Other Scientific Purposes (21). All mice were maintained under pathogen-free conditions in the animal facility at the Centro de Biología Molecular, Universidad Autónoma de Madrid (Madrid, Spain). The animal protocol was approved by the Comité de Ética de la Investigación de la Universidad Autónoma de Madrid. Animals had free access to food and water and were handled in compliance with European norms. Mice were euthanized in a CO_2 chamber, and all efforts were made to minimize suffering.

Elicitation of organs and T, CD11b, and Ly6G magnetic cell sorting

In each experiment, 5–15 BALB/c or C57BL/6 mice were infected i.p. Mice were euthanized, at different days postinfection, in a CO_2 chamber, and hearts were aseptically removed, perfused with 10 ml PBS–heparin solution, and kept in cold HBSS. Then, hearts were pooled in a cell culture dish, washed thoroughly with HBSS, and minced into small pieces with a sterile surgical blade. Heart pieces were then processed with a GentleMacs (Miltenyi Biotech) and with an enzyme mixture following the directions of the manufacturer. The cell pellet was resuspended in RPMI 1640 supplemented with 5% FBS. Blood from infected and noninfected mice was obtained by cardiac puncture and treated with heparin. Spleen cells were obtained by mechanical disruption of spleens and passed through a 40-μm cell strainer (BD Falcon). Single-cell suspension of PBMCs and spleen cells was depleted of erythrocytes by hypotonic lysis and washed with cold PBS. Peritoneal cell exudates were obtained after peritoneal cavity lavage of noninfected mice with 7 ml of a solution of sucrose (116 g/l) in PBS. CD11b$^+$ cells were purified from heart, blood, spleen, and peritoneal lavage cells using CD11b microbeads (Miltenyi Biotec). T cells were isolated from spleen cells of noninfected mice with the Pan T cell kit using MACS LS columns and MACS Separators (Miltenyi Biotec) following the manufacturer's instructions. CD11b$^+$ and T sorted cells were analyzed by flow cytometry and showed 95% cell purity. For Ly6G$^+$ cell sorting, an anti-Ly6G microbead kit (Miltenyi Biotec) was used with the above-mentioned separating system. The Ly6G$^-$ fraction of the cell suspension was 95% pure and was afterward processed for CD11b sorting and Giemsa staining.

mRNA analysis by quantitative RT-PCR

Total RNA was extracted from heart, blood, or isolated cells in TRIzol reagent (Invitrogen) as indicated by the manufacturer. For quantitative RT-PCR analysis, in indicated experiments, reverse transcription of total RNA was performed using the components of the High Capacity cDNA Archive Kit (Applied Biosystems), and amplification of different genes [*Arginase* (*Arg*)*1, Arg2, NO synthase* (*Nos*)*2, Tlr2, Tlr4, PG* (*Pstg*)*1, Ptgs2, Ccl2, Ccl3, Ccl5, Ccl17, Cxc2, Cxcl9, Cxcl10, Cxcl12, Il1b, Il4, Il6, Il10, Il12a, Il13, Tnf, Ifng, Tgfb,* S100 calcium binding protein (*S100*)*a8* and *S100a9*, and ribosomal housekeeping *S18*] was performed using the corresponding mouse TaqMan MGB probes and the TaqMan Universal PCR Master Mix (Applied Biosystems) on an ABI Prism 7900 HT instrument (Applied Biosystems). M2 gene signature expression was carried out, in indicated experiments, using Superscript II reverse transcriptase (Invitrogen) for reverse transcription and iQ SYBR Green Supermix (Bio-Rad, Hercules, CA) for quantitative RT-PCR in an iCycler (Bio-Rad) for the identified common M2 signature including *macrophage mannose receptor* (*Mrc1*), *found in inflammatory zone* (*Fizz*) *1* (*Retlna*), *macrophage galactose-type C-type lectin* (*Mgl*)*2*, Chitinase 3-like 3/4 (*Ch3l3/4*), *cadherin-1* (*Cdh1*), plasma *platelet–activating factor acetylhydrolase* (*Pla2g7*), *prosaposin* (*Psap*), *selenoprotein* (*Sepp*)*1*, folate receptor (*Folr*)*2*, and *triggering receptor expressed on myeloid cells* (*Trem*)*2* as previously described (12). All samples were run in triplicate. Quantification of gene expression by real-time PCR was calculated by the comparative threshold cycle (C_T) method following the manufacturer's instructions. All quantifications were normalized to the housekeeping gene, as indicated, to account for the variability in the initial concentration of RNA and in the conversion efficiency of the reverse transcription reaction (ΔC_T) and to values from control samples (CD11b$^+$ cells from blood or peritoneal exudates, as indicated) from noninfected mice ($\Delta\Delta C_T$). The relative quantity (RQ) when using TaqMan probes was calculated as $RQ = 2^{-\Delta\Delta C_T}$. Graphs were plotted as RQ or log RQ. The fold induction for M2 gene expression analysis was normalized against the housekeeping gene *S12*.

Protein expression analyses

Protein was determined by Western blot analyses. Protein extracts were prepared in PBS containing 0.1% Triton X-100, 100 μg/ml pepstatin, 100 μg/ml aprotinin, and 100 μg/ml antipain. Protein concentration was determined by the bicinchoninic acid (BCA) method (Pierce). Western blot analyses were performed as follows: 20 μg tissue extract was fractionated on SDS 10 or 15% polyacrylamide gel and transferred to a nitrocellulose membrane (Hybond-ECL; Amersham). When indicated, protein loading was visualized by Ponceau staining (Sigma). Primary Abs were diluted as follows: goat anti-mouse arginase I (V-20; Santa Cruz Biotechnology) 1:1000, S100A8 and S100A9 (R&D Systems) 1:500, purified anti-mouse iNOS (BD Transduction) 1:500, and goat anti-mouse actin (I-19; Santa Cruz Biotechnology) 1:1000. Then, the membranes were incubated with HRP-conjugated rabbit anti-goat (Sigma) 1:10,000 or goat anti-mouse (Pierce) 1:1000 Abs. Detection was carried out with Supersignal detection reagent (Pierce) and photographic film exposure.

Flow cytometry

Staining was performed in 96-well plates (Nunc). Single-cell suspensions were fixated with paraformaldehyde 1% in PBS for 1 h at 4°C. Cells were

washed with cold PBS throughout the whole staining procedure. Fc receptors on cells were blocked by incubating with purified anti-CD16/CD32 Ab (Mouse BD Fc Block; BD Pharmingen) for 15 min at 4°C. Cells were then stained with the different conjugated Abs, washed, and acquired on a FACSCanto Cytometer (Becton Dickinson). For intracellular staining, after the staining of surface molecules, cells were incubated 15 min in the presence of 0.2% saponin, washed, and incubated for 20 min with anti-CD68, washed again, and acquired as mentioned above. All data were analyzed with the FlowJo software (Tree Star).

Abs used were the following: PE–Cy7–conjugated or Alexa Fluor 647-conjugated anti-CD11b (clone M1/70; BD Pharmingen), FITC-conjugated or PE-conjugated anti-Ly6G/Ly6C (Gr-1, clone RB6-8C5; BD Pharmingen), Alexa Fluor 647-conjugated anti-Ly6C (clone AL-21; AbD Serotec), PE-conjugated anti-CD68 (FA-11; AbD Serotec), PE-conjugated anti-MHC class II (I-A/I-E, clone M5/114.15.2; eBioscience), PE-conjugated anti-F4/80 (clone BM8; AbD Serotec), PE-conjugated anti-CD11c (clone HL3; BD Pharmingen), FITC-conjugated anti-CD49b (clone DX5; eBioscience), and FITC-conjugated anti-CCR3 (clone 83101; R&D Systems). PE-conjugated Armenian hamster IgG1 (BD Pharmingen), PE-conjugated rat IgG2a (BD Pharmingen), FITC-conjugated rat IgG2a (BD Pharmingen), Alexa Fluor 647-conjugated rat IgG2a (AbD Serotec), PE–Cy7–conjugated rat IgG2b (BD Pharmingen), and FITC-conjugated rat IgM (eBioscience) Abs were used as isotypic controls.

Proliferation assays

Purified CD11b$^+$ cells from hearts of infected mice and blood from noninfected mice were obtained as described earlier, counted, and resuspended in complete RPMI 1640 with 0, 100, and 1000 μM L-arginine supplemented with 5% FBS. A total of 2×10^5 cells per well were plated in flat 96-well plates (Nunc). T cells sorted from the spleens of noninfected mice were resuspended in the same media and plated with or without CD11b$^+$ purified cells isolated from hearts of infected mice or blood or spleens from noninfected mice in a 1:1 ratio. Cell cultures were stimulated with 5 μg/ml purified anti-CD3 (BD Pharmingen) and 1 μg/ml purified anti-CD28 Ab (BD Pharmingen), and, when indicated, 24 μM N^{ω}-hydroxy-nor-L-arginine (nor-NOHA; Calbiochem) or 2 mM N^{G}-monomethyl-L-arginine (L-NMMA; Calbiochem) were added. After incubation at 37°C and 5% CO_2 for 24 h, 1 μCi [^{3}H]thymidine (Amersham Pharmacia Biotech) was added to each well. Cells were then harvested on a glass-fiber filter by use of a Cell Harvester (Skatron Instruments), and radioactivity was estimated in a microβ counter (Maxwell) and incorporation expressed as counts per minute.

L-Arginine determination in plasma and culture supernatants

Plasma and 1:10 diluted supernatants from cultured cells were centrifuged at 14,000 rpm to remove protein precipitates, and 5 μl was subjected to HPLC analysis for L-arginine determination using an HPLC chromatograph coupled to a triple quadrupole mass spectrometer (Varian 1200L; Agilent Technologies).

Statistical analysis

For in vivo experiments, data are reported as means ± SEM from triplicate determination of a representative experiment of at least two independent experiments with different experimental conditions. Results shown from in vitro experiments are representative of at least two experiments performed in triplicate. Significance was evaluated by Student *t* test with GraphPad Prism version 5.00 for Windows (GraphPad Software, San Diego CA); the Welsh correction was applied when different variances were observed. All differences mentioned were significant compared with controls ($*p < 0.05$, $**p < 0.01$, and $***p < 0.001$).

Results

Characterization of CD11b$^+$ cells from the hearts of T. cruzi*-infected mice*

We previously described a population of myeloid cells expressing arginase I infiltrating the hearts of mice during acute *T. cruzi* infection (19). To characterize further the myeloid-infiltrating cells, CD11b$^+$ populations from hearts of infected mice (HI) were isolated at the time in which arginase I heart tissue expression was maximal [14 d postinfection (dpi) and 21 dpi in C57BL/6 and BALB/c mice, respectively] (19). For comparison purposes, we used CD11b$^+$ cells from peripheral blood of noninfected mice (BNI) because hearts from the latter mice were devoid of CD11b$^+$ cell infiltration. CD11b$^+$ cells from the blood of infected mice (BI) were also purified and characterized. The results showed that arginase I protein expression was strongly upregulated in CD11b$^+$ HI cells in comparison with CD11b$^+$ BNI cells both in C57BL/6 and BALB/c infected mice (Fig. 1). Arginase I protein was also expressed in CD11b$^+$ BI cells, but at lower level than that in CD11b$^+$ HI cells. Arginase I protein expression was higher in BALB/c than in C57BL/6 mice in the three cell types investigated likely reflecting the fact that BALB/c mice are more prone to develop Th2 and M2 responses (22). Notably, iNOS protein expression was detected in CD11b$^+$ HI cells, but not in CD11b$^+$ BI and BNI cells from C57BL/6 and BALB/c mice (Fig. 1).

We analyzed the expression of several genes by quantitative RT-PCR in CD11b$^+$ HI purified cells from infected BALB/c mice at 21 dpi, including: proinflammatory/M1-associated cytokines and chemokines genes required for protection against *T. cruzi* infection; anti-inflammatory/regulatory/M2-associated cytokines and chemokines that favor parasite replication; and TLRs involved in *T. cruzi* recognition. Gene expression analysis of the genes coding for arginase I (*Arg1*) and iNOS (*Nos2*) in infected BALB/c paralleled the protein expression data (Fig. 2*A* versus Fig. 1). The expression of *Arg2* in CD11b$^+$ HI and BI cells was impaired compared with that in CD11b$^+$ BNI cells. In contrast, in CD11b$^+$ HI cells, gene expression of *Tlr2* in comparison with that in CD11b$^+$ BNI cells was increased, whereas *Tlr4* was reduced (Fig. 2*B*). *Ptgs1* and *Ptgs 2* genes coding for cyclooxygenase 1 and 2 enzymes and involved in the production of inflammatory mediators were downregulated and upregulated, respectively, in CD11b$^+$ HI cells in comparison with that in the CD11b$^+$ BNI cells (Fig. 2*C*). M1 chemokine genes, previously reported to be expressed in heart tissue during *T. cruzi* infection, such as *Ccl2* and *Cxcl9* (23) were found to be expressed at higher levels in CD11b$^+$ HI cells with respect to CD11b$^+$ BNI cells, whereas *Ccl3*, *Ccl5*, *Cxcl2*, *Cxcl10*, and *Cxcl12* showed a more discrete induced expression. The M2-associated chemokine gene *Ccl17* did not show a significant increment of expression in CD11b$^+$ HI cells (Fig. 2*D*). CD11b$^+$ HI cells also showed strong gene expression encoding for the regulatory cytokine IL-10 (*Il10*) and, at a lower level, proinflammatory cytokines such as *Il6*, *Ifng*, *Il12a*, and *Tnf*, whereas other anti-inflammatory cytokines showed downregulation (*Il4*, *Il13*, *and Tgfb1*; Fig. 2*E*). It should be mentioned that in general, the trend of the modulation of expression was similar in CD11b$^+$ HI and BI cells of the different genes tested, with the exception of

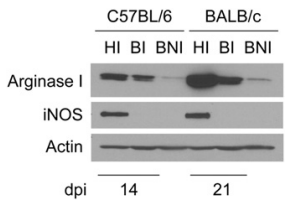

FIGURE 1. Expression of iNOS and arginase I proteins in CD11b$^+$ HI cells from *T. cruzi*-infected C57BL/6 and BALB/c mice. Mice were infected i.p. with 2×10^3 blood trypomastigotes of the Y strain and sacrificed at day 14 and 21 postinfection as indicated, and infected hearts and blood from infected and noninfected mice were collected. After mechanical and enzymatic digestion of heart tissue and PBMCs purification, CD11b$^+$ cells were purified with CD11b microbeads. Protein extracts were isolated; 20 μg loaded in 10% SDS-PAGE gels and subjected to Western blot analyses using anti-arginase I or anti-iNOS Abs. Data are representative of three independent experiments.

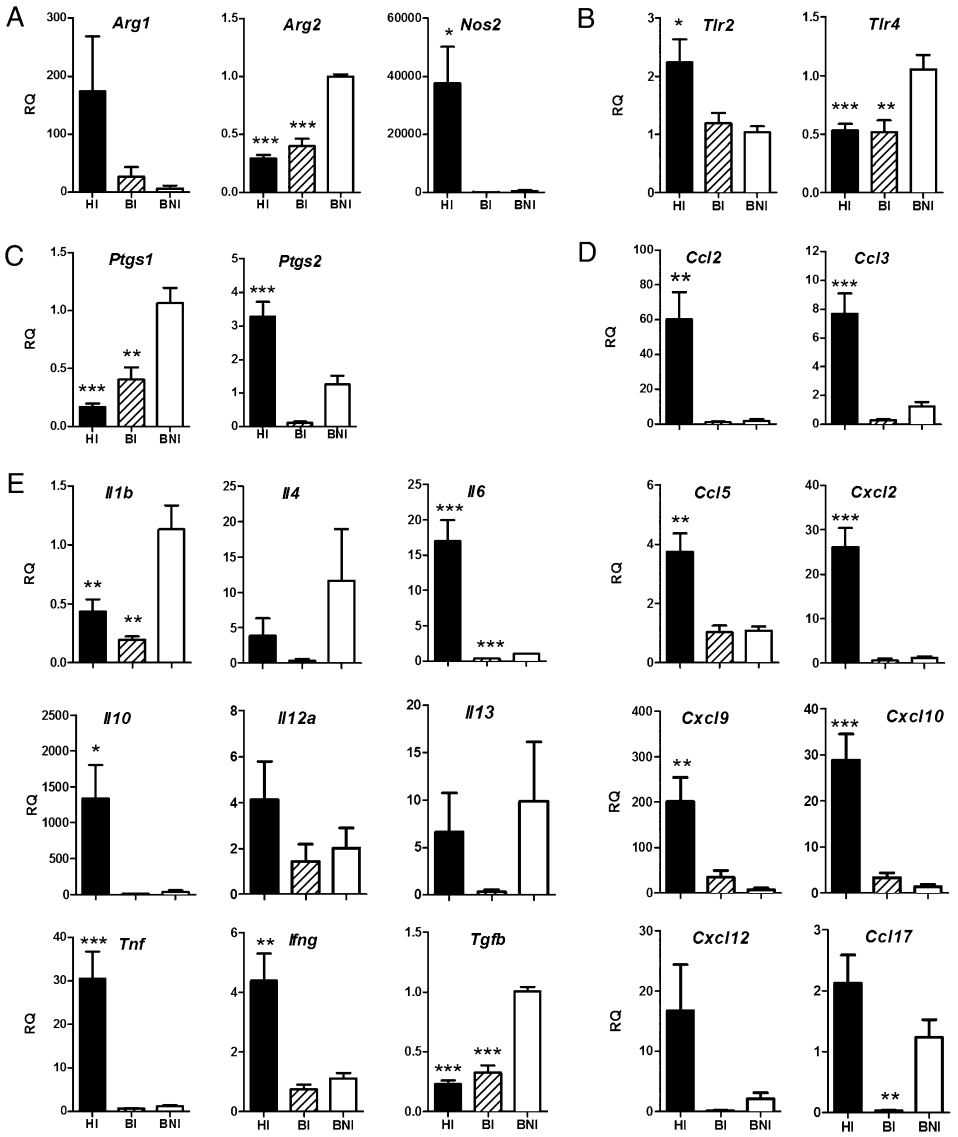

FIGURE 2. Gene expression in CD11b$^+$ cells purified from hearts of *T. cruzi*-infected BALB/c mice. BALB/c mice were infected i.p. with 2×10^3 blood trypomastigotes of the Y strain. Mice were sacrificed at day 21 postinfection, and infected hearts and blood from infected and noninfected mice were elicited. After mechanical and enzymatic digestion of heart tissue and PBMCs purification, CD11b$^+$ cells were purified with CD11b microbeads. HI, black bars; BI, dashed bars; BNI, white bars. mRNA was isolated from cells, and (*A*) *ArgI*, *ArgII*, and *Nos2*, (*B*) *Tlr2* and *Tlr4*, (*C*) *Ptgs1* and *Ptgs2*, (*D*) chemokines (*Ccl2*, *Ccl3*, *Ccl5*, *Cxcl2*, *Cxcl9*, *Cxcl10*, *Cxcl12*, and *Ccl17*), and (*E*) cytokines (*Il1β*, *Il4*, *Il6*, *Il10*, *Il12a*, *Il13*, *Tnf*, *Ifng*, and *Tgfb1*) expression was analyzed by quantitative RT-PCR using TaqMan probes. Data are the mean of three independent experiments. Statistically significant differences of HI and BI with respect to BNI are shown: $*p < 0.05$, $**p < 0.01$, $***p < 0.001$.

the genes coding for *Ptgs2*, *Il4*, and *Ccl17*, which were downregulated in BI cells but upregulated in HI cells compared with that in BNI cells (Fig. 2). We also investigated gene expression of the CD11b$^+$ HI isolated cells by quantitative RT-PCR of 10 markers of M2 activation previously described (12). The results showed that some M2 genes such as *Psap*, *Trem2*, *Ch3l3/4*, *Cdh1*, and *Folr2*, but not others such as *Retlna*, *Sepp1*, and *Mgl2*, were significantly overexpressed in CD11b$^+$ HI cells compared with that in purified CD11b$^+$ of noninfected BALB/c mice (Table I). Therefore, we can conclude that heart-infiltrating CD11b$^+$ cells during *T. cruzi* infection do not show a typical M1 or M2 signature, likely reflecting the heterogeneity of the CD11b$^+$ population.

Heterogeneity of the CD11b$^+$ cells purified from the hearts of T. cruzi*-infected mice*

Next, the composition of the CD11b$^+$ HI sorted population was analyzed by flow cytometry. Within purified CD11b$^+$ cells, ~70% were Ly6G$^-$ and 25% were Ly6G$^+$ (Fig. 3*A*), suggesting the presence of two major subpopulations, respectively a monocytic and a granulocytic subpopulation. This was supported by the

Table I. M2 gene signature expression levels in CD11b$^+$ HI as determined by real-time PCR

Gene	Fold Increase[a]
Fizz (*Retlna*)	Not detected
Pla2g7	2.05
Psap	16.71[b]
Sepp1	0.15
Trem2	5.81[b]
Mgl2	0.1
Ch3l3/4	26,075.97[b]
Mrc1	5.33[b]
Cdh1	112.89[b]
Folr2	6.81[b]

[a]On day 21 postinfection, normalized with the ribosomal S12 gene and expressed relative to peritoneal exudates cells from noninfected mice. Data are shown as mean of three individual experiments.
[b]Fold increase >5.

observation that 1) CD11b$^+$Ly6G$^-$ cells expressed higher levels of Ly6C (monocytic marker), CD68 (mature macrophage marker), and MHC class II molecules compared with those of CD11b$^+$ Ly6G$^+$ cells and 2) the CD11b$^+$Ly6G$^+$ cells included a higher percentage of CCR3$^+$ eosinophils than that of the CD11b$^+$Ly6G$^-$ cells. DX5$^+$ NK cells were detected only in the CD11b$^+$Ly6G$^+$ cell population. Finally, neither CD11b$^+$Ly6G$^-$ nor CD11b$^+$Ly6G$^+$ cell subpopulations expressed the B cell marker B220 (data not shown), the macrophage marker F4/80, or the dendritic cell marker CD11c (Fig. 3*B*). Together, these data show that CD11b$^+$ HI cell composition is heterogeneous with mainly a monocytic and a granulocytic/NK cell fraction.

CD11b$^+$ cells isolated from heart tissue of infected mice suppress T cell proliferation by an NO-dependent mechanism

In addition to arginase I and iNOS expression, suppression of T cell proliferation is the characteristic that best defines MDSCs (10, 13). Thus, we analyzed T cell proliferation upon anti-CD3/anti-CD28 Ab stimulation in the presence of CD11b$^+$ HI cells using CD11b$^+$ BNI cells as control. Fig. 4*A* shows that compared with CD11b$^+$ BNI cells, CD11b$^+$ HI cells were able to suppress proliferation of stimulated T cells. The addition of iNOS inhibitor L-NMMA to the cultures, but not of arginase inhibitor nor-NOHA, partially restored T cell proliferation (Fig. 4*A*), suggesting that CD11b$^+$ HI-mediated suppression was likely mediated by an NO-dependent mechanism. However, it is known that extracellular L-arginine concentrations below 100 μM impair fully functional T cell proliferation (15). Therefore, we studied T cell proliferation in medium containing different concentrations of L-arginine (0, 100, and 1000 μM) in the presence and absence of CD11b$^+$ cells from spleens of noninfected mice (NI), (Fig. 4*B* and 4*C*, respectively). The results showed that T cell proliferation was dependent on L-arginine concentration, and addition of CD11b$^+$ cells to the culture significantly incremented T cell proliferation with respect to T cells alone. Therefore, to test the contribution of arginase I to T cell suppression by L-arginine depletion, we lowered L-arginine concentration in the culture medium to 100 μM and compared the effect of CD11b$^+$ HI cells (Fig. 4*D*) with cultures of T cells alone. The results showed that when T cells were cultured with CD11b$^+$ HI cells, there was a strong suppressive effect on T cell proliferation. Addition of iNOS and arginase I inhibitors to activated T cells cultured alone did not significantly affect their proliferation. However, similar to cultures performed in >1 mM L-arginine (Fig. 4*A*), there was a partial recovery of T cell proliferation in the presence of L-NMMA, but not in the presence of

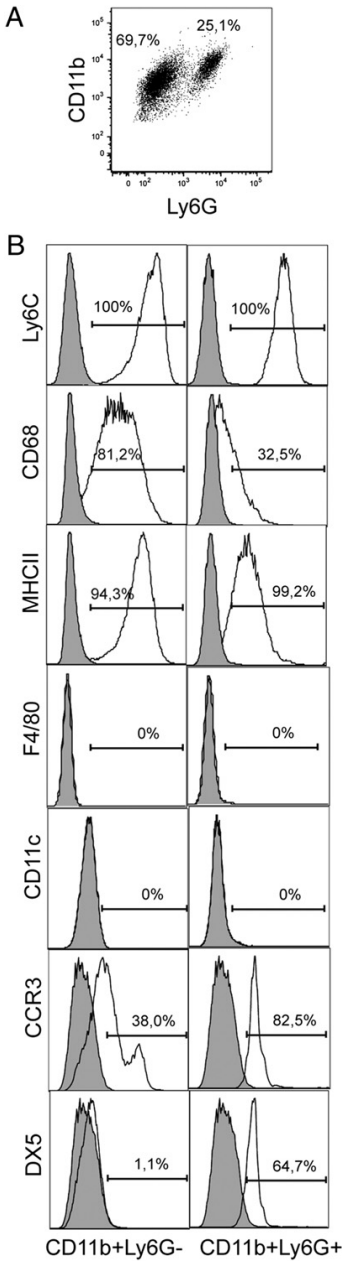

FIGURE 3. Flow cytometry analysis of CD11b$^+$ cells purified from hearts of *T. cruzi*-infected BALB/c mice. Mice were infected i.p. with 2×10^3 blood trypomastigotes of the Y strain. Mice were sacrificed at day 21 postinfection, and infected hearts were elicited. After mechanical and enzymatic digestion of heart tissue, CD11b$^+$ cells were purified with CD11b microbeads. Cells were stained with anti-CD11b–PE–Cy7 or anti-CD11b–Alexa Fluor 647, anti-Ly6G/Ly6C(Gr-1)–FITC or anti-Ly6G/Ly6C(Gr-1)–PE, anti-Ly6C–Alexa Fluor 647, anti-CD68–PE, anti-MHCII–PE, anti-F4/80–PE, anti-CD11c–PE, anti-CCR3–FITC, and anti-CD49b(DX5)–FITC Abs and analyzed in FACSCanto. Gray histograms represent isotypic Ab labeling and white histograms specific staining as indicated. *A*, Double staining with Ly6G/Ly6C and CD11b Abs. *B*, Staining of CD11b$^+$Ly6G$^-$ and CD11b$^+$Ly6G$^+$ gated populations with Ly6C, CD68, F4/80, MHCII, CD11c, CCR3, and DX5 Abs. Data are representative of at least three independent experiments. MHCII, MHC class II.

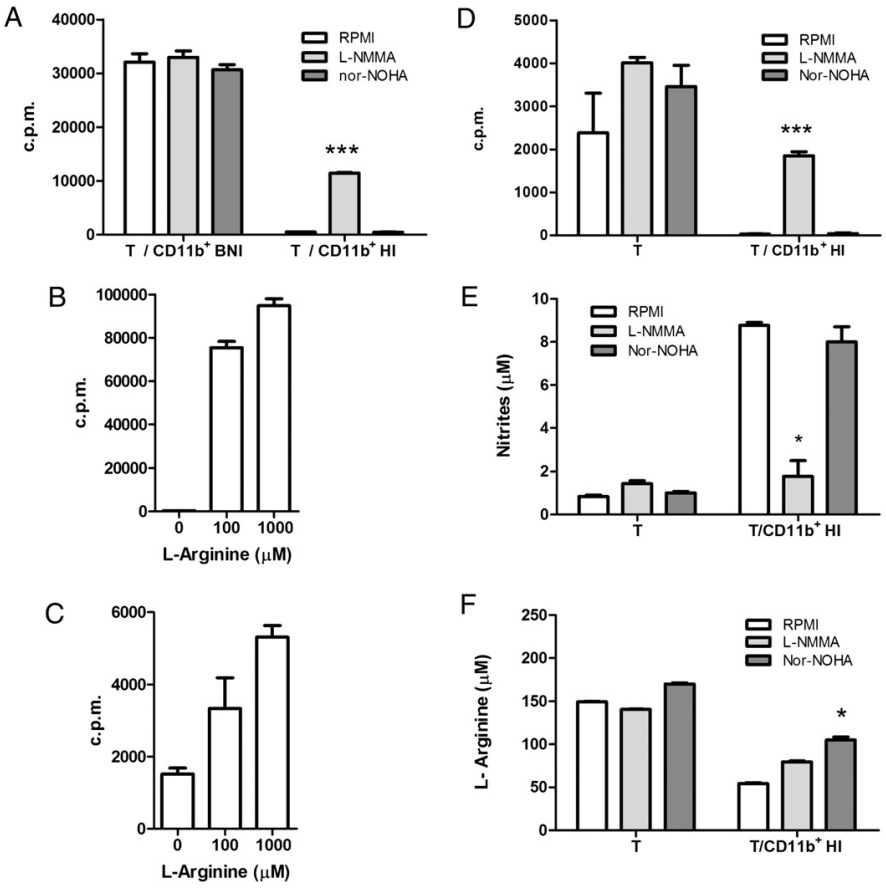

FIGURE 4. Suppression of T cell proliferation in the presence of CD11b$^+$ HI cells from *T. cruzi*-infected BALB/c mice. Mice were infected i.p. with 2×10^3 blood trypomastigotes of the Y strain. Mice were sacrificed at day 21 postinfection, and infected hearts were collected. After mechanical and enzymatic digestion of infected heart tissue (HI) and isolation of blood from noninfected mice (BNI), CD11b$^+$ cells were purified with CD11b microbeads. T cells were isolated from spleens of noninfected mice (T) with the Pan T cell kit, and the proliferation assays were set up as follows. *A*, T cells were activated with anti-CD3 and anti-CD28 Abs and cultured with RPMI 1640 with 1 mM L-arginine in the presence of CD11b$^+$ BNI or CD11b$^+$ HI cells and the presence or absence of iNOS (L-NMMA) and arginase I (nor-NOHA) inhibitors. *B* and *C*, Activated T cells were cultured with CD11b$^+$ cells isolated from noninfected mice (*B*) or alone (*C*) in presence of indicated concentrations of L-arginine. *D*, Activated T cells were cultured with 100 μM L-arginine in the presence or absence of CD11b$^+$ HI cells and inhibitors (L-NMMA and nor-NOHA). *E*, Concentration of nitrites (NO_2Na) was measured in the supernatants of the cultures from *D* with the Griess reagent. *F*, Concentration of extracellular L-arginine was measured in the supernatants of the cultures from *D* using an HPLC chromatograph coupled to a mass detector. Data are representative of at least two independent experiments. Statistically significant differences with respect to cultures with RPMI medium of each condition are shown: $*p < 0.05$, $***p < 0.001$.

nor-NOHA (Fig. 4*B*), suggesting that, in vitro, even at reduced L-arginine concentration, suppression of proliferation is mostly mediated by NO. In agreement, the concentration of nitrite increased significantly in the culture supernatants in the presence of CD11b$^+$ cells, and this was inhibited upon addition of L-NMMA (Fig. 4*E*). Finally, Fig. 4*F* shows that the concentration of L-arginine was still above the threshold that allows basal T cell proliferation (~100 μM). Additional L-arginine present in the supernatants (150 μM) could come from the FBS added to the RPMI 1640 medium and from intracellular pools. Notably, CD11b$^+$ HI cells caused a drastic reduction of L-arginine concentration in medium when these cells were cocultured with activated T cells. This was significantly recovered in the presence of arginase inhibitor, indicating that arginase is active in CD11b$^+$ HI cells. Taken together, the above results indicate that CD11b$^+$ HI cell in vitro T cell immunosuppression is mediated by iNOS.

Purified CD11b$^+$Ly6G$^-$ monocytic cells isolated from heart tissue of infected mice express iNOS and arginase I and suppress, in vitro, T cell proliferation by an NO-dependent mechanism

To characterize in more detail the cells expressing arginase I and iNOS, Ly6G$^+$, CD11b$^+$Ly6G$^-$, and CD11b$^-$Ly6G$^-$ cells isolated from hearts of *T. cruzi*-infected mice were cultured with activated T cells. Fig. 5*A* and Table II show that, after magnetic sorting, ~35% of the cells were Ly6G$^+$ and 65% were Ly6G$^-$, in agreement with flow cytometry analysis (Fig. 3). We recovered an average of 1.57×10^5 ($\pm 0.30 \times 10^5$) Ly6G$^+$ cells and 2.96×10^5 ($\pm 0.57 \times 10^5$) Ly6G$^-$ per heart of BALB/c infected mice. Microscopic examination of 20 different fields of Giemsa-stained cells showed that the phenotype of the Ly6G$^-$ cells was predominantly monocytic, whereas Ly6G$^+$ cells were ~70% granulocytic and 30% nongranulocytic (Table II and Supplemental

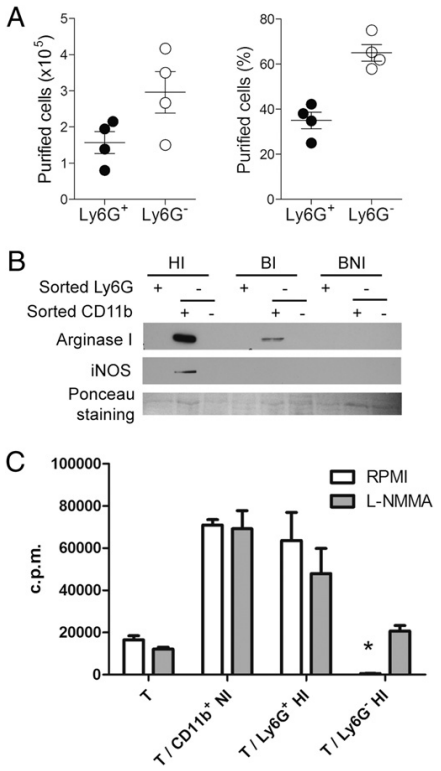

FIGURE 5. Expression of iNOS and arginase I in $CD11b^+$ $Ly6G^-$ HI cells suppresses T cell proliferation. BALB/c mice were infected i.p. with 2×10^3 blood trypomastigotes of the Y strain. Mice were sacrificed at day 21 postinfection, and infected hearts and blood were elicited. Hearts were mechanically and enzymatically digested and PBMCs purified from blood of infected and noninfected mice. Cells were purified with Ly6G microbeads, and the resulting $Ly6G^-$ cells were subsequently purified with CD11b microbeads. *A*, Average number and percentage of purified cells per heart of *T. cruzi*-infected BALB/c mice. *B*, Protein content was quantified by BCA method and analyzed; 20 μg loaded in 10% SDS-PAGE gels and subjected to Western blot with Abs against arginase I and iNOS. A representative Ponceau-stained band is shown as loading control. *C*, Proliferative assay of anti-CD3– and anti-CD28–stimulated T cells in the absence and presence of purified $CD11b^+$ cells isolated from noninfected mice ($CD11b^+$ NI cells), $Ly6G^+$ HI cells, and $Ly6G^-$ HI cells. Data are representative of at least two independent experiments. The statistically significant difference with respect to cultures of T cells alone and in the presence of $CD11b^+$ cells from noninfected mice is shown: $*p < 0.05$.

Fig. 1). $CD11b^+Ly6G^-$ cells, but not $Ly6G^+$ cells, expressed arginase I and iNOS by Western blot (Fig. 5*B*). We also detected arginase I expression in $CD11b^+Ly6G^-$ cells isolated from the blood of infected mice but not from noninfected mice (Fig. 5*B*), in agreement with previous observations in PBMC lysates (19). $CD11b^+Ly6G^-$ cells, but not $Ly6G^+$ cells, from hearts of infected mice suppressed anti-CD3/anti-CD28–stimulated T cell proliferation in comparison with T cells alone and T cells cultured with $CD11b^+$ NI (Fig. 5*C*). Suppression was partially reverted in the presence of L-NMMA, indicating that it is mediated by NO. These results strongly support that $CD11b^+Ly6G^-$ are MDSCs.

Table II. Phenotype of magnetically sorted cells isolated from hearts of mice at 21 dpi according to Giemsa staining

Cell Type	Microscopic Examination % (20 Fields)
$CD11b^+Ly6G^+$	70 granulocytic 30 nongranulocytic
$CD11b^+Ly6G^-$	98 monocytic 2 nonmonocytic

$Ly6G^+$ granulocytic cells isolated from heart tissue of infected mice express S100A8 and S100A9

MDSC recruitment into several tissues has been shown to be dependent on S100A8 and S100A9 proteins (24). Coinciding with the presence of monocytic MDSCs, our results showed that *S100a8* and *S100a9* gene and corresponding protein expression (Fig. 6*A* and 6*B*, respectively) were detected in heart tissue in the acute phase of *T. cruzi* infection in BALB/c mice, showing highest expression at 21 dpi coincident with previously described maximum arginase I and iNOS expression (19). We also detected expression of *S100a8* and *S100a9* gene and protein in C57BL/6 infected mice (Supplemental Fig. 2), although lower than that in BALB/c mice, correlating with the different kinetics of arginase I expression in heart tissue of this strain of mice infected with *T. cruzi* (19). In agreement with previous observations, the expression of another important chemokine involved in monocyte heart recruitment in *T. cruzi* infection, CCL2 (25), showed itself to be overexpressed in $CD11b^+$ HI cells with respect to control cells (Fig. 2*D*) following similar kinetics as S100A8 and S100A9 in heart tissue of both BALB/c and C57BL/6 mice (Supplemental Fig. 3).

We next investigated the cellular origin of S100A8 and S100A9 in the heart infiltrate of *T. cruzi* infected mice. We found that S100A8 and S100A9 proteins were expressed in $Ly6G^+$, which did not express iNOS and arginase I, but not in $CD11b^+Ly6G^-$ cells, which do express iNOS and arginase I (Figs. 4 and 6*C*). Therefore, S100A8 and S100A9 proteins expressed by granulocytic cells might be implicated in the recruitment and/or differentiation of heart-infiltrated, arginase I/iNOS-expressing MDSCs in *T. cruzi*-infected mice.

T. cruzi *infection in mice causes plasma* L*-arginine depletion*

Arginase I expression in MDSCs during *T. cruzi* infection can decrease L-arginine availability. Thus, we studied whether circulating L-arginine levels were affected in infected mice. In C57BL/6 mice, there was a substantial decrease in plasma L-arginine concentration (<50 μM) at 14 dpi, and in BALB/c mice the reduction was observed for longer periods (at 14 and 21 dpi) (Fig. 7*A*, 7*B*). These results correlated with our previous kinetics of arginase I expression in the hearts of both C57BL/6 and BALB/c mice (19) and indicated that during in vivo infection, arginase I-expressing cells in heart tissue and/or in peripheral blood could cause plasma L-arginine depletion that can account for suppression of T cell proliferation observed in the acute phase.

To evaluate the relevance of MDSCs in hearts of *T. cruzi*-infected mice, we treated mice with the iNOS inhibitor L-NAME. The inhibition of iNOS resulted in a dramatic increase in parasitemia, mortality, and parasite load in heart tissue with respect to untreated mice (Supplemental Fig. 4). This result confirms the in vivo relevance of iNOS and, by extension, NO-producing MDSCs in *T. cruzi* infection. Of greater interest, L-arginine supplementation reduced parasite burden in heart tissue (Fig. 7*C*), indicating that restoration of L-arginine levels is beneficial for the host.

Discussion

The understanding of the pathogenesis of myocarditis induced by *T. cruzi* is crucial to develop therapeutic strategies aiming to ameliorate the inflammation that leads to heart dysfunction. In this

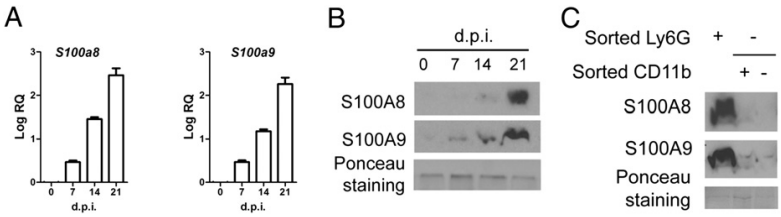

FIGURE 6. S100A8/S100A9 expression in hearts from *T. cruzi*-infected BALB/c mice and in hearts isolated cells after Ly6G and CD11b magnetic sorting. Groups of 5–15 BALB/c mice were infected i.p. with 2×10^3 blood trypomastigotes of the Y strain. Mice were sacrificed at 0, 7, 14, and 21 dpi. *A*, mRNA was extracted from hearts, and *S100a8* and *S100a9* expression was analyzed by quantitative RT-PCR. *B*, Protein extracts were isolated from heart tissue from BALB/c mice at different days postinfection; 20 μg loaded in 15% SDS-PAGE gels and subjected to Western blot analysis with anti S100A8 and S100A9 Abs. A representative Ponceau-stained band is shown as loading control. Data are representative of at least two independent experiments. *C*, Hearts were mechanically and enzymatically digested. Cells were purified with Ly6G microbeads, and the resulting $Ly6G^-$ cells were subsequently purified with CD11b microbeads. Protein content was quantified by BCA method; 20 μg loaded in 15% SDS-PAGE gels and subjected to Western blot with Abs against S100A8 and S100A9. A representative Ponceau-stained band is shown as loading control. Data are representative of at least two independent experiments.

regard, the mouse model of *T. cruzi* infection recapitulates many of the functional and pathological alterations of the human disease. Thus, in the myocardium of acutely infected mice, there is an inflammatory reaction characterized by lymphoid and myeloid cell infiltration and expression of inflammatory mediators thought to be responsible for the pathogenesis (19). To date, most of the research has focused on the characterization of the infiltrating T lymphocytes in the myocarditis associated with *T. cruzi* infection whereas very little is known about myeloid cells present in this heart inflammatory infiltrate. Our previous results showed that myeloid cells infiltrating the heart, and to a minor extent PBMCs from *T. cruzi*-infected mice, expressed arginase I (19). In this study, we have purified those cells and analyzed their gene expression, phenotype, and function.

The myeloid $CD11b^+$ population in the hearts of mice acutely infected with *T. cruzi* expresses markers of M1 and M2 subsets and is composed of two main subpopulations: immature monocytic $Ly6G^-$ and granulocytic $Ly6G^+$. The monocytic $Ly6G^-$ cells, but not the granulocytic $Ly6G^+$ cells, express iNOS and arginase I and are able to suppress T cell proliferation. The granulocytic $Ly6G^+$ cells, but not monocytic $Ly6G^-$ cells, express S110A8 and S100A9 proteins. According to marker expression and especially suppressive function, our results indicate that monocytic $Ly6G^-$ cells are indeed MDSCs. Recruitment of MDSCs to the heart could be potentiated by granulocytic $Ly6G^+$ cells through S100A8 and S100A9 protein expression. T cell suppression in vitro by those $CD11b^+Ly6G^-$ cells is mostly mediated by NO, and the in vivo high level of expression of arginase I by MDSCs produces systemic depletion of L-arginine that may contribute to systemic immunosuppression in the acute phase of infection.

We found that isolated $CD11b^+$ cells from the hearts of infected mice expressed both arginase I and iNOS but not arginase II. In addition, gene expression of several type 1 chemokines and cytokines was found to be selectively upregulated by $CD11b^+$ HI cells. Notably, the regulatory cytokine *Il10* was also highly induced, as well as markers of M2 populations. We focused our studies in the BALB/c model, which presented higher infiltration of those cells; however, similar qualitative results were obtained in the C57BL/6 model (data not shown). The expression of M1 and M2 genes could be the result of heterogeneity of the $CD11b^+$ isolated population. Nonetheless, it is accepted that coexpression of M1/M2 genes is characteristic of MDSCs (26). Moreover, a striking similar profiling of M1/M2 genes (*Il10*, *Ccl2*, and *Ccl5*, IFN-inducible chemokines *Cxcl9* and *Cxcl10*) has been described in MDSCs infiltrating tumors (27, 28). Giemsa staining of the isolated $CD11b^+Ly6G^-$ HI cells revealed a monocytic phenotype. Therefore, the monocytic $CD11b^+Ly6G^-$ isolated subpopulation expressing both iNOS and arginase I could be considered as bona fide MDSCs accumulating in the hearts of *T. cruzi*-infected mice. The $Ly6G^+$ sorted population was more heterogeneous and showed a predominant granulocytic phenotype that was devoid of iNOS and arginase I expression. In a different model, the existence of a $Ly6C^+$ granulocytic population has been described in the injured myocardium, which is recruited via CCR2 and thought to digest damaged tissue (29). In addition, $CD11b^+Gr\text{-}1^+F4/80^+$ populations that presented mixed M2/MDSCs phenotype have been described infiltrating the heart during Coxsackie virus B3 (CVB3) viral myocarditis (9). Neither iNOS expression nor suppressor activity had been reported in the injured heart or in CVB3 myocarditis. It is worth mentioning that $CD11b^+$ HI cells were $F4/80^-$ but $CD68^+$, being both mature macrophage markers. Our

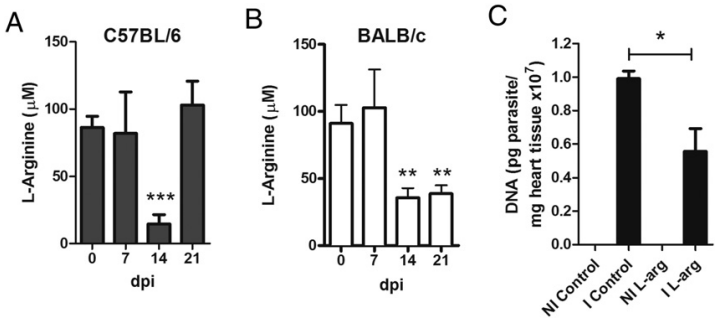

FIGURE 7. Plasma L-arginine depletion in mice infected with *T. cruzi*. BALB/c and C57BL/6 mice were infected i.p. with 2×10^3 blood trypomastigotes of the Y strain. Plasma was isolated at indicated days postinfection and L-arginine concentration determined. *A*, Values for C57BL/6 mice. *B*, Values for BALB/c mice. *C*, *T. cruzi* parasite load determined by quantitative PCR in mice with or without dietary L-arginine supplement. Data are representative of at least two independent experiments. Statistically significant difference with respect to noninfected mice (*A*, *B*) and untreated infected mice (*C*) is shown: $*p < 0.05$, $**p < 0.01$, $***p < 0.001$.

results indicate that *T. cruzi* infection induces the recruitment of a particular phenotype of cells different from the ones described in CVB3 myocarditis.

It is known that MDSCs express arginase I that can cause suppression of T cell proliferation by extracellular L-arginine depletion. We observed that during acute *T. cruzi* infection, there is plasma L-arginine depletion at day 14 postinfection in less susceptible C57BL/6 mice and at days 14 and 21 postinfection in more susceptible BALB/c mice. These results suggest that fast recovery from L-arginine plasma depletion in C57BL/6 mice is linked to their low susceptibility to infection. In addition, L-arginine plasma depletion nicely correlated with the kinetics of arginase I expression in isolated blood and heart $CD11b^+$ cells (19) and with systemic immunosuppression (5). The mechanism of T cell suppression in vitro in *T. cruzi*-infected mice by $CD11b^+$ $Ly6G^-$ cells is mediated by NO, and in vivo systemic depletion of L-arginine, likely mediated by high level of expression of arginase I by those cells, may contribute to systemic immunosuppression in the acute phase of infection. Thus, according to markers, phenotype, and suppressive function, these cells are in fact bona fide MDSCs.

$CD11b^+$ BI cells did not express iNOS compared with $CD11b^+$ HI cells. Thus, induction of arginase I and iNOS in $CD11b^+$ cells could occur after their recruitment from periphery to heart tissue, similar to what happens in tumor infiltration by myeloid cells (10, 28). In this regard, we found that only the $Ly6G^+$ cells isolated from heart tissue of infected mice expressed S100A8 and S100A9 proteins. Those molecules have been described to regulate the accumulation of MDSCs (24). Thus, a plausible explanation is that $Ly6G^+$ infiltrated in heart tissue could be triggering recruitment of $Ly6G^-$ cells through expression of S100A8 and S100A9 proteins, which also prevent further differentiation of MDSCs to macrophages and dendritic cells. Nonetheless, we cannot discard the involvement of other chemokines as CCL2 in this recruitment. In contrast, it could be possible that blood cells expressing arginase I (but no iNOS) are M2 macrophages, a possibility that has not been addressed in this study. Alternatively, MDSCs in heart may result from expansion of resident tissue macrophages, but this is unlikely, as they do not express the mature macrophage marker F4/80. Also, the spleen has been described to function as a source of monocytes that have further ability to infiltrate the heart (30), therefore it could be that $CD11b^+$ HI cells are originated and mobilized from the spleen. In this regard, we have found that spleens of *T. cruzi*-infected animals in the same days postinfection contain a $CD11b^+Gr1^+$ population that inhibits T cell proliferation via NO (5).

The goal of immune regulation is to avoid excessive production of immune mediators that could be detrimental to the host and even cause its death, as it seems to be in *T. cruzi* myocarditis (3). Thus, $CD11b^+$ HI MDSCs may regulate the excessive T cell-dependent inflammation in the heart at the onset of infection, which could much later determine the severity of cardiomyopathy. Among the genes expressed by $CD11b^+$ HI cells are the chemokines *Ccl2*, *Ccl5*, *Cxcl9*, and *Cxcl10* that were previously shown to be expressed in the hearts of *T. cruzi*-infected mice during the acute phase, and they play a protective role in *T. cruzi* infection but not in association with the heart inflammatory phenotype (23, 25). This indirectly would suggest a protective role of $CD11b^+$ HI cells in *T. cruzi*-induced myocarditis. On the contrary, in susceptible mice, expression of iNOS and arginase I by MDSCs is higher and more prolonged in time than in nonsusceptible C57BL/6 mice, suggesting an association between MDSCs, iNOS/arginase I expression, and higher parasite burden followed by worst outcome of the disease.

A formal demonstration of the exact role of MSDCs in *T. cruzi* infection is difficult because there are no conclusive markers of those cells to allow their selective elimination in infected animals. To evaluate the relevance of MDSCs, we followed an alternative approach: we inhibited iNOS with L-NAME treatment of infected mice resulting in a dramatic increase in parasitemia, mortality, and parasite load in heart tissue with respect to untreated mice, showing that iNOS, and by extension NO-producing MDSCs, are necessary to control the *T. cruzi* infection (31–34). In addition, L-arginine supplementation reduced parasite burden in heart tissue, indicating that restoration of L-arginine levels is beneficial for the host. Because L-arginine is one of the rate-limiting factors in NO production (35), it is possible that L-arginine supplementation increases NO production in infected mice, which would end in a more efficient control of the infection. Therefore, L-arginine supplementation can have two different effects: 1) it could fuel iNOS-derived NO production, thus reducing parasite replication that is evidenced by a reduction in heart parasite load; 2) it can revert immunosuppression, thus allowing a more efficient control of infection by the immune system. Moreover, there is a strong correlation between the appearance of those cells and severity of the disease. More importantly, antagonizing or preventing the effect of arginase I and iNOS, enzymes that best define their function, modulates parasite load in heart tissue and mortality. Our results support the hypothesis that iNOS- and arginase I-expressing MDSCs are beneficial in *T. cruzi* infection when L-arginine is available but detrimental for the host when they cause persistent L-arginine depletion.

In summary, we describe in this study for the first time to our knowledge that monocytic MDSCs that express iNOS and arginase I are present in heart tissue in the acute phase of *T. cruzi* infection, where they have the potential to suppress T lymphocytes present in the infiltrate. This is the first description of MDSCs found infiltrating the heart during *T. cruzi* infection and, to our knowledge, in the context of cardiac inflammation. The presence of MDSCs correlates with depletion of L-arginine from plasma that can have a systemic suppressor effect on T cell function extending to other inflamed organs and tissues. MDSC iNOS activity may be required for efficient control of parasite load in the heart that leads to survival of infected mice, but iNOS in combination with arginase I also could be detrimental for the host when iNOS/arginase I expression is persistent through the acute phase of infection causing plasma L-arginine depletion. Cardiac and systemic effects of MDSCs are transient, and the outcome of disease may depend as well on components of the innate, adaptive, and regulatory immune responses.

Acknowledgments

We thank Beatriz Barrocal and Ella Omasta for animal care and Maria A. Chorro, Carlos Chillón, Ricardo Ramos, and Rosa Sedano for technical assistance. We also thank Kiavash Movahedi and Tom Bosschaerts for discussion of the data.

Disclosures

The authors have no financial conflicts of interest.

References

1. WHO. 2002. *World Health Report.* WHO, Geneva, Switzerland.
2. Gironès, N., and M. Fresno. 2003. Etiology of Chagas disease myocarditis: autoimmunity, parasite persistence, or both? *Trends Parasitol.* 19: 19–22.
3. Marin-Neto, J. A., E. Cunha-Neto, B. C. Maciel, and M. V. Simões. 2007. Pathogenesis of chronic Chagas heart disease. *Circulation* 115: 1109–1123.
4. Muñoz-Fernández, M. A., M. A. Fernández, and M. Fresno. 1992. Synergism between tumor necrosis factor-alpha and interferon-gamma on macrophage activation for the killing of intracellular *Trypanosoma cruzi* through a nitric oxide-dependent mechanism. *Eur. J. Immunol.* 22: 301–307.

5. Goñi, O., P. Alcaide, and M. Fresno. 2002. Immunosuppression during acute *Trypanosoma cruzi* infection: involvement of Ly6G (Gr1(+))CD11b(+) immature myeloid suppressor cells. *Int. Immunol.* 14: 1125–1134.
6. Gomes, J. A., L. M. Bahia-Oliveira, M. O. Rocha, O. A. Martins-Filho, G. Gazzinelli, and R. Correa-Oliveira. 2003. Evidence that development of severe cardiomyopathy in human Chagas' disease is due to a Th1-specific immune response. *Infect. Immun.* 71: 1185–1193.
7. Bergeron, M., and M. Olivier. 2006. *Trypanosoma cruzi*-mediated IFN-gamma-inducible nitric oxide output in macrophages is regulated by iNOS mRNA stability. *J. Immunol.* 177: 6271–6280.
8. Stempin, C. C., T. B. Tanos, O. A. Coso, and F. M. Cerbán. 2004. Arginase induction promotes *Trypanosoma cruzi* intracellular replication in Cruzipain-treated J774 cells through the activation of multiple signaling pathways. *Eur. J. Immunol.* 34: 200–209.
9. Fairweather, D., and D. Cihakova. 2009. Alternatively activated macrophages in infection and autoimmunity. *J. Autoimmun.* 33: 222–230.
10. Gabrilovich, D. I., and S. Nagaraj. 2009. Myeloid-derived suppressor cells as regulators of the immune system. *Nat. Rev. Immunol.* 9: 162–174.
11. Vincendeau, P., A. P. Gobert, S. Daulouède, D. Moynet, and M. D. Mossalayi. 2003. Arginases in parasitic diseases. *Trends Parasitol.* 19: 9–12.
12. Ghassabeh, G. H., P. De Baetselier, L. Brys, W. Noël, J. A. Van Ginderachter, S. Meerschaut, A. Beschin, F. Brombacher, and G. Raes. 2006. Identification of a common gene signature for type II cytokine-associated myeloid cells elicited in vivo in different pathologic conditions. *Blood* 108: 575–583.
13. Marigo, I., L. Dolcetti, P. Serafini, P. Zanovello, and V. Bronte. 2008. Tumor-induced tolerance and immune suppression by myeloid derived suppressor cells. *Immunol. Rev.* 222: 162–179.
14. Movahedi, K., M. Guilliams, J. Van den Bossche, R. Van den Bergh, C. Gysemans, A. Beschin, P. De Baetselier, and J. A. Van Ginderachter. 2008. Identification of discrete tumor-induced myeloid-derived suppressor cell subpopulations with distinct T cell-suppressive activity. *Blood* 111: 4233–4244.
15. Choi, B. S., I. C. Martinez-Falero, C. Corset, M. Munder, M. Modolell, I. Müller, and P. Kropf. 2009. Differential impact of L-arginine deprivation on the activation and effector functions of T cells and macrophages. *J. Leukoc. Biol.* 85: 268–277.
16. Bronte, V., P. Serafini, A. Mazzoni, D. M. Segal, and P. Zanovello. 2003. L-arginine metabolism in myeloid cells controls T-lymphocyte functions. *Trends Immunol.* 24: 302–306.
17. Brys, L., A. Beschin, G. Raes, G. H. Ghassabeh, W. Noël, J. Brandt, F. Brombacher, and P. De Baetselier. 2005. Reactive oxygen species and 12/15-lipoxygenase contribute to the antiproliferative capacity of alternatively activated myeloid cells elicited during helminth infection. *J. Immunol.* 174: 6095–6104.
18. Abrahamsohn, I. A., and R. L. Coffman. 1995. Cytokine and nitric oxide regulation of the immunosuppression in *Trypanosoma cruzi* infection. *J. Immunol.* 155: 3955–3963.
19. Cuervo, H., M. A. Pineda, M. P. Aoki, S. Gea, M. Fresno, and N. Gironès. 2008. Inducible nitric oxide synthase and arginase expression in heart tissue during acute *Trypanosoma cruzi* infection in mice: arginase I is expressed in infiltrating CD68+ macrophages. *J. Infect. Dis.* 197: 1772–1782.
20. Brener, Z. 1962. Therapeutic activity and criterion of cure on mice experimentally infected with *Trypanosoma cruzi*. *Rev. Inst. Med. Trop. Sao Paulo* 4: 389–396.
21. European Council. 1986 (March 18). *Council Directive from the Convention for the Protection of Vertebrate Animals Used for Experimental and Other Scientific Purposes*. Eurpoean Council, Strasbourg, France.
22. Mills, C. D., K. Kincaid, J. M. Alt, M. J. Heilman, and A. M. Hill. 2000. M-1/M-2 macrophages and the Th1/Th2 paradigm. *J. Immunol.* 164: 6166–6173.
23. Hardison, J. L., R. A. Wrightsman, P. M. Carpenter, T. E. Lane, and J. E. Manning. 2006. The chemokines CXCL9 and CXCL10 promote a protective immune response but do not contribute to cardiac inflammation following infection with *Trypanosoma cruzi*. *Infect. Immun.* 74: 125–134.
24. Sinha, P., C. Okoro, D. Foell, H. H. Freeze, S. Ostrand-Rosenberg, and G. Srikrishna. 2008. Proinflammatory S100 proteins regulate the accumulation of myeloid-derived suppressor cells. *J. Immunol.* 181: 4666–4675.
25. Paiva, C. N., R. T. Figueiredo, K. Kroll-Palhares, A. A. Silva, J. C. Silvério, D. Gibaldi, Ados. S. Pyrrho, C. F. Benjamim, J. Lannes-Vieira, and M. T. Bozza. 2009. CCL2/MCP-1 controls parasite burden, cell infiltration, and mononuclear activation during acute *Trypanosoma cruzi* infection. *J. Leukoc. Biol.* 86: 1239–1246.
26. Umemura, N., M. Saio, T. Suwa, Y. Kitoh, J. Bai, K. Nonaka, G. F. Ouyang, M. Okada, M. Balazs, R. Adany, et al. 2008. Tumor-infiltrating myeloid-derived suppressor cells are pleiotropic-inflamed monocytes/macrophages that bear M1- and M2-type characteristics. *J. Leukoc. Biol.* 83: 1136–1144.
27. Biswas, S. K., L. Gangi, S. Paul, T. Schioppa, A. Saccani, M. Sironi, B. Bottazzi, A. Doni, B. Vincenzo, F. Pasqualini, et al. 2006. A distinct and unique transcriptional program expressed by tumor-associated macrophages (defective NF-kappaB and enhanced IRF-3/STAT1 activation). *Blood* 107: 2112–2122.
28. Bronte, V., and P. Zanovello. 2005. Regulation of immune responses by L-arginine metabolism. *Nat. Rev. Immunol.* 5: 641–654.
29. Nahrendorf, M., F. K. Swirski, E. Aikawa, L. Stangenberg, T. Wurdinger, J. L. Figueiredo, P. Libby, R. Weissleder, and M. J. Pittet. 2007. The healing myocardium sequentially mobilizes two monocyte subsets with divergent and complementary functions. *J. Exp. Med.* 204: 3037–3047.
30. Swirski, F. K., M. Nahrendorf, M. Etzrodt, M. Wildgruber, V. Cortez-Retamozo, P. Panizzi, J. L. Figueiredo, R. H. Kohler, A. Chudnovskiy, P. Waterman, et al. 2009. Identification of splenic reservoir monocytes and their deployment to inflammatory sites. *Science* 325: 612–616.
31. Naviliat, M., G. Gualco, A. Cayota, and R. Radi. 2005. Protein 3-nitrotyrosine formation during *Trypanosoma cruzi* infection in mice. *Braz. J. Med. Biol. Res.* 38: 1825–1834.
32. Petray, P., E. Castaños-Velez, S. Grinstein, A. Orn, and M. E. Rottenberg. 1995. Role of nitric oxide in resistance and histopathology during experimental infection with *Trypanosoma cruzi*. *Immunol. Lett.* 47: 121–126.
33. Saeftel, M., B. Fleischer, and A. Hoerauf. 2001. Stage-dependent role of nitric oxide in control of *Trypanosoma cruzi* infection. *Infect. Immun.* 69: 2252–2259.
34. Vespa, G. N., F. Q. Cunha, and J. S. Silva. 1994. Nitric oxide is involved in control of *Trypanosoma cruzi*-induced parasitemia and directly kills the parasite in vitro. *Infect. Immun.* 62: 5177–5182.
35. Mori, M., and T. Gotoh. 2000. Regulation of nitric oxide production by arginine metabolic enzymes. *Biochem. Biophys. Res. Commun.* 275: 715–719.

OPEN ACCESS Freely available online

PLOS | NEGLECTED TROPICAL DISEASES

Appraisal of a *Leishmania major* Strain Stably Expressing mCherry Fluorescent Protein for Both *In Vitro* and *In Vivo* Studies of Potential Drugs and Vaccine against Cutaneous Leishmaniasis

Estefania Calvo-Álvarez[1☯], Nestor Adrian Guerrero[2☯], Raquel Álvarez-Velilla[1], Christopher Fernández Prada[1], Jose María Requena[2], Carmen Punzón[3], Miguel Ángel Llamas[3], Francisco J. Arévalo[3], Luis Rivas[4], Manuel Fresno[2,3], Yolanda Pérez-Pertejo[1], Rafael Balaña-Fouce[1]*, Rosa M. Reguera[1]

1 Departamento de Ciencias Biomédicas, Universidad de León, León, Spain, **2** Centro de Biología Molecular "Severo Ochoa", Universidad Autónoma de Madrid, Madrid, Spain, **3** Diomune, Parque Cientifico de Madrid, Madrid, Spain, **4** Centro de Investigaciones Biológicas, Madrid, Spain

Abstract

Background: *Leishmania major* cutaneous leishmaniasis is an infectious zoonotic disease. It is produced by a digenetic parasite, which resides in the phagolysosomal compartment of different mammalian macrophage populations. There is an urgent need to develop new therapies (drugs) against this neglected disease that hits developing countries. The main goal of this work is to establish an easier and cheaper tool of choice for real-time monitoring of the establishment and progression of this pathology either in BALB/c mice or *in vitro* assays. To validate this new technique we vaccinated mice with an attenuated Δhsp70-II strain of *Leishmania* to assess protection against this disease.

Methodology: We engineered a transgenic *L. major* strain expressing the mCherry red-fluorescent protein for real-time monitoring of the parasitic load. This is achieved via measurement of fluorescence emission, allowing a weekly record of the footpads over eight weeks after the inoculation of BALB/c mice.

Results: *In vitro* results show a linear correlation between the number of parasites and fluorescence emission over a range of four logs. The minimum number of parasites (amastigote isolated from lesion) detected by their fluorescent phenotype was 10,000. The effect of antileishmanial drugs against mCherry+*L. major* infecting peritoneal macrophages were evaluated by direct assay of fluorescence emission, with IC_{50} values of 0.12, 0.56 and 9.20 μM for amphotericin B, miltefosine and paromomycin, respectively. An experimental vaccination trial based on the protection conferred by an attenuated Δhsp70-II mutant of *Leishmania* was used to validate the suitability of this technique *in vivo*.

Conclusions: A *Leishmania major* strain expressing mCherry red-fluorescent protein enables the monitoring of parasitic load via measurement of fluorescence emission. This approach allows a simpler, faster, non-invasive and cost-effective technique to assess the clinical progression of the infection after drug or vaccine therapy.

Citation: Calvo-Álvarez E, Guerrero NA, Álvarez-Velilla R, Prada CF, Requena JM, et al. (2012) Appraisal of a *Leishmania major* Strain Stably Expressing mCherry Fluorescent Protein for Both *In Vitro* and *In Vivo* Studies of Potential Drugs and Vaccine against Cutaneous Leishmaniasis. PLoS Negl Trop Dis 6(11): e1927. doi:10.1371/journal.pntd.0001927

Editor: Genevieve Milon, Institut Pasteur, France

Received April 30, 2012; **Accepted** October 16, 2012; **Published** November 29, 2012

Funding: This research was supported by Ministerio de Ciencia y Tecnología (grants AGL2010 16078/GAN), Instituto de Salud Carlos III (grant PI09/0448 and the Network of Tropical Diseases RICET RD06/0021/1004). RAV, CFP and ECA are pre-doctoral fellows granted by RICET (ISCIII), Junta de Castilla y León (ESF; European Social Founding) and University of León, respectively to RMR. Instituto de Salud Carlos III (Network of Tropical Disasese RICET RD06/0021/0016), Ministerio de Ciencia e Innovación (SAF2010-17833), ChagasEpiNet 223034 European Union Seventh Framework Programme and Fundación Ramón Areces to MF. Funding by ISCIII-RETIC RD06/0021/0008-FEDER to JMR and ISCIII-RETIC RD06/0021/0006-FEDER to LR is also acknowledged. The funders had no role in study design, data collection and analysis, decision to publish, or preparation of the manuscript.

Competing Interests: The authors have declared that no competing interests exist.

* E-mail: rbalf@unileon.es

☯ These authors contributed equally to this work.

Introduction

Leishmania major is the main cause of cutaneous leishmaniasis (CL) in the Old World. Parasites are transmitted by *Phlebotominae* sandflies whilst blood feeding on infected mammalian hosts. CL is widely spread in the developing world, affecting people in 88 countries with 1.5 million new cases reported each year. CL usually produces ulcers on the exposed parts of the body that often leave disfiguring scars, which in turn, can cause serious social prejudice [1].

Conventional *in vivo* animal models for the study of parasite-host relationships involve large number of animals. These animals are required to be slaughtered at different time points in order to identify both anatomical distribution and parasite numbers in

Role of *Trypanosoma cruzi* Autoreactive T Cells in the Generation of Cardiac Pathology

NÚRIA GIRONÈS,[a] EUGENIO CARRASCO-MARIN,[b] HENAR CUERVO,[a] NÉSTOR ADRIÁN GUERRERO,[a] CRISTINA SANOJA,[a] JOHN SPARROW,[c] REYES FLORES-HERRÁEZ,[d] LORENA FERNÁNDEZ-PRIETO,[b] ISABEL CHICO-CALERO,[a] HUGO SALGADO,[a] JAVIER CARRIÓN,[a] AND MANUEL FRESNO[a]

[a]*Centro de Biología Molecular, CSIC-UAM, Universidad Autónoma de Madrid, Madrid, Spain*

[b]*Departamento de Inmunología, Hospital Universitario Marqués de Valdecilla, Santander, Spain*

[c]*Glaxo SmithKline, Tres Cantos, Madrid, Spain*

[d]*Departamento de Biología Celular, Facultad de Medicina, Universidad Complutense de Madrid, Madrid, Spain*

ABSTRACT: Chagas disease, caused by *Trypanosoma cruzi*, affects several million people in Central and South America. About 30% of chronic patients develop cardiomyopathy probably caused by parasite persistence and/or autoimmunity. While several cross-reactive antibodies generated during mammal *T. cruzi* infection have been described, very few cross-reactive T cells have been identified. We performed adoptive transfer experiments of T cells isolated from chronically infected mice. The results showed the generation of cardiac pathology in the absence of parasites. We also transferred cross-reactive SAPA-specific T cells and observed unspecific alterations in heart repolarization, cardiac inflammatory infiltration, and tissue damage.

KEYWORDS: *T. cruzi*; autoreactive T cells; autoimmunity; Chagas disease

INTRODUCTION

Chagas disease is a debilitating multisystemic disorder that affects several million people (approximately 18 million individuals are infected with

Address for correspondence: Manuel Fresno, Centro de Biología Molecular, CSIC-UAM, Universidad Autónoma de Madrid, Cantoblanco, E-28049 Madrid, Spain. Voice: 34-91-3978413; fax: 34-91-3974799.
mafresno@cbm.uam.es

Ann. N.Y. Acad. Sci. 1107: 434–444 (2007).
doi: 10.1196/annals.1381.046